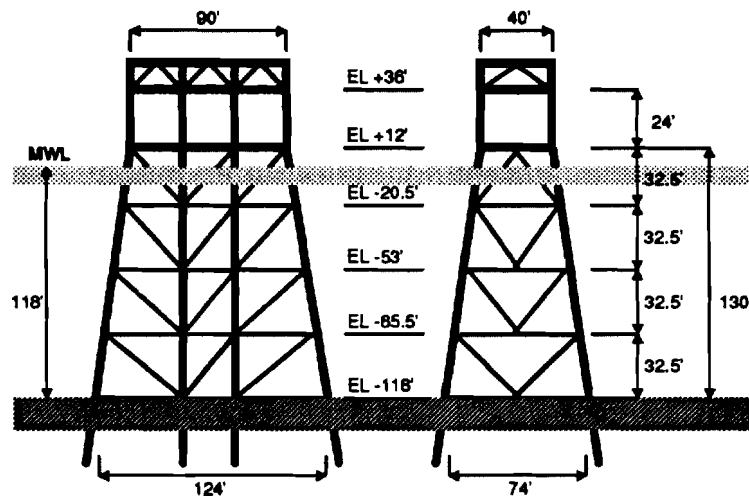β

Marine Technology & Management Group Project

SCREENING METHODOLOGIES
FOR USE IN PLATFORM
ASSESSMENTS & REQUALIFICATIONS

Final Project Report

by

Mehrdad Mortazavi

and

Professor Robert G. Bea

Department of Civil Engineering
UNIVERSITY OF CALIFORNIA, BERKELEY

January 1996

224 E

EXECUTIVE SUMMARY

There are over 7,000 offshore platforms worldwide with more than 3,800 in the Gulf of Mexico. This offshore infrastructure is used by the oil and gas industry to furnish over twenty percent of the worlds hydrocarbon requirements. Many of these offshore platforms are called upon for extended service beyond their original design life. This makes the need to assess and requalify these structures a high priority concern.

Detailed nonlinear structural analyses are complex and difficult to perform. The programs developed to help engineers perform such analyses require high degrees of expertise to operate properly, are expensive to purchase and maintain, and require large amounts of manpower and time to complete the analyses. Therefore, detailed structural analyses are not the appropriate first step in the process of assessment and requalification of every offshore platform. Resources are limited and have to be competed for. These facts and the large number of platforms that need to be assessed and requalified highlight the need for a practical methodology for screening large fleets of offshore platforms.

The objective of this research was to develop and verify a simplified analytical method for assessment of structural reliability of template-type offshore platforms subjected to severe storm conditions. Verification of these procedures has been accomplished by comparing the results from the simplified analyses with the results from three dimensional, nonlinear analyses of a variety of template-type platforms, with actual field performance of these platforms during past hurricanes, and with the results from large-scale frame tests.

The methodology developed during this research can be used in the process of screening platform fleets that are being evaluated for extended service. In addition, it can be used to help verify results from complex analytical models that are intended to determine the ultimate limit state lateral loading capacities of platforms. Lastly, the simplified procedure can be applied as a preliminary design tool for design of new platforms.

ACKNOWLEDGMENTS

TABLE OF CONTENTS

LIST OF FIGURES

LIST OF TABLES

CHAPTER 1

INTRODUCTION

1.1 Problem Statement

The first oil and gas operations over water took place in Summerland, California as early as 1896, where wells were drilled from piers extending from shore. By the early 1930's, the oil industry had moved into shallow waters of Gulf of Mexico using existing technology for timber structures. The first steel platforms were installed in 1947 in the Gulf of Mexico. Since then, they have been used extensively in development of offshore fields around the world. Today, there are over 7,000 offshore structures worldwide with more than 3,800 in the Gulf of Mexico. This offshore infrastructure is used by the oil and gas industry to furnish over twenty percent of the worlds hydrocarbon requirements (Weidler, 1993).

It was not until 1969 that the industry had its first offshore design standards with the publication of the first edition of API RP 2A (American Petroleum Institute Recommended Practice for Planning, Designing and Constructing Fixed Offshore Platforms). Before this date, there did not exist any common design guidelines and the individual designers were on their own. Platforms were designed based on experience gained from design and construction of onshore high-rise buildings and bridges and designers judgment. Since these early days, design criteria for offshore platforms has

changed significantly over the past four decades. The design basis for many of the early generations of platforms is now obsolete.

The marine environment is extremely hostile and accelerates the natural processes of aging and deterioration of offshore platforms. In addition to fatigue and corrosion damage, some of these structures are damaged by collisions with supply boats and objects dropped from the platform decks. Member overload during intense storms have been another source of damage to main load carrying elements like vertical diagonal braces, tubular joints and foundation piles and soils. Installation and maintenance activities are often a source of damage to offshore platforms.

With the oil economics of today on one hand and new technology extending the life of the old oil fields on the other hand, many of these structures are now called upon for extended service beyond their original design life. Approximately one-third of the platforms in the Gulf of Mexico (~1000 structures) are now beyond their original design life (20-25 years) and are now being called upon for extended service. This makes the need to assess and requalify platforms a high priority concern. Hurricanes of considerable magnitude and with significant impact have highlighted this need (Hilda and Betsy in the 1960's, Camille in 1974 and Andrew in 1992). Interest in safety assessment and maintaining the safety of offshore platforms against loss of life, environmental pollution, and loss of resources and property has recently increased due to the awareness of the public of the consequences of their failure.

The problem of risk management of existing facilities is not unique to offshore industry. The electric power generation industry and the chemical industry have been addressing the same problem. The 1971 San Fernando, 1989 Loma Prieta, and 1994 Northridge earthquakes in California have repeatedly focused the attentions on existing infrastructure. In particular, questions were raised concerning safety of buildings and bridges.

During the past three decades, an immense amount of effort has been devoted to development of sophisticated computer programs to assess storm wind, wave, and current loadings and the ultimate limit state capacity characteristics of conventional, pile-supported, template-type offshore platforms. There are many alternatives in modeling the structure and its components and in interpreting the results. There is little validation of software. The few existing studies indicate relatively large deviations and inconsistencies among the results of different software packages. Quite different results are demonstrated in the literature, in terms both of failure modes and capacity for the same structure (Billington et al., 1993b).

The programs developed to help engineers perform such detailed analyses require high degrees of expertise to operate properly, are expensive to purchase and maintain, and require large amounts of manpower and time to complete the analyses. Due to the sophistication of these programs, they are prone to human error. Experience has shown

3

that it is easy to make mistakes that are difficult to detect and that can have significant influences on the results.

In addition to structural modeling uncertainties, large uncertainties are associated with environmental conditions (wave height and period, wind and current speed), calculated forces, and structure and foundation condition and capacities. These uncertainties add another dimension to the complexity of the process of assessment and requalification of offshore platforms.

Detailed structural reliability analyses are extremely prohibitive to perform in terms of time and cost. Therefore, they are not the appropriate first step in the process of assessment and requalification of every offshore platform. Resources are limited and have to be competed for. These facts and the large number of platforms that need to be assessed and requalified highlight the need for a practical method for screening and assessing the structural integrity of existing offshore platforms.

1.2   Research Objective and Scope

The fundamental question addressed by this research is whether it is possible to develop a rational and simplified analytical method to evaluate the loadings on and capacities of existing platforms so that a complete structural reevaluation for a majority of these structures would be unnecessary. The objective of this research is to answer this question by developing and verifying such a method. This dissertation documents the development

and verification of simplified quantitative procedures that can be used to assess the structural safety of steel template-type offshore platforms. The following issues are addressed in this research:

a) Storm loadings acting on offshore platforms

b) Capacity of intact, damaged, and grout repaired structural elements and components of paltforms

c) Static ultimate lateral loading capacity of platform systems

d) Structural reliability of platforms

e) Verification of the simplified method with results from detailed nonlinear structural analyses, actual field performance, and large-scale frame tests

f) Development of a software that helps performing the simplified analyses

Offshore platforms are subject to various environmental, operational and accidental loads. Environmental loads include waves, currents, wind, earthquakes, subsea mudslides, and ice loads. Operational loads include those that are imposed on the platform as a result of the operational activities such as crane movements on the platform main deck. Accidental loads include those that result from collisions, dropped objects, or explosions. These loads are in general dynamic in nature and depending on the structure's characteristics (mass and stiffness properties) and type of analyses (local vs. global or nominal vs. extreme conditions) have to be considered as such. This research focused on waves, currents, and wind forces developed during intense storms and acting on offshore platforms. A simplified load model was developed. Based on an idealized structure, aerodynamic and

5

hydrodynamic loads acting on a platform were formulated. This load model was verified with results from more sophisticated current and wave load generating programs commonly used in industry.

Prediction of ultimate and residual capacities of a platform system requires realistic modeling of the behavior of elements and components that comprise the platform. The structural elements include tubular braces and joints, deck and jacket legs, pipe piles and foundation soils. The primary structural components include the deck portal, the jacket bays, and the foundation (Figure 1.1). In this research, simplified formulations were developed to estimate the ultimate capacities of these structural elements and components. Based on presumed collapse mechanisms, the principle of virtual work was utilized to formulate the ultimate capacity for each component. Material and geometric nonlinearities were considered. Where possible, these capacity formulations were verified with and calibrated against existing empirical equations given in current design guidelines (API, 1993b).

In offshore operations, accidents like collisions and dropped objects are not a rarity. Steel members are exposed to an extremely corrosive environment. Damage such as dents, global bending, and corrosion can significantly affect the ultimate strength of an offshore platform. Given the physical properties of damage, an estimate of the ultimate and residual strength of the damaged members is necessary to perform a strength assessment of a platform. Given a significant reduction in overall platform capacity due to damaged
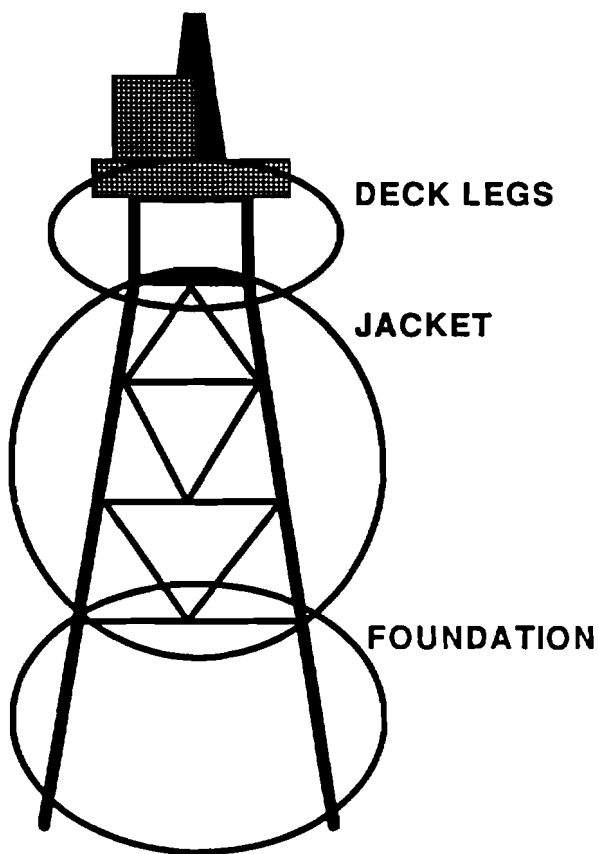
Figure 1.1: Primary Structural Components of Template-Type Platforms

elements, remedial actions need to be undertaken and their effectiveness on reinstating the element and system ultimate strengths need to be assessed. In the recent years, numerous investigators have studied this subject and several theoretical approaches have been developed addressing different types of damage to tubular members and alternative repair strategies. Small and large scale experiments have been performed to verify the analytical capacity formulations of the ultimate and post ultimate behavior of damaged and repaired tubular members. A literature review was performed on the ultimate strength behavior of damaged and repaired tubular braces with dents, global out-of-straightness, and corrosion.

7

Simplified methods were identified to estimate the ultimate and residual capacity of such members. These methods were integrated in the framework of a global simplified platform assessment procedure.

Using the loading and component capacity prediction procedures developed during this research, and based on previous research performed at the University of California at Berkeley (Bea and DesRoches, 1993), a simplified approach was developed to assess the structural integrity of a platform system. This procedure identifies the weak-link in the platform system. The ultimate lateral loading capacity of the platform is reached when the weak-link reaches its lateral capacity.

In extreme storm conditions, and unlike earthquake loading, experience has shown that the dynamic nature of the loads do not play a major role in the ultimate limit state performance of conventional, pile-supported, jacket-type offshore platforms. This fact is also reflected in the design practice of such structures where, based on wave data, a single design wave height is selected and static structural analyses are performed. Hence, the focus of this research was upon static pushover analyses, where a load pattern is selected, applied to the platform, and incrementally increased until the platform is no longer capable of resisting the lateral storm and vertical deck loads. At this point, the base shear or the total lateral load acting on the structure defines the ultimate lateral loading capacity of the platform.

An initial objective of this research was to develop deterministic loading and capacity formulations based on mean values or best estimates of input variables. During the research, it was recognized that the large uncertainties associated with capacity and loading parameters and their effect on overall platform safety needed to be addressed. Based on the fundamentals of structural reliability theory and using the deterministic load and capacity modeling procedures developed during this research, a simplified structural component and system reliability analysis procedure was developed to identify the potential failure modes of the structure and to estimate the failure probability of the platform.

A major part of this research effort has been to verify and calibrate the simplified deterministic loading and capacity prediction formulations. Three levels of verification were performed using results from

a)   detailed, three-dimensional, nonlinear pushover analyses,

b)   actual field performance of platforms during intense storms, and

c)   large-scale frame tests.

In this effort, using the simplified method developed during this research, the ultimate element and system capacities of actual offshore platforms and test frames were estimated and compared with results from detailed nonlinear pushover analyses, actual platform response to storm loadings and actual ultimate capacity behavior of test frames.

Finally, a computer program has been developed to perform the simplified analyses. Reasonable simplifications and high degrees of user-friendliness have been employed in development of the software to reduce the engineering effort, expertise, and costs associated with the analyses.

The methodology developed and verified during this research is believed to be a significant contribution to the field of offshore structural engineering. The following potential application areas are identified:

a)   screening large fleets of platforms,

b)   parametric studies and sensitivity analyses,

c)   reliability analyses,

d)   checking complex models and analyses,

e)   preliminary design and design optimizations.

Given that a detailed structural assessment of a single platform is an extremely prohibitive task, the simplified method developed can be used to perform risk analyses for a large number of platforms. The platforms can be prioritized based on their likelihoods and potential consequences of failure. Limited resources can then be focused on high priority platforms. Detailed risk assessment, evaluation, and mitigation programs can be applied to these structures in an efficient and timely manner.

While assessing the structural integrity of an intact or damaged platform, and before a detailed risk analysis is performed, the simplified analysis procedure can be used to identify the potential failure modes, the effect of member damage on overall platform strength, and the effectiveness of grout-repair of damaged members in reinstating the full strength of the platform. These preliminary results can provide the analysts with valuable insight into the probable performance of the structure and help the engineers plan the detailed analysis accordingly.

Detailed nonlinear structural analyses require the use of sophisticated hardware and software. A typical offshore platform is a relatively complex structure. Modeling of such complex structures is not a straightforward task. Due to this sophistication and complexity, the process of detailed risk analysis of an offshore platform is prone to human and system error. The simplified methodology presents an ideal tool to "roughly" check the results of complex analyses.

Lastly, but not least importantly, the simplified procedures can be used in preliminary design of offshore platforms. Given the environmental conditions and required working areas and deck loads (topside facilities and equipment), platform configuration, bracing pattern, member dimensions and the total steel tonnage can be rapidly estimated. Using this methodology, important design issues like robustness (ductility, redundancy, and excess capacity) can be studied and integrated into platform design at a conceptual design phase.

Develop Simplified Analysis Procedure

Verify w. Detailed Analyses

Verify w. Actual Field Performance

Verify w. Frame Tests
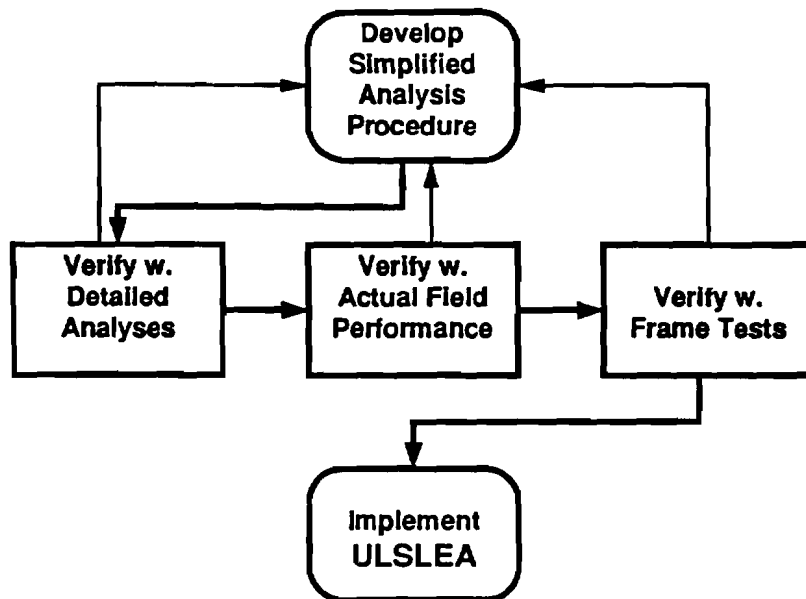
Implement ULSLEA

Figure 1.2: Interactive Development, Verification, and Calibration of ULSLEA

1.3 Research Methodology

Figure 1.2 shows the principal approach used to develop, verify, and implement the simplified collapse analysis procedures. Based on fundamentals of mechanics of materials, statics, fluid dynamics, and structural reliability theory, simplified load and capacity prediction and reliability analysis procedures were developed in this thesis. Use was made of research results of various researchers and engineers who have been working on related topics. The simplified procedures were verified and calibrated with results from detailed nonlinear analyses, actual field performance of some Gulf of Mexico platforms, and large-scale frame tests. The product of this simultaneous development, verification, and

calibration effort is identified as ULSLEA (Ultimate Limit State Limit Equilibrium Analysis).

The environmental loads were formulated based on a simplified model of the structure, water particle kinematics, and a semi-empirical force transfer function. The simplified structural model incorporated all of the platform's structural and nonstructural elements that are capable of resisting and transferring the environmental loads. These included the superstructure (decks and the topside facilities), the substructure (the jacket including all vertical and horizontal framing), and the appurtenances (boatlandings, barge bumpers, risers, etc.). The water particle kinematics were formulated based on the storm type (tropical or extra-tropical) and environmental conditions, including water and storm surge depths, wave height and period, current velocity profile, and wind speed at a reference elevation. The aerodynamic and hydrodynamic forces were determined based on the velocity pressures.

Simplified formulations are developed to estimate the ultimate lateral shear capacity of the three primary structural components of a platform. Elements within these components are identified first. These are deck legs, tubular braces and their connections (tubular joints) and pipe piles. For each component to fail, all elements within that component have to fail. Based on past numerical analyses and experience, failure modes are assumed for different platform components. Using the concept of plastic hinge theory, the principle of virtual work is utilized to formulate the component capacities; the virtual displacement is taken to

be the actual collapse mechanism and an equilibrium equation is derived for each component at ultimate limit state. Where of significance, geometric nonlinearities are also taken into account.

Theoretical approaches and experiments addressing the ultimate strength behavior of damaged and grout-repaired tubular braces were reviewed. Simplified methods have been identified to estimate the ultimate and residual capacity of such members. These formulations have been integrated in ULSLEA.

Taking into account the uncertainties associated with capacity and loading parameters, a simplified structural component and system reliability analysis procedure was developed. The objective was to identify the potential failure modes of an offshore structure and to estimate bounds on its probability of failure. In this approach, the maximum static force acting on and the capacity of a platform were treated as functions of random variables. The simplified load and capacity prediction procedures developed earlier were utilized to estimate the expected or best estimate loads acting on and capacity of the platform. The uncertainties associated with loads and capacities were derived considering the uncertainties associated with environmental conditions, structure conditions, kinematics, material properties, and force and capacity calculation procedures.

Verification of the simplified load and capacity prediction procedures was accomplished by comparing the results from the simplified analyses with the results from three

dimensional nonlinear analyses of a variety of template-type platforms. The verification platforms included four-leg well protector and quarter structures and eight-leg drilling and production structures in the Gulf of Mexico. These structures employed a variety of types of bracing patterns and joints. Several of these structures were subjected to intense hurricane storm loadings during hurricanes Andrew, Camille, Carmen and Frederic. Within the population of verification platforms are several that failed or were very close to failure. Finally, the ultimate strength performance of three-dimensional large-scale test frames, determined during three major frame test projects performed in the last decade, were used to verify the simplified ULSLEA method.

1.4   Summary of Approach Developed

A template-type offshore platform is comprised of three primary structural components (Figure 1.1). Superstructure, or deck, supports the topside facilities. Substructure, or jacket, resists and transfers the vertical dead loads and lateral operational and environmental live loads to the foundation. Pile foundation finally transfers the loads to the ocean ground. In the following, the simplified approach for structural safety assessment of such structures, developed during this research, is summarized.

Figure 1.3 illustrates the steps involved in the overall process of the simplified limit equilibrium analysis of an offshore platform. The geometry of the platform is defined by specifying a minimum amount of data. The environmental conditions are defined and include the water depth, wave height and associated period, storm surge depth, current velocity profile and wind speed at a reference elevation. These values are assumed to be
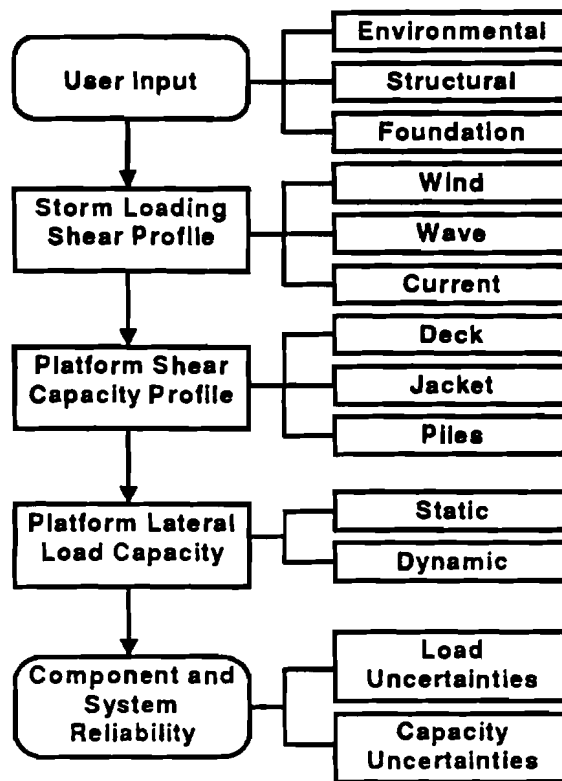
Figure 1.3: Simplified Loading, Capacity, and Reliability Analyses Process

collinear and to be the values that occur at the same time. The wave period is generally

taken to be expected period associated with the expected maximum wave height. The

structure is defined by specifying the following parameters: the effective deck areas, the

proportion and topology of jacket legs, braces, joints, foundation piles and conductors.

The projected area characteristics of appurtenances such as boat landings, risers, and well

conductors are also specified. If marine fouling is present, the variation of the fouling

thickness with depth is defined. Specialized elements are designated including grouted or

ungrouted joints, braces, and legs. In addition, damaged or defective elements are

included. Dent depth and initial out-of-straightness are specified for braces with dents and global bending defects. Element capacity reduction factors are introduced to account for other types of damage to joints, braces, and foundation (corrosion, fatigue cracks, etc.). Steel elastic modulus, yield strength, and effective buckling length factor for vertical diagonal braces are specified. Soil characteristics are specified as the depth variation of effective undrained shear strength for cohesive soils or the effective internal angle of friction for cohessionless soils. Scour depth around the piles is also specified.

Wave, current and wind forces are considered. For the purpose of load calculation, all of the structure elements are modeled as equivalent vertical cylinders that are located at the wave crest. Appurtenances (boat landings, risers) are modeled in a similar manner. For inclined members, the effective vertical projected area is determined by multiplying the product of member length and diameter by the cube of the cosine of its angle with the horizontal. Wave horizontal velocities are based on Stokes fifth-order theory. The total horizontal water particle velocities are taken as the sum of the wave horizontal velocities and the current velocities. Modification factors are introduced to recognize the effects of wave directional spreading and current blockage. The maximum drag force acting on the portions of structure below the wave crest is based on the fluid velocity pressure. For wave crest elevations that reach the lower decks, the horizontal hydrodynamic forces acting on the lower decks are computed based on the projected area of the portions of the structure that would be able to withstand the high pressures. The wind force acting on the exposed decks is based on the wind velocity pressure.

To develop a resistance profile, collapse mechanisms are assumed for the deck legs, the jacket, and the pile foundation. Based on the presumed failure modes, the principle of virtual work is utilized to estimate the ultimate lateral capacity for each component and a profile of horizontal shear capacity of the platform is developed.

Comparison of the storm shear profile with the platform shear capacity profile identifies the weak-link in the platform system. The base shear or total lateral loading at which the capacity of this weak-link is exceeded defines the static ultimate lateral capacity of the platform R_{us}. The static lateral loading capacity, addressed by this research, can be corrected with a loading effects modifier, F_v, to recognize the interactive effects of transient wave loadings and nonlinear hysteretic platform response (Bea and Young, 1993)

$$R_u = R_{us} F_v \qquad (1.1)$$

A platform can be considered as a combination of series components and parallel elements. The series components are the superstructure (deck), the substructure (jacket), and the foundation. The capacity of the platform is assumed to be reached when the capacity of any one of these components is reached. Within each component there are parallel elements; deck legs, braces, joints, and piles. In order for a component to fail, all of its parallel elements have to fail. The maximum static force acting on and capacities of platform elements and components are treated as functions of random variables. By taking

18

into account the biases and uncertainties associated with loads and capacities and using a First Order Second Moment (FOSM) approach, bounds on probability of system failure are estimated

A typical output of the deterministic failure analysis procedure is illustrated in Figure 1.4. Storm shear and platform shear resistance profiles are plotted versus platform elevation. The cumulative storm shear at a given elevation, includes the integrated wind, wave and current forces acting on the portions of platform above that elevation. The storm shear at the top of the plot corresponds to total wind, wave and current forces acting on the deck areas of the platform. The storm shear at the mudline defines the total base shear. The upper-bound capacity of a given bay is based on failure of all of the resisting elements. The lower-bound capacity of a given bay is based on first member failure and is plotted in addition to upper-bound capacity for jacket bays. Comparison of the storm shear and platform capacity profiles identifies the weak-link of the platform. When the lateral load acting on the weakest component equals the shear resistance of this component, the corresponding total base shear defines the ultimate lateral loading capacity of the platform.

Figure 1.5 shows a typical output of the probabilistic failure analysis procedure. The outcome of this procedure is expressed in terms of reliability indices. Reliability index is a measure of safety. For each loading direction, reliability indices, β, are plotted for all failure modes. In addition to the expected values of loadings and capacities, the reliability indices reflect the uncertainties associated with these variables. The probability of failure

Platform Elevation   **Storm Shear / Platform Shear Capacity**
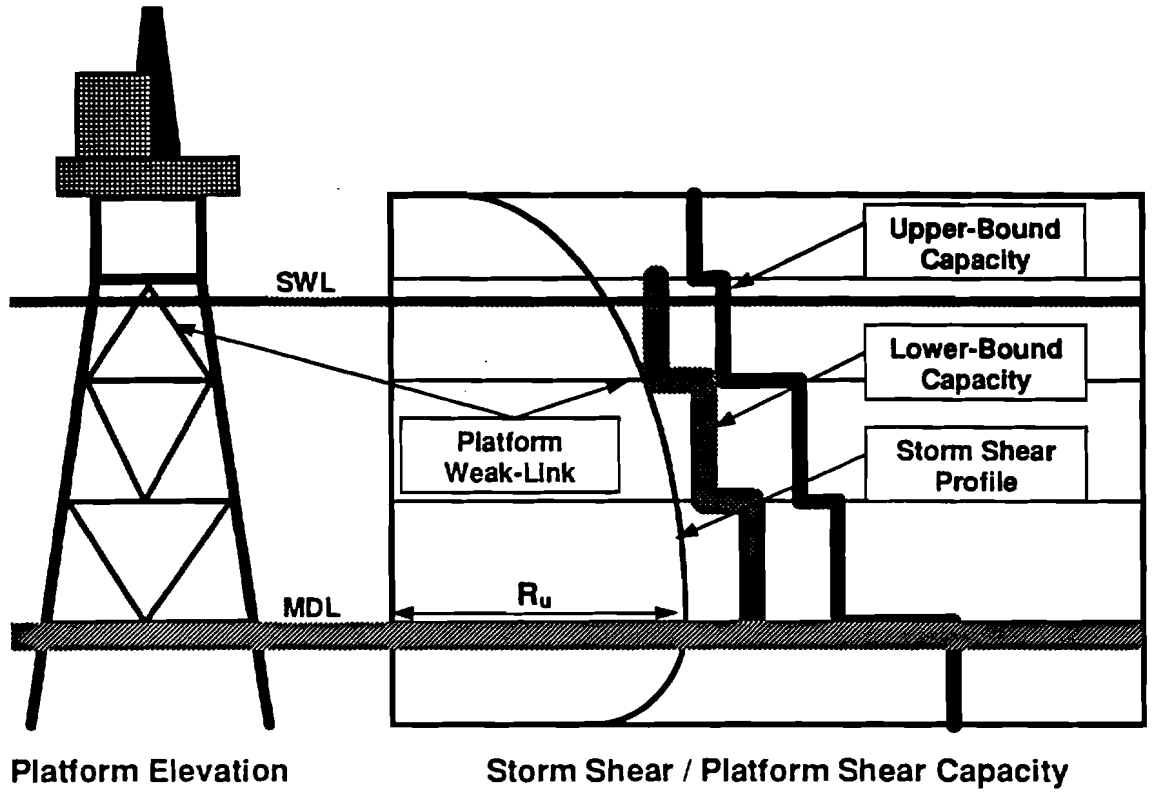
Figure 1.4: Typical Output of the Deterministic Failure Analysis

Deck Legs

Bay I

Bay II

Bay III

Foundation

SWL

MDL

Platform Elevation

Lateral

Axial

β (Reliability Index)
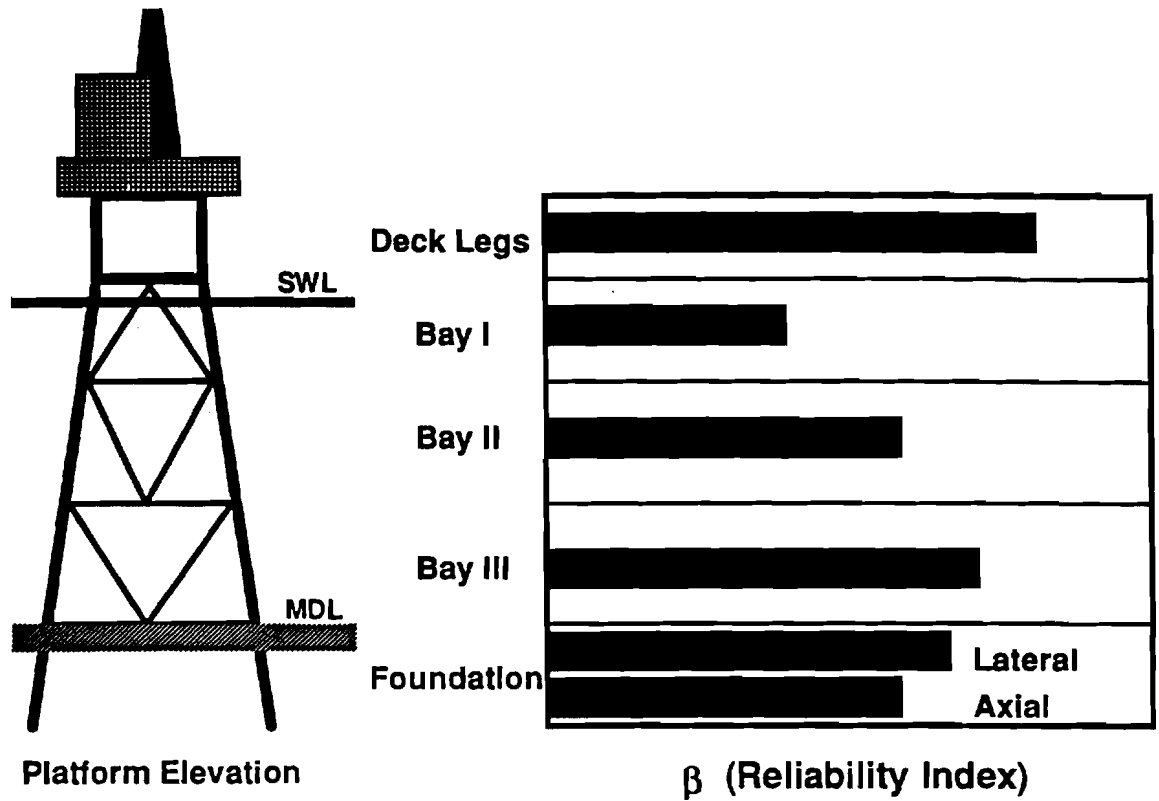
Figure 1.5: Typical Output of the Probabilistic Failure Analysis

of each component, p_{fi}, is estimated as $\Phi(-\beta)$, the normal cumulative distribution function evaluated at $-\beta$. Bounds on the probability of failure of the platform system are estimated as

$$max\ P_{fi} < P_{fs} < \sum_i P_{fi} \tag{1.2}$$

1.5 Organization of Dissertation

Chapter 2 contains a background on different aspects of platform assessment and requalification process. Past and recent research in the subject area is summarized and

developments in industry are reviewed and discussed in this chapter. The structural modeling and simplified environmental loading calculation procedures are detailed in Chapter 3. Simplified structural component capacity formulations based on the concept of limit equilibrium analysis are presented and discussed in Chapter 4. Taking into account the uncertainties associated with loadings and capacities, a simplified structural reliability analysis method is introduced, discussed, and implemented in a case study in Chapter 5. Chapter 6 is devoted to the verification studies performed to check the validity and calibrate the simplified ULSLEA method. The loadings on and capacities of 6 Gulf of Mexico platforms are estimated using both the simplified ULSLEA and the nonlinear finite element analysis programs USFOS (Sintef, Norway) and SEASTAR (PMB Systems Engineering, USA). The studies are described in detail and the results are discussed. Both sets of results are also compared with the actual performance of the platforms during intense storms. Finally, the frame test verification results are reported and discussed in this chapter. Chapter 7 contains a summary of the developments and findings of this research. Potential future research topics are also identified and discussed in this chapter.

Input and output files of CALREL (a reliability analysis software developed at University of California at Berkeley; Liu et al., 1987) for an example platform are contained in Appendix A. Appendix B contains the modified element capacity formulations for damaged and repaired members as given by Loh (1993) and Parsanejad (1987). Appendix C documents the computer program ULSLEA. A detailed program description and user-manual is contained in this appendix.

CHAPTER 2

OVERVIEW & BACKGROUND

2.1 Platform Assessments and Requalifications

The process of assessment and requalification of an existing structure commonly involves the following steps:

a)   Inspection and condition assessment,

b)   environmental loading assessment,

c)   structural and foundation performance assessment,

d)   maintenance and repair assessment, and

e)   risk assessment and evaluation.

In the case of existing offshore platforms, this process is associated with an immense amount of effort and is extremely costly and time consuming. Every single step of this process is associated with high degrees of uncertainty. These facts and the large number of platforms that need to be assessed and requalified pose an unprecedented challenge to the offshore structural engineering community.

Over the years, confronted with the problem of risk management of its aging platform fleets, the offshore oil and gas industry has developed and implemented internal measures of action. Some owner/operator companies have developed in-house programs to prioritize, inspect, maintain and repair their inventory of platforms. These measures range from rating systems developed based on past experience and expert judgment to

sophisticated state of the art reliability analyses (Marshall, 1993; Nair, et al., 1992). However until recently, no industry-wide accepted common rules and procedures of practice existed.

Recently, U.S. Minerals Management Service (MMS) held an international workshop on assessment and requalification of offshore production structures. The workshop was organized by the University of California at Berkeley and Texas A&M University and held in New Orleans, Louisiana, in December 1993. Many leaders and representatives of offshore industry and other interest groups attended the workshop. Working groups were charged with the task of identifying and prioritizing issues and research needs for assessment and requalification procedures. Areas of significance that were addressed included a) inspections, surveys and data management, b) environmental conditions and forces, c) structural and foundation elements, systems and analysis, d) operational analysis, and e) policy considerations and consequences. In the proceedings of the workshop, Dunlap and Ibbs (1993) summarized the inputs from working groups regarding research needs for each area. The major findings of this workshop, among others, are summarized and discussed in the following sections.

In early 1992, the American Petroleum Institute (API) initiated an effort to develop a Recommended Practice (RP) for Assessment of Existing Platforms. An API task group was charged with developing procedures for inspection and acceptance criteria. The initial draft of the API RP 2A Section 17 was published in 1993 and contained a global

framework and recommended a multi-level screening approach. Based on this working draft, a document was ballot released for a one year review/comment to assist the process of acceptance and use. Incorporating industry feedback received at the requalification workshop and a trial application of the Section 17 process on a number of existing platforms by several organizations, API officially issued a draft Supplement 1 for both the WSD and LRFD versions of API RP 2A in April 1995. Figure 2.1 shows the platform assessment process for metocean (meteorological and oceanographic) loading as contained in Section 17 (Digre et al., 1995).

The following sections contain the background and status of industry practice. The shortcomings of the state-of-the-practice and needs for research and development regarding the overall process of platform assessment and requalification are presented and discussed. Special attention is given to the subject of environmental conditions and forces and structural and foundation element and system analyses.

2.2 Structural Integrity Assessments

Scarce resources and the prohibitive nature of comprehensive risk analyses underline the need to develop a screening methodology with the goal of prioritizing structures and identifying those that pose the highest risk and need the most immediate attention. A few investigators have addressed this problem and developed ideas to solve it (Aggarwal et al., 1990; Aggarwal, 1991; Bea, 1992; Marshall, 1992; Bea and Craig, 1993; Nair, 1993). One

Figure 2.1 (continue): Platform Assessment Process (API RP 2A - Section 17)

ANALYSIS CHECKS
All analysis to be conducted using present RP 2A procedures, as modified in Section 17.7

Design Level Analysis

Perform design level analysis applying proper loading from Table 17.5.2a, b
(see Notes 1,2 and Section 17.7)

Passes → **Platform passes assessment**

Fails

Implement mitigation alternatives ?
(see Section 17.8)

Yes

No

Ultimate Strength Analysis

Perform ultimate stength analysis applying proper loading from Table 17.5.2a, b (see Section 17.7)

Passes → **Platform passes assessment**

Fails

Implement mitigation alternatives ?
(see Section 17.8)

Yes

No

Platform does not pass assessment

Figure 2.1 (continue): Platform Assessment Process (API RP 2A - Section 17)

common aspect, addressed by all investigators, is the development of a multi-level screening process. Marshall (1992) identified the following levels of analysis:

1) Back-of-the-envelope, where platforms are rated based on nominal design information

2) Elastic analysis or state of the practice, using conventional analysis tools

3) Over-load analysis, using state-of-the-art software and expert consultants

4) Research level, studying methodology issues and further developing analysis tools to deal with complex problems associated with the details of the forgoing levels of analysis

Marshall suggested the use of these levels of analysis to perform the following sequence of steps in reassessing an old platform: a) classification, b) demand/capacity screening, c) risk rating, and d) evaluating options. Nair et al. (1992) described a two-level assessment approach including screening or relative ranking based on experience and analytical approaches with varying levels of detail depending on the nature of the problem.

Aggarwal et al. (1990) and Bea and Craig (1993) presented a multi-level approach which was based on a progressive screening process that involved four cycles of analysis with increasing level of detail (Figure 2.2).

"Cycle 1: qualitative scoring factors are used to evaluate the platform capacity and loadings and the potential consequences associated with the failure of the platform. Cycle 2: coarse quantitative analyses are used to define the capacity and loadings and the potential consequences of failure.
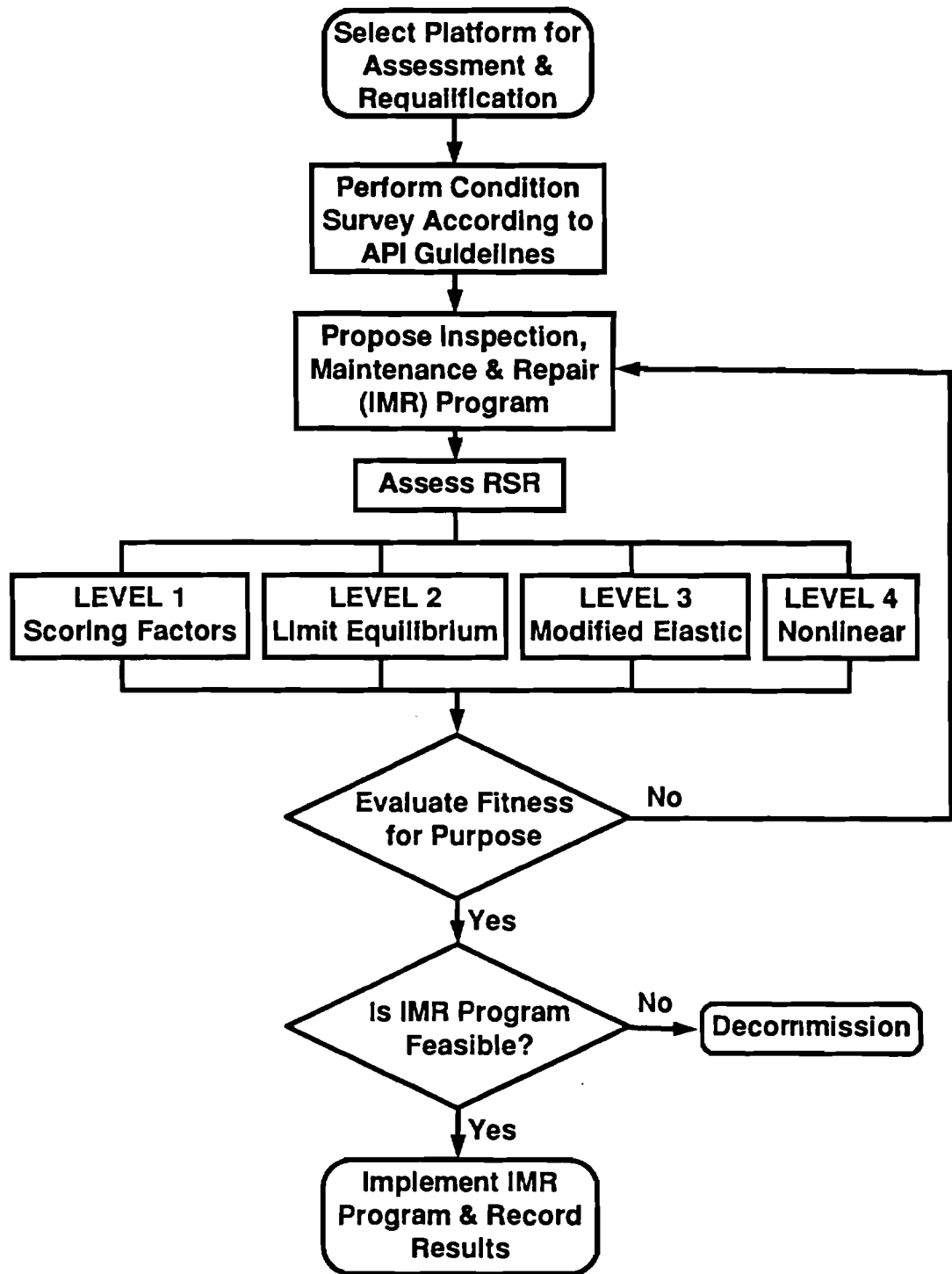
Figure 2.2: Assessment and Requalification Approach Based on RSR (Adopted from Bea and Craig, 1993)

30

Cycle 3: detailed quantitative state-of-the-practice analyses of platform capacity, loadings and potential consequences are performed.

Cycle 4: very detailed quantitative state-of-the-art analyses are used to evaluate platform performance characteristics, the probabilistic aspects of the loadings and capacities, and the likelihood and consequences associated with failure."

This four cycle assessment approach could be used for a periodic reassessment and evaluation of the safety and serviceability of large fleets of platforms. Having identified the most critical platforms, attention and resources could be focused on them and detailed evaluation of the reserve strength and consequence of failure would be required for only a few platforms.

Reserve Strength Ratio (RSR) has been often used as a measure of structural integrity. RSR is defined as the ratio of ultimate capacity, R_u, over a reference base shear

$$RSR = \frac{R_u}{S_r} \tag{2.1}$$

S_r denotes the reference storm total lateral loading and is usually taken as the design load. The ultimate capacity should be determined based on a realistic load pattern. Generally, RSR of a given platform is determined by increasing the magnitude of the reference load pattern acting on the structure until the platform reaches its ultimate capacity. However, this approach may not lead to a realistic RSR, if the reference load pattern does not include loads acting on the deck areas. When the wave crest elevation exceeds that of the platform lower decks, the load pattern changes significantly. Deck inundation can result in

very large lateral deck loads. By not including these loads in RSR, not only are the results based on an unrealistic load pattern, but a potential failure mode is eliminated as well (collapse of deck portal).

Level 1 screening is the logical first step in requalifying a platform. Bea and Craig (1993) used several loading and capacity related factors to define a Level 1 RSR. Based on experience and judgment, they gave guidelines on how to define scores for each factor. Nair et al. (1992) defined a "relative risk" as the linear summation of five penalty factors addressing issues like platform age, condition, etc. Although the procedures involved in a level 1 screening approach may seem to be too simplistic, they attempt to capture the most important factors that can have a significant contribution to the overall risk. This rating system approach has been successfully implemented elsewhere (e.g. existing dams in Washington State, Shaefer, 1992).

Aggarwal et al. (1990) described the basic approach for a Level 2 screening cycle which was based on simplified quantitative load and capacity prediction procedures. Bea and DesRoches (1993) further developed the analytical procedures and applied them in case of five eight-leg self-contained drilling and production platforms and one five-leg well protector in the Gulf of Mexico. The simplified analysis results were verified against the observed and computed loadings and capacities of the platforms.

A Level 3 screening involves linear elastic or state of the practice analysis of a platform. Since linear elastic structural analyses are unable to capture the nonlinear element and system response behavior, capacity modification factors are introduced and safety factors are removed to capture the first significant member failure. Static, linear elastic finite element analyses are relatively easy to perform. The linear elastic analysis procedures have been long established and used in design of almost all existing offshore platforms. These facts and the complex and prohibitive nature of nonlinear finite element analyses have motivated some investigators to develop modifications to these programs so that they can predict the ultimate capacity of platforms. Vannan et al. (1994) developed and introduced such a simplified approach to estimate a lower-bound ultimate strength based on linear analysis. Their approach included nonlinear soil-structure interaction and linear structure behavior modeling above the mudline. Neither material nor geometric nonlinearity was accounted for. Member overstress equations given by API RP 2A-LRFD (API, 1993b) were used. Using this simplified elastic approach, the authors analyzed five platforms and compared the results with those gained from full nonlinear analyses. The two sets of results did not seem to correlate too well in terms of failure mode and ultimate capacity. Differences in structural, foundation and loading assumptions for the two sets of analyses was reported to be the reason for discrepancy in results.

Level 4 screening involves three-dimensional, full nonlinear, state-of-the-art structural analysis of platforms. The objective of this analysis cycle is to model the true response characteristics of elements and the system as a whole and to predict the true ultimate

capacity of the structure. Based on linear elastic design assumptions, a structure can be loaded up to its design load without experiencing yielding at any point. There are many sources of additional or reserve strength in the system so that in general a further increase in the loads beyond the design load would not lead to collapse or even yielding at any point of the structure. Titus and Banon (1988) identified the following sources of explicit and implicit reserve strengths in a structural system: a) conservatism or overdesign, b) code safety factors, c) material reserve strength, d) member reserve strength, e) system redundancy, and f) other factors.

In the past decades, an immense amount of effort has been devoted to development of nonlinear finite element analysis programs. Accurate modeling of ultimate and post-ultimate behavior of axially and laterally loaded tubular braces, tubular joints and foundation soils is of crucial importance to correct prediction of the reserve strength. The computer programs developed so far have reached a high level of sophistication. In most instances, they need experts to use them and to interpret the results. There are many alternatives to model a structure and its elements and to select loading combinations. In general, these programs have not been validated against each other and frame test results (Billington et al., 1993b). In the few cases that comparisons have been made, quite different results have been reported both in terms of collapse mechanism and ultimate capacity (Nordal, 1991). A state of the art review of the subject of reserve, residual and ultimate strength analysis of offshore structures is documented by Billington et al. (1993b).

Particularly interesting are the results of a benchmarking effort that was recently performed to determine the variability of the results of ultimate strength analyses (Digre et al., 1995). This effort was part of a joint government-industry project to perform a trial application of API RP 2A Draft Section 17. A "benchmark structure" was selected and a number of participants were asked to evaluate the ultimate capacity performance of the platform. Nine different software packages were used, which represent most of the available programs in the industry. The benchmark platform was an existing four-legged structure located in Gulf of Mexico in a water depth of 157 ft (verification platform C, Chapter 6). Initially, the coefficient of variation (COV) of the hydrodynamic loading, estimated by participants, was reported to be 24 percent. The COV of wind loading was 33 percent and that of wave and current loads on the deck was 77 percent. The COV of the ultimate capacity was 23 percent with a range of 1,500 kips to 3,150 kips. Different failure modes were reported by different analysts to have governed the ultimate capacity of the platform from pile axial compression failure to yielding of pile segments to failure in the jacket.

The large variations in loading and capacity predictions were found to have originated from the following sources: a) "gross" errors (e.g. in selecting environmental criteria), b) differences in modeling (e.g. pile-soil interaction), c) sensitivity of wave-in-deck load to wave height, d) lack of skill and inconsistency among participants in using design guidelines (API RP 2A-WSD 20th edition, 1993). After these sources of variability in

results were removed, overall COV's of 12% and 16% were reported for the hydrodynamic load and ultimate capacity respectively.

One important issue related to Level 4 analyses is gross errors. In general, human and system error can have a significant influence on the reliability of engineered systems (Bea, 1990; Moore, 1993). These errors can occur in design, construction and operation of such systems. One important source of structural failure is error in design (Moan, 1981). Factors affecting human error include fatigue, negligence, bad judgment, inadequate training, wishful thinking, etc. Factors affecting system error include complexity, latent flaws, sever demands on user, small tolerances, etc. (Bea, 1990). Oftentimes, the interaction between humans and systems magnifies the potential for errors. Loch and Bea (1995) documented some of the common errors and pitfalls of Level 4 ultimate limit state analyses. These analyses require highly sophisticated software and high powered hardware. The complex process puts a high level of demand on the user in terms of interface, experience and judgment. Due to their sophistication, these programs are prone to human error. It is easy to make mistakes that are generally difficult to detect and that can have significant influences on the results (Loch and Bea, 1995).

Despite their complexity and high demand on expertise, time and cost, Level 4 analysis procedures are the best we know to analytically assess the structural integrity of offshore platforms. The question is how to efficiently use the state-of-the-art tools that are available and to verify their results.

2.3 Other Related Issues

Assessment of environmental loadings on and ultimate capacities of existing offshore platforms are two important steps involved in an overall risk management scheme but not the only steps. Comprehensive risk management programs for offshore platforms are proposed and described by Bea and Smith (1987), Bea et al. (1988), and Aggarwal (1991). They view the risk management program as "a structured approach to efficiently solve the problem of maintaining a platform in a fit-for-purpose state over its remaining life to safely and economically perform the originally planned or modified operations". These programs, in general, address the following steps in the process of risk management: a) risk identification, b) risk assessment, c) risk evaluation d) risk mitigation and e) risk maintenance. Risk identification requires implementation of a periodic survey and inspection program and maintenance of records. Risk assessment requires not only the determination of likelihoods of failure but also the consequences of failure. Risk mitigation involves identification and selection of suitable techniques to reduce the risk level associated with a structure. Risk maintenance involves implementing the selected risk mitigation measures and making a decision on the period for implementation of the next risk management cycle.

Although not directly the subject of this research, the issues of inspections, data management, risk evaluation, and risk mitigation are summarized and briefly discussed for the sake of completeness in the following sections.

2.3.1 Inspections and Condition Surveys

Before any structural models can be built and any valid analyses can be performed, the existing condition of the structure has to be determined. The candidate structures need to be inspected with the objective of identifying and quantifying all sources of deviation of the platforms' condition from the original design drawings. These include missing members, damaged members (bent, dented, corroded, fatigue cracked), misalignments and imperfections, marine growth, cathodic protection, and scour around foundation piles. Underwater inspections are extremely expensive to perform. Premature failure of a structure, on the other hand, can have significant consequences. These facts underline the need for an efficient and optimized inspection methodology. The questions are: What should be inspected and how? What should be the level and frequency of inspection? What should the inspection report contain?

It is crucial that the individual responsible for inspection planning has full understanding of the history of the structure in terms of design criteria, fabrication and installation processes, operational activities and loadings, and past exposure. This individual should also be highly familiar with inspection methods, tools, and processes. In establishing the level and frequency of inspections, the following factors need to be considered (Hennegan et al., 1993): a) robustness of the structure, b) fabrication and construction practice (e.g. welding techniques used), c) quality control during fabrication and construction, d) cathodic protection history, e) experience with other structures at the same location, f)

consequence of failure, g) age of the structure, h) location, and i) past inspection results. The final output of the inspection process should include all data necessary to build a realistic structural model for further analyses and evaluations.

2.3.2 Data Management

A significant amount and wide range of information and data are needed for and produced during the process of platform requalification. The efficiency of the process strongly depends on how the data and information are collected, preserved, and retrieved when and where they are needed. This information includes data on inspection and monitoring, maintenance, repairs and modifications, design, material characteristics, fabrication, installation, accidents, field performance observations, and different levels of risk analysis including likelihoods and consequences of failure. At the present time, there are no comprehensive information management and data processing systems available in the offshore industry which address these needs.

Today, the tools and techniques used to capture and store inspection and condition survey data vary considerably in degree of sophistication from manual sketches to electronic devices and computers. The trend is to capture most of the data in electronic format. Real time capture and entry of data is already being used in some cases (e.g. cathodic potential readings using video tapes). Object oriented databases are likely to be employed in the next future. Information gathered during design, fabrication and installation can be crucial to assessment of an existing platform and lead to enormous savings in cost and time.

Indeed, requalification programs should be a design consideration. The design information that need to be collected and preserved include design basis and report, analytical models and analysis results, material characteristics, weld procedures and as-built drawings (Billington, et al., 1993b). The information gathered during installation and construction can be most useful to reassess the foundation integrity. Based on this data, design assumptions can be updated and the foundation model modified if necessary.

The preceding were some examples of how and where an efficient information management system could enhance the platform requalification process. Development of a comprehensive Information Management System (IMS) as a decision support tool is the subject of present research at University of California at Berkeley. The goal of this research is "to develop a computerized information system for the management of engineering analyses in the screening of large numbers of structures, supporting engineers and decision makers in the corporate and regulatory environment". IMS is intended to provide engineers and managers with information on various engineering analyses performed in the framework of an overall reassessment process (Staneff, et al., 1995).

2.3.3 Risk Evaluation

So far in the process of platform assessment and requalification, the focus has been on problems associated with the assessment of failure probability. To requalify a platform, or to determine whether a platform is fit for purpose, potential consequences of failure need also to be assessed. Total risk can be determined as the product of likelihood and

consequence of failure. Given the notional (or calculated) risk is determined, requalification guidelines and acceptance criteria are needed to evaluate the risk and determine whether a platform is fit for purpose. Risk is a fact of life and as such unavoidable. The challenge is to manage (identify, assess, evaluate, mitigate, maintain) the risk. In the following, some of the key issues related to risk evaluation are addressed.

The fundamental question is: how safe is safe enough? Clearly, this is a subjective question to which different parties with different interests and risk attitudes would give different answers. The logical next question that arises is: who determines the acceptable level of risk and how? In answering and discussing these questions the following facts need to be considered (Wenk et al., 1993):

a)   According to U.S. and international law, offshore oil and gas resources are considered a common property resource that must be managed by federal and state governments as a public trust.

b)   In United States and some other countries, the private sector has been exploring and developing these resources motivated by free market incentives.

Clearly, there are conflicting interests at stake; those of private and public sectors: profit focused priorities determined by economic imperatives of the market versus public expectations and societal intolerance for loss of life and environmental pollution. Obviously, private and public sectors have to work together and reach consensus on acceptable levels of safety.

Over decades, two fundamental approaches have evolved to develop judgments concerning acceptable probabilities of failure: utility evaluations and experience evaluations (Bea, 1990). Utility evaluation approach is based on resource optimization (e.g. total cost minimization). Based on this approach, optimal reliability measures are derived which are then used as risk evaluation criteria. Figure 2.3 shows an example where the utility is measured in monetary terms. Optimal probabilities of loss of serviceability are determined by minimizing the total costs. The utility evaluation approach is not based strictly on monetary terms. This is an advantage since in some cases it is difficult to incorporate the intangible consequences in monetary terms such as fatalities and environmental impact. In such cases, in addition to possible consequences, the decision maker's preference plays a roll. Based on utility evaluations, sensitivity analyses can be performed. Such analyses provide useful insight into how the utility of a development alternative changes if the input variables are changed (e.g. consequences, likelihoods, preferences). In fact the result can be treated as a random variable for which complete probability distributions can be developed.

The experience evaluation approach uses risk acceptance criteria (or tolerable risk) that is indirectly defined by the society through experience and over time. In Figure 2.4 annual probabilities of failure are plotted against consequences associated with the failure of various engineered structures in terms of number of fatalities and actual costs. The lines indicating the acceptability of risk are based on research evaluations on how the public and industries have historically accepted the risk of failures. This approach is based on

42
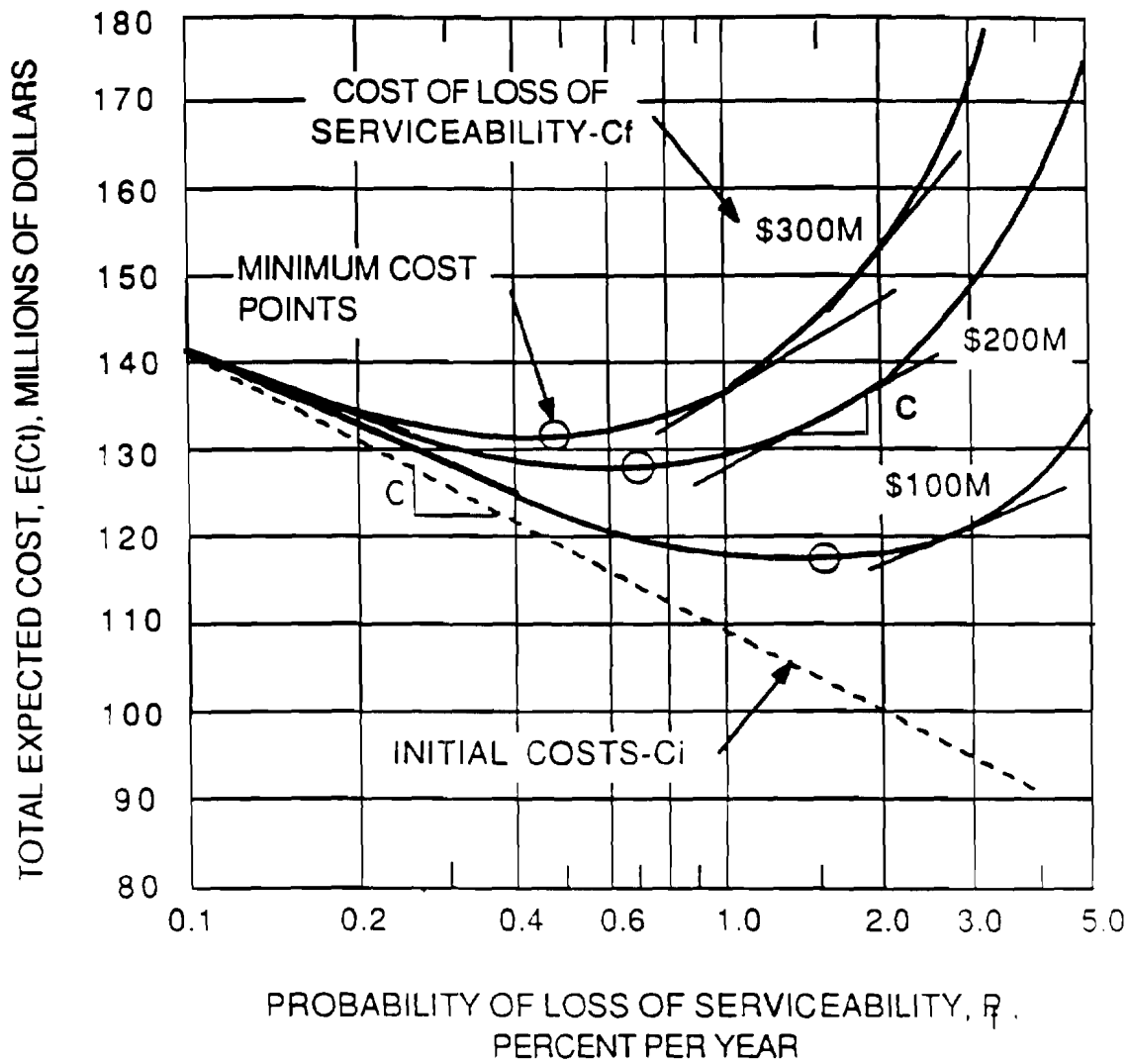
Figure 2.3: Optimized Utility-Cost-Benefit Evaluations (Bea, 1990)
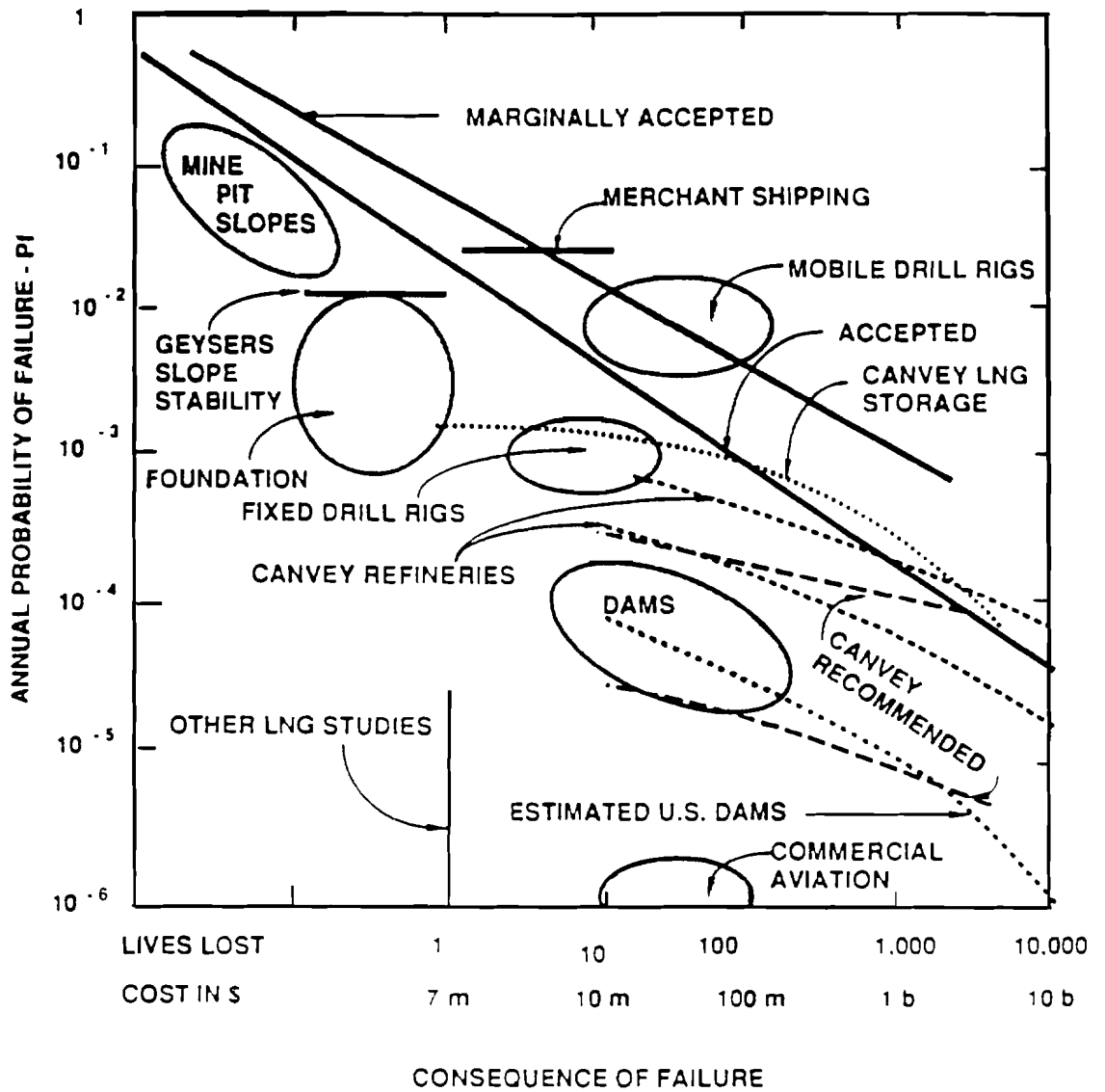
Figure 2.4: Historical Relationship of Risks and Consequences for Engineered Structures (Bea, 1990)

historical data. For example, the safety margins defined in the design codes are empirical and based on experience and lessons learnt by failures in the past. The actual level of safety of a structure designed to these codes can be regarded as acceptable to society. The following disadvantages are associated with the experience evaluation approach:

a)   The notional risks are not always consistent with actuarial risks.

b)   In some cases the historical risks are based on a limited set of data which include mixed populations (e.g. different causes and consequences).

c)   In general, acceptable risk is a function of time. Risk levels that have been accepted in the past may not be adequate for present or future.

These two approaches are thought to be complimentary and should be both used to develop judgment concerning acceptable levels of risk (Bea, 1990).

2.3.4   Risk Mitigation

Given that a platform does not pass any of the screening levels, it is not fit for purpose. In such a case, the alternative options are to mitigate the risk and make the platform fit for purpose or to decommission it. There are principally two measures of risk mitigation:

1)   reduce likelihood of failure by reducing loads and/or increasing capacities, and

2)   reduce consequence of failure.

In the case of a probabilistic risk assessment, a third measure of risk mitigation is to reduce the uncertainties associated with loads and capacities. Load reduction can be

achieved by removing equipment from lower decks to higher elevations, removing unnecessary appurtenances such as boat landings and unused conductors, elevating the platform decks, etc. Upgrading the strength of a structure can be costly and hence should be carefully planned and evaluated. Measures of strengthening include grinding, grout-filling, welding, clamping, use of adhesives for the superstructure and jacket upgrading and adding insert piles or "outrigger" piles for upgrading the pile foundations. The consequences of failure can be grouped into three categories: a) loss of life, b) environmental pollution, and c) loss of resources, property and production. The following are some measures of reducing the consequence of failure (Billington, et al., 1993a):

a) increase the life safety by de-manning before extreme effects or permanently,

b) reduce the environmental consequence by using safety shutdown valves and/or removing oil storage from platform, and

c) minimize the economical consequence by moving key facilities and equipment to other platforms and/or redrilling at other locations.

In the case of probabilistic risk assessment, the statistical and modeling uncertainties associated with environmental loadings and foundation capacities can be reduced by installing instruments and collecting more data.

CHAPTER 3

ENVIRONMENTAL LOADS

3.1   Introduction

One important step in designing a new or assessing an existing offshore platform is to

determine the environmental loads acting on the structure. In general, these loads are due

to wind, waves, currents, earthquakes, ice and subsea mudslides. This research primarily

focuses on wind, wave, and current loads.

Due to complexity and random nature of these loads, it is difficult, if not impossible, to

develop theoretical models that accurately predict these loads and their effects on offshore

structures. This is why offshore engineering research has traditionally used field

measurements and laboratory experiments to calibrate existing loading models. The

Conoco Test Structure (Bea et al., 1986) and the Ocean Test Structure (Haring et al.,

1979) are two example platforms highly instrumented for the purpose of measuring wind

and wave forces on offshore structures.

Traditionally two different approaches have been utilized to predict the hydrodynamic

loads on offshore installations; deterministic and stochastic (Bea and Lai, 1978). The

deterministic approach itself can be pseudo-static or time-dependent. The pseudo-static

deterministic approach uses the wave kinematics which result in maximum loads. These

loads are then used to perform static structural analyses. In the time-dependent

deterministic approach, loads are calculated as a function of time and used to perform dynamic structural analyses. The stochastic approach treats the loading as a random process where the loading condition is described by spectral densities. Figure 3.1 summarizes these approaches and the major steps involved in each approach. The different methods are used to perform different types of analyses from static pushover for extreme conditions to fatigue analyses for nominal conditions.

To develop understanding and formulate the current and wave forces on offshore platforms two areas of fundamental research need to be addressed; a) fluid mechanics of steady and unsteady flows passing a body and b) fluid motion in a wave described by a wave theory (Sarpkaya and Isaacson, 1981). For an overview of historical developments in the subject of hydrodynamic loads on offshore structures and a more detailed treatment of the subject, refer to Sarpkaya and Isaacson (1981).

The purpose of this research is to develop a simple procedure that helps determining the aerodynamic and hydrodynamic loads acting on an offshore platform. In the following sections, wind loads are formulated and discussed first. The fluid mechanics background that is necessary to develop a simplified load calculation approach is also discussed. Finally, a simplified load model is introduced that uses an idealized structure and Stokes fifth-order wave theory to predict the wave loads acting on offshore platforms. This load model is verified with results from more sophisticated current and wave load generating programs commonly used in industry.

DETERMINISTIC Pseudo-Static	DETERMINISTIC Time-Dependent	STOCHASTIC
Wave Records	Wave Height Spectrum	Wave Height Spectrum
Design Wave	Multi-Harmonic Sea State Simulation	Hydrodynamic Energy Spectral Density
Time-Independent Hydrodynamic Forces	Time-Dependent Hydrodynamic Forces	Response Displacement Spectral Density
Time-Independent Displacements	Time-Dependent Displacements	RMS Displacements
Time-Independent Shears & Moments	Time-Dependent Shears & Moments	RMS Shears & Moments

Figure 3.1: Alternative Procedures to Wave Loading Analysis (Bea and Lai, 1978)

3.2   Aerodynamic Loads

Wind forces acting on the exposed portions of offshore platforms are in general not as significant as the wave forces acting on these structures. However, their effect has to be included in the global and particularly in the local structural analyses of the deck structure and the topside facilities and equipment tie-downs. Wind forces are generally composed of two components: a sustained (or steady) component averaged over a longer period of time (usually over one minute) and a gust (or fluctuating) component averaged over a shorter period of time (usually less than one minute). Sustained wind velocities are used to analyze the global platform behavior and gust velocities are used to analyze the local member behavior. In case of dynamically sensitive structures such as compliant towers or tension leg platforms, more detailed dynamic wind load analyses are necessary. In such cases, wind energy representations in form of spectral densities are utilized (Ochi et al., 1986). Typical Gulf of Mexico jacket-type platforms respond to wind forces in a static way. In this research, the dynamic aspects of wind loading are neglected.

Due to surface friction, the geostrophic wind velocity is reduced in the vicinity of ocean surface. API RP 2A (API, 1993a) gives the following approximation to the wind profile

$$u(1hr, z) = u(1hr, z_R)\left(z \big/ z_R\right)^{0.125} \tag{3.1}$$

where z_R denotes a reference height usually taken as 10 meters. Given the wind velocity, the maximum wind force, S_a, acting on the exposed decks of the platform is given as

50

$$S_a = \frac{\rho_a}{2} C_s A_d V_d^2 \qquad\qquad (3.2)$$

where ρ_a is the mass density of air, C_s the wind velocity pressure (or shape) coefficient, A_d the effective projected area of the exposed decks, and V_d the wind velocity at the deck elevation and for an appropriate time interval. The wind shape coefficient is a function of air turbulence, structure geometry and surface roughness.

3.3   Hydrodynamic Loads

To establish the hydrodynamic loads acting on an offshore platform, the following steps need to be taken: a) establish wave, current, and storm surge information based on site specific studies including recorded or hindcasted data, b) use an appropriate wave theory to describe the fluid motion and water particle kinematics, and c) use a force transfer function to determine the loads acting on platform members. In the following sections, the last two steps, b and c, are described and discussed in detail.

3.3.1   Water Particle Kinematics

3.3.1.1   Wave Theories

The problem of describing the wave motion has been dealt with for more than a century now. Numerous text books have been devoted to development of various wave theories and describing their results (refer to Sarpkaya and Isaacson, 1981, for a comprehensive list of references). All of these wave theories are based on the following common assumptions: the waves are two-dimensional and propagate in horizontal direction in waters with constant depth and a smooth bed. It is further assumed that the wave train

51
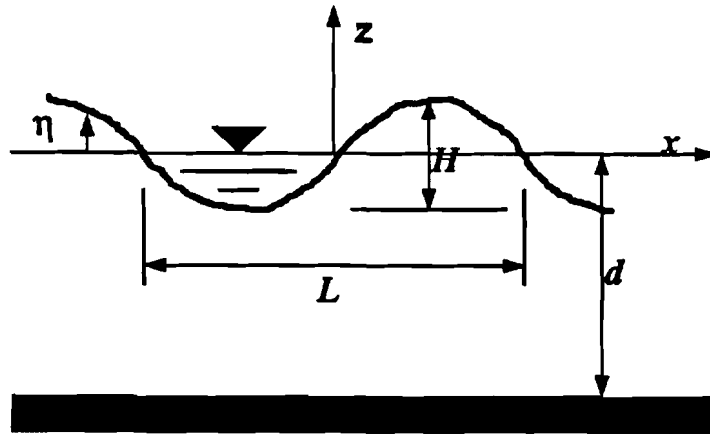
Figure 3.2: Wave Train Definition Sketch

profile does not change with time, no underlying current exist, and the water surface is tension-free (uncontaminated). Water itself is assumed to be incompressible, inviscid (ideal fluid), and irrotational. Figure 3.2 shows the definition sketch of a wave train with H, L, d, and η, denoting wave height and length, water depth and surface elevation respectively. The governing equations of wave motion can be found in any classical text book on fluid mechanics (e.g. Sarpkaya and Isaacson 1981) and are given below for the sake of completeness.

Defining a scalar function $\phi=\phi(x,z,t)$ so that the fluid velocity vector can be given by the gradient of ϕ, it can be shown that based on the assumptions stated above ϕ, the so-called velocity potential, satisfies the two-dimensional Laplace equation

$$\nabla^2 \phi = \frac{\partial^2 \phi}{\partial x^2} + \frac{\partial^2 \phi}{\partial z^2} = 0 \qquad (3.3)$$

and is subject to the following boundary conditions at water surface and seabed:

$$\frac{\partial \phi}{\partial z} = 0 \qquad\qquad \text{at } z = -d \qquad (3.4)$$

$$\frac{\partial \eta}{\partial t} + \frac{\partial \phi}{\partial x}\frac{\partial \eta}{\partial x} - \frac{\partial \phi}{\partial z} = 0 \qquad\qquad \text{at } z = \eta \qquad (3.5)$$

$$\frac{\partial \phi}{\partial t} + \frac{1}{2}\left[\left(\frac{\partial \phi}{\partial x}\right)^2 + \left(\frac{\partial \phi}{\partial z}\right)^2 \right] + g\eta = f(t) \qquad\qquad \text{at } z = \eta \qquad (3.6)$$

$$\phi(x,z,t) = \phi(x - ct, z) \qquad (3.7)$$

The boundary condition at the seabed states that the velocity vector has no component in vertical direction (Equation 3.4). The kinematic boundary condition at the water surface states that the velocity component normal to the water surface is equal to the velocity of water surface in that same direction (Equation 3.5). The dynamic boundary condition at the water surface states that the pressure along the surface is constant (equal to atmospheric pressure) (Equation 3.6). Equation (3.7) is based on the assumption of periodicity of the wave train where $c = L/T$ denotes the wave celerity.

Given the wave height, period and the water depth, the question is what shape does the wave take and how to describe the water particles motion (displacements, velocities, and accelerations) throughout the flow. In solving the governing Laplace Equation (3.3) subject to boundary conditions explained in Equations (3.4-3.6), the following problems

53

are encountered: the boundary conditions at the water surface are nonlinear and specified at a surface elevation η, which is itself unknown. The various wave theories developed in the past have tried to solve these problems with reasonable approximations. These include linear or Airy wave theory (also known as small amplitude wave theory), Stokes finite amplitude wave theories, Dean's stream function theory, and nonlinear shallow wave theories (such as Cnoidal wave theory). The question of suitability of a given wave theory for a particular application is a difficult one. One selection criteria is the amount of effort needed to produce the desired results. The more advanced the theory is, the more sophisticated the tools need to be to perform the analyses. Theoretical charts have been developed that show the ranges of best fit to the free surface boundary conditions for different wave theories (e.g. Figure 3.3). Experimental comparisons of different wave theories have not resulted in clear trends regarding the applicability of any particular wave theory (Sarpkaya and Isaacson, 1981). For the sake of simplicity and within the framework of a simplified analysis, only Airy small amplitude and Stokes finite amplitude wave theories are considered in this research.

The linear wave theory provides a first approximation of the wave motion. It is derived based on the assumption of relatively small wave heights, it is $H<<L,d$. The boundary conditions are satisfied at $z=0$. Airy wave theory is very attractive to use for many engineering applications. It is simple and does not require computer analysis. There are approximations to linear wave theory for shallow water, intermediate depth and deep water ranges (see e.g. Sarpkaya and Isaacson, 1981). A practical approximation to Airy wave theory is the "depth-stretched" linear wave theory. In this approach, the water

54
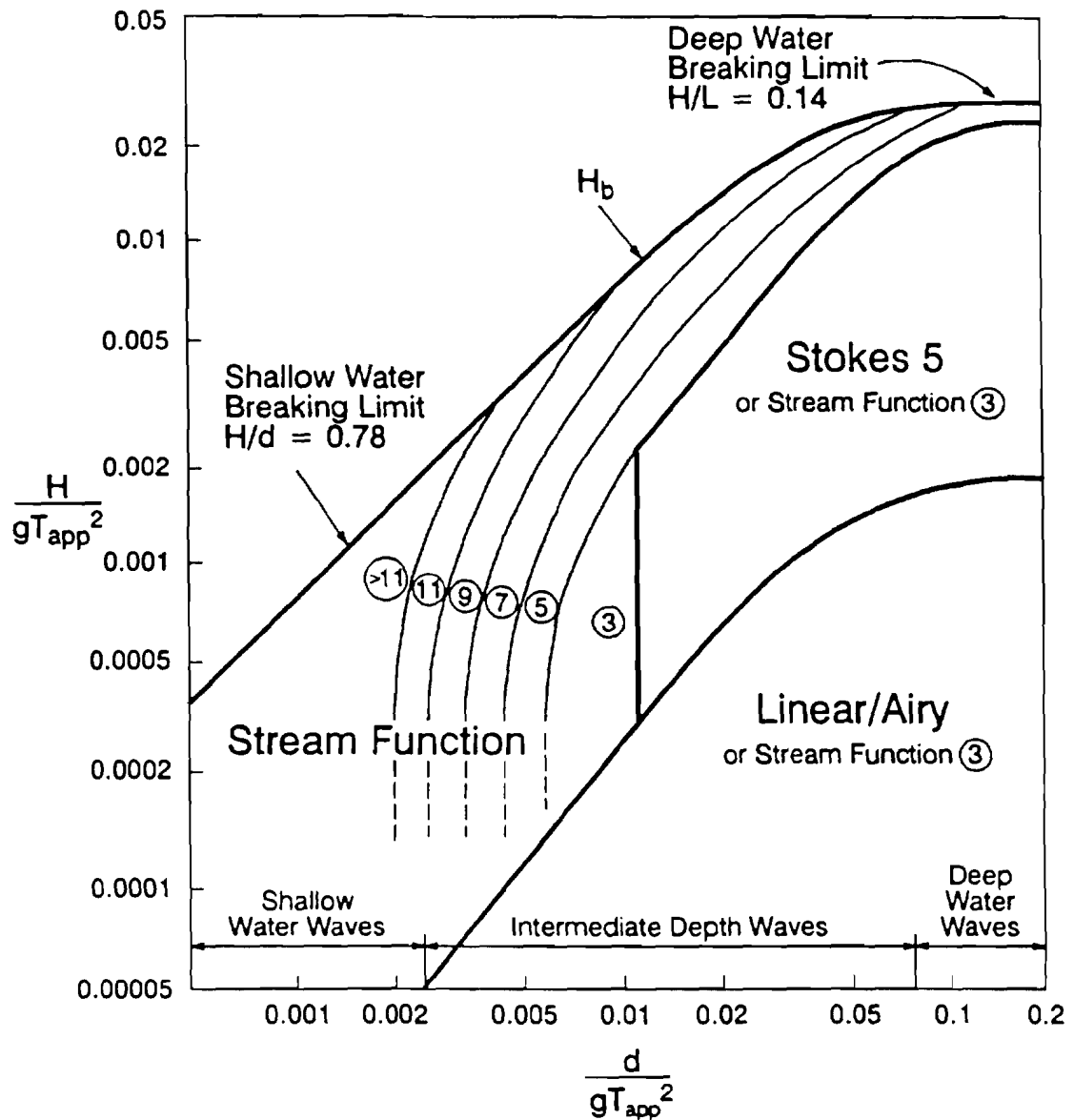
H/gT_{app}^2: Dimensionless wave steepness   d: Mean water depth
d/gT_{app}^2: Dimensionless relative depth T_{app}: Wave period
     H: Wave height   g: Acceleration of gravity
    H_b: Breaking wave height

Figure 3.3: Regions of Applicability of Stream Function, Stokes V, and Linear Wave Theory (API, 1993)

surface is "stretched" to the wave crest elevation. The water particle kinematics are estimated according to the Airy small amplitude wave theory.

Based on a perturbation method, Stokes finite amplitude wave theories attempt to solve Equation (3.3) subjected to boundary conditions explained in Equations (3.4-3.6) more closely. However, like many other wave theories, convergence conditions put numerical limitations on wave heights in certain water depths. Work by Skjelbreia and Hendrickson (1960) and Fenton (1985) on a fifth-order Stokes wave theory has found widespread interest and usage in engineering applications. Their formulations do not require extensive computer programming effort and is used in this research to develop a simplified load model.

3.3.1.2   Wave Directional Spreading

Real storm conditions include waves from multiple directions. Directional spreading of the waves reduces the loads acting on marine structures which are computed based on a two dimensional, long crested, regular wave grid propagating in a single horizontal direction. This load reduction is mainly due to change in water particle kinematics. Wave components from different directions can partially cancel each other. The effects of wave directionality have been investigated by many authors (e.g. Dean, 1977).

The detailed treatment of the subject is not within the scope of this work. In engineering practice, wave directional spreading effects are captured by a single wave kinematics

56

modification factor. The actual water particle velocity is estimated by multiplying the velocities based on a two-dimensional wave theory with the wave kinematics modification factor. Measurements indicate a range of 0.85 to 1.0 for highly directional seas during tropical storms to extra-tropical storm conditions (API, 1993a).

3.3.1.3 Currents and Current Blockage

Currents can be a major contributor to total hydrodynamic forces acting on an offshore platform. In general, currents are generated in three ways; there are tidal, circulational, and storm generated currents. Tidal currents can be important in shallow waters of continental shelves (coastal regions and inlets). The Gulf Stream in the Atlantic Ocean and the Loop Current in the Gulf of Mexico are examples for large-scale circulational currents. Winds and pressure gradients during storms are the source of storm generated currents. These currents can be roughly estimated to have surface speeds of 1-3% of the one hour sustained wind speed during storms (API, 1993a). The profile of storm generated currents is largely unknown and the subject of research.

In determining the water particle kinematics due to currents, it should be recognized that, due to existence of the structure, the current is disturbed and its speed in the vicinity of the platform differs from that in the free field. Based on experimental test data, approximate current blockage factors for typical jacket-type platforms are given in API RP 2A (API, 1993a). The actual current velocity in the vicinity of the structure is obtained by

multiplying the free field current speed with the current blockage factor. These factors range from 0.7 for end-on loading of eight-leg platforms to 0.9 for tripods (API, 1993a).

3.3.2 Wave and Current Loads

Morison, Johnson, O'Brien and Schaff (1950) proposed the following formulation for the force acting on a section of a pile due to wave motion

$$F = F_i + F_d = C_m \rho V \frac{du}{dt} + \frac{1}{2} C_d \rho A u |u| \tag{3.8}$$

This formulation is widely known as Morison equation. According to Morison et al. (1950), this force is composed of two components; an inertia component related to the acceleration of an ideal fluid around the body, F_i, and a drag component related to the steady flow of a real fluid around the body, F_d. C_m is the so-called inertia coefficient, ρ is the mass density of fluid, V is the volume of the body and du/dt is the fluid acceleration. C_d is the so-called drag coefficient, A denotes the projected area of the body normal to the flow direction, and u is the incident flow velocity relative to pile.

Vortex shedding, drag and lift forces are all phenomena observed in real (viscous) fluids due to wake formation when the fluid passes a body. These phenomena do not exist in an ideal (inviscid) fluid. They have been the subject of comprehensive research for many decades and are now well understood and described for simple, idealized cases. In such cases, numerical computations are able to simulate these phenomena with reasonable degrees of accuracy. However, these programs are not yet efficient enough to be used by engineers and designers to calculate the forces on "real" marine structures.

58

Although extremely simple, the Morison's equation has been used for many years by researchers and engineers to calculate the wave forces on "slender" marine structures. An important assumption implicit in the Morison equation is that the incident flow remains undisturbed in the vicinity of the body. This condition is satisfied when the body is small relative to the wave length. If the body is large relative to the wave length, the incident flow will not remain uniform and will be refracted due to presence of the body. In this case the refraction problem needs to be solved. For detailed treatment of the subject refer to Sarpkaya and Isaacson (1981). The refraction problem is not considered in this research since the platform dimensions are much smaller than the wave length in the extreme conditions underlying the ultimate strength analysis.

The drag and inertia coefficients in Morison equation have empirical nature and depend on many factors including flow characteristics, shape and roughness of the body and its proximity to sea floor or free surface. One important flow parameter reflecting its uniformity is Keulegan-Carpenter (KC) number which is defined as

$$ KC = \frac{UT}{D} \tag{3.9} $$

where U and T are the velocity amplitude and period of the oscillatory flow and D is the diameter of the cylinder. Reynolds number, Re, is another important parameter that characterizes the flow regime reflecting its turbulence and is defined as

$$ Re = \frac{UD}{\nu} \tag{3.10} $$

59

where v denotes the fluid viscosity. Past field tests have indicated a large scatter in the values of drag and inertia coefficients when they are plotted against either the Reynolds number or the Keulegan-Carpenter number. This scatter is largely attributable to the irregular nature of the ocean waves. Typical values for Reynolds and Keulegan-Carpenter numbers in extreme conditions are $Re > 10^6$ and $KC > 30$. For these ranges and based on experimental and field test data, mean drag and inertia coefficients are established for cylinders with smooth and rough surface (e.g. API, 1993a).

3.4   A Simplified Load Model

Based on the background developed in the previous sections, a simplified load calculation model is developed and discussed in the following. Wave, current and wind forces are considered. In the case of wave loading, only the drag force component of Morison equation is estimated. Due to 90 degree phase angle difference between the maximum drag and inertia force components and the relatively small dimensions of a typical jacket-type platform with respect to wave lengths and heights in an extreme condition, at the time the drag forces acting on the platform reach a maximum value the inertia forces are relatively small and hence neglected in this work.

Wave horizontal velocities are based on Stokes fifth-order theory. Using equations given by Skjelbreia and Hendrickson (1961) and Fenton (1985), a computer program was developed to determine the wave kinematics (Preston, 1994). Given the wave height H,

period T and water depth d, the vertical profile of maximum horizontal velocities beneath the wave crest is given as

$$u = K_{ds} c \sum_{n=1}^{s} n \phi_n' \cosh(nks)$$ (3.11)

where K_{ds} is a coefficient that recognizes the effects of directional spreading and wave irregularity on the Stokes wave theory based velocities. k is the wave number and s is the vertical coordinate counting positive upward from the sea floor. c is the wave celerity and given by

$$\frac{c^2}{gd} = \frac{\tanh(kd)}{kd} \left[1 + \lambda^2 C_1 + \lambda^4 C_2 \right]$$ (3.12)

The crest elevation η is estimated by

$$k\eta = \sum_{n=1}^{s} \eta_n'$$ (3.13)

ϕ_n' and η_n' are given functions of λ and kd. C_n are known functions of kd only and given by Skjelbreia and Hendrickson (1961). The wave number k is obtained by implicitly solving the following equation given by Fenton (1985)

$$\frac{2\pi}{T(gk)^{0.5}} - C_0 - \left(\frac{kH}{2} \right)^2 C_1 - \left(\frac{kH}{2} \right)^4 C_4 = 0$$ (3.14)

The parameter λ is then calculated using the equation given by Skjelbreia and Hendrickson (1961)

$$\frac{2\pi d}{gT^2} = \frac{d}{L} \tanh(kd) \left[1 + \lambda^2 C_1 + \lambda^4 C_2 \right]$$ (3.15)

Having the parameters λ and *kd*, Equations (3.11) and (3.13) can be used to estimate the horizontal water particle velocities and the wave crest elevation. The specified variation of current velocities with depth is stretched to the wave crest and modified to recognize the effects of structure blockage on the currents. The total horizontal water particle velocities are taken as the sum of the wave horizontal velocities and the current velocities.

The maximum drag force acting on the portions of structure below the wave crest is based on the fluid velocity pressure

$$F_d = \frac{1}{2} C_d \rho A u |u|$$
(3.16)

where ρ is the mass density of water, *A* the effective vertical projected area of the exposed structure element, and *u* the horizontal velocity of water at a given point on the submerged portion of the structure element.

All of the structure elements are modeled as equivalent vertical cylinders that are located at the wave crest (Figure 3.4). Appurtenances (boat landings, risers) are modeled in a similar manner. For inclined members, the effective vertical projected area is determined by multiplying the product of member length and diameter by the cube of the cosine of its angle with the horizontal.

For wave crest elevations that reach the lower decks, the horizontal hydrodynamic forces acting on the lower decks are computed based on the projected area of the portions of the
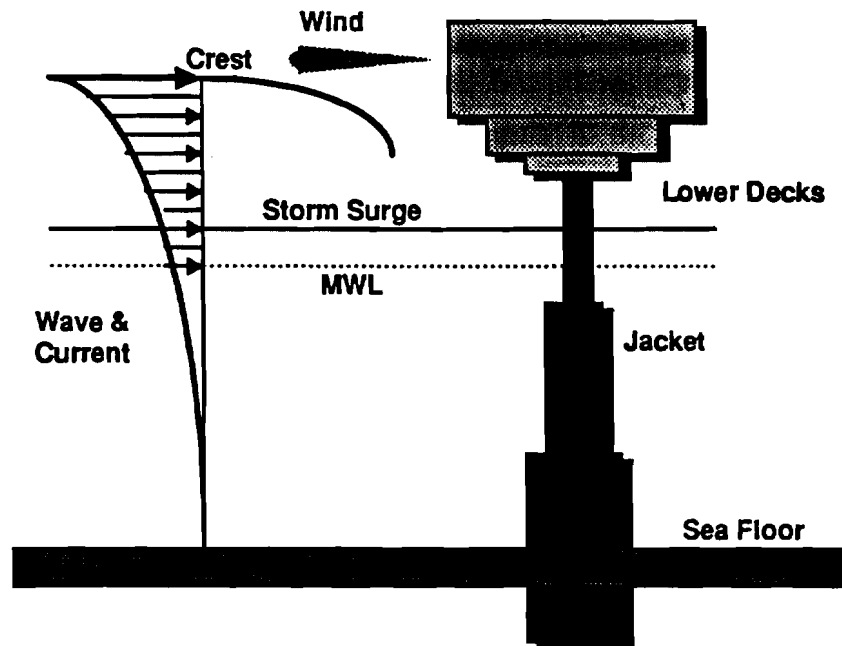
Figure 3.4: Simplified Load Model

structure that would be able to withstand the high pressures. The fluid velocities and pressures are calculated in the same manner as for the other submerged portions of the structure with the exception of the definition of C_d. In recognition of rectangular shapes of the structural members in the decks a higher C_d is taken. This value is assumed to be developed at a depth equal to two velocity heads (U^2/g) below the wave crest. In recognition of the near wave surface flow distortion effects, C_d is assumed to vary linearly from its value at two velocity heads below the wave crest to zero at the wave crest. (McDonald et al., 1990; Bea and DesRoches, 1993).

3.5 Verification of the Simplified Load Model

The procedure used to estimate the wave forces acting on jacket structures has been verified and calibrated against results from more sophisticated computer programs. In an initial verification effort, the computer output for four design wave cases on single surface piercing cylindrical piles were used. These data were produced during an analytical wave force study conducted by Exxon and Shell Research Companies and documented by Bea (1973). In this study, the maximum wave force acting on a 3 ft diameter surface piercing cylinder was estimated where nondimensional water depths d/gT^2 ranged from 0.022 to 0.146. Based on the simplified procedure developed in the previous sections of this chapter, the maximum wave force acting the same cylinder is also estimated using Stokes fifth-order and depth stretched linear wave theories. A drag coefficient of C_d=0.6 is used in all cases. The results are also compared to those gained by using Dean's Charts that are developed based on ninth-order stream function theory (Dean, 1973). The results are summarized in Figures 3.5- 3.8.

Figure 3.5 shows the results for deep water conditions. Stokes V results in an estimate of base shear that is in good agreement with results reported in Exxon-Shell wave force study. Dean's Charts slightly underpredict the total force. Surprising is the result gained by using depth-stretched linear wave theory, which gives a base shear that is almost 40% less than that given by Stokes V. Figures 3.6 and 3.7 show the results for deep to intermediate water depths. Again, it can be seen that Stokes V results are in good agreement with those reported in Exxon-Shell study. Depth-stretched linear wave theory underpredicts the base

shear by 40% to 50%. Dean's Charts result in total forces that are also close to those gained by using Stokes V. Figure 3.8 shows the results for intermediate to shallow water conditions. Stokes V base shear is about 10% to 15% larger than the base shear predicted by Exxon-Shell study and that gained by using Dean's Charts. In this case, Airy wave based prediction makes up only 20% of Stokes V results.

Field measurements in intermediate water depths indicate that depth-stretched Airy theory provides an acceptable fit to the actual wave kinematics. With this in mind, the results plotted in Figures 3.5-3.8 indicate that wave force predictions based on finite amplitude wave theories (Stokes V or stream function) might be conservatively biased. Biases and uncertainties associated with wave force predictions are discussed in Chapter 5.

Based on the results of this initial verification case study, Stokes fifth-order theory was used in this research. A second comprehensive verification effort was also performed using analytical models of actual Gulf of Mexico Platforms. This second set of verification case studies are documented and discussed in Chapter 6.

3.6 Summary

A simplified environmental loading model is developed in this chapter that is able to predict estimates of total lateral wind, wave and current loadings acting on jacket-type offshore platforms. Based on sustained wind velocity at a reference height, wind forces are estimated according to API RP 2A (API, 1993a). The wave loading prediction model

utilizes Stokes fifth-order wave theory. The current velocity profile is added to the wave velocity profile. Wave directional spreading and current blockage are taken into account. The hydrodynamic drag force acting on a simplified model of the structure is estimated using the drag force component in the Morison's equation.

The simplified load prediction procedure was verified with results reported in a wave force study performed by Exxon and Shell Research Companies (Bea, 1973). Good agreement has been achieved for wave loading on a surface piercing cylinder in deep water and transitional water depth conditions using Stokes V theory. In water depths close to shallow water conditions, the simplified procedure tends to slightly overpredict the base shear. For the studied cases, the depth-stretched linear wave theory substantially underpredicted the forces and was hence not used in this research.

Verification studies have also been performed on actual platforms. The results are documented in Chapter 6 of this report. Using Stokes fifth-order theory, the results indicated an overprediction of total base shear of about 10% in average compared to results gained from a sophisticated three dimensional wave loading program, WAJAC (DNV, 1993). The reason for this overprediction is explained and discussed in Chapter 6 of this report.
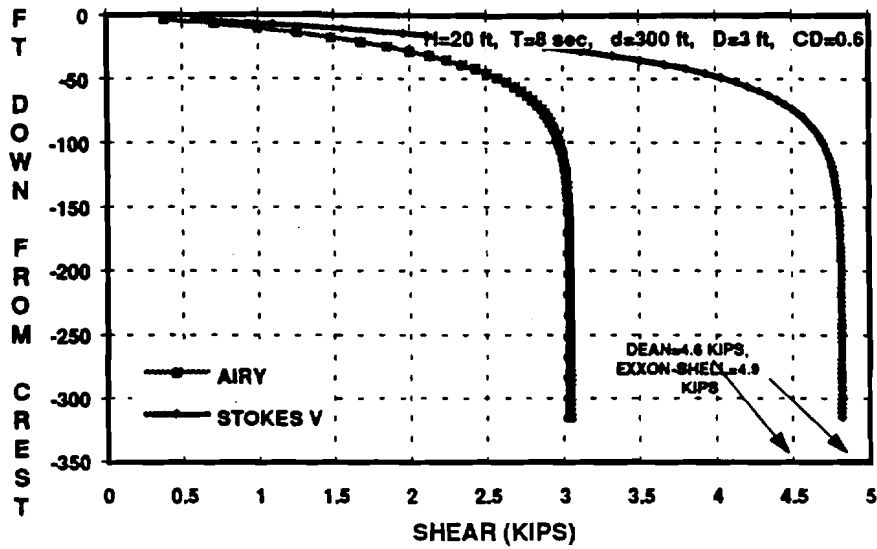
Figure 3.5: Wave Force on a Vertical Surface Piercing Cylinder in Deep Water
$(d / gT^2 = 0.146)$
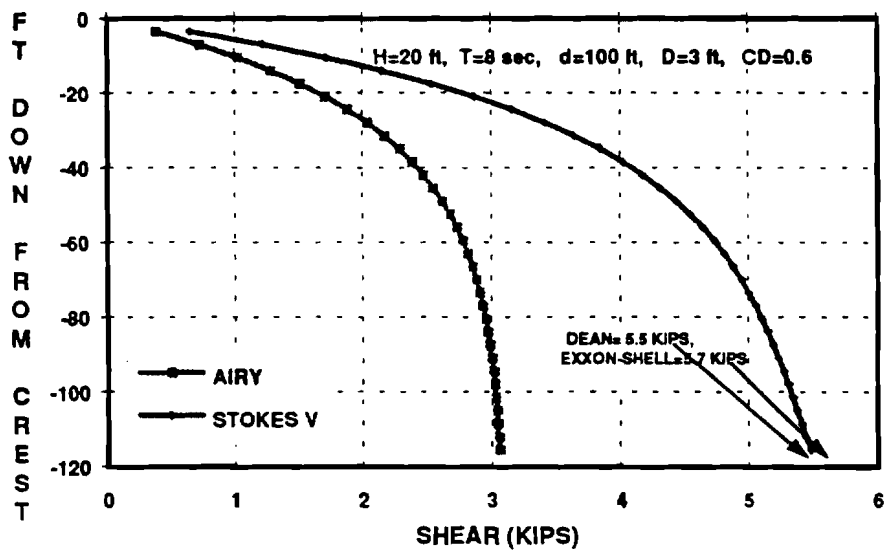
Figure 3.6: Wave Force on a Vertical Surface Piercing Cylinder in Transitional
Water Depth $(d / gT^2 = 0.049)$

67
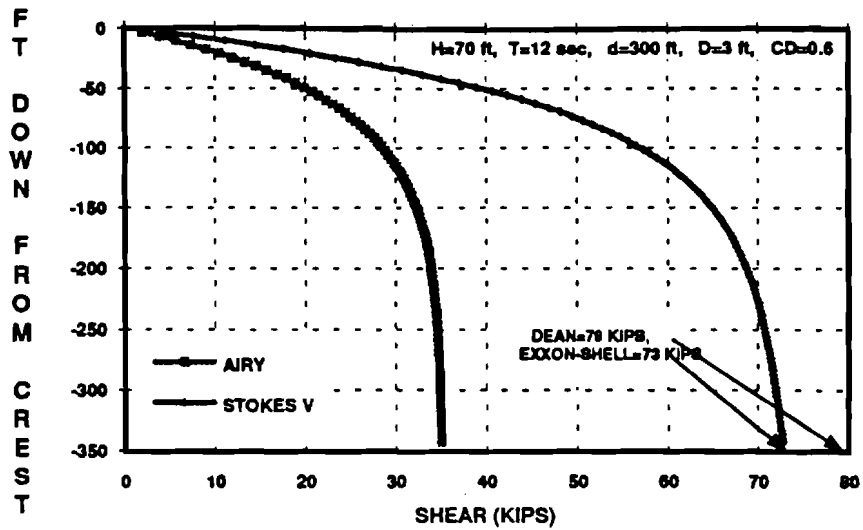
Figure 3.7: Wave Force on a Vertical Surface Piercing Cylinder in Transitional Water Depth (d / gT² = 0.065)
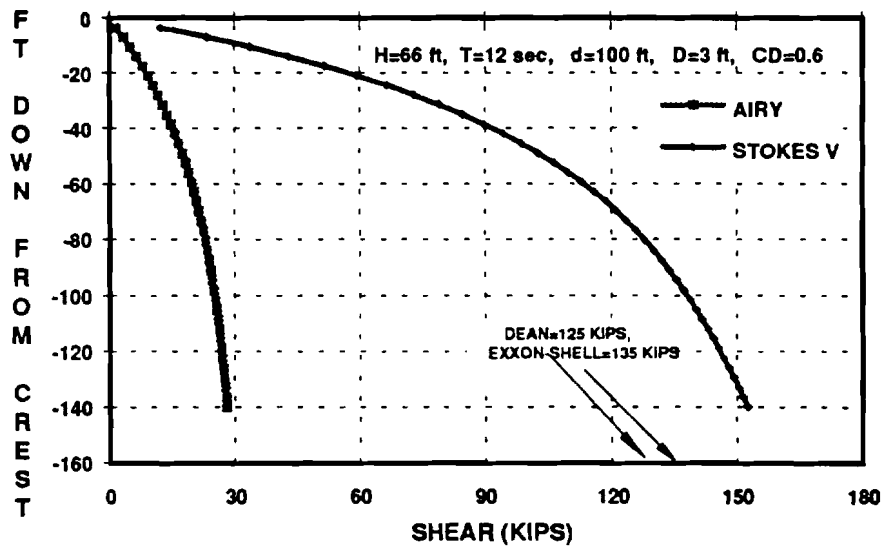
Figure 3.8: Wave Force on a Vertical Surface Piercing Cylinder in Transitional Water Depth (d / gT² = 0.022)

68

CHAPTER 4

ULTIMATE STRENGTH OF PLATFORM COMPONENTS

4.1 Introduction

The development of simplified element and component capacity estimation procedures used to predict the ultimate lateral loading capacity of a platform system are described in this chapter. Using the concept of plastic hinge theory, limit equilibrium is formulated by implementing the principle of virtual work. This is the key to the simplified ultimate limit state analysis method. Where of importance, geometric and material nonlinearities are considered. This method is being increasingly used in plastic design of simple structures or structural elements (e.g. moment frames, continuous beams). Due to the impracticality of such analyses for more complicated structures, these methods have not found broad use in design or assessment of complex structures; all possible failure modes need to be considered and evaluated to capture the "true" collapse mechanism and the associated ultimate lateral load.

Actual field experience and numerical results from three-dimensional, nonlinear analyses performed on a variety of template-type platforms indicate that in most cases certain failure modes govern the ultimate capacity of such platforms: a) plastic hinge formation in the deck legs and subsequent collapse of the deck portal, b) buckling of the main load carrying vertical diagonal braces in the jacket, c) lateral failure of the foundation piles due

to plastic hinge formation in the piles and plastification of foundation soil, and d) pile pullout or pile plunging due to exceedance of axial pile and soil capacities.

Within the framework of a simplified analysis and based on experience, collapse mechanisms are assumed for the three primary components that comprise a template-type platform: the deck legs, the jacket, and the pile foundation. Based on the presumed failure modes, the principle of virtual work is utilized to estimate the ultimate lateral capacity for each component. In the following sections, this process is described in detail for the primary components of a platform.

4.2   Deck Bay

The ultimate shear that can be resisted by an unbraced deck portal is estimated based on bending moment capacities of the tubular deck legs that support the upper decks. A collapse mechanism in the deck bay would form by plastic yielding of the leg sections at the top and bottom of all of the deck legs (Figure 4.1). The interaction of bending moment and axial force is taken into account. The maximum bending moment and axial force that can be developed in a tubular deck leg is limited by local buckling of leg cross-sections. The vertical dead loads of the decks are assumed to be equally shared among the deck legs. Due to relatively large axial loads (weight of the decks and topside facilities) and large relative displacements at collapse (deck bay drift), P-Δ effect plays a role in reducing the lateral shear capacity and hence is taken into account.
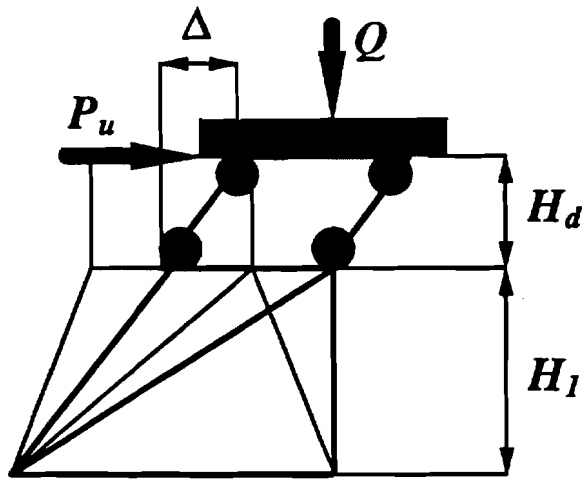
Figure 4.1 : Deck Portal at Ultimate Lateral Load

4.2.1 Deck Bay Drift at Collapse

To derive an estimate of P-Δ effect with out leaving the framework of a simplified analysis, simplifying assumptions are made. It is assumed that the deck structure is rigid. It is further assumed that plastic yielding of the sections at the bottom of the deck legs occur simultaneously, following the plastic yielding of the sections at the top of the legs and hence an estimate of plastic hinge rotations to calculate the deck bay drift is unnecessary. Finally, to estimate the deck bay drift at collapse, Δ, the jacket is replaced by rotational springs at the bottom of each deck leg. The spring rotational stiffness, C_r, is approximated by applying external moments, which are equal in magnitude and have the same direction, to the top of jacket legs at the uppermost jacket bay. Assuming rigid horizontal braces and fixed boundary conditions at the bottom of these jacket legs, the rotation of cross-sections at the top of the legs and hence the rotational stiffness, C_r, is determined

$$\frac{1}{C_r} = \frac{H_1}{E I_1 \cos \beta} \left(1 - \frac{3 C_s H_1^3}{4 C_s H_1^3 + 12 E I_1 \cos \beta} \right) \qquad (4.1)$$

where C_s is an equivalent lateral stiffness coefficient

$$C_s = \frac{1}{2} \sum_i \frac{\cos^2 \theta_i E_i A_i}{L_i} \qquad (4.2)$$

summed over all diagonal braces within the uppermost jacket bay. I_1 and H_1 denote the moment of inertia of the jacket leg and the first jacket bay height respectively. E is the Young modulus, β and θ are the batter angle of the jacket legs and vertical diagonal braces respectively.

The principle of virtual force is implemented to calculate the deck bay horizontal drift at collapse

$$\Delta = M_u H_d \left(\frac{H_d}{6 E I_d} + \frac{1}{C_r} \right) \qquad (4.3)$$

H_d and I_d are the height and moment of inertia of the deck legs. M_u is the ultimate moment that can be resisted by the cross-section in the presence of axial load and can be derived from the M-P interaction equation for tubular cross-sections

$$M_u = M_{cr} \cos\left(\frac{\pi}{2} \frac{Q / n}{P_{crl}} \right) \qquad (4.4)$$

M_{cr} and P_{crl} denote the critical moment and axial load associated with local buckling of the tubular cross-section. Q denotes the total vertical deck load and n is the number of supporting deck legs.

72

4.2.2 Deck Legs Lateral Shear Strength

Using the formulation developed above for the deck bay drift at collapse, the lateral shear capacity of the deck portal can be estimated. Equilibrium is formulated using the principle of virtual displacement. Using the actual collapse mechanism as the virtually imposed displacement, the equilibrium equation for the lateral shear capacity of the unbraced deck portal is derived including the second-order P-Δ effect

$$P_u = \frac{1}{H_d}(2n\,M_u - Q\Delta) \tag{4.5}$$

4.3 Jacket Bays

The shear capacity of each of the bays of vertical bracing that comprise the jacket is estimated including the tensile and compressive capacity of the diagonal braces and the associated joint capacities. The capacity of a given brace is taken as the minimum of the capacity of the brace or the capacity of either its joints. The batter component of axial force in the jacket legs and piles inside the jacket legs are taken into account. Where of significance, the shear forces in the legs and piles are also considered.

4.3.1 Ultimate Axial Strength of Tubular Braces

The diagonal braces near the free surface are exposed to high combined bending moments and axial forces. In general, the existing bending moment result in a reduction of the ultimate axial load capacity of the brace. At the ultimate state, the large deflections result
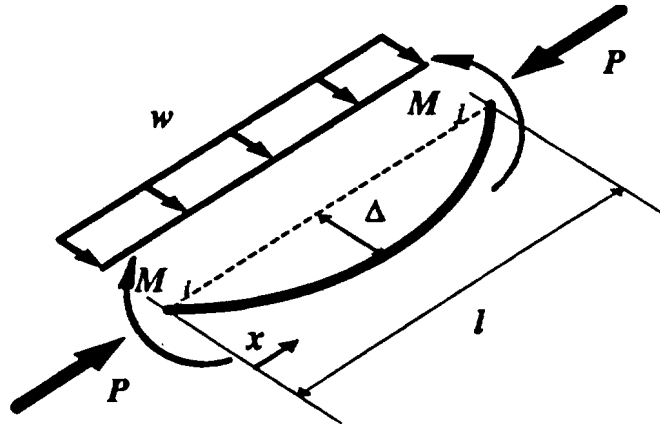
Figure 4.2: Brace Element Under Compressive and Transverse Loading

in inelastic strains. Generally an elastic-plastic load deflection $(P\text{-}\delta)$ analysis should be performed to determine the ultimate strength of the brace. The braces are treated as though there are no net hydrostatic pressures (e.g. flooded members). The governing differential equation of the beam-column can be given as

$$M_{xx} + \frac{P}{EI} M = -w - 8P \frac{\Delta_o}{l^2}$$
(4.6)

where M_{xx} stands for the second derivative of bending moment with regard to the coordinate x (Figure 4.2). Δ_o, P, and l are the initial out-of-straightness, axial force and unbraced length of the member respectively. The following substitutions

$$\xi = \frac{x}{l} \quad , \quad \varepsilon = l\sqrt{\frac{P}{EI}}$$
(4.7) , (4.8)

result in the transformed differential equation

$$M_{\xi\xi} + \varepsilon^2 M = -w l^2 - 8 P \Delta_o$$
(4.9)

which has the following closed-form solution

74

$$M(\xi) = \frac{\sin\varepsilon(1-\xi)}{\sin\varepsilon} M(\xi=0) + \frac{\sin\varepsilon\xi}{\sin\varepsilon} M(\xi=1) + \frac{1}{\varepsilon^2}\left(\frac{\cos\varepsilon(0.5-\xi)}{\cos\frac{\varepsilon}{2}} - 1\right)\left(w\,l^2 + 8P\,\Delta_o\right)$$

(4.10)

Based on a three-hinge failure mode, the exact solution of the second-order differential equation for the bending moment of a beam-column (Equation 4.10) is implemented to formulate the equilibrium at collapse

$$M(\xi=0.5) = -M(\xi=0) = -M(\xi=1) = M_u$$

(4.11)

$$M_u = \left(\frac{1}{1 + 2\frac{\sin 0.5\varepsilon}{\sin\varepsilon}}\right)\frac{1}{\varepsilon^2}\left(\frac{1}{\cos\frac{\varepsilon}{2}} - 1\right)\left(w\,l^2 + 8\,P_u\Delta_o\right)$$

(4.12)

Elastic-perfectly plastic material behavior is assumed. The ultimate compression capacity is reached when full plastification of the cross-sections at the member ends and mid-span occur (Figure 4.3). It is further assumed that plastic hinges at member ends form first followed by plastic hinge formation at mid-span. M-P interaction condition for tubular cross-sections provides a second equation for the unknown ultimate moment M_u and axial force P_u in plastic hinges at collapse

$$\frac{M_u}{M_p} - \cos\left(\frac{\pi}{2}\frac{P_u}{P_p}\right) = 0$$

(4.13)
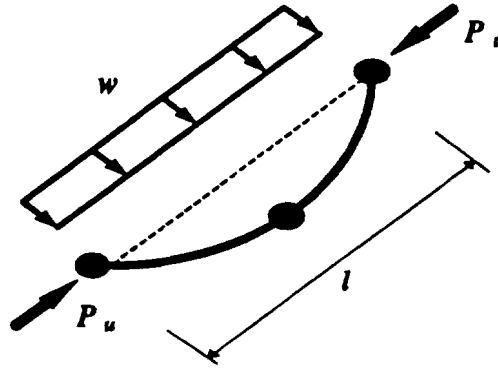
Figure 4.3: Three Hinge Failure Mode for Diagonal Braces

The results have been verified with results from the nonlinear finite element program USFOS (Sintef, 1994); using the same initial out-of-straightness, Δ_0, for both simplified and complex analyses, the axial compression capacity of several critical diagonal members of different structures has been estimated. The simplified method slightly overpredicts the axial capacity of compression members (less than 10%). The initial out-of-straightness, Δ_0, is used to calibrate the axial compression capacity of braces to the column buckling curves according to API RP 2A-LRFD (API, 1993b)

$$\Delta_0 = \frac{M_p \cos\left(\frac{\pi}{2}\frac{P_{cr}}{P_p}\right)}{\left(\frac{1}{1+2\frac{\sin 0.5\varepsilon}{\sin\varepsilon}}\right)\frac{1}{\varepsilon^2}\left(\frac{1}{\cos\frac{\varepsilon}{2}}-1\right)(8\,P_{cr})}$$

(4.14)

where P_{cr} is the buckling load of a given brace according to API RP 2A-LRFD. Using appropriate buckling length factors, the calibrated results are in close agreement with results from USFOS (Hellan et al., 1994).

4.3.2 Ultimate Strength of Tubular Joints

Because of their favorable drag characteristics, cross-sectional symmetry and the ability to provide buoyancy, tubular members are widely used in offshore structures. The stress analysis of their welded connections, often referred to as tubular joints, and the theoretical prediction of their ultimate strength has proven to be difficult. Elastic stress analysis of different joint types and geometries can be performed using a range of analytical approaches from shell theory to finite element analyses. The following parameters have a significant influence on the capacity of a tubular joint (Marshall, 1986):

a)   Chord yield strength (f_y),

b)   chord radius to thickness ratio (γ),

c)   type of load (axial tension, axial compression),

d)   load pattern (type of joint : K, Y, T, DT, X),

e)   geometric parameters (diameter ratio, ratio of gap between braces in a K-joint to brace diameter), and

f)   existing load in chord.

Experience has shown that tubular connections have a high plastic reserve strength beyond first yield, which can not be addressed by conventional linear elastic methods. Hence,

empirical capacity equations based on test results have been used to predict the joint

ultimate strength. Based on a data base of 137 tests of tubular joints, Yura et al. (1980)

recommended one formula for both compressive and tensile ultimate capacity in the

branch of a K-joint. This formula is identical to that for T and Y joints except for the

additional gap factor. The test capacity was taken as the lowest of the loads at first crack,

at an excessive deformation, or at first yield. For simple tubular joints with no gussets,

diaphragms, or stiffeners, the capacity equations are given in Table 4.1. The same capacity

equations are adopted by API RP 2A-LRFD (API, 1993b).

Joint Type	Tension	Compression
T , Y	$\dfrac{f_y T^2 (3.4 + 19\beta)}{\sin\Theta}$	$\dfrac{f_y T^2 (3.4 + 19\beta)}{\sin\Theta}$
DT , X	$\dfrac{f_y T^2 (3.4 + 19\beta)}{\sin\Theta}$	$\dfrac{f_y T^2 (3.4 + 13\beta)}{\sin\Theta} Q_\beta$
K	$\dfrac{f_y T^2 (3.4 + 19\beta)}{\sin\Theta} Q_g$	$\dfrac{f_y T^2 (3.4 + 19\beta)}{\sin\Theta} Q_g$

Table 4.1: Capacity Equations for Simple Tubular Joints (Yura et al., 1980)

Q_β is a factor accounting for geometry and Q_g is a gap modifying factor and are estimated

according to the following equations

$$Q_g = 1.8 - 0.1 \frac{g}{T} \qquad \text{for} \qquad \gamma \leq 20 \tag{4.15}$$

$$Q_g = 1.8 - 4 \frac{g}{D} \qquad \text{for} \qquad \gamma > 20 \tag{4.16}$$

$$Q_\beta = \frac{0.3}{\beta(1 - 0.833\beta)} \qquad \text{for} \qquad \beta > 0.6 \tag{4.17}$$

$$Q_p = 1.0 \qquad \text{for} \qquad \beta \le 0.6 \qquad\qquad (4.18)$$

g denotes the gap between branches of K-joints, $\beta = d/D$, and $\gamma = d/2T$. D, d and T are the branch and chord diameter and thickness respectively.

The capacity equations given above are known to be conservative (API, 1993b). Assessment of biases and uncertainties in ultimate strength of tubular joints is an area of current research. In addition, joint stiffness and load deflection characteristics, joint ductility, hysteretic behavior, low cycle fatigue failure and tensile fracture are other potential areas for future research in particular in the context of assessment and requalification of existing platforms. In this research, the capacity equations given in Table 4.1 are used and modified with bias factors that are based on existing test data.

4.3.3   Effect of Shear Force in Jacket Legs and Piles

Within the framework of a simplified analysis, the jacket has been treated as a trusswork. Plastic hinge formation in the jacket legs was not considered because this hinge development occurs at a lateral deformation that is much larger than is required to mobilize the axial capacities of the vertical diagonal braces. At the large lateral deformations required to mobilize the lateral shear capacities of the legs, the diagonal brace capacities have decreased significantly due to column buckling or tensile rupture. In general, the effect of bending moment distribution along the jacket legs on the lateral capacity has been neglected. This assumption is justified by the following example.
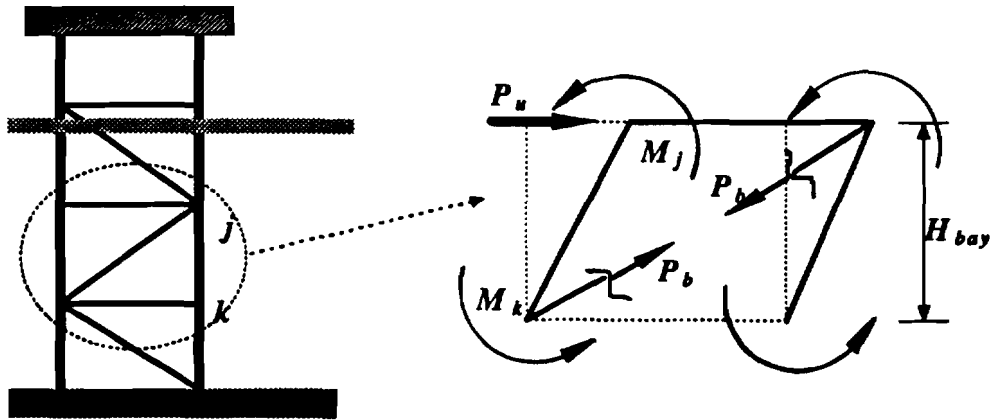
Figure 4.4 : Lateral Capacity of a Jacket Bay

We impose a virtual displacement to the ith jacket bay of a two-dimensional jacket frame (Figure 4.4) and equate the external and internal work

$$W^{(E)} = W^{(I)}$$

(4.19)

which leads to the following equilibrium equation for the given jacket bay

$$P_u = P_{bh} + \frac{2(M_j + M_k)}{H_{bay}}$$

(4.20)

where P_{bh} denotes the horizontal component of brace axial force. Assuming that the magnitude of bending moment in the jacket legs is negligible

$$M_j = M_k = 0$$

(4.21)

the following simplified relationship results

$$P_u = P_{bh}$$

(4.22)

This assumption leads to estimates of lateral capacity of a jacket bay that are either conservative or unconservative depending on the actual bending moment distribution in

80

the legs. However, this conservatism or unconservatism is negligible for all but the uppermost and lowest jacket bays. Due to frame action in the deck portal and rotational restraint of the legs at mud level, the jacket legs and piles inside the legs experience relatively large bending moments at these two bays. The bending moment in the legs at the lowest bay has the direction of a resisting moment and hence not considering it can only be conservative. In contrary, the shear force due to the large moment gradient at the uppermost jacket bay has the same direction as the global lateral loading. If this effect is not taken into account, the lateral capacity will be overestimated.

A simplified procedure is developed to account for the effect of shear force in the top jacket bay. We are interested in moment distribution along the legs at this bay due to frame action in the deck portal (Figure 4.5). Given the geometry of the deck portal and the load acting on deck areas, the moment distribution along the deck legs can be estimated

$$M_o = \frac{\dfrac{P_d L_d^2}{2EI} + \dfrac{P_d L_d}{C_r}}{\dfrac{L_d}{EI} + \dfrac{1}{C_r}} \leq M_p \tag{4.23}$$

$$M_1 = M_o - P_d L_d \leq M_p \tag{4.24}$$

Thinking of a jacket leg as a continuous beam which is supported by horizontal framings, the applied moment at the top of the leg rapidly decreases towards the bottom. Based on geometry of the structure, in particular jacket bay heights and the cross-sectional properties of the jacket leg (if nonprismatic), and in the limiting case of rigid supports, an

81
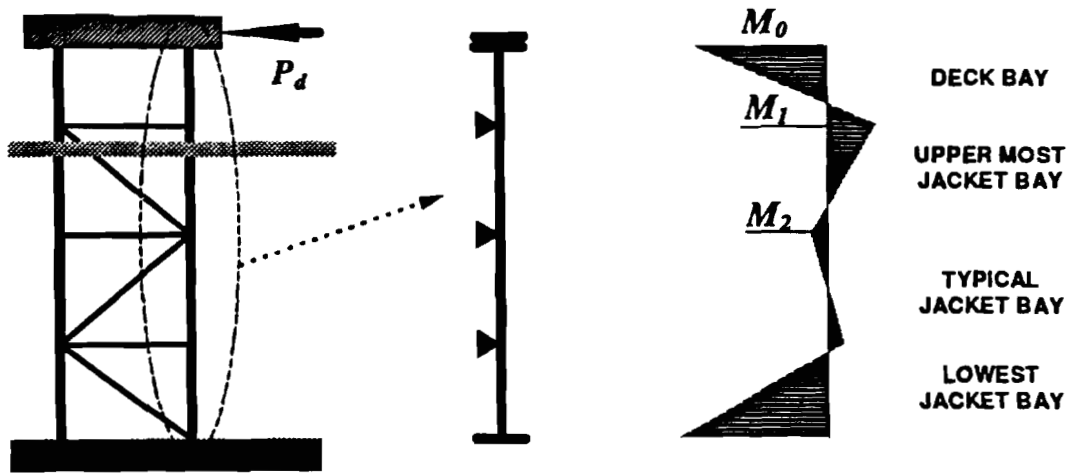
Figure 4.5 : Typical Moment Distribution in Jacket Legs under Lateral Loading

upper bound for the desired moment distribution is estimated. For equal spans, constant moment of inertia and limiting case of rigid supports the following relationship can be derived

$$|M_2| \le 0.286 |M_1|$$

(4.25)

4.3.4   Jacket Bays Lateral Shear Strength

To derive a lower-bound capacity formulation, the notion of Most Likely To Fail (MLTF) element is introduced. MLTF element is defined as the member with the lowest capacity over stiffness ratio. The lower-bound lateral capacity of a jacket bay is estimated by adding the horizontal force components of all load carrying members in the given bay at the instant of first member failure. A linear multi-spring model is used to relate the forces and displacements of diagonal braces within a bay. It is assumed that the horizontal braces

are rigid. The axial force in the jacket legs due to lateral overturning moment is estimated at each bay and its batter component is added to the lateral capacity.

$$P_{uJ} = \sum_i \left(\frac{P_{u,MLTF}}{K_{MLTF}} \right) K_i + F_L \tag{4.26}$$

The summation is over all vertical diagonal braces within a given jacket bay. P_{uJ} denotes the lower-bound lateral shear capacity of the jacket bay, P_u is the horizontal component of axial force in a given diagonal brace, F_L is the sum of batter components of leg forces, and K_i denotes the lateral stiffness of brace i

$$K_i = \frac{E_i A_i cos^2 \theta}{L_i} \tag{4.27}$$

where L, E, A, and θ denote the length, Young modulus, cross-sectional area, and the angle between the diagonal brace and the horizon respectively.

An upper-bound capacity is also formulated for each bay. After the MLTF member in compression reaches its axial capacity, it can not maintain the peak load and any further increase in lateral displacement will result in unloading of this member. Presuming that the load path remains intact (inter-connecting horizontals do not fail), a load redistribution follows and other members carry the load of the lost members until the last brace reaches its peak capacity. An empirical residual capacity modification factor, α, is introduced. Assuming elasto-perfectly plastic material behavior, α is equal to 1.0 for members in tension (neglecting strain hardening effects) and less than 1.0 for members in compression due to $P-\delta$ effects (generally in the range of 0.15 to 0.5). The upper-bound lateral shear

83

capacity of a given jacket bay, $P_{u,u}$, is estimated by adding the horizontal component of the residual strength of all of the braces within the bay

$$P_{u,u} = \sum_i P_{u,i} \alpha_i + F_L \tag{4.28}$$

4.4 Foundation Bay

Realistic modeling of pile foundations is crucial to the validity of the results of static and dynamic structural analyses of offshore platforms. Too often in the past have foundation failures been predicted to be the dominant failure mode of platforms. Seldom have the observed failure modes included failure of foundation elements (PMB, 1995). This fact indicates that the traditional methods of predicting the ultimate capacity of pile foundations are in general conservatively biased.

Assessing the structural integrity of an offshore platform requires due consideration of all biases and uncertainties associated with loadings and capacities. In the case of foundations, this requirement translates into the need of better understanding of their performance and more realistic modeling of their behavior. Major sources of bias are found to be the dynamic nature of loadings and soil sampling and testing. Bea (1987) found two of the important influences of dynamic loadings on offshore pile foundations to be the: a) decrease in the capacity and stiffness due to cyclic loading and b) increase in the capacity and stiffness due to high rates of loading.

During an intense storm a platform in the Gulf of Mexico and Northern North Sea experiences some 10^3 to 10^4 load cycles from which, in general, less than 10 are larger than 70 to 80 percent of the maximum force (Bea, 1987). Test results on axially loaded piles in clay have shown that at cyclic displacements that do not exceed the displacement at which the maximum static pile strength is developed, only little decrease in pile axial capacity is observed (Bea, 1987). On the other hand, it is well known that high strain rates tend to increase the material stiffness and strength. Bea (1987) gives the following logarithmic relationship for the strength ratio (strength at a given time of loading to failure to the strength at 100 seconds)

$$\beta_R = 1 + F \log \frac{t_r}{t_s} \tag{4.29}$$

where t_r denotes the actual loading rate and t_s is the reference loading rate. F is a soil material dependent parameter and ranges from 0.01 to 0.03 for sands and from 0.02 to 0.12 for clays.

Those familiar with geotechnical practices, in particular with soil sampling practices, know that soil sample disturbance is unavoidable. Some of the sources of sample disturbance are drilling, sampling, significant pressure relief, packaging, transport and preparation for testing (Bea, 1987). Laboratory testing is another source of bias in soil strength parameters.

In the following sections, simplified foundation capacity formulations are developed and discussed. These formulations are derived based on the assumption of limit equilibrium. Two basic failure modes are considered: lateral and axial. In Chapter 5 of this dissertation a simplified probabilistic failure analysis approach is developed where the biases and uncertainties are also considered and included in the analyses.

4.4.1 Ultimate Lateral Strength of Pile Foundations

The pile lateral shear capacity is based on an analysis similar to that of deck legs with the exception that the lateral support provided by the foundation soils and the batter shear component of the piles are included. It is assumed that each pile reaches its ultimate lateral capacity when two plastic hinges form: one at the mudline and the other at a lower depth where the bending moment reaches a maximum (Figure 4.6). Figure 4.7 shows the assumed lateral pile failure mode in cohesive soils.

For cohesive soils, the distribution of lateral soil resistance along the pile per unit length, p_s, is assumed to be

$$p_s = 9 \, S_u \, D \tag{4.30}$$

where S_u is the effective undrained shear strength of the soil and D is the pile diameter. This formulation is supported by studies of Matlock (1970) and Randolf et al. (1984) for smooth piles. Findings by Reese et al. (1975) support a lateral soil resistance of

$$p_s = 11 \, S_u \, D \tag{4.31}$$
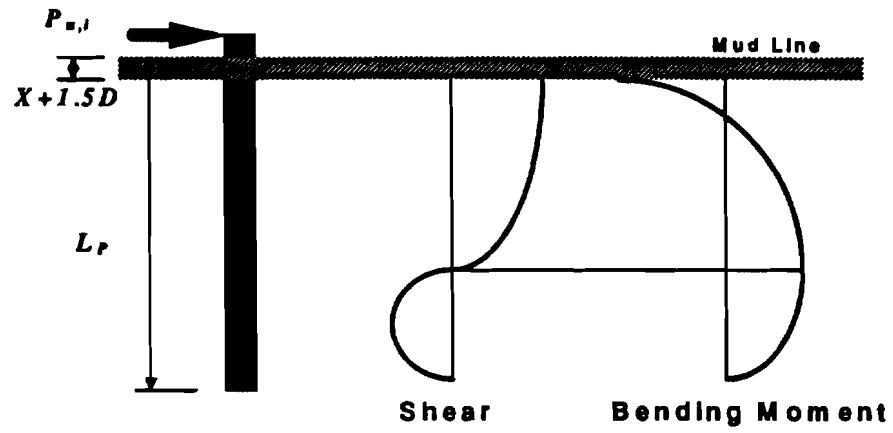
Figure 4.6 : Typical Internal Force Distribution in a Vertical Laterally Loaded Pile
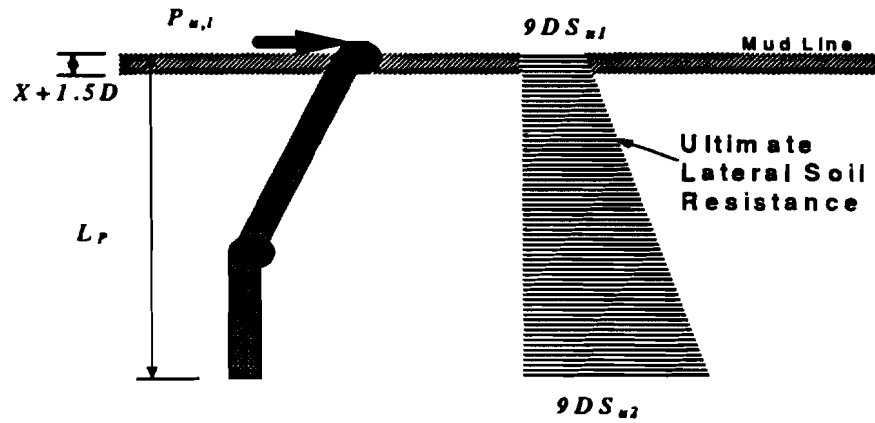
Figure 4.7 : Lateral Pile Failure Mode in Cohesive Soil

Murff et al. (1993) developed a method to predict the ultimate lateral capacity of piles in undrained clays. The procedure makes use of the upper-bound method of plasticity and is based on a three-dimensional failure mechanism. In their approach strength nonhomogenity, soil-pile adhesion, and suction on the back of the pile can be accounted for. It was found in their paper that adhesion can increase the unit resistance along the pile by some 20 to 30 percent. Experimental results reported by Hamilton et al. (1991) supported this finding. In addition, soil unit resistance was estimated by measurement of bending moments along the test piles and subsequent differentiation of moment diagram. An average unit soil resistance of $11S_uD$ was reported for all depths from a distance close to seabed to the pile tip.

Based on Equation (4.30) and for a constant undrained shear strength, S_u, over the pile length and for a given scour depth, X, the ultimate lateral force that can be developed at the pile top is (Tang, 1990)

$$P_{uj} = 0.5 \left\{ -\left(27D^2 S_u + 18 S_u XD\right) + \left[\left(27D^2 S_u + 18 S_u XD\right)^2 + 144 S_u D M_u\right]^{0.5} \right\}$$

(4.31)

where M_u is the plastic moment capacity of the pile cross-section computed using the M-P interaction equation for tubular cross sections. In the case of linearly increasing shear strength with depth the ultimate lateral capacity of the pile, $P_{u,l}$, can be estimated from the following equation

$$P_{u,l}\left(C + \xi\right) - 2 M_u - \left(A + \eta \xi\right)\frac{C^2}{2} - \left(\frac{\eta}{2}\right)\frac{C^3}{3} = 0$$

(4.32)

where

$$C = \frac{1}{\eta}\left[(-A+\eta\xi) + \sqrt{(A+\eta\xi)^2 + 2\eta\, P_{u,l}}\,\right]$$

(4.33)

$$\eta = \frac{B-A}{L_p}$$

(4.34)

$$\xi = 15D + X$$

(4.35)

$$A = 9\,S_{u1}D \quad \text{and} \quad B = 9\,S_{u2}D$$

(4.36) , (4.37)

S_{u1} and S_{u2} denote the undrained shear strength at mudline and at the pile tip respectively (Figure 4.7). For cohesionless soils, the distribution of lateral soil pressure along a pile at a depth z, is assumed to be

$$p_s = 3\gamma z\, K_p$$

(4.38)

where

$$K_p = \tan^2\left(45 + \frac{\Phi}{2}\right)$$

(4.39)

Φ is the effective angle of internal friction of the soil and γ is the submerged unit weight of the soil. The ultimate lateral force that can be developed at the pile top with no scour is (Tang, 1990)

$$P_{u,l} = 2.382\; M_p^{2/3}\left(\gamma D\, K_p\right)^{1/3}$$

(4.40)

For a scour depth equal to X, the ultimate lateral force is given implicitly by

(4.41)

$$P_{u,l} = \frac{2\, M_p}{\left[X + 0.544\left(\dfrac{P_{u,l}}{\gamma D\, K_p}\right)\right]^{0.5}}$$

89
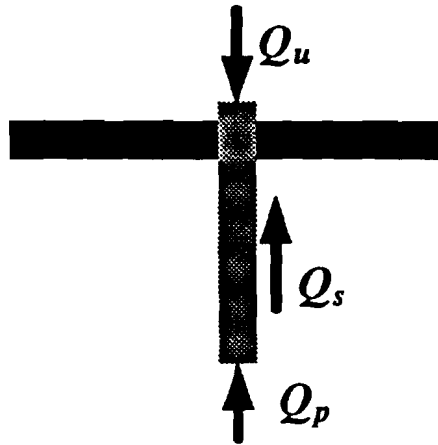
Figure 4.8 : Axial Pile Capacity

The equilibrium equations (4.31), (4.32), (4.40) and (4.41) are derived using the principle of virtual displacement. The horizontal batter component of the pile top axial force is added to estimate the total lateral shear capacity of the piles. This component is computed based on axial loads carried by the piles due to storm force overturning moment.

4.4.2 Ultimate Axial Strength of Pile Foundations

The axial resistance of a pile is based on the combined effects of a shear yield force acting on the lateral surface of the pile and a normal yield force acting over the entire base end of the pile (Figure 4.8). Thus the ultimate axial capacity Q_u, can be expressed as

$$Q_u = Q_s + Q_p = q \ A_p + f_{av} A_{sk} \tag{4.42}$$

Q_p denotes the ultimate end bearing and Q_s is the ultimate shaft capacity, q is the normal end yield force per unit of pile-end area acting on the area of pile tip A_p, and f_{av} denotes the ultimate average shear yield force per unit of lateral surface area of the pile acting on embedded area of pile shaft A_{sh}. It is assumed that the pile is rigid and that shaft friction and end bearing forces are activated simultaneously. It is further assumed that the spacing of the piles is sufficiently large so that there is no interaction between the piles.

After considering the weight of the pile and the soil plug (for open-end piles), the ultimate compressive loading capacity of the pile, Q_c, can be calculated as

$$Q_c = \frac{q\pi D_o^2}{4} + \left(f_{av}\pi D_o - w_p\right)L_p \tag{4.43}$$

$$w_p = \gamma_{st} A_{st} + \gamma_s A_s = \frac{1}{4}\left[\gamma_{st}\pi\left(D_o^2 - D_i^2\right) + \gamma_s\pi D_i^2\right] \tag{4.44}$$

where

A_{st}	= cross-sectional area of the steel pile
A_s	= cross-sectional area of the soil plug
D_o	= outside diameter of the pile
D_i	= inside diameter of the pile
f_y	= yield stress
γ_{st}	= submerged specific weight of steel
γ_s	= submerged specific weight of soil
L_p	= pile embedded length
w_p	= weight of pile and soil plug per unit length

The end bearing capacity can be fully activated only when the shaft frictional capacity of the internal soil plug exceeds the full end bearing (Focht and Kraft, 1986). This condition can be formulated as

$$\frac{q\pi D_i^2}{4} < \left(f_{av}\pi D_i + w_s\right)L_p \tag{4.45}$$

The tensile capacity is similarly estimated as

$$Q_t = \left(f_{av}\pi D_o + w_p\right)L_p \tag{4.46}$$

For cohesive soils with an undrained shear strength, S_u, the ultimate bearing capacity is taken as the end bearing of a pile in clay

$$q = 9S_u \tag{4.47}$$

The ultimate shaft friction is taken as

$$f_{av} = \kappa S_{u,av} \tag{4.48}$$

where κ is the side resistance factor and a function of the average undrained shear strength $S_{u,av}$ as given in Table 4.2. For cohesionless soils, the ultimate bearing capacity of a deeply embedded pile is estimated as

$$q = N_q \sigma_v \tag{4.49}$$

N_q is a bearing capacity factor and a function of the friction angle of the soil Φ, and σ_v denotes the effective pressure at the pile tip. Since sand soils possess high permeability, the pore water quickly flows out of the soil mass and the effective stress is assumed equal to applied stress. The unit shaft resistance on pile increment is estimated as

$$f_i = k \sigma_{vi} \tan\delta \tag{4.50}$$

92

where k is an earth lateral pressure coefficient assumed to be 0.8 for both tension and compression loads, σ_{vi} denotes the effective overburden pressure at the given depth, and δ denotes the friction angle between the soil and pile material and is taken as

$$\delta = \Phi - 5^\circ \qquad (4.51)$$

The unit shaft resistance and the unit end bearing capacity can not indefinitely increase with the penetration. The ultimate axial capacity of piles in sand soils is estimated based on commonly used limiting values for N_q, q_{max} and f_{max} given by Focht and Kraft (1986), (Table 4.3).

Undrained Shear Strength $S_{u,av}$ (ksf)	Side Resistance Factor κ
<0.5	1
0.5 - 1.5	1 - 0.5
>1.5	0.5

Table 4.2: Side Resistance Factor for Cohesive Soils (Focht et al., 1986)

Friction Angle Φ	Bearing Cap. Factor, N_q	Bearing Cap. q_{max}(ksf)	Shaft Friction f_{max}(ksf)
20	8	40	1.0
25	12	60	1.4
30	20	100	1.7
35	40	200	2.0

Table 4.3: Frequently Used Values for Medium Dense Materials (Focht et al., 1986)

4.5 Damaged and Repaired Members

A major problem associated with assessment of an older platform is locating and evaluating the effects of defects and member damage on platform response to extreme loadings. Damage such as dents, global bending, corrosion, and fatigue cracks can significantly affect the ultimate strength of an offshore platform. Given the physical properties of damage, an estimate of the ultimate and residual strength of the damaged members is necessary to perform a strength assessment of an offshore platform system. Recently, numerous investigators have devoted their attention to this subject and several theoretical approaches have been developed addressing different types of damage (e.g. Ellinas, 1984; Ricles et al., 1992; Loh, 1993; Kim, 1992). Small and large-scale experiments have been performed to verify the analytical capacity formulations and to gain better understanding of the ultimate and post ultimate behavior of damaged and repaired tubular members.

A literature review was performed on the ultimate strength behavior of damaged and repaired tubular braces with dents, global out-of-straightness, and corrosion. Simplified methods were identified to estimate the ultimate and residual capacity of such members. In the following section, this literature review is summarized and discussed. The results of the simplified capacity estimation methods are compared with existing theoretical and experimental test results given in literature.

4.5.1 Dents and Global Bending Damage

Dent-damaged tubular bracing members have been analytically studied since late 70's. The analytical methods of strength prediction developed so far can be classified into three categories (Ricles, 1993):

a)   Beam-column analysis (Ellinas, 1984, Ricles et al, 1992, Loh, 1993)

b)   Numerical integration methods (Kim, 1992)

c)   Nonlinear finite element (FE) methods

Beam-column analysis is based on formulation of equilibrium of the damaged member in its deformed shape. The P-δ effects including the effects of out-of-straightness are considered in the equilibrium equations. The effect of dent depth is taken into account by modifying the cross-sectional properties. Numerical integration methods use empirical moment-axial load-curvature relationships to iteratively solve the differential equation of axially loaded damaged member. The empirical M-P-Φ relationship is usually based on experimental test results or finite element studies of dented tubular segments. Nonlinear FE analyses represent the most general and rigorous method of analysis. However, their accuracy and efficiency require evaluation and they are expensive and time consuming to perform.

Loh's Interaction Equations

Developed at Exxon Production Research Company, BCDENT is a general computer program that uses M-P-Φ approach to evaluate the full behavior of dented member (Loh,

1993). The behavior of the dent section is treated phenomenologically using a set of M-P-Φ expressions. Compared with the experimental results, BCDENT gives mean strength predictions for both dented and undented members. Based on BCDENT results, Loh (1993) presented a set of new unity check equations for evaluating the residual strength of dented tubular members. The unity check equations have been calibrated to the lower bound of all existing test data. The equations cover axial compression and tension loading, in combination with multi-directional bending with respect to dent orientation. When the dent depth approaches zero, the recommended equations are identical to API RP 2A equation for undamaged members(API, 1993b). Loh's equations for dent damaged members and those with global bending damage have been integrated in ULSLEA. These equations are listed in Appendix B.

Comparison Between Experimental and Predicted Capacities

Based on a comparison between the experimental ultimate capacities and the corresponding predicted capacities of dented tubulars using different methods of analysis, Ricles (1993) concluded that Ellinas' formulation, which is based on first yield in the dent saddle, is overly conservative. In general, it has been found that Ellinas' approach can be either conservative or unconservative depending on the dent depth, member slenderness, and out-of-straightness. Ricles further concluded that DENTA (a computer program developed by Taby (1988)), Loh's interaction equations, numerical integration based on M-P-Φ relationships, and the nonlinear FEM are able to predict the capacity of the test members reasonably well.
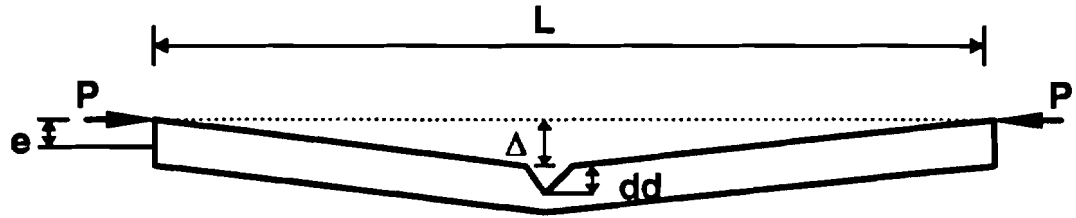
Figure 4.9 : Definition Sketch for a Damaged Tubular Brace

Also, a joint industry project on testing and evaluation of damaged jacket braces was performed by PMB Engineering and Texas A&M University (1990). Twenty salvaged braces were tested and their strength behavior compared with results gained from analyses using finite element beam column models of damaged braces. It was found that on average the analyses would overpredict the capacities by 21%. The agreement in this case is not as good as that presented by other investigators. Use of new and artificially damaged braces in other investigations may explain this inconsistency. Generally, corrosion is found to add large uncertainties to the properties of the entire member. Figure 4.9 shows the definition sketch of a dent-damaged member with global out-of-straightness. Using ultimate capacity equations formulated by Ellinas (1984) and Loh (1993), the ratio of damaged compressive capacity over intact buckling capacity was estimated for ten tubular braces. The intact buckling capacity of a tubular brace was taken to be that given by API (1993b). The capacity ratios are plotted for two separate cases. Figure 4.10 shows the results for no dent damage and varying global out-of-straightness, whereas Figure 4.11 shows the results for no global bending damage and varying dent depth. In case of global bending damage,
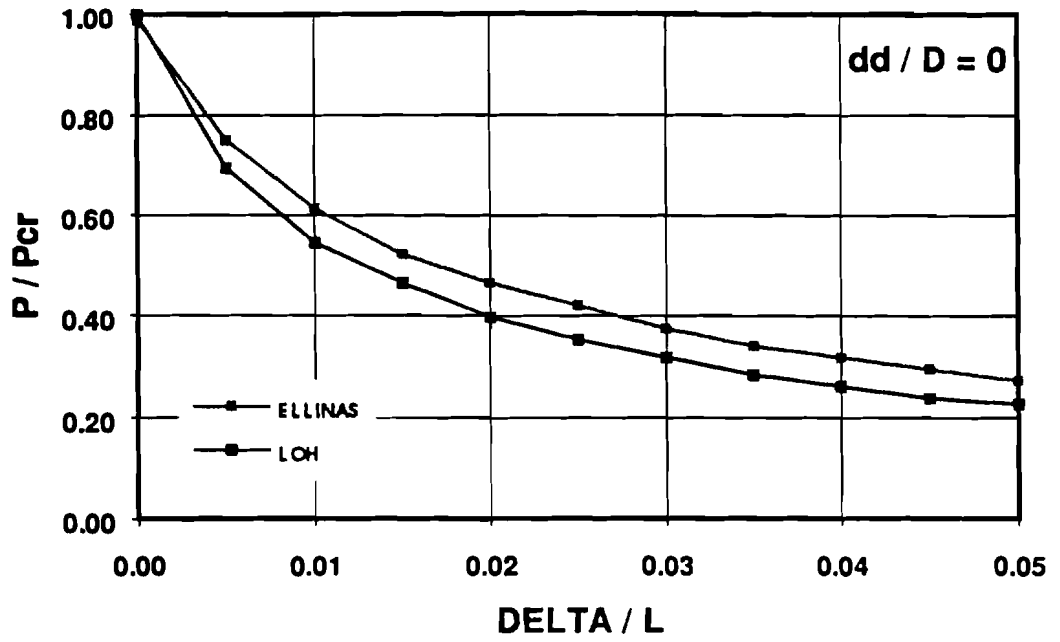
Figure 4.10 : Comparison of Capacity Predictions for Tubulars with Global Bending Damage
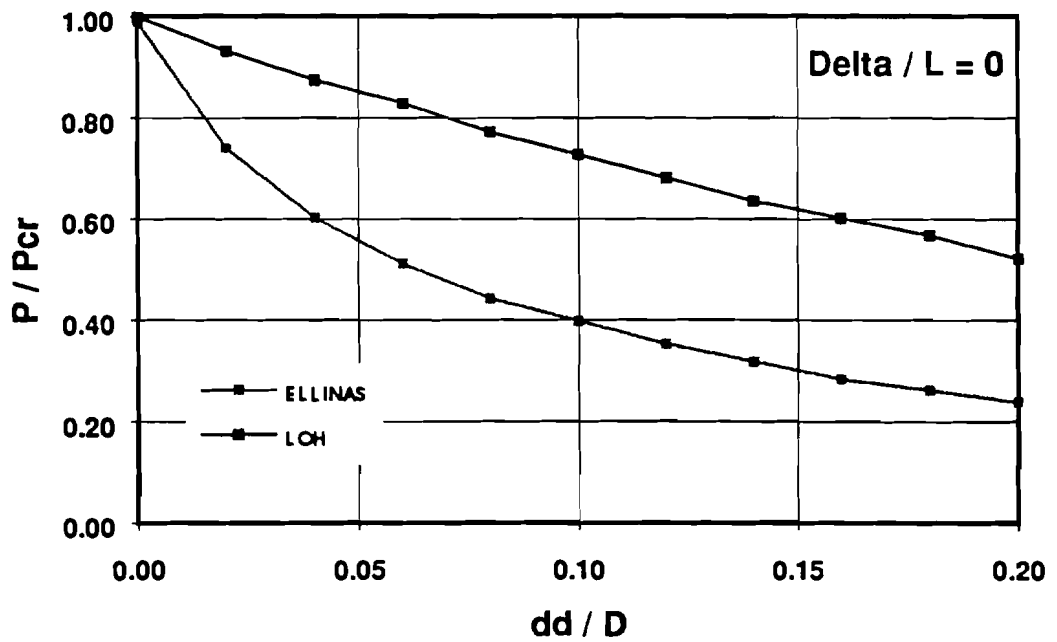
Figure 4.11 : Comparison of Capacity Predictions for Tubulars with Dent Damage

the two sets of results are in close agreement indicating that the second-order P-δ effects are captured coherently by both sets of formulations (Figure 4.10). In case of dent-damaged tubulars, however, the results indicate significant differences in capacity predictions by the two sets of formulations. These results confirm those previously published in the literature regarding the level of conservatism of capacity equations developed by Ellinas. An attempt was made to compare the results of different theoretical approaches to predict the compressive capacities of damaged tubulars. Nine specimen were selected from a database that represents all of the test results currently in the public domain (Loh, et al., 1992). Table 4.4 contains the member sizes and material and damage properties. The test results are compared with those gained from the programs BCDENT (Loh, 1993), UC-DENT (Ricles et al., 1992), and capacity equations given by Ellinas (1983) and Loh (1993). The numerical results are given in Table 4.5 and plotted in Figure 4.12. The results indicate that for the data points presented, BCDENT capacity predictions are unbiased. Loh's formulations lead to capacity predictions that are close lower bounds of test results. Ellinas' formulation is in most cases overly conservative. UC-DENT predicts capacities that are close approximations of test results.

Based on experimental test results and parametric studies using different analytical methods, the following observations have been made and presented in the literature:

a) The residual strength decreases significantly as the dent depth increases.

99

b) For a given dent depth, the analyses show a decrease in residual strength for members with higher D/t ratio.

c) The axial compression capacity decreases as the out-of-straightness increases, but the impact on ultimate moment is negligible.

d) A mid-length dent location can be assumed for any dent within the middle-half section of members effective length.

e) Accounting for strain hardening has only a small effect on the maximum predicted capacity.

f) Lateral loadings, such as those caused by wave forces, can significantly affect dented brace capacity.

g) The behavior of members with multiple forms of damage are generally dominated by one damage site.

Test	D [IN]	t [IN]	L [IN]	Sy [KSI]	E [KSI]	dd/D [%]	delta/L [%]	e/L [%]
A1	2.50	0.08	84.63	33.06	29145		0.02	
A2	2.50	0.08	84.63	33.21	30160		0.03	0.46
A3	2.50	0.08	84.63	32.77	28710	0.046	0.55	
B3	3.13	0.07	84.63	28.71	31030	0.08	0.5	
C1	4.00	0.07	84.63	30.60	29145		0.05	
C2	4.00	0.07	84.63	41.18	29870		0.05	0.46
C3	4.00	0.07	84.63	33.79	28565	0.034	0.04	
F1	16.02	0.39	305.24	44.23	28710		0.07	
F2	15.98	0.39	305.24	42.49	31030	0.124	0.18	

Table 4.4: Test Specimen Properties

Test	dd/D	delta/L [%]	e/L [%]	Ptest [KN]	BCDENT [KN]	LOH [KN]	ELLINAS [KN]	RICLES [KN]
A1		0.02		78.10	76.50	63.46	60.94	
A2		0.03	0.46	46.00	41.60	38.86	41.88	
A3	0.05	0.55		44.20	43.80	33.68	28.23	
B3	0.08	0.50		43.30	41.50	35.97	25.04	43.96
C1		0.05		121.00	104.80	95.37	96.48	119.66
C2		0.05	0.46	89.40	97.10	90.66	97.84	
C3	0.03	0.04		95.70	101.90	93.61	68.85	86.00
F1		0.07		3238.70	3509.90	3160.30	3192.10	3862.30
F2	0.12	0.18		2056.90	2031.70	1962.40	1068.00	2051.40

Table 4.5: Experimental and Theoretical Capacities of Damaged Tubulars
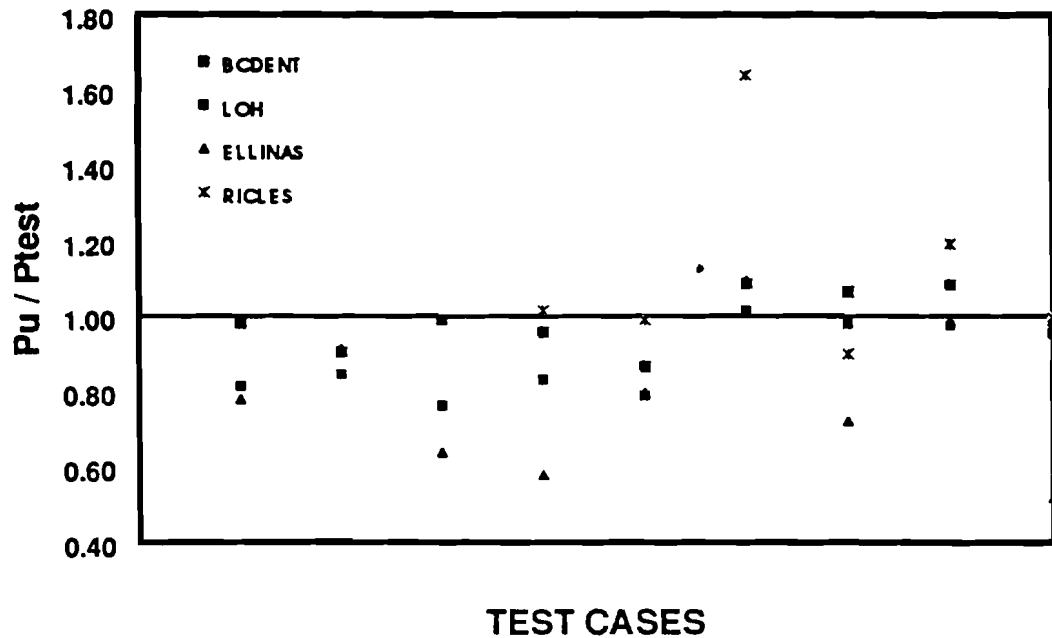
Figure 4.12 : Comparison of Capacity Predictions for Tubulars with Dents and Global Bending Damage (Table 4.5)

4.5.2 Corrosion Damage

The marine environment is extremely corrosive. Although cathodic protection systems and protective coatings have been applied to prevent corrosion of steel members, in numerous

cases corrosion damage of offshore platforms has still been observed. Corrosion results in a reduced wall thickness of the steel members which can lead to premature local buckling at the corroded areas.

Ostapenko et al. (1993) conducted experimental test on corroded tubulars from salvaged Gulf of Mexico platforms. Local buckling was reported at the most severely corroded area and an up to 50% reduction in capacity was observed. It was found that the patch with the most severe corrosion controls the local buckling of the member. Ricles and Hebor (1994) performed and presented an analytical and experimental study on patch-corroded steel tubular members. They used the results of an experimental program to verify a non-linear finite element model. The calibrated FE model was then used to perform parametric studies and develop relationships between the residual strength of the damaged members and corrosion patch geometry. Based on a multi-variable, nonlinear regression analysis, a closed-form solution for patch-corroded tubular member strength was derived as a function of D/t ratio and corrosion patch geometry.

4.5.3 Grout-Repaired Tubular Members

Given that the loss of strength of a member due to damage has a significant impact on strength and reliability of the platform system, it is desirable to apply some measure of strengthening the damaged member. Internal full-grouting or using grouted steel clamps are two economically attractive alternatives. Experimental results have shown that grouting significantly increases the capacity of damaged tubular members and therefore is

a viable mean of strengthening such members. In the past practicing engineers have been applying existing analytical expressions for composite members to estimate the capacity of grout-filled damaged tubular members.

Parsanejad Method

Responding to the need for some sort of analytical expressions, Parsanejad (1987) presented a simple analytical expression for estimating the ultimate capacity of grout-filled damaged tubular members. The analysis was based on the following simplifying assumptions:

a) full interaction exists between grout and the damaged tube and

b) grout provides sufficient support to the tube wall in the damaged region to prevent premature local buckling.

The first yield collapse criterion was adopted by Parsanejad; it was assumed that the ultimate capacity of damaged tubular member is reached when the compressive stress in the steel tube at the dent equals the yield stress. The damaged member was treated as a beam-column with uniform cross-sectional properties represented by the dented region. The total eccentricity was taken as the sum of eccentricities due to initial out-of-straightness, external load, and the distance between the original center of the tube and the centroid of the transformed cross section at the dent. Comparing the analytical results with the limited experimental results existent at the time, Parsanejad reported good agreement: the analytical results presented close lower-bound estimates of test results. The equations

developed for grout repaired tubulars by Parsanejad has been integrated in ULSLEA and are listed in Appendix B.

Comparison Between Experimental and Predicted Capacities

Ricles et al. (1993) performed experiments on thirteen large-scale damaged and repaired tubular members with the following objectives:

a) assessing the residual strength of dent damaged steel tubular bracing members under combined flexural and axial load and

b) determining the effectiveness of using internal complete grouting and grouted steel clamps to repair dent damaged members.

The residual strength of damaged unrepaired and grout repaired specimens were compared to the undamaged design strength according to WSD and LRFD formats respectively. Test results were also compared to results gained from the modified Ellinas equation, computer program DENTA, and Parsanejad formulation. The following conclusions regarding grout-filled damaged tubular members are drawn by Ricles et al (1993):

a) Internal grout and grouted steel clamp repairs of a 0.1D dent damaged brace are successful in reinstating the original undamaged member's strength by arresting dent growth inwards.

b) The predicted strength of internally grout-repaired members based on Parsanejad's method provided a close lower bound to experimental data.

4.6   Summary

A template-type offshore platform is comprised of three main structural components. The superstructure, or deck, supports the topside facilities. The substructure, or jacket, resists and transfers the vertical dead loads and lateral operational and environmental live loads to the foundation. The pile foundation finally transfers the loads to the ocean ground.

In this chapter, simplified formulations were developed to estimate the ultimate lateral shear capacity of the three above-mentioned primary structural components of a platform. Elements within these components were identified first. These are deck legs, tubular braces and their connections (tubular joints) and pipe piles. For each component to fail, all elements within that component have to fail. Based on past numerical analyses and experience, failure modes were assumed for different platform components. Using the concept of plastic hinge theory, the principle of virtual work was utilized to formulate the component capacities; the virtual displacement was taken to be the actual collapse mechanism and an equilibrium equation was derived for each component at ultimate limit state. Where of significance, geometric nonlinearities were taken into account.

Based on a literature survey, simplified analysis methods to predict the ultimate capacity of damaged and grout-repaired tubular braces have been identified. These methods were presented and discussed in this chapter.

CHAPTER 5

A SIMPLIFIED STRUCTURAL SYSTEM RELIABILITY ANALYSIS

5.1 Introduction

Extreme-condition environmental loadings acting on offshore platforms are dynamic in nature. In general, given the load time-history, nonlinear time-domain structural analyses need to be performed to predict the "true" response of the platform subject to such loadings. Such analyses are complex and difficult to perform. Nonlinear cyclic-dynamic response characteristics of platform elements need to be described. However, in extreme storm conditions, and unlike earthquake loading, experience has shown that the dynamic nature of the loads do not play a major role in the ultimate limit state performance of conventional jacket-type offshore platforms.

Static nonlinear structural analyses are being increasingly used to determine the structural integrity (reserve and residual strength) of offshore platforms (Hellan et al., 1993). In the past three decades an immense amount of effort has been devoted to development of software to help analysts perform such analyses. In general, these analyses are complex. There is a need for experts and a significant amount of time to perform such analyses. There are many alternatives to model a structure (Billington et al., 1993). In many cases, the output is highly sensitive to these modeling assumptions. Only recently has some of the existing software been validated and calibrated by comparison with other programs

(Digree et al., 1995) and against large scale test results (Grenda et al., 1988, Bolt et al., 1994, Bolt, 1995). Due to the complexity of software, these programs are prone to human and system error. Experience has shown that it is easy to make mistakes that are difficult to detect and that can have significant influence on the results (Loch and Bea, 1995).

Large uncertainties associated with loadings and capacities add another dimension to the complexity of the problem of structural integrity assessment of offshore platforms. Due to this large uncertainties and relatively high consequences of failure of offshore platforms, in particular in North Sea region, these structures have been the subject of comprehensive reliability analyses in the past (e.g. Thoft-Christensen et al., 1982, Nordal et al., 1988). In general, there are two types of uncertainty; natural or aleatory (Type I) and unnatural or epistemic (Type II). The source of the aleatory uncertainties is the inherent randomness of stochastic processes (e.g. the uncertainty associated with the prediction of the annual maximum wave height for a given site). Basically, this type of uncertainty is information insensitive and can not be reduced. The epistemic uncertainties are partially due to our lack of thorough understanding of the physics of the problem (physical modeling uncertainties) and partially due to lack of data (statistical modeling uncertainties)(e.g. uncertainties associated with the wave kinematics given the wave height and period). This type of uncertainty is in general information sensitive and can be reduced. More research can lead to our better understanding of the physical processes and help enhance the physical modelings and hence reduce the uncertainties associated with them. More experiments and field measurements can lead to improvements of statistical modelings and

help reduce the uncertainties associated with the modeling parameters. It is often difficult to clearly distinguish between the two types of uncertainty.

One effective mean of representing Type II uncertainties is through characterizing "biases". Bias is defined as the ratio of the true to the predicted value of a random variable. By establishing and evaluating the statistical properties of the bias (mean and standard deviation), conservatism or unconservatism implicit in the simplified modeling assumptions can be captured and taken into account.

Based upon the background developed in Chapters 3 and 4 of this dissertation, a simplified deterministic structural integrity assessment approach has been developed for offshore platforms. This approach is described in the following section. Taking into account the Type I and Type II uncertainties associated with loadings and capacities and using the concepts of structural reliability theory and the deterministic safety assessment formulations developed in this and previous chapters, a simplified probabilistic safety assessment approach has been also developed and is described in this chapter.

5.2   Deterministic Failure Analysis

The process is summarized in Figure 5.1. The geometry of the platform is defined by specifying a minimum amount of data. These include the effective deck areas, the proportion and topology of jacket legs, braces, and joints and of the foundation piles and

```
                    ┌─────────────┐
                    │ User Input  │
                    └──────┬──────┘
              ┌────────────┴────────────┐
              ▼                         ▼
      ┌───────────────┐         ┌───────────────┐
      │ Storm Loading │         │ Platform Shear│
      │ Shear Profile │         │   Resistance  │
      └───────┬───────┘         └───────┬───────┘
              └────────────┬────────────┘
                           ▼
                   ┌───────────────┐
                   │IdentifyPlatform│
                   │  Weak-Link    │
                   └───────┬───────┘
                           ▼
                   ╭───────────────╮
                   │ RSR = Rᵤ / Sᵣ │
                   ╰───────────────╯
```

$$RSR = R_u / S_r$$
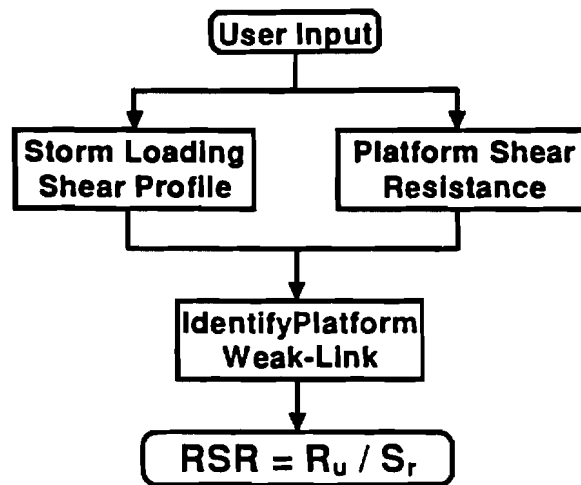
Figure 5.1: Deterministic Failure Analysis

conductors. The projected area characteristics of appurtenances such as boat landings, risers, and well conductors are specified. If marine fouling is present, the variation of the fouling thickness with depth is also defined. Specialized elements are designated including grouted or ungrouted joints, braces, and legs. In addition, damaged or defective elements are included. Dent depth and initial out-of-straightness are specified for braces with dents and global bending defects. Element capacity reduction factors are introduced to account for other types of damage to joints, braces, and foundation (corrosion, fatigue cracks, etc.). Steel elastic modulus, yield strength, and effective buckling length factor for vertical diagonal braces are specified. Soil characteristics are specified as the depth variation of effective undrained shear strength for cohesive soils or the effective internal angle of friction for cohessionless soils. Scour depth around the piles is also specified.

Collapse mechanisms are assumed for the three primary components that comprise a template-type platform: the deck legs, the jacket, and the pile foundation. Based on the presumed failure modes, the principle of virtual work is utilized to estimate the ultimate lateral capacity for each component and a profile of horizontal shear capacity of the platform is developed (Chapter 4).

Storm wind speed at the deck elevation, wave height and period, current velocity profile, and storm water depth need to be defined. These values are assumed to be collinear and to be the values that occur at the same time. Generally the load combination is chosen to be wind speed component and current component that occur at the same time and in the same principal direction as the expected maximum wave height. The wave period is generally taken to be expected period associated with the expected maximum wave height. To calculate wind loadings acting on the exposed decks the effective drag coefficient needs to be defined. Similarly, the hydrodynamic drag coefficients for smooth and marine fouled members have to be defined. Modification factors are introduced to recognize the effects of wave directional spreading and current blockage.

Comparison of the storm shear profile with the platform shear capacity profile identifies the weak link in the platform system (Figure 1.4). The base shear or total lateral loading at which the capacity of this weak link is exceeded defines the static ultimate lateral capacity of the platform R_{us}. The static lateral loading capacity is corrected with a loading effects

110

modifier, F_v, to recognize the interactive effects of transient wave loadings and nonlinear hysteretic platform response (Bea and Young, 1993)

$$R_u = R_{ur} F_v$$ (5.1)

With these results, the Reserve Strength Ratio (RSR) can be determined as

$$RSR = \frac{R_u}{S_r}$$ (5.2)

where S_r denotes the reference storm total maximum lateral loading.

5.3 Probabilistic Failure Analysis

The development of a simplified method to assess the structural reliability of conventional template-type offshore platforms is described in this section. The primary objectives are to identify the potential failure modes and weak-links of the structure and to estimate bounds on the probability of system failure by taking into account the biases and uncertainties associated with loadings and capacities (Figure 5.2).

With this in mind, the maximum static force acting on a platform is treated as a function of random variables. Its statistical properties are derived considering the uncertainties associated with environmental conditions, structure conditions, kinematics, and force calculation procedures. The expected capacity of the platform and the uncertainty associated with it are also characterized. The simplified ultimate limit state analysis procedures described in previous chapters are utilized to estimate an expected or best estimate capacity of the platform. The uncertainties associated with this capacity are

111

```
                    ┌─────────────┐
                    │ User Input  │
                    └─────────────┘
          ┌───────────────┴───────────────┐
          ▼                                ▼
┌──────────────────────┐       ┌──────────────────────┐
│    Probabilistic     │       │    Probabilistic     │
│Characteristics of Storm│      │  Characteristics of  │
│  Loading on Platform  │       │  Platform Component  │
│   Components, $S_i$   │       │   Capacities, $R_i$  │
└──────────────────────┘       └──────────────────────┘
          └───────────────┬───────────────┘
                          ▼
           ┌──────────────────────────────┐
           │     Component Reliability    │
           │       $G_i = R_i - S_i$      │
           │     $p_{fi} = P[G_i < 0]$    │
           └──────────────────────────────┘
                          ▼
           ╭──────────────────────────────╮
           │      System Reliability      │
           │ $max\,P_{fi} < P_{fs} < \sum P_{fi}$ │
           ╰──────────────────────────────╯
```
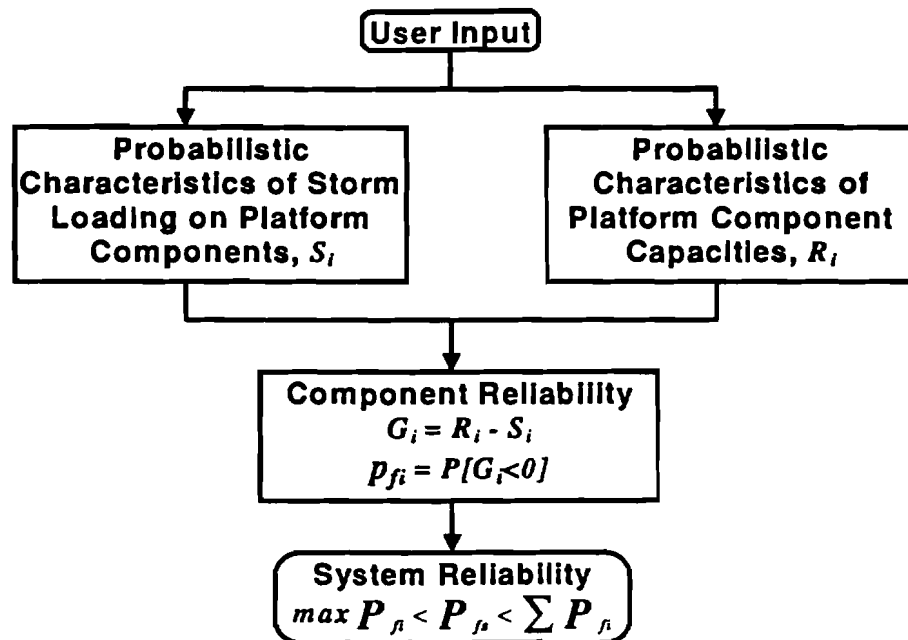
Figure 5.2: Probabilistic Failure Analysis

estimated using a combination of series components and parallel elements. The series components are the superstructure (deck), the substructure (jacket), and the foundation. The capacity of the platform is assumed to be reached when the capacity of anyone of these components is reached. Within each component there are parallel elements; deck legs, braces, joints, and piles. In order for a component to reach its upper-bound capacity, all of the parallel elements have to fail.

The proposed reliability analysis in this chapter is based on a first order second moment (FOSM) approach. A study is made of the implications of the simplified FOSM method. In

112

the case of an eight-leg drilling and production platform located in Gulf of Mexico (verification platform A), the results from FOSM reliability analysis are compared with those from first and second order reliability methods (FORM and SORM).

5.3.1 Structural Component and System Reliability

5.3.1.1 Component Reliability

The reliability analysis formulated in this chapter is based on the assumption of two-state structural components; a component can be in a safe- or fail-state. Furthermore it is assumed that the uncertainties associated with the state of the component can be described by random variables. For the basic structural component with the resistance R and load S, the probability of failure is equal to the probability that the load exceeds the resistance

$$p_f = P[R < S] \tag{5.3}$$

Assuming that R and S are random variables with the joint probability density function $f_{RS}(r,s)$, the probability of failure can be written as

$$p_f = \iint_{r \leq s} f_{RS}(r,s)drds \tag{5.4}$$

In general, the resistance R and the load S are themselves functions of random variables. Assuming $X(x_1, x_2, ..., x_n)$ to be a set of random variables that completely describe the load and resistance characteristics with a joint probability density function $f_X(x)$, and further assuming that the state of the component is described by a function $g(x)$ so that $g(x) = <0$ indicates failure, the probability of failure can be given by the n-fold integral

$$p_f = \int_{g(x) \leq 0} f_X(x)dx \tag{5.5}$$

g(x) is often referred to as limit state function. Problems associated with evaluating the above integral include: a) $f_x(x)$ may not be completely known due to lack of statistical data, b) the limit state function, *g(x)*, may not completely describe the true state of the component, and c) even in absence of problems stated above, integrating the above integral can be a formidable task (Der Kiureghian, 1994).

To circumvent these problems, reliability measures under incomplete statistical information have been developed. Indeed much of the early work on reliability analysis was based on such measures. The complete handling of the subject is not within the scope of this dissertation, however, the background used to develop simplified reliability analysis formulations for jacket offshore structures is summarized in the following.

Based on a mean value first order second moment (MVFOSM) approximation and using the load and capacity equations formulated earlier in this and other chapters, the mean and standard deviation of loads acting on and capacities of platform components can be estimated. Given that the resistance *R* of a component is a function of random variables $(x_1, x_2, ..., x_n)$, its first two statistical moments can be given by

$$\mu_R \approx R (M_x)$$ (5.6)

and

$$\sigma_R^2 \approx \nabla R \mid_{M_x} \Sigma \nabla R^T \mid_{M_x}$$ (5.7)

where

$$M_x = \begin{bmatrix} \mu_{x1} & \mu_{x2} & \cdots & \mu_{xn} \end{bmatrix}$$ (5.8)

is the mean vector of the resistance function and

$$\Sigma = \begin{bmatrix} \sigma_{x1}^2 & \rho_{12}\sigma_{x1}\sigma_{x2} & \cdots & \rho_{1n}\sigma_{x1}\sigma_{xn} \\ \rho_{21}\sigma_{x2}\sigma_{x1} & \sigma_{x2}^2 & \cdots & \rho_{2n}\sigma_{x2}\sigma_{xn} \\ \cdots & \cdots & \cdots & \cdots \\ \rho_{n1}\sigma_{xn}\sigma_{x1} & \rho_{n2}\sigma_{xn}\sigma_{x2} & \cdots & \sigma_{xn}^2 \end{bmatrix}$$ (5.9)

defines the covariance matrix, whereas

$$\nabla R = \begin{bmatrix} \dfrac{\partial R}{\partial x_1} & \dfrac{\partial R}{\partial x_2} & \cdots & \dfrac{\partial R}{\partial x_n} \end{bmatrix}$$ (5.10)

is the gradient vector of the resistance function which is evaluated at the mean vector in Equation (5.8). The same formulations can be written for the load function S. Defining a safety margin as:

$$M = \ln R - \ln S$$ (5.11)

the probability of failure can be given by:

$$p_f = CDF(U)$$ (5.12)

where

$$U = \frac{(M - \mu_M)}{\sigma_M}$$ (5.13)

is a standard variate with zero mean and unit standard deviation. μ_M and σ_M are the mean and standard deviation of the safety margin respectively. Presuming lognormal distribution for loads and capacities, the exact reliability index can be given as:

$$\beta = \frac{\mu_M}{\sigma_M} \tag{5.14}$$

where

$$\mu_M = ln\left(\frac{\mu_R}{\mu_S}\sqrt{\frac{1+V_S^2}{1+V_R^2}}\right) \tag{5.15}$$

$$\sigma_M^2 = ln\left(1+V_R^2\right)+ln\left(1+V_S^2\right)-2ln\left(1+\rho_{RS}V_RV_S\right) \tag{5.16}$$

and

$$P_f = \Phi\left(-\beta\right) \tag{5.17}$$

where $\Phi(.)$ is the cumulative standard normal function. Note that these equations and those derived for jointly normally distributed loads and capacities are the only known exact and closed form solutions of the probability of failure for non-trivial distributions of loads and capacities.

5.3.1.2   System Reliability

Unimodal bounds on probability of failure of a series system, p_{fs}, can be estimated by

$$max\; P_{fi} < P_{fs} < \sum_i P_{fi} \tag{5.18}$$

where p_{fi} denotes the probability of failure of the ith component. The lower bound is based upon the assumption of perfect correlation among all component failure modes. The upper bound is based upon the assumption of no correlation among the component failure modes. In general, unimodal bounds are useful when there exists a dominating failure mode. However, in case of offshore platforms, the failure of different structural

116

components has been shown to be strongly correlated mainly due to common dominating uncertainties in loading variables (Thoft-Christensen and Baker, 1982, Nordal et al., 1988).

5.3.2 Probabilistic Loading and Capacity Formulations

Probablisitc characteristics of long term extreme storm conditions and hydrodynamic loads acting on fixed offshore platforms are the focus of this research. These characteristics can be very different from those of short term nominal environmental conditions and loads. Although the short term distribution of wave heights can be described by a Rayleigh distribution, a theoretical long term wave height distribution has not been derived (Bea, 1990). Lognormal and Weibul probability distributions have been shown to provide acceptable fits to the data for many applications.

Given the wave height and its associated period, there are uncertainties associated with predicting the wave kinematics (water particle velocities and accelerations). The primary source of these uncertainties is the incomplete physical modeling of the complex processes. Wave theories that try to predict the wave kinematics have been developed based on many idealizing assumptions, including wave regularity, directionality, and propagation (Chapter 3). Given the water particle kinematics, there also are uncertainties associated with predicted local and global forces acting on an offshore platform. The primary source of these uncertainties is the force calculation model and the associated empirical drag and inertia coefficients (Bea, 1990; Haver, 1995).

Offshore engineering research has traditionally used field measurements and laboratory experiments to calibrate existing wave kinematics and load models and establish the uncertainties associated with the predictions of these models. The Conoco Test Structure (Bea et al. 1986) and Ocean Test Structure (Haring et al. 1979) are two examples of highly instrumented platforms to measure wave kinematics and forces on offshore structures. The measured data indicates that the primary difference between predicted and measured wave kinematics and forces is due to irregularity and directional spreading of real waves generated during intense storms.

Given the wave height, the API wave and current force calculation procedure is expected to result in unbiased estimates of the forces acting on offshore platforms provided appropriate coefficients are used (Heideman and Weaver, 1992). The kinematics modification factors and the force coefficients recommended in API RP 2A (API, 1993a) guidelines are based on large numbers of experimental test data and field measurements. For a given Keulegan-Carpenter number (e.g. KC>30), the uncertainties associated with the force coefficients are found to be rather small (COV=0.05) (Haver, 1995).

Wave height is the governing parameter in the API load calculation procedure. However, various investigators have found that wave forces can be more closely correlated to wave crest elevations (Haver, 1995). This is particularly true, if the crest elevation exceeds the elevation of lower platform decks. The probabilistic characteristics of wave-in-deck

118

loadings are of extreme importance for structural risk assessment studies of offshore platforms. Tromans et al. (1992) found that the only significant source of modeling uncertainty relates to wave-in-deck forces which is due to modeling uncertainties in local water particle kinematics close to the free surface. For predicted wave-in-deck forces, a total coefficient of variation of 70% has been suggested by Petrauskas et al. (1994). For a given wave height, a conditional COV for predicted wave-in-deck force of 0.35 has been recommended by API (1994).

Hydrodynamic wave forces on platform decks are not only important due to their magnitude, but also because of their effect on the global load pattern. A load pattern that includes relatively large deck forces can result in failure modes different from those predicted based on a load pattern that does not include wave-in-deck forces (Loch and Bea, 1995).

To perform structural risk analyses of a platform, it is necessary to characterize the limit states of the structure and the uncertainties associated with them. In this research, the ultimate limit state of the structure at collapse is considered (as opposed to serviceability limit state). With the exception of foundation capacities, the uncertainties associated with the ultimate static capacity of structural components are small compared to loading related uncertainties. In some case studies, the platform capacity is assumed to be a deterministic value (Bea and Smith, 1987; Haver, 1995). This capacity is estimated by performing nonlinear structural analyses (e.g. pushover analyses) using mean values or best estimates

for capacity parameters. The probability of failure is estimated as the likelihood that the random load exceeds the deterministic capacity. In a general case, however, the uncertainties associated with platform component capacities need to be considered. This is particularly true, when a foundation failure mode is a potential collapse mechanism. The large uncertainties associated with foundation axial and lateral capacities are primarily due to the inherent variability of ocean floor soils, soil sampling and testing procedures, the complexity of marine sub-sea construction, and modeling of pile-soil and loading interaction (Bea, 1990).

Considering a platform as a series of structural components, its structural reliability can be evaluated by using the formulations given earlier. The series components are the superstructure (deck), each bay of the substructure (jacket), and the foundation. The capacity of the platform is reached when the capacity of any one of these components is reached. Within each component there are parallel elements; deck legs, braces, joints, and piles. In order for a component to reach its upper-bound capacity, all of the parallel elements have to fail.

Using a first-order Taylor-series approximation around the mean point, the required means and standard deviations of loads and capacities can be computed. By specifying the means of input variables, the mean lateral load acting on components and the mean component capacities are estimated. Simplified loading and capacity equations have been developed in

the previous Chapters 3 and 4. Some of these equation are used in this section and are repeated for the sake of completeness.

5.3.2.1 Loading Formulation

A combination of storm wind load and hydrodynamic wave and current loads is considered

$$S = S_w + S_h \tag{5.19}$$

The wind load is given by

$$S_w = K_w V_{wd}^2 \tag{5.20}$$

where K_w is a structure dependent loading parameter, and V_{wd} is the wind speed that occurs at the same time as the maximum wave height.

The total integrated hydrodynamic drag force acting on a surface piercing vertical cylinder can be expressed as

$$S_h = K_d K_u H^2 \tag{5.21}$$

K_u is an integration function that integrates the velocities along the cylinder and is a function of wave steepness and the wave theory used to estimate the velocities. K_d is a force coefficient and a function of mass density of water ρ, diameter of the cylinder D, and drag coefficient C_d. The mean forces acting on the elements are integrated and the shear force at each component level is calculated. These integrated shear forces define the means of the load variables S_D for deck, S_{Ji} for each jacket bay, and the base shear S_F for the foundation bay. The coefficient of variation of the wave load is given as

$$V_s = \sqrt{V^2_{K_i} + V^2_{K_i} + \left(2V_H\right)^2}$$ (5.22)

The dominating storm loading parameters are the maximum wave height and its associated period. An evaluation of the uncertainties in the wind forces does not play a major role and is not included.

5.3.2.2 Capacity Formulation

Deck Legs' Shear Capacity

A mechanism in the deck leg bay would form when plastic hinges are developed at the top and bottom of all of the deck legs. Using this failure mode as a virtual displacement, virtual work principle can be utilized to estimate the deck leg shear resistance R_d (Chapter 4)

$$R_d = \frac{1}{L_d}\left(2n\,M_u - Q\Delta\right)$$ (5.23)

where

$$\Delta = M_U\,L_d\left(\frac{L_d}{6EI} + \frac{1}{C_r}\right)$$ (5.24)

$$\frac{M_u}{M_{cr}} - cos\left(\frac{\pi}{2}\frac{Q\,/\,n}{P_{crl}}\right) = 0$$ (5.25)

The moment capacity of the legs M_{cr} and the local buckling capacity P_{crl} are treated as random variables. Assuming perfect correlation between M_{cr} and P_{crl}, the variance of deck legs capacity can be given as

$$\sigma_{R_d}^2 = \sigma_{M_{cr}}^2\left(\frac{\partial R_d}{\partial M_{cr}}\right)^2 + \sigma_{P_{crl}}^2\left(\frac{\partial R_d}{\partial P_{crl}}\right)^2 + 2\sigma_{M_{cr}}\sigma_{P_{crl}}\left(\frac{\partial R_d}{\partial M_{cr}}\right)\left(\frac{\partial R_d}{\partial P_{crl}}\right) \tag{5.26}$$

where $\dfrac{\partial R_d}{\partial M_{cr}}$ and $\dfrac{\partial R_d}{\partial P_{crl}}$ are the partial derivatives of the deck legs shear capacity R_d with

respect to critical moment and buckling capacities M_{cr} and P_{crl}, evaluated at the mean

values $\mu_{M_{cr}}$ and $\mu_{P_{crl}}$.

Jacket Bays' Shear Capacity

Shear capacity in a given jacket bay is assumed to be reached when the vertical diagonal

braces or their joints are no longer capable of resisting the lateral load acting on the jacket

bay. Tensile and compressive capacity of the diagonal braces, the associated joint

capacities, and the batter component of axial forces in the legs due to overturning moment

are included to estimate the jacket bay shear capacity. The capacity of a given brace is

taken as the minimum of the capacity of the brace or the capacity of either its joints.

It should be noted that the diagonal brace capacities are negatively correlated with the

lateral loading. To implicitly account for this correlation, Equation (4.12) is rewritten in

the following format

$$P_u = \frac{M_u}{8\Delta_o\left(\dfrac{1}{1+2\dfrac{\sin 0.5\varepsilon}{\sin\varepsilon}}\right)\dfrac{1}{\varepsilon^2}\left(\dfrac{1}{\cos\dfrac{\varepsilon}{2}}-1\right)} - \frac{wl^2}{8\Delta_o} \tag{5.27}$$

Thus the variance of the compression capacity of a brace can be given by

123

$$\sigma^2_{P_u} = \sigma^2_{P_{cr}} + \left(\frac{l^2}{8\Delta_0}\right)^2 \sigma^2_w \qquad (5.28)$$

where it is assumed that Δ_0 is a deterministic parameter and that the first term in Equation (5.27) equals the buckling load of the brace in the absence of lateral distributed load w

$$P_{cr} = \frac{M_u}{8\Delta_0 \left(\frac{1}{1 + 2\frac{\sin 0.5\varepsilon}{\sin \varepsilon}}\right)\frac{1}{\varepsilon^2}\left(\frac{1}{\cos\frac{\varepsilon}{2}} - 1\right)} \qquad (5.29)$$

To obtain the statistical properties of the joint-brace-joint system, it is assumed that the tensile and compressive capacities of joint and vertical diagonal braces are lognormally distributed. Using the results of structural system reliability for series systems, the cumulative distribution function of the ultimate capacity of a joint-brace-joint system can be given as

$$F_R(r) = 1 - \prod_i \left[1 - \Phi\left(\frac{\ln r - \lambda_i}{\xi_i}\right)\right] \qquad (5.30)$$

where

$$\lambda_i = \ln(\mu_i) - \frac{1}{2}\xi_i^2 \qquad (5.31)$$

$$\xi_i^2 = \ln\left(1 + \frac{\sigma_i^2}{\mu_i^2}\right) \qquad (5.32)$$

where μ_i and σ_i ($i=1$ to 3) denote the mean and standard deviation of the tensile or compression capacity of the brace and its associated joints. Given the capacity distribution

124

function $F_R(r)$, μ_R and σ_R the mean and standard deviation of the capacity of joint-brace-joint system can be estimated using numerical integration.

To estimate the lateral capacity of a given jacket bay, it is assumed that interconnecting horizontal brace elements are rigid. Thus, the lower-bound capacity of the nth jacket bay R_{Jn}, which is associated with the first member failure in that bay, can be given as (Chapter 4)

$$R_{Jn} = \sum_i \overline{\alpha}_n K_i + F_L \qquad (5.33)$$

where F_L is the sum of batter components of axial pile and leg forces in the given bay and

$$\overline{\alpha}_n = \frac{P_{u,MLTF}}{K_{MLTF}} \qquad (5.34)$$

is the lateral drift of the nth jacket bay at the onset of first member failure. K_i are deterministic factors accounting for geometry and relative member stiffness ($\overline{\alpha} K_i$ = horizontal shear force of brace element i at the onset of first brace or joint failure within the given bay). Assuming that there is no correlation between the capacity of the MLTF member and lateral shear in the jacket legs, the variance of the lower-bound capacity of the nth jacket bay can be given as

$$\sigma^2_{R_{Jn}} = \left(\sum_i K_i \right)^2 \sigma^2_{\overline{\alpha}} + B^2_{F_L} \sigma^2_{F_L} \qquad (5.35)$$

where

$$\sigma_{\overline{\alpha}} = \frac{\sigma_{Pu,MLTF}}{K_{MLTF}} \qquad (5.36)$$

125

B_{FL} denotes the bias associated with the batter component of axial leg forces F_L.

The upper-bound capacity of the nth jacket bay R_{Jn}, which is associated with failure of all main load carrying members in that bay, can be given as (Chapter 4)

$$R_{Jn} = \sum_i \alpha_i R_i + F_L \qquad (5.37)$$

where R_i is the horizontal component of resisting force of the joint-brace element i. α_i account for the post-yielding behavior of semi-brittle brace or joint elements ($\alpha_i R_i$ = residual strength of element i) and are assumed to have deterministic values. Assuming perfect correlation among the member capacities R_i and R_j within the given bay, the variance of the upper-bound capacity of the nth jacket bay can be given as

$$\sigma^2_{RJn} = \sum_{i,j} \alpha_i \alpha_j \sigma_{Ri} \sigma_{Rj} + \left(B_{FL} \sigma_{FL} \right)^2 \qquad (5.38)$$

Foundation Capacity

Two basic types of failure mode in the foundation are considered: lateral and axial. The lateral failure mode of the piles is similar to that of the deck legs. In addition to moment resistance of the piles, the lateral support provided by foundation soils and the batter shear component of the piles are considered. The lateral and axial capacity equations for piles in sand and clay are given in Chapter 4. These formulations are used to calculate the best estimate capacities. Considering the uncertainties in soil and pile material properties, the uncertainties associated with foundation capacities can also be estimated. However, due to lack of data regarding modeling uncertainties, the total uncertainties associated with axial

and lateral pile capacities are used in this research, which implicitly include the uncertainties associated with soil and pile parameters and capacity modeling. The uncertainty associated with the batter component of the pile force is added to the total capacity uncertainty for vertically driven piles.

Load tests and recent post-hurricane Andrew studies on marine foundations (PMB, 1995) have indicated that the traditional foundation capacity prediction procedures are conservatively biased (Chapter 4). Major sources of bias are found to be the dynamic nature of loadings and soil sampling and testing.

Bea (1987) found the following to be two of the important influences of dynamic loadings on offshore pile foundations: a) decrease in the capacity and stiffness due to cyclic loading and b) increase in the capacity and stiffness due to high rates of loading. Another source of bias in the foundation capacities is the quality of soil samples. Soil sample disturbance is unavoidable. Some of the sources of sample disturbance are drilling, sampling, significant pressure relief, packaging, transport and preparation for testing (Bea, 1987). Laboratory testing is also a source of bias in soil strength parameters.

5.3.3 Example Application

Using the formulations developed in the previous sections, the structural reliability of an offshore platform is determined. Located in the main pass area of the Gulf of Mexico, the 8-leg template-type platform is installed in a water depth of approximately 271 feet

(Figure 5.3). Designed and installed in 1968-70, the platform is exposed to high environmental loading developed by hurricanes passing through the Gulf. Because of its dominance, only wave force is considered. According to oceanographic studies performed for the site, the 100 year return period wave height, H_{100}, is 70 feet. The uncertainties associated with the expected annual maximum wave height predictions are assumed and given in Table 5.1. Considering these uncertainties result in a total bias of $B_H = 1.1$ and a coefficient of variation of $V_H = 0.34$. Assuming Lognormal and Type I Extreme Value distributions, the probabilistic characteristics of the expected annual maximum wave height are given in Table 5.2. The wave height distribution parameters were determined by fitting the tails of the distributions to the predicted extreme wave heights. The variabilities of the force coefficients given by Bea (1990) were used to estimate the uncertainties associated with the wave forces (Table 5.3). These estimates are consistent with the simplified analytical models employed to calculate the loadings.

It should be noted that once the wave crest elevation exceeds the platform lower deck elevation, the load pattern changes significantly and the total forces acting on the platform increase much faster than before. In the presented example, this fact has not been accounted for. In general, the problem can be circumvented by considering conditional probabilities (p_f/H). In this case, the total probability of failure can be estimated by

$$p_f = \int_h p_{f/H} f_H(h) dh \qquad (5.39)$$
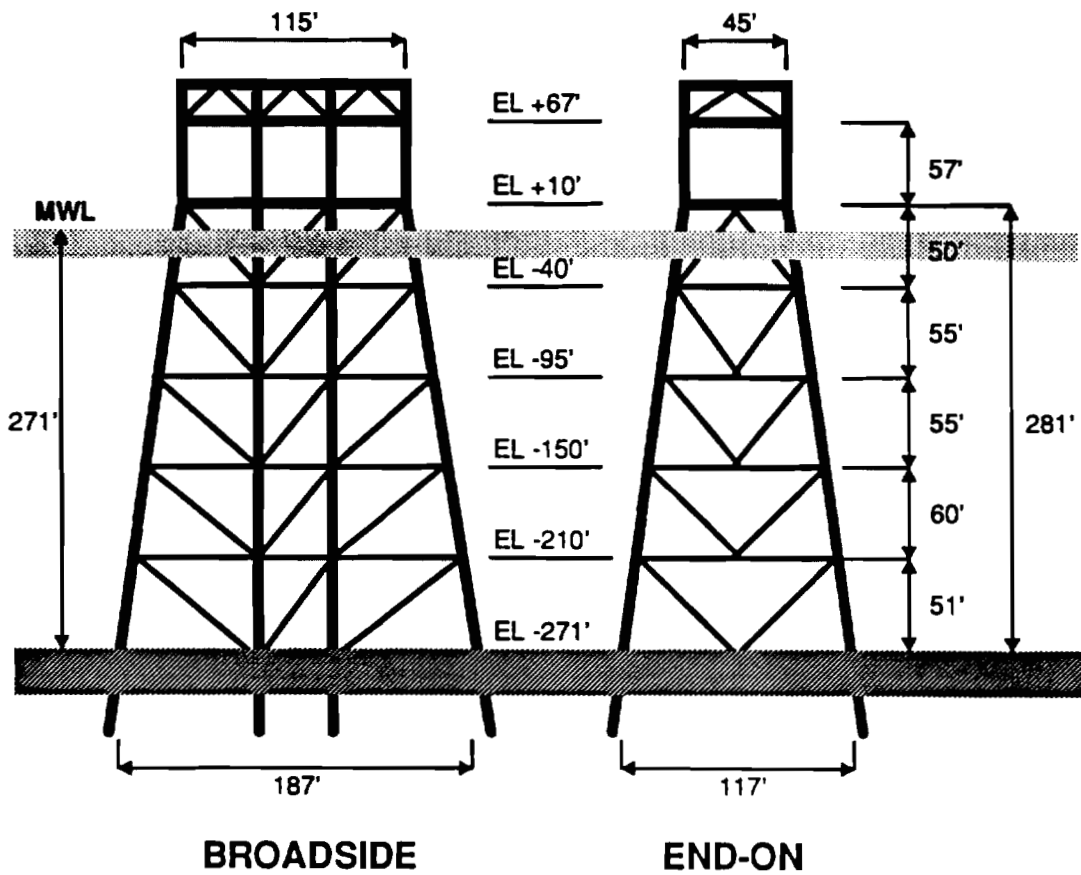
Figure 5.3: Example Platform Elevations

	σ_{lnH}	*Bias (B_H)*	σ_{lnBH}
H_{max}	0.3	1.1	0.13

Table 5.1: Wave Height Uncertainties (Example Platform)

$f_H(h)$	μ_H *(ft)*	σ_H *(ft)*
Lognormal	34.5	11.7
Type I largest	34.0	11.4

Table 5.2: Probabilistic Characteristics of the Maximum Wave Height
(Example Platform)

	σ_{lnK}	Bias (B_k)	σ_{lnBk}
K_u	0.1	0.41	0.47
K_d	0.1	1.67	0.23

Table 5.3: Force Coefficient Uncertainties (Bea, 1990)

Based on the background developed in the previous sections of this chapter, structural reliability of the example platform is studied for the two principal orthogonal directions. For each load direction, eight different failure modes are identified and analyzed; one in the superstructure, five in the substructure, and two foundation failure modes.

For critical bending moment M_{cr}, local buckling capacity P_{crl}, and global buckling capacity of diagonal braces P_{cr}, the mean-value curves given by Cox (1987) are utilized. These are

$$M_{cr} = M_p \left[1.113 \exp\left(\frac{-1.638 f_y D}{Et} \right) \right] \tag{5.40}$$

$$P_{crl} = P_y \left[1.79 - 0.25 \left(\frac{D}{t} \right)^{0.25} \right] \tag{5.41}$$

$$P_{cr} = P_y \left(1.03 - 0.24 \lambda^2 \right) \quad for \ 0 < \lambda < 1.7 \tag{5.42}$$

where

$$M_p = Z f_y \tag{5.43}$$

$$P_y = A f_y \tag{5.44}$$

$$\lambda = \left(\frac{1}{\pi} \right) \left(\frac{KL}{r} \right) \sqrt{\frac{f_y}{E}} \tag{5.45}$$

where Z, λ, and K are the plastic section modulus of the cross-section, slenderness ratio of the member, and buckling length factor respectively. For bending resistance, a combined coefficient of variation (COV) of 0.106 is given by Cox(1987). The COV for local buckling is 0.117, which includes the test uncertainties, uncertainties in steel yield

strength, and uncertainties associated with fabrication. This value is reported to be constant over the entire range of practical values of Et/fyD and D/t respectively. The uncertainties of column resistance over a practical range of λ are given in Table 5.4 (Cox, 1987). In addition to uncertainties associated with test and fabrication, the uncertainties associated with yield stress f_y, elastic modulus E, and effective column length factor K are included in the column resistance uncertainty.

λ	0.4	0.6	0.8	1.0	1.2	1.4
COV	0.099	0.100	0.106	0.119	0.150	0.212

Table 5.4: Column Resistance Uncertainties (Cox, 1987)

A tubular joint failure mode is not included in the presented reliability analysis since the leg-pile annulus and the joints are grouted and the joints are significantly stronger than the braces. In a general case, the joints' capacity and the uncertainties associated with it can be considered.

In the presented example, the upper-bound capacity formulation is used for the jacket bays. Deterministic values are assigned to brace residual strength factors α, which are calibrated to give results consistent with those gained from a detailed nonlinear pushover analysis of the studied platform (Bea, et al. 1995). In a general case however, the α factor is unknown and can be considered as a random variable itself. The uncertainty associated with this variable reflects the modeling uncertainty introduced by using simplifying

132

assumptions regarding residual strength of compression braces and stiffness properties of inter-connecting horizontal braces.

Lateral Capacity in:	Bias	COV
Clay	0.92	0.20
Sand	0.81	0.21

Table 5.5: Lateral Pile Capacity Uncertainties (Tang, 1990)

Axial Pile Capacity in:	Bias	COV
Sand	0.9	0.47 - 0.56
Clay	1.3 - 3.7	0.32 - 0.53

Table 5.6: Axial Pile Capacity Uncertainties (Tang, 1988)

Due to lack of data regarding the pile capacity modeling uncertainty, the total uncertainties recommended by Tang and Gilbert (1990) are used, which are based on test results and implicitly include the model uncertainties (Table 5.5). The uncertainty associated with the batter component of the pile force is added to the total capacity uncertainty given for vertical piles. Available test data on axially loaded piles indicate a very wide range in capacity bias. The uncertainties associated with axial capacities of driven piles are given by Tang (1988) (Table 5.6). Current studies of the performance characteristics of platforms subjected to storm loadings indicates that the mean biases in

133

lateral and axial pile capacities indicated in Tables 5.5 and 5.6 represent a lower bound (mean biases in the range of 2 to 3) (Bea et al. 1995b; 1995c).

To study the effect on FOSM results of different probability distributions of maximum wave height and nonlinear limit state functions, the computer program CALREL (Liu et. al., 1989) was used to perform FORM and SORM analyses in addition to FOSM analysis (Appendix B). In the case of lognormally distributed loads and capacities, the results from the simplified FOSM analysis and those from more sophisticated FORM and SORM are given in Tables 5.7 and 5.8 and Figures 5.3 and 5.4. FORM and SORM analyses have also been performed assuming Type I Extreme Value distribution for annual maximum wave height. No significant changes in the reliability indices are observed. The FOSM safety indices are close approximations to those determined from the FORM and SORM analyses.

The results indicate that the most probable failure mode in both loading cases involves the failure of the diagonals in the second jacket bay. The large uncertainties in storm loadings are due to uncertainties in force calculations and those associated with predicted wave heights. The large uncertainties in jacket bay capacities are mainly due to uncertainties associated with the lateral loading and the load-capacity correlation which is implicitly accounted for in this analysis. The uncertainties in lateral capacity of jacket bays are larger for the broadside loading direction than the end-on loading direction. This can be explained by the fact that for the broadside loading case, compressive buckling of diagonal

134

BROADSIDE LOADING	LOAD (KIPS)	BIAS	C.O.V.	CAP (KIPS)	BIAS	C.O.V.	FOSM β	Pf	FORM β	SORM β
DECK LEGS	197	0.83	1.03	2606	1.00	0.11	3.64	1.34E-04	3.51	3.51
JACKET										
BAY1	644	0.83	1.03	2932	1.00	0.08	2.61	4.52E-03	2.48	2.48
BAY2	621	0.83	1.03	2621	1.00	0.24	2.22	1.32E-02	2.08	2.12
BAY3	638	0.83	1.03	4130	1.00	0.45	2.41	8.07E-03	2.41	2.47
BAY4	641	0.83	1.03	5702	1.00	0.49	2.67	3.85E-03	2.75	2.80
BAY5	643	0.83	1.03	6157	1.00	0.48	2.75	2.94E-03	2.84	2.90
FOUNDATION										
LATERAL	643	0.83	1.03	7700	0.81	0.56	2.69	3.58E-03	2.67	2.67
AXIAL	1035	0.83	1.03	4063	1.5	0.31	2.52	5.79E-03	2.49	2.49

Table 5.7: Component Reliabilities Based on FOSM, FORM and SORM Analyses, Broadside Loading (Example Platform)

END-ON LOADING	LOAD (KIPS)	BIAS	C.O.V.	CAP (KIPS)	BIAS	C.O.V.	FOSM β	Pf	FORM β	SORM β
DECK LEGS	120	0.83	1.03	2606	1.00	0.11	4.22	1.20E-05	4.10	4.10
JACKET										
BAY1	424	0.83	1.03	1954	1.00	0.07	2.43	7.51E-03	2.29	2.29
BAY2	499	0.83	1.03	2046	1.00	0.10	2.28	1.13E-02	2.12	2.14
BAY3	515	0.83	1.03	2360	1.00	0.15	2.39	8.54E-03	2.25	2.28
BAY4	518	0.83	1.03	2538	1.00	0.20	2.43	7.62E-03	2.28	2.32
BAY5	520	0.83	1.03	2892	1.00	0.26	2.51	6.02E-03	2.38	2.43
FOUNDATION										
LATERAL	520	0.83	1.03	7200	0.81	0.53	2.88	1.96E-03	2.85	2.85
AXIAL	856	0.83	1.03	4063	1.5	0.31	2.74	3.12E-03	2.70	2.70

Table 5.8: Component Reliabilities Based on FOSM, FORM and SORM Analyses, End-on Loading (Example Platform)

Loading	Lower-Bound p_{fs}	Upper-Bound p_{fs}
End-on	0.011	0.046
Broadside	0.013	0.042

Table 5.9: Unimodal Bounds on annual p_f (Example Platform)

135
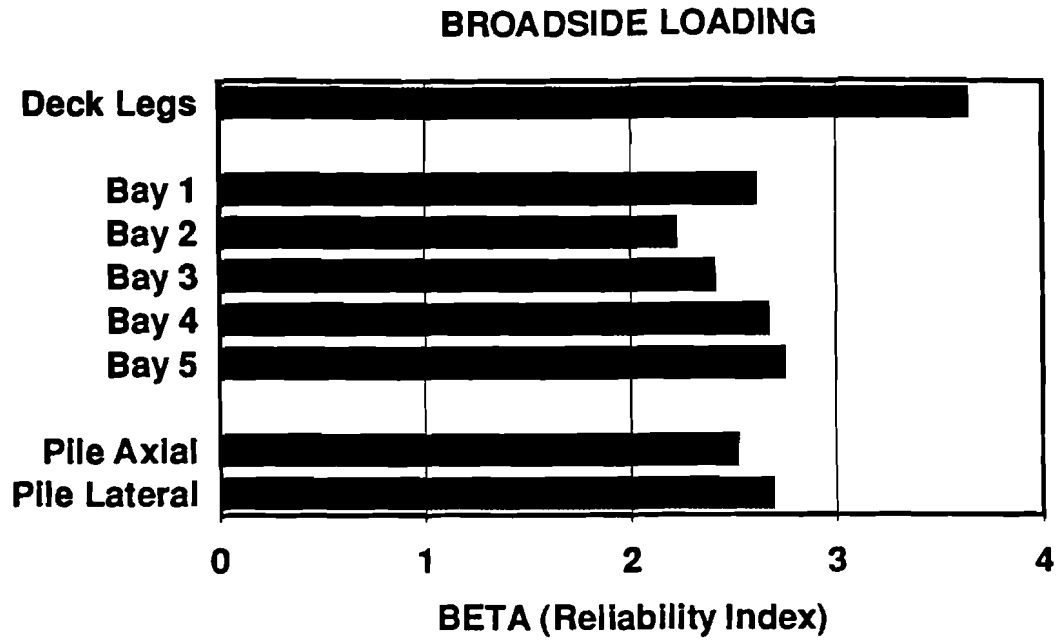
BROADSIDE LOADING

Figure 5.4: Annual Component Safety Indices for Broadside Loading
(Example Platform)
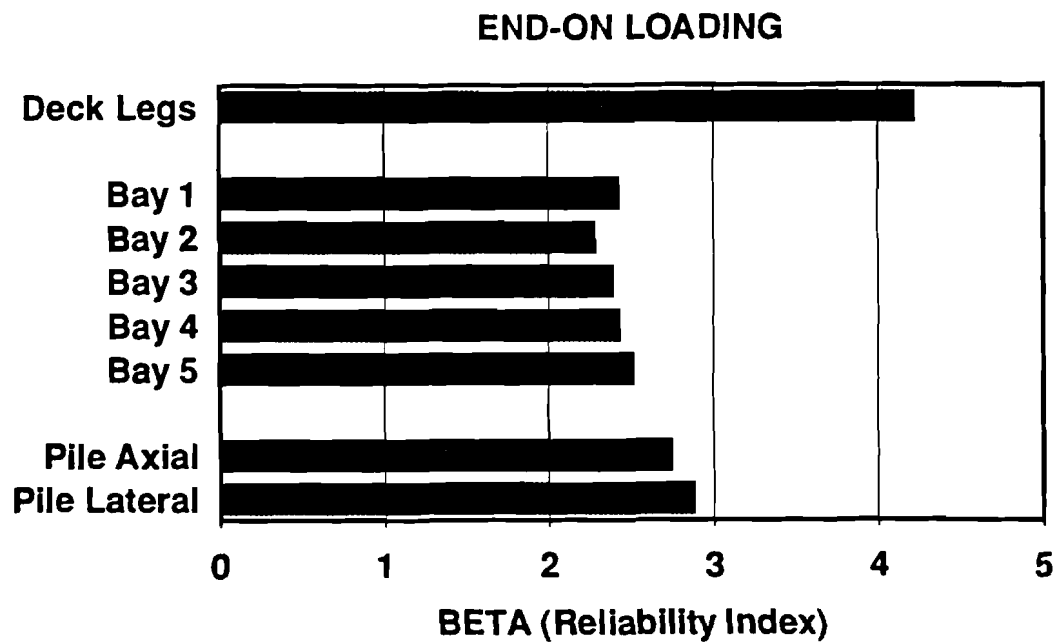
END-ON LOADING

Figure 5.5: Annual Component Safety Indices for End-on Loading
(Example Platform)

K-braces govern the failure of the jacket, whereas in the case of end-on loading, tensile yielding of diagonal braces govern the ultimate lateral loading capacity of the jacket. The compressive buckling of the braces is associated with much larger uncertainties than the tensile yielding. The foundation piles have safety indices that are comparable with those in the superstructure.

Based on the FOSM results, unimodal bounds on annual probabilities of failure are estimated for both loading directions and given in Table 5.9. The failure probabilities range from about 1% per year to 4% per year depending on the assumptions regarding correlation of the failure modes. Given the large loading uncertainties relative to those of the component capacities, one would expect the correlation of the failure modes to be nearly unity (Nordal et al. 1988). Thus, the most realistic failure probability would be represented by the lower-bound results.

5.4 Summary

A simplified procedure has been presented to perform structural reliability analysis of conventional, steel jacket-type, offshore platforms. This procedure can be used in the process of assessment and requalification of older platforms, or it can be used in the preliminary design phase of a new platform. The reliability analysis is based on a first order second moment approach. It is assumed that the loads and capacities are lognormally distributed.

A case study is performed and the structural reliability of an eight-leg offshore drilling and production platform located in Gulf of Mexico is studied. In addition to reliability indices for different failure modes, unimodal bounds for the system probability of failure is estimated. Using the computer program CALREL, first order and second order reliabilities are also computed. Two different distributions are selected for the maximum wave height; Lognormal and Type I Largest Value. In both cases the results are in good agreement with those from the simplified FOSM analysis.

CHAPTER 6

VERIFICATION CASE STUDIES

6.1   Introduction

This chapter summarizes the verification studies conducted during this research. The objective of this work was to examine the validity of the results of the simplified load and capacity calculation procedures. Three levels of verification were performed using results from

a)   detailed, three-dimensional, nonlinear pushover analyses,

b)   actual field performance of platforms during intense storms, and

c)   large-scale frame tests.

The simplified estimates of total forces acting on the platforms during intense storms and predictions of ultimate member strength and platform capacity were verified with results from detailed nonlinear analyses (Loch, Bea 1995). Thorough verification studies on six Gulf of Mexico (GOM) platforms were performed. Some of the studied platforms were on or very close to the path of hurricanes Frederic, Camille and Andrew. The available data on the actual field performance of these platforms (survival w/o damage, survival with damage, failure and failure mode) have been used to verify the predictions of the simplified procedures.

One effective way of verifying and calibrating the results of nonlinear finite element software programs is to perform large-scale frame tests. It is important to design such test programs so that the results are representative of actual behavior of offshore platforms. Large-scale test programs are expensive to perform. As a result, there are only a few performed in the past (e.g. Zayas et al., 1980; Grenda et al., 1988; Bolt et al., 1994; Bolt, 1995). The three recent test programs addressed the collapse performance of K-braced and X-braced frames representative of fixed template-type offshore platforms. The results of these tests have been used as a last level of verification of the simplified ULSLEA method. In the following sections, each test program is described and the verification results are reported and discussed.

6.2   Detailed Nonlinear Analyses and Actual Field Performance

Detailed three-dimensional nonlinear analyses were performed on six conventional Gulf of Mexico platforms (platforms A-F). The verification cases included five eight-leg and one four-leg drilling and production platforms. The characteristics of these structures are summarized in the following sections. For detailed description of the modeling process for platforms B-E refer to Loch (1995). Detailed modeling of platform F is documented by Stear and Bea (1995). In case of platform A, the results available from a detailed nonlinear pushover analysis were used to verify the simplified analysis' results (Bea and DesRoches, 1993). In the case of platforms B, C, D, E and F, the nonlinear finite element computer program USFOS (Sintef, 1993) was utilized to perform the static pushover analyses. In this analyses, wave and wind loads in the deck are manually calculated and applied as

nodal loads. The hydrodynamic forces on jacket were generated using the WAJAC wave load program (DNV, 1993). Stokes 5th-order wave theory was used to estimate the water particle kinematics. Member loads were calculated based on Morison (MJOS) equation. Wind forces were computed using the API RP 2A formulation assuming a drag coefficient of $C_s = 1.0$ for clear decks, 1.5 for cluttered and 2.0 for blocked decks. Hydrodynamic force coefficients and kinematic modification factors (drag and inertia coefficients, current blockage and directional spreading factors) were selected based on API RP 2A, 20th edition (API, 1993a). All verification platforms were analyzed for two principal orthogonal loading directions; end-on and broadside.

In the presented cases, the simplified analyses have been performed assuming elastic-perfectly plastic behavior for members in both tension and compression (a residual strength factor of $\alpha=1.0$) to estimate the upper-bound capacities of jacket bays. In all cases, the same oceanographic conditions and hydrodynamic coefficients utilized in the detailed analyses have been used to perform simplified analyses.

A detailed structural reliability analysis was performed on verification platform A and the results presented in Chapter 5. In addition to component reliability indices, bounds on the annual probabilities of failure were estimated for two different loading directions. Simplified structural reliability analyses were also performed for verification platforms B-F. Conditional component reliability indices were estimated for these platforms. The estimated reliability indices were conditional on maximum wave heights and their

associated periods that were used in performing deterministic pushover analyses of the same platforms (Bea et al., 1995c). In general, the uncertainties associated with loading and capacity parameters given in Chapter 5 were used for all studied platforms (Tables 5.3-5.6). Results are presented in terms of component reliability indices conditional on wave height and direction.

It should be noted that, for the presented case studies, neither in the deterministic pushover analyses nor in the probabilistic failure analyses has the contribution of well conductors to the lateral foundation capacity been taken into account. Nor has the increase in foundation capacities due to loading rate effects been considered (Chapter 4). The contribution of well conductors to the lateral foundation capacity and the loading rate effects would lead to an increase in the reliability indices associated with foundation failure modes.

6.2.1 Platform A

Platform A is an eight-leg drilling and production structure located in the Main Pass area of the Gulf of Mexico in a water depth of 271 feet (Figure 6.1). Designed and installed in 1968-70, the platform has been exposed to high environmental loading developed by hurricanes passing through the Gulf. The structure foundation consists of eight 42 in. piles which penetrate to a depth of 270 ft into medium sands overlaying stiff clays. The jacket legs are battered in two directions and the leg-pile annulus is grouted. The lower and upper decks are located at +46 ft and +63 ft respectively.

For this platform, a detailed nonlinear analysis was performed using a 9th-order stream function to compute wave crest elevations. A wave steepness of 1/12 was used (wave period of 12.8 seconds for the 100-year wave). According to 1988 wave crest elevations, waves with return period greater than hundred years will result in deck inundation. Marine growth at the site was taken as 1 in. and considered for all members located between the waterline and -100 ft. A three-dimensional platform computer model and a two-dimensional wave grid were used to compute the forces acting on the platform. The loading on each member throughout the platform was summed to determine the platform's base shear. The process was repeated as the wave was moved through the structure in 24 increments to compute the maximum base shear. The drag coefficient was taken as $C_d = 0.7$ and the inertia coefficient was taken as $C_m = 1.5$.

The maximum lateral forces were computed using both the simplified and detailed analyses. These forces are plotted versus the return period. This is done for both broadside and end-on directions. Compared to the results of detailed analyses, total lateral forces were overpredicted by up to 20% (Figures 6.2 and 6.3). The principal difference was traced to modeling assumptions in the simplified analysis: all of the platform elements are modeled as equivalent vertical cylinders that are concentrated at a single vertical position in the wave crest.

The ultimate limit states were determined for the platform's orthogonal directions. In the case of broadside loading with wave crest reaching the deck, the ultimate capacity was reported to be 2,935 kips (Figure 6.4). In this case, the failure was due to buckling of compression braces at the second jacket bay. In the case of end-on loading, the wave-in-deck condition resulted in an ultimate capacity of 2,607 kips. Most of the member failures were due to compressive buckling of braces (Figure 6.6). The analysis indicated a brittle strength behavior and little effective redundancy which is a typical result for K-braced platform systems.

In broadside loading direction, the simplified analysis predicted a failure mode in the second jacket bay at a total base shear of about 3,400 kips (Figure 6.5). In end-on loading direction, the simplified analysis indicated a failure due to buckling of compression braces in the uppermost jacket bay at a lateral load of 2,900 kips (Figure 6.7). These results are 10 to 15% higher than those gained from detailed nonlinear analyses. The principal difference lies in the differences between the two programs (SEASTAR/ULSLEA) in nonlinear modeling of vertical diagonal braces.

This platform was very close to the path of hurricane Frederic. It survived the storm without significant damage. Both the simplified and detailed nonlinear analyses were able to predict the observed performance of the platform during the storm. The analyses indicated that the platform should have survived the storm, and it did.

144
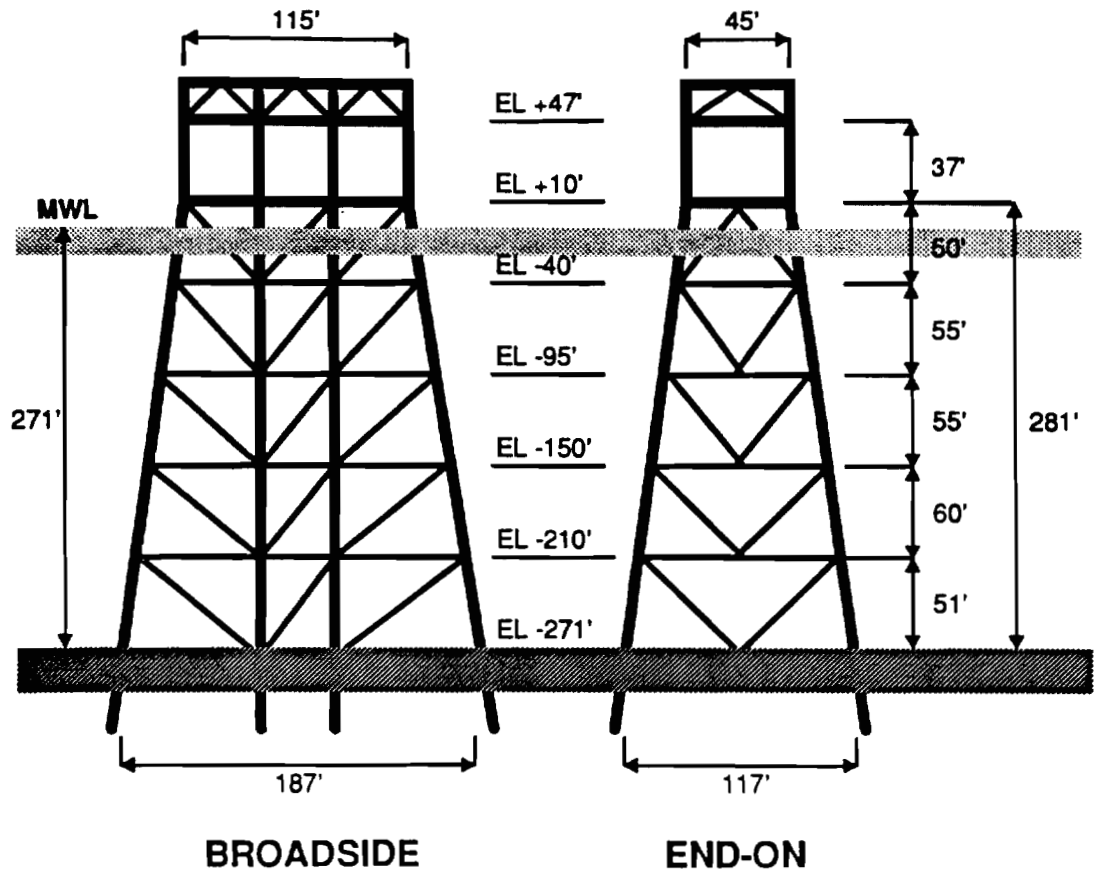
Figure 6.1: Platform A Elevations

145

TOTAL LATERAL FORCE (BROADSIDE)
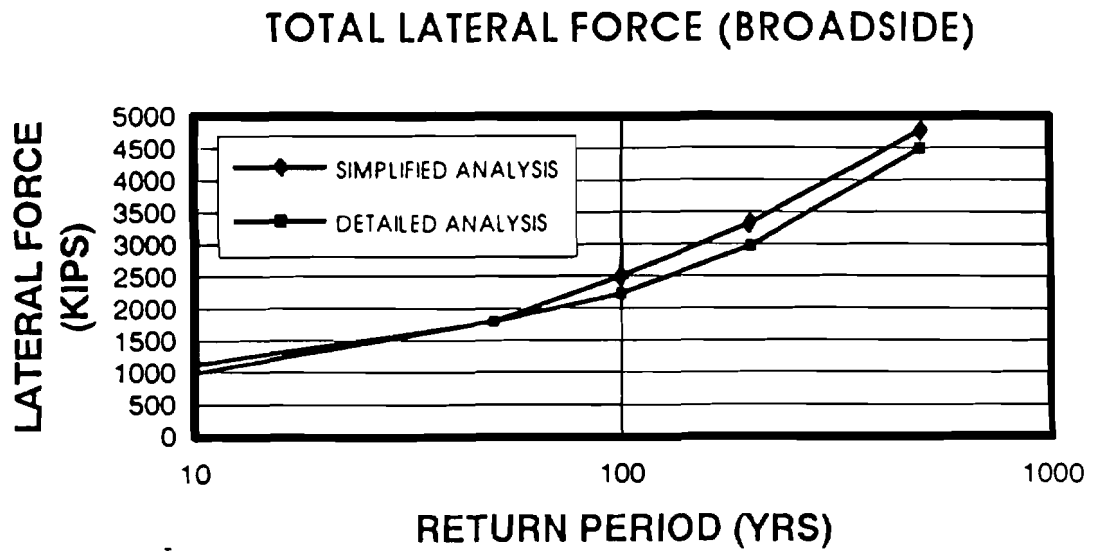
Figure 6.2 : Platform   A   Broadside Loading

TOTAL LATERAL FORCE (END-ON)
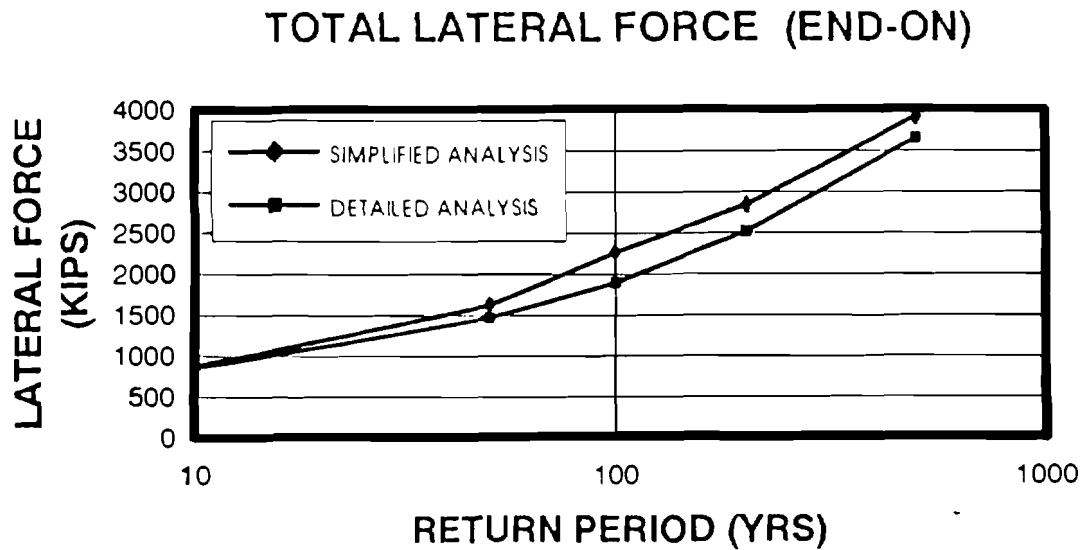
Figure 6.5 : Platform   A   End-on Loading

146
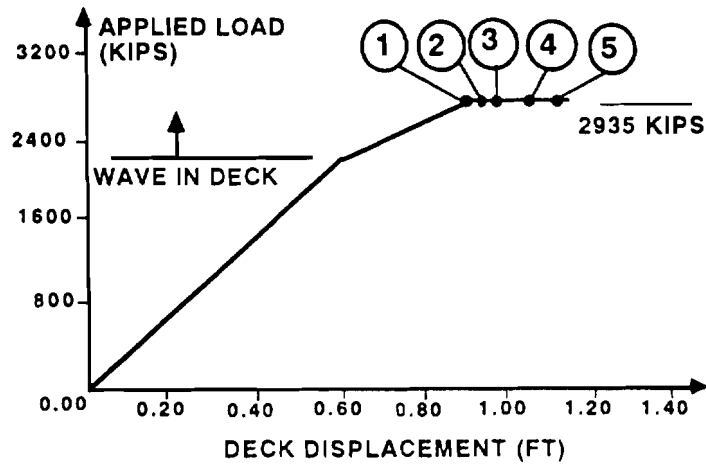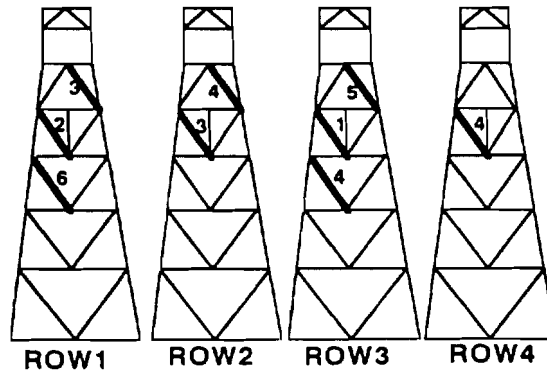
Figure 6.3 : Platform   A   Broadside Capacity (SEASTAR)

Storm Shear / Platform Shear Capacity (kips)
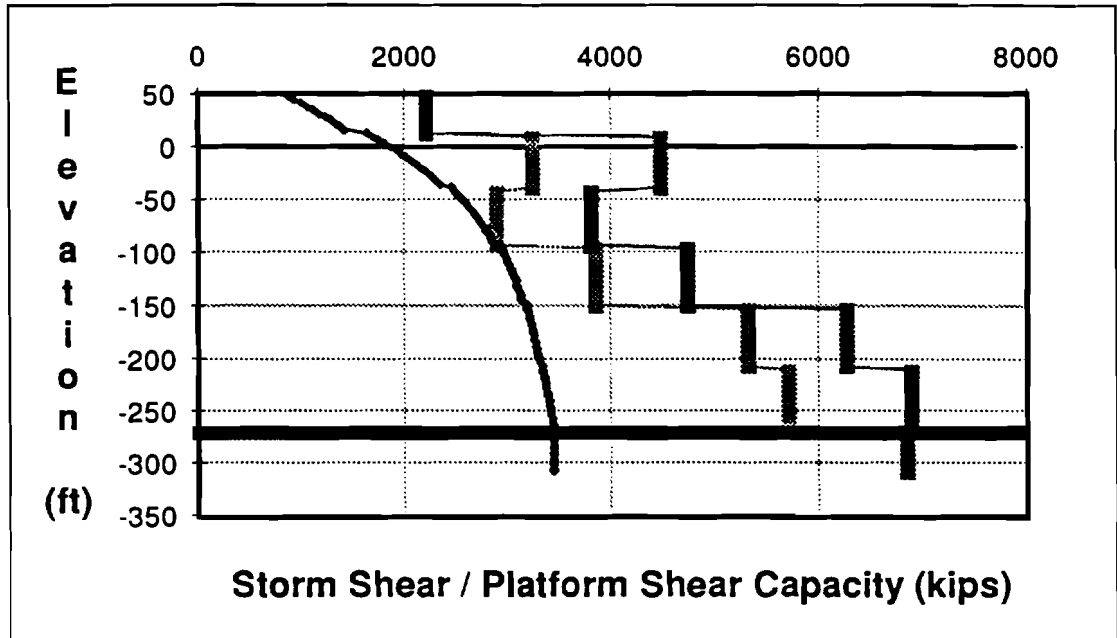
Figure 6.4 : Platform   A   Broadside Shear Capacity (ULSLEA)

147
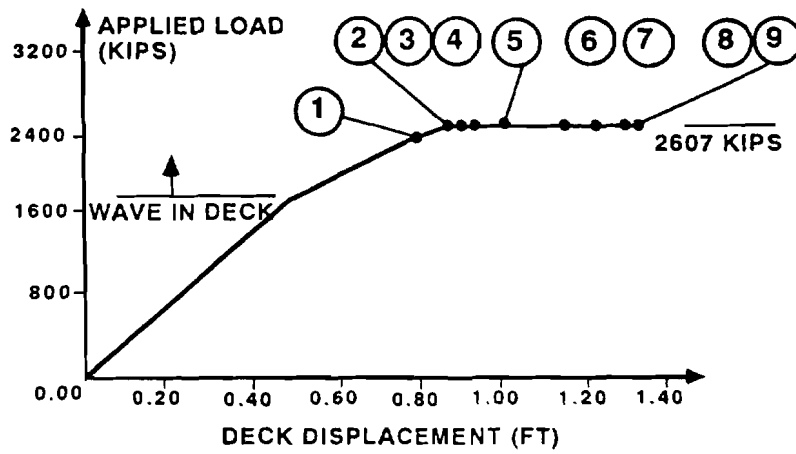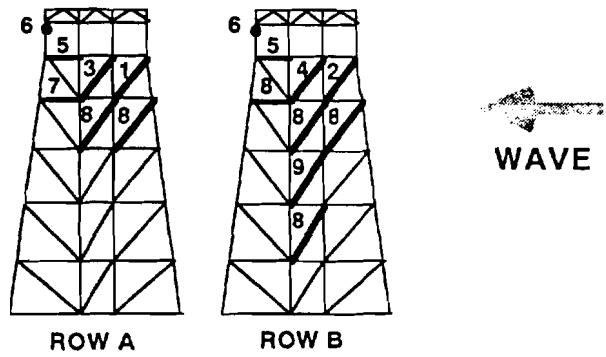
Figure 6.6 : Platform A End-on Capacity (SEASTAR)

Storm Shear / Platform Shear Capacity (kips)
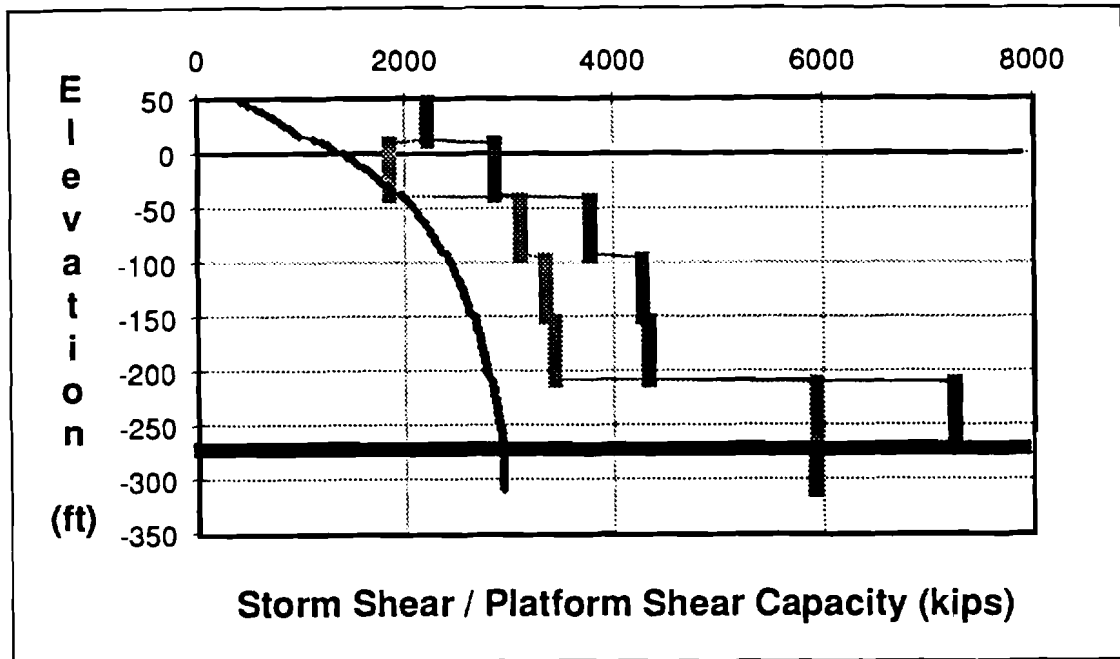
Figure 6.7 : Platform A End-on Shear Capacity (ULSLEA)

6.2.2 Platform B

Platform B is an eight-leg structure located in the Gulf of Mexico's South Timbalier region in a water depth of 118 ft (Figure 6.8). The platform was designed using a design wave height of 55 ft. The cellar and main decks are located at +36 ft and +47 ft, respectively. The 39 in. jacket legs are battered in two directions and have no joint cans. The 36 in. piles are grouted inside the jacket legs and driven to a depth of 190 ft. The foundation soils consist primarily of gray clay. Expected steel yield stresses of 58 and 43 ksi were used for diagonal braces and jacket legs (and piles) respectively.

Nonlinear pushover analysis results indicated that the platform is capable of resisting 3,850 kips in broadside loading (Figure 6.13). The failure mechanism developed in the uppermost jacket bay due to buckling of the compression braces. The analysis indicated a brittle strength behavior and no effective redundancy. The analysis indicated the platform's end-on resistance capacity to be approximately 3,900 kips (Figure 6.17). Failure began in the uppermost jacket bay, where the four diagonal compression braces buckled almost simultaneously. The failure mechanism was completed when the horizontal struts in the upper jacket bay buckled in addition to compression braces.

A simplified limit equilibrium analysis was also performed for this platform. Since the same procedure was used to estimate the wind and wave forces on the projected deck areas, they were essentially the same for both detailed and simplified analyses. In broadside loading direction, the simplified force calculation procedures overestimated the

hydrodynamic loads on the jacket by 7% (Figures 6.9 and 6.10). In end-on loading direction, the jacket loads were overestimated by 15% (Figures 6.15 and 6.16). For each loading direction, the predicted performance of MLTF (most likely to fail) vertical diagonal brace was verified. Using the same initial out-of-straightness for both simplified (ULSLEA) and complex (USFOS) analyses, the simplified column buckling formulation overpredicted the peak member load (given by USFOS) by 6% and 9% for end-on and broadside loading directions respectively. Using the calibrated format of simplified column buckling equations with a buckling length factor of K=0.65, the simplified analysis underpredicted the peak load by 7% and 1% for end-on and broadside loading directions respectively.

To study the effect of K-factor on predicted buckling load, a sensitivity analysis was performed. The calibrated buckling capacity formulation gave the "exact" result (given by USFOS) when buckling length factors of K=0.63 and 0.57 were used for MLTF members in compression for broadside and end-on loading directions respectively (Figures 6.11 and 6.12). Note that in the latter case, the brace is connected to jacket legs at both ends and is therefore stiffer. It is interesting to note that this result is in good agreement with those presented by Hellan et al. (1994).

The platform shear capacity and storm shear profiles are plotted versus platform elevation (Figures 6.14 and 6.18). In case of broadside loading and using a buckling length factor of K=0.65 for braces in compression, the simplified analysis predicted a failure mode in the

150

deck legs and uppermost jacket bay at a total base shear of about 3,600 kips, which is in good agreement with the results from nonlinear analysis (~ 6% underprediction) (Figures 6.13 and 6.14). In case of end-on loading with a buckling length factor of K=0.55 for compression braces, the simplified analysis predicted a collapse load of 3,100 kips (~ 20% underprediction) due to failure of compression braces in the top jacket bay (Figures 6.17 and 6.18). The source of this underprediction is found to be the somewhat conservative shear force correction procedure, which is developed in Chapter 4 of this report.

The conditional component reliability indices are plotted in Figures 6.19 and 6.20 for broadside and end-on loading directions respectively. These results are conditional on the wave height and direction. Figure 6.19 indicates that in case of broadside loading, the uppermost jacket bay, the deck legs, and the piles in lateral mode are the most likely to fail components of the platform. The axial foundation failure is the least likely collapse mechanism. Relatively large reliability indices for axial foundation failure mode are typical results for the studied platforms with stiff clay as the dominant foundation soil material. In the presented studies, a bias factor of 3.0 is used for axial pile capacity in clay (Tang, 1988). The low reliability indices associated with the uppermost jacket bay and deck legs are in agreement with the deterministic analysis results (Figure 6.14). However, the low reliability index associated with a lateral foundation failure mode is not in agreement with the deterministic analysis results. This discrepancy is due to large uncertainties associated with the lateral loads and foundation capacity, which are accounted for in the reliability analysis. Similar conclusions can be drawn for the end-on loading direction (Figure 6.20).

Hurricanes Carmen (1974) and Andrew (1992) passed within a few miles of verification platform B. Damage to the lower decks of the platform suggested that the structure had been subjected to up to 58 feet waves during hurricane Carmen. A post-hurricane platform condition assessment revealed some damage to the vertical diagonal joints at the top of the uppermost jacket bay. In 1988, the platform was the subject of a comprehensive risk analysis. Consequent risk mitigation measures included removal of the conductors and all equipment from the lower decks. In 1992, damage to the cellar deck and hindcast studies performed following the passage of hurricane Andrew suggested maximum wave heights of 60 to 64 feet approximately 15 degrees off of platform broadside. The platform survived with some yielding damage to the K-joints at the top of the uppermost jacket bay. It was estimated that the absence of the conductors and equipment on the lower decks reduced the total base shear by 20 percent.

For a broadside loading scenario, ULSLEA predicted failure of the brace-joint system at the uppermost jacket bay at a total base shear of 3,600 kips (Figure 6.14). The load pattern used was based on a 64 feet wave and a storm tide of 6 feet. The lower-bound lateral loading capacity of the platform was reached at roughly 90% of this load. This result indicated that the platform was very close to failure during hurricane Andrew. The predicted failure mode was also in agreement with the observed damage.
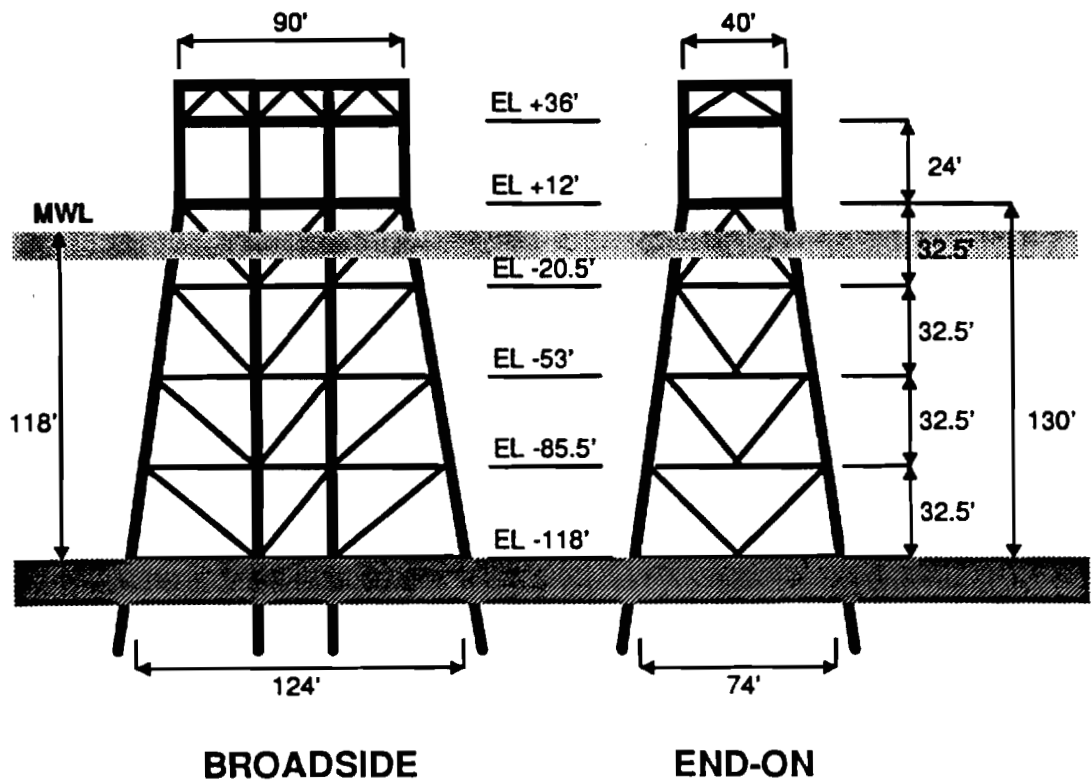
Figure 6.8 : Platform B Elevations
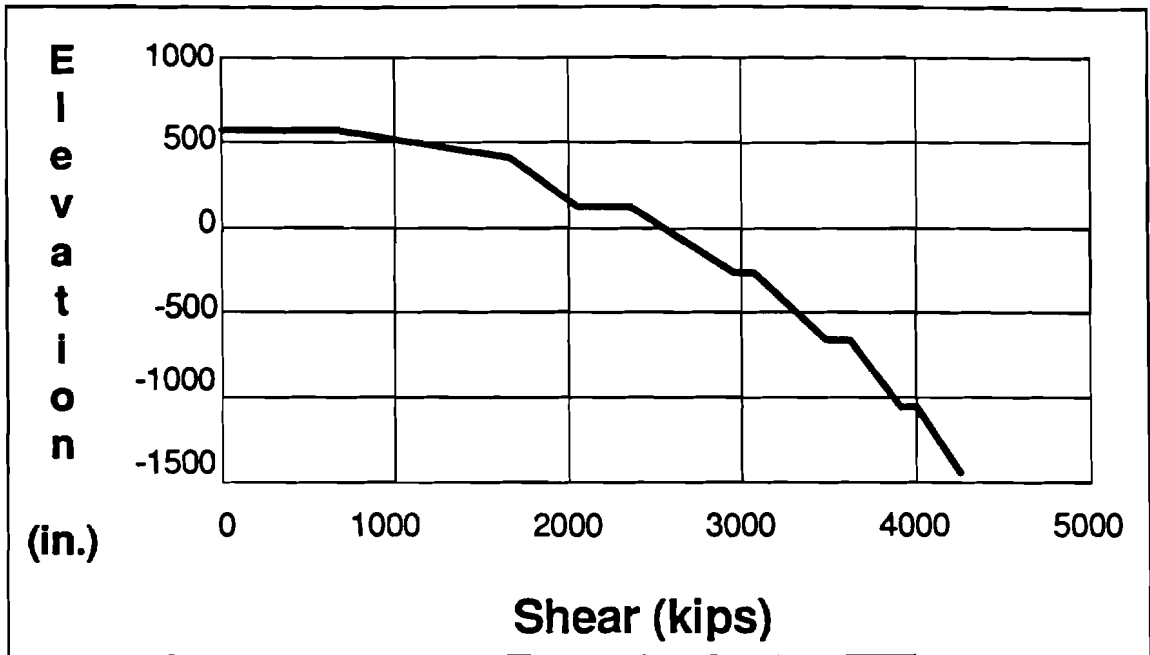
Figure 6.9: Platform B Broadside Reference Storm Shear Profile (WAJAC)
(Loch, 1995)
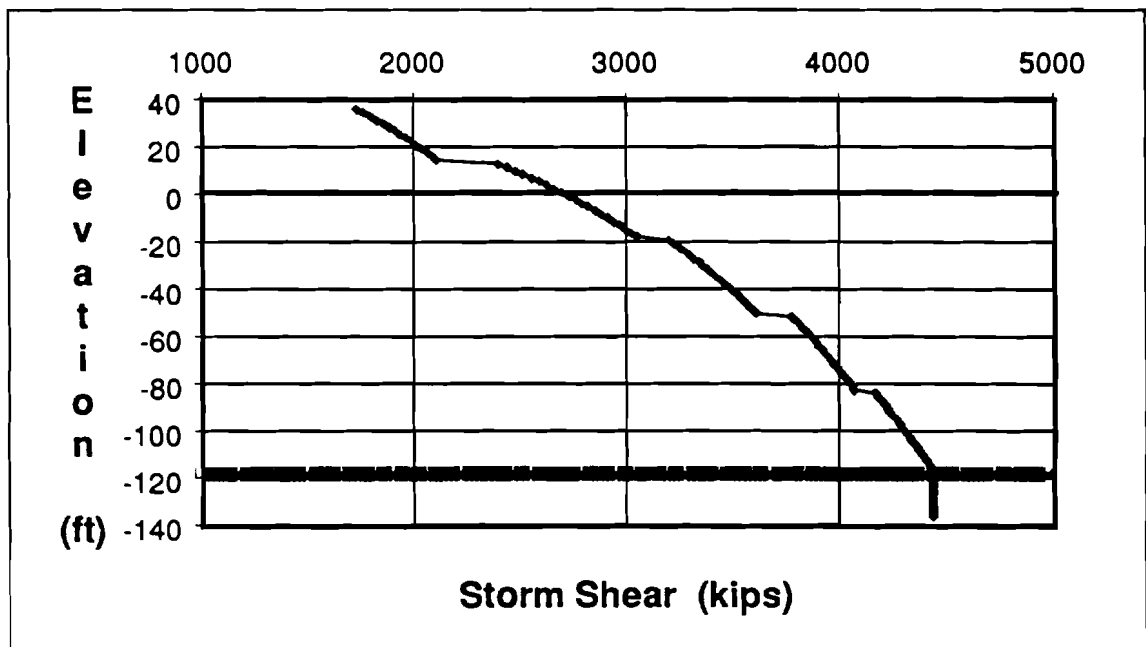
Figure 6.10: Platform B Broadside Reference Storm Shear Profile (ULSLEA)
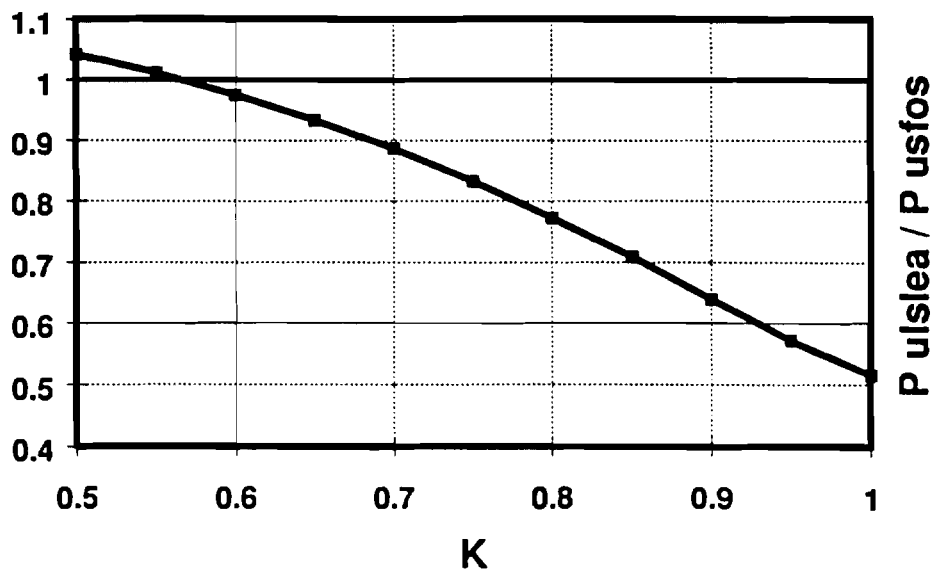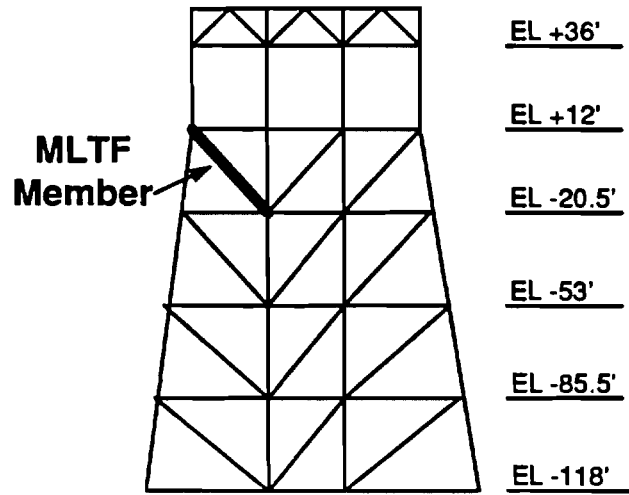
Figure 6.11 :Predicted Buckling Load vs. Buckling Length Factor, K
(Platform B, End-on Loading, MLTF Member)
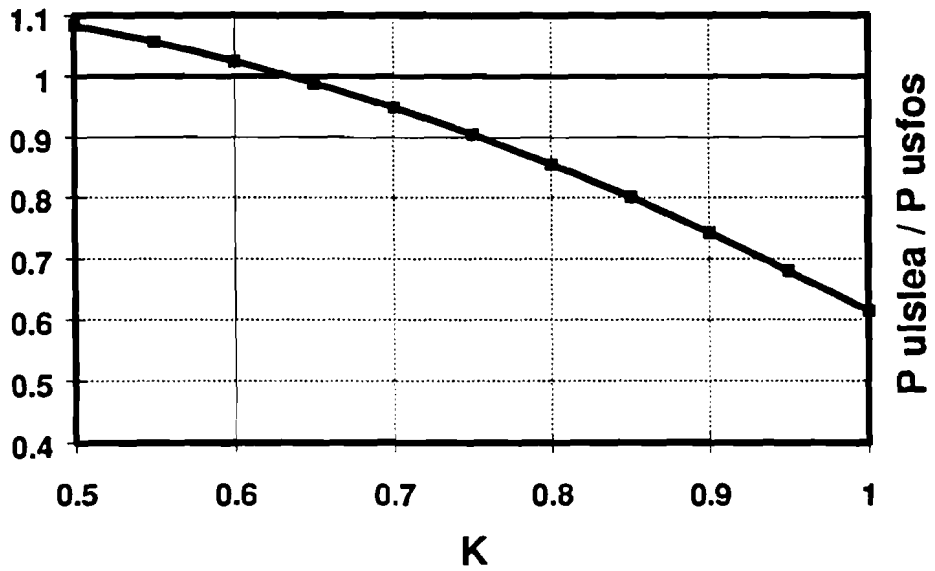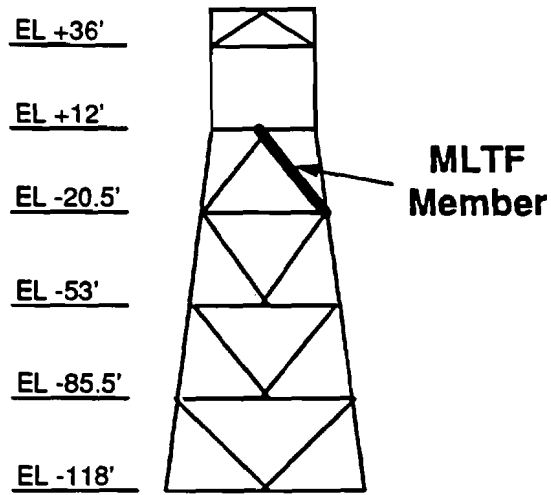
Figure 6.12 :Predicted Buckling Load vs. Buckling Length Factor, K
(Platform B, Broadside Loading, MLTF Member)
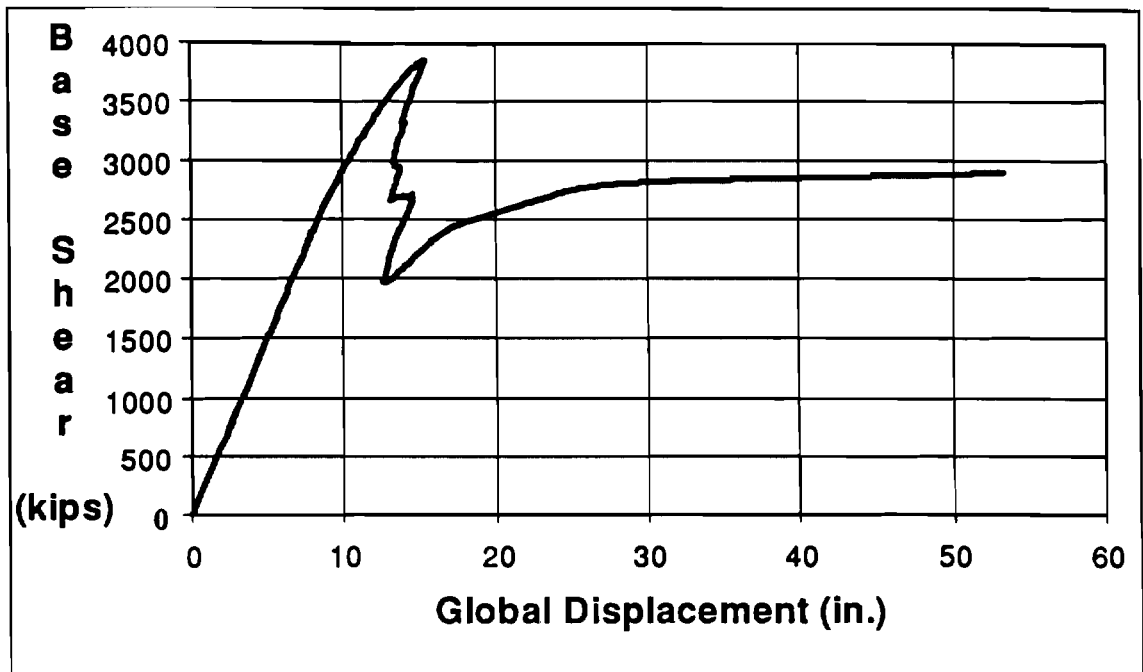
Figure 6.13: Platform B Broadside Force-Displacement History (USFOS) (Loch, 1995)
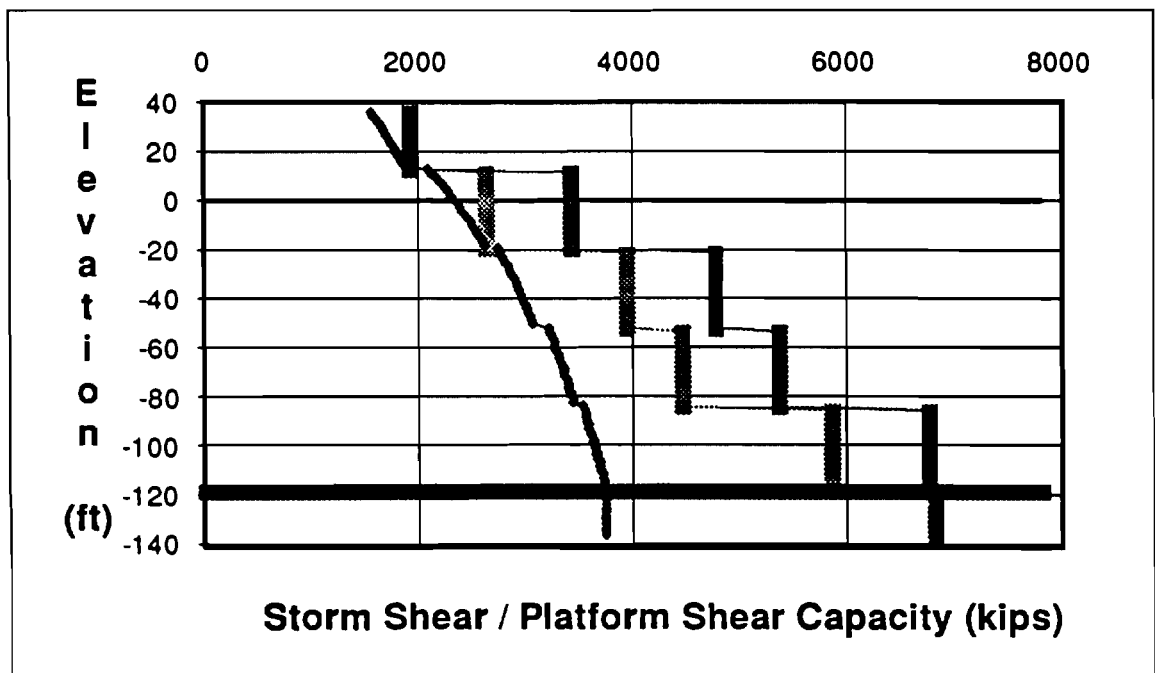
Figure 6.14: Platform B Broadside Shear Capacity (ULSLEA)
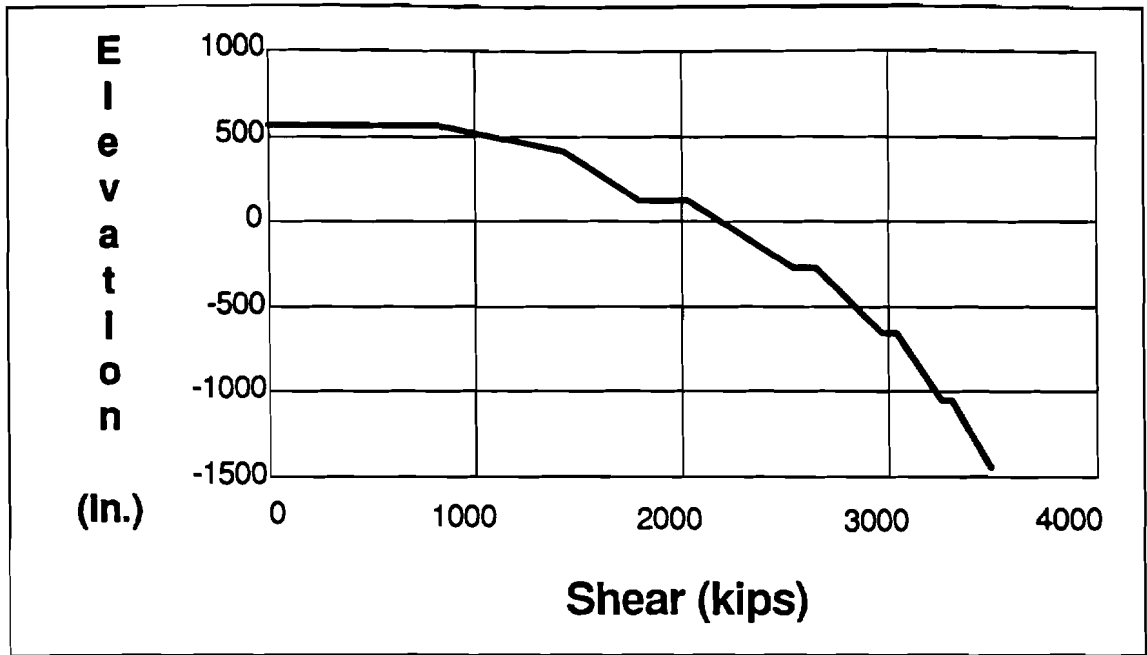
Figure 6.15 : Platform B End-On Reference Storm Shear Profile (USFOS)
(Loch, 1995)
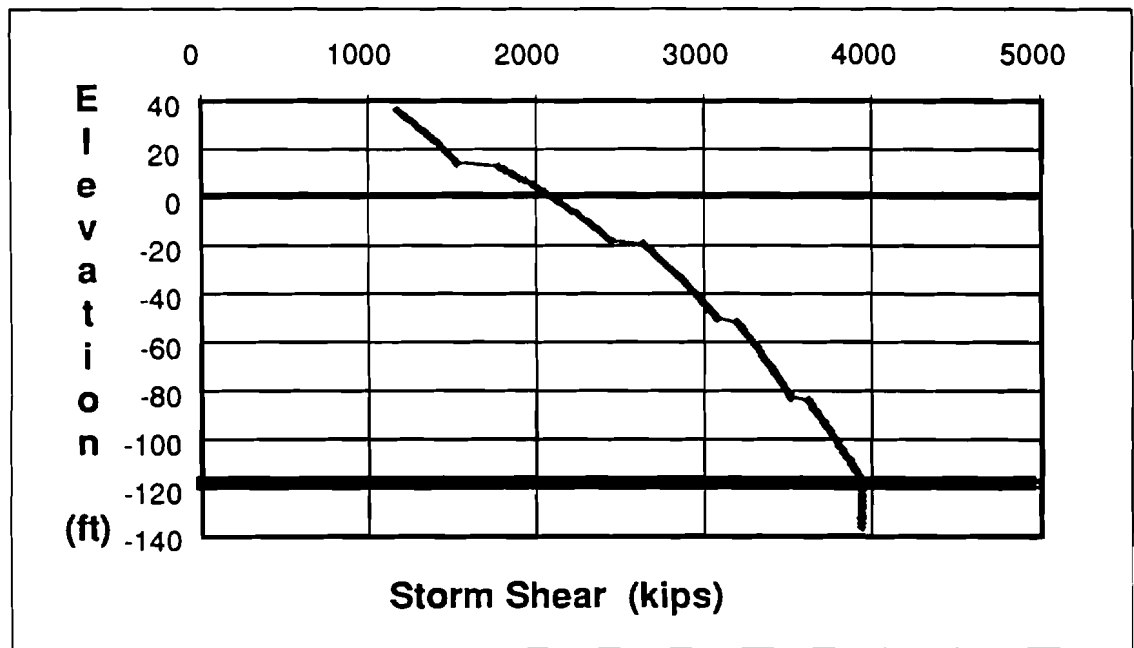
Figure 6.16 : Platform B End-on Reference Storm Shear Profile (ULSLEA)
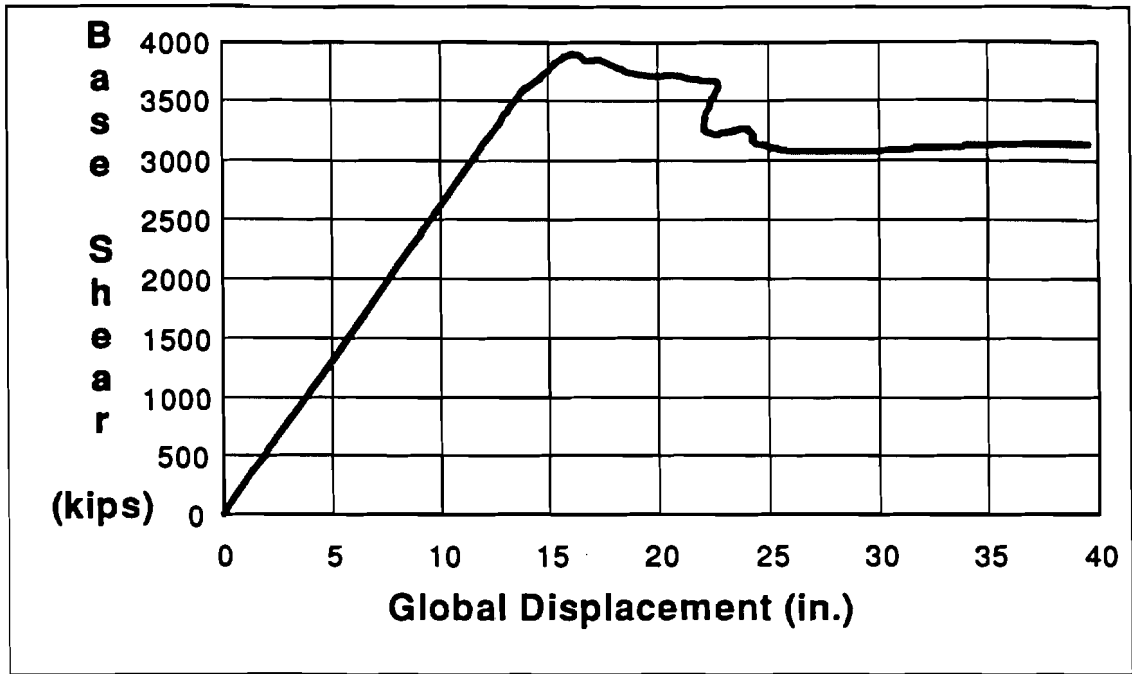
Figure 6.17: Platform B End-On Force-Displacement History (USFOS) (Loch, 1995)
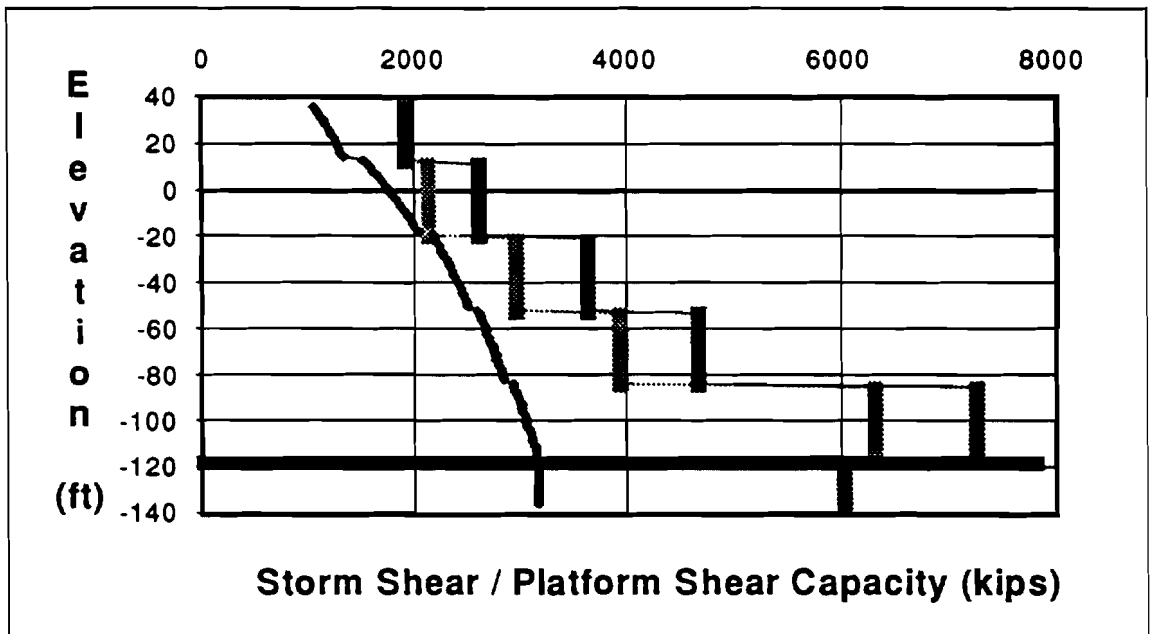
Figure 6.18 : Platform B End-on Shear Capacity (ULSLEA)

BROADSIDE LOADING
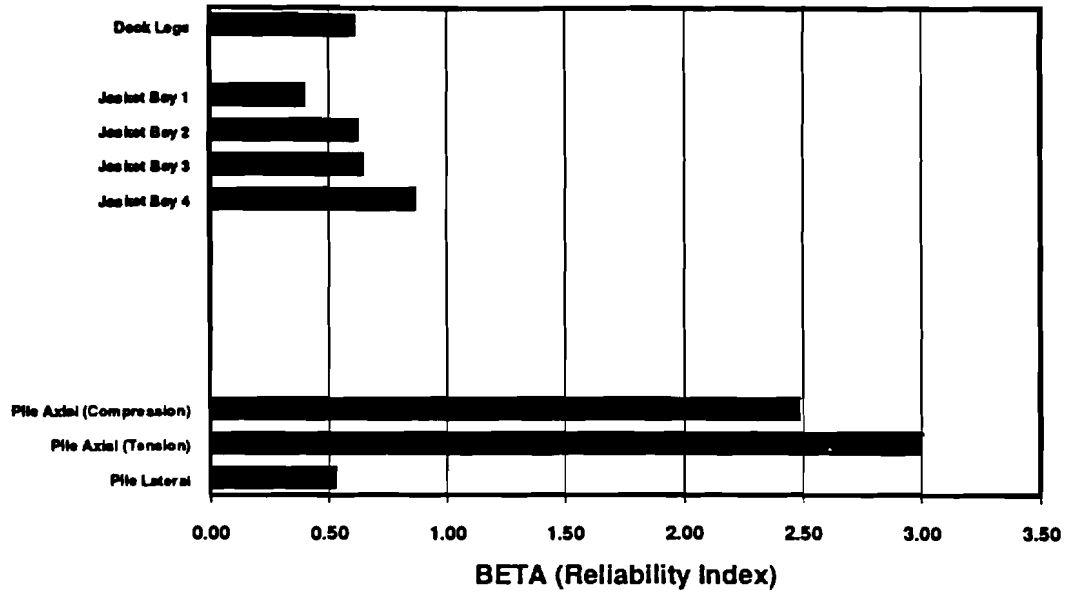
Figure 6.19: Platform B Component Safety Indices ($\beta|_{\text{Wave Height}}$) - Broadside Loading

END-ON LOADING

Figure 6.20: Platform B Component Safety Indices ($\beta|_{\text{Wave Height}}$) - End-on Loading

160

6.2.3 Platform C

Platform C is a self-contained four-pile drilling and production platform (Figure 6.21). It was installed in the Gulf of Mexico's Ship Shoal region in a water depth of 157 ft in 1971. The platform has four decks at elevations +33 ft, +43 ft, +56 ft, and +71 ft. The jacket legs are battered in two directions and have joint cans. The leg-pile annulus is ungrouted and the piles attached to the jacket with welded shimmed connections at the top of the jacket. The piles reach a penetration of 355 ft in soft to stiff gray clay. An expected steel yield stress of 43 ksi was used for all structural elements of this platform.

This platform has been the subject of extensive structural analyses. As an industry wide effort to assess the variability in predicted performance of offshore platforms in extreme storms, the ultimate capacity of this platform has been assessed by many investigators using a variety of nonlinear analysis software packages (Digre, et al., 1995).

The force-displacement history for broadside loading is shown in Figure 6.23. This curve indicates that platform failed at a total base shear of 1,673 kips. Since the foundation was shown to be the weak link in the platform, a fixed base analysis was also performed. This was accomplished by analyzing the platform while rigidly fixing the piles at the mudline. In this case, the braces in the sixth jacket bay became the weak link. The analysis indicated that compression braces in the sixth bay from top buckled at a total base shear of 3,440 kips (Figure 6.24). After the compression braces in the sixth jacket bay buckled, the braces in the fifth jacket bay buckled and the jacket began to collapse.

Using ULSLEA for a reference wave height of 67 ft, a wave period of 14.3 sec and a uniform current velocity of 3.1 ft/sec, the total base shear for an orthogonal loading direction was estimated to be 3,050 kips (Figure 6.22). Using a buckling length factor of 0.65 for compression braces, the limit equilibrium analysis indicated platform collapse at a base shear of 3,200 kips due to simultaneous failure of compression braces at different jacket bays (Figure 6.25). For this lateral loading, the mean axial pile capacity in compression was exceeded by approximately 30% (RSR=0.7). According to this best-estimate result based on static pile capacities, a failure mode in foundation would govern the ultimate capacity of the platform.

These results are in good agreement with those gained from USFOS analysis. The comparison indicated that the simplified method overestimated the current and wave loads in jacket by 17%. The ultimate capacity of the platform with dynamic pile capacities was underpredicted by 6%. The axial compression capacity of piles were overestimated by 14%. After including the self-weight of the jacket to the axial pile loading, the pile capacities were in close agreement. Due to how the piles are installed and the potential loadings carried by the mudline braces and mudmats, whether or not the dead loads are fully carried by the supporting piles is uncertain.

The results of the simplified reliability analysis are plotted in Figure 6.26. These results indicate that a lateral foundation failure mode is as likely as a failure mode initiated in the

jacket. This potential failure mode was not captured by the deterministic analysis. The conditional component reliability indices for different jacket bays are generally in agreement with the deterministic analysis results (Figure 6.25). The relatively large reliability indices associated with axial foundation failure is due to the large bias factor of 3.0 used to correct the predicted axial capacity of piles in clay (Chapter 5).

This platform was located close to the path of hurricane Andrew. Hindcast studies for the site revealed an estimated maximum wave height of approximately 60 ft. The platform survived the storm without significant damage. The results of the simplified and detailed nonlinear analyses were both in conformance with the observed performance of the platform.
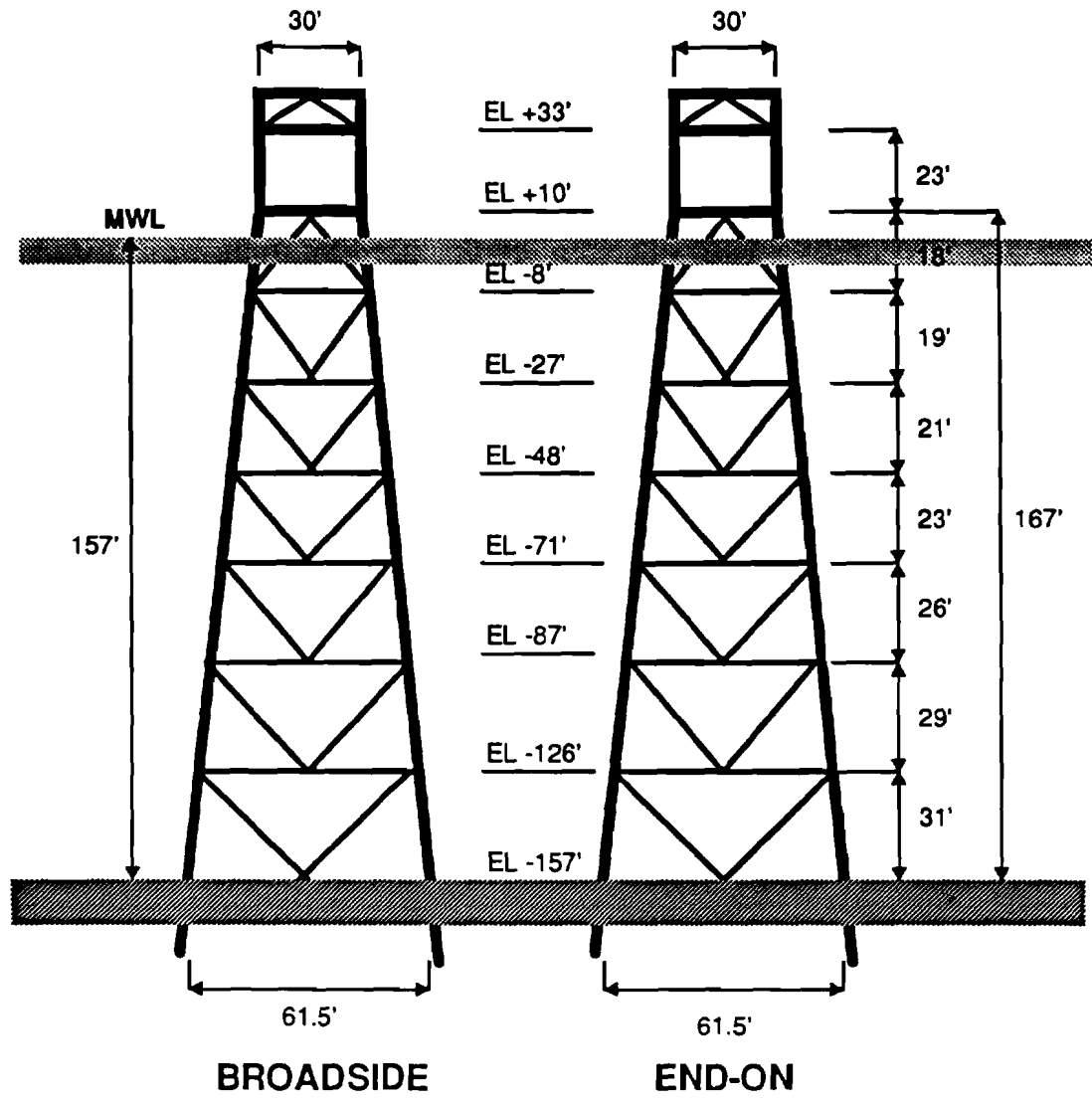
Figure 6.21: Platform C Elevations

164
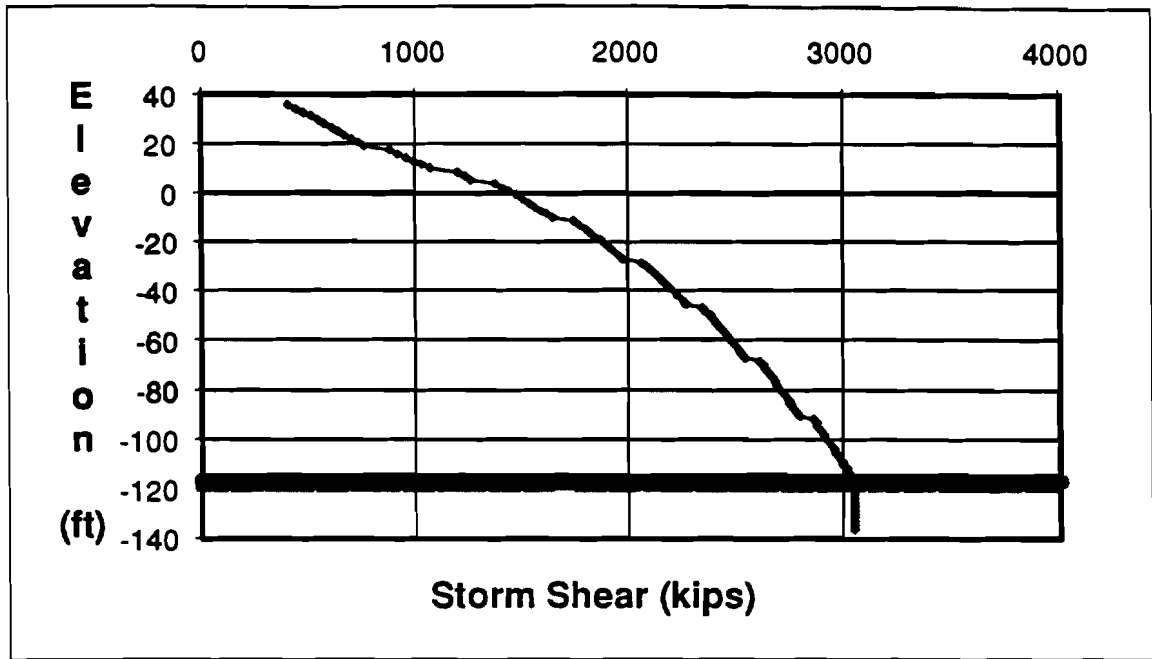
Figure 6.22: Platform C Reference Storm Shear (ULSLEA)
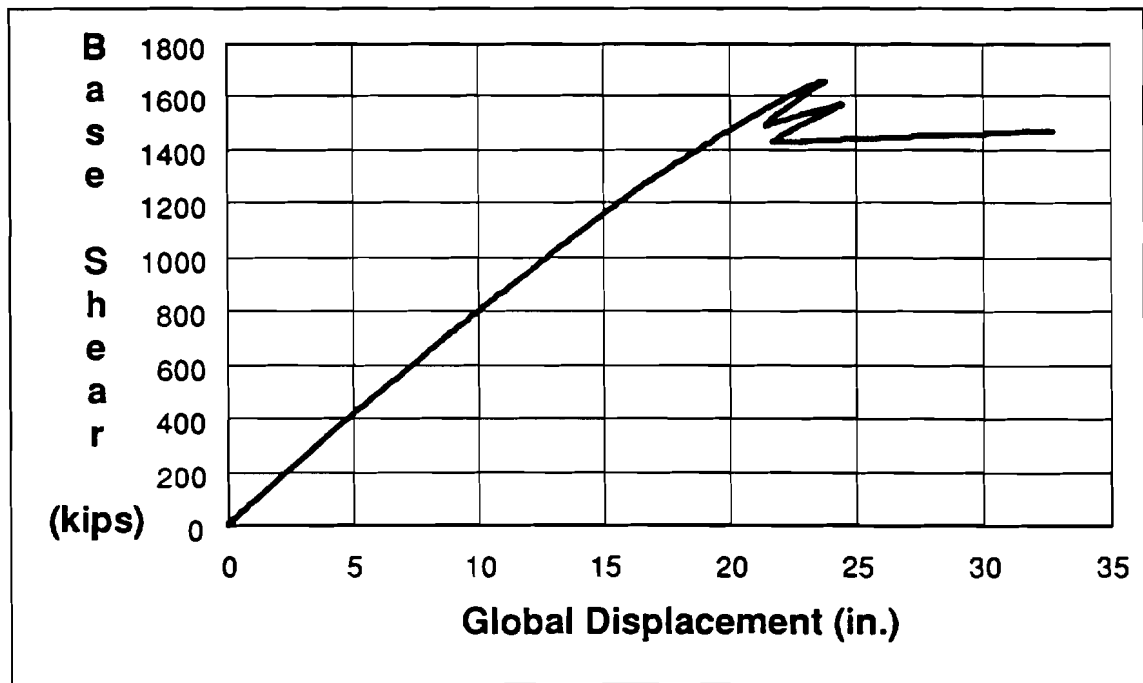
Figure 6.23: Platform C Force-Displacement History (USFOS)
(Loch, 1995)

165
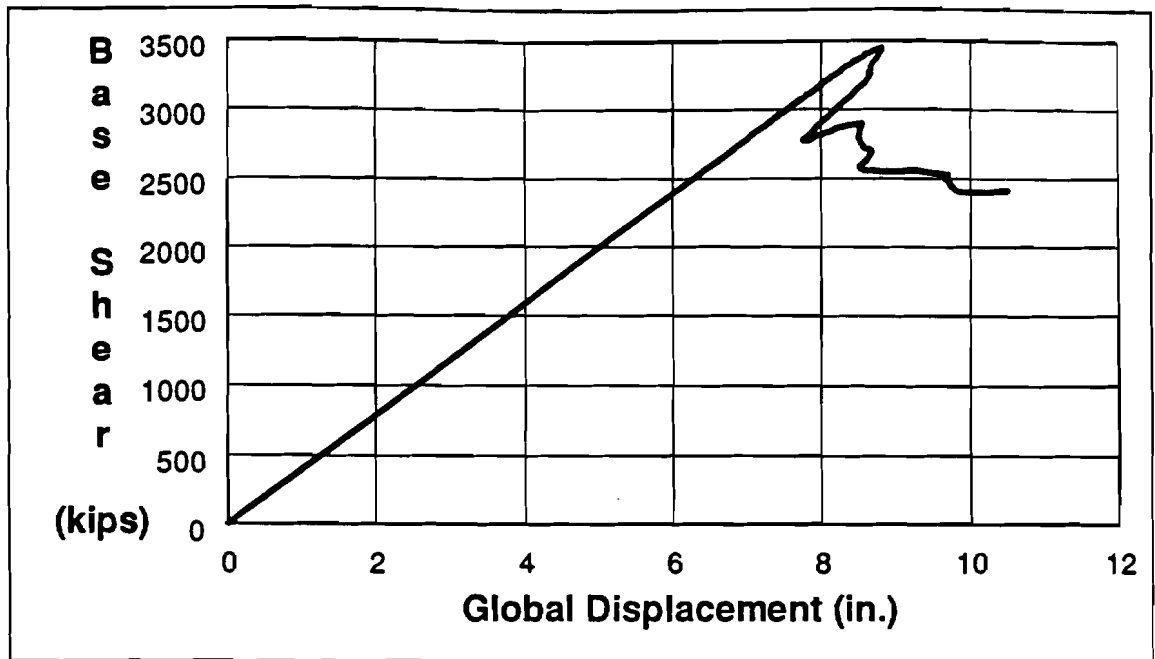
Figure 6.24: Platform C Fixed Base Force Displacement History (USFOS)
(Loch, 1995)
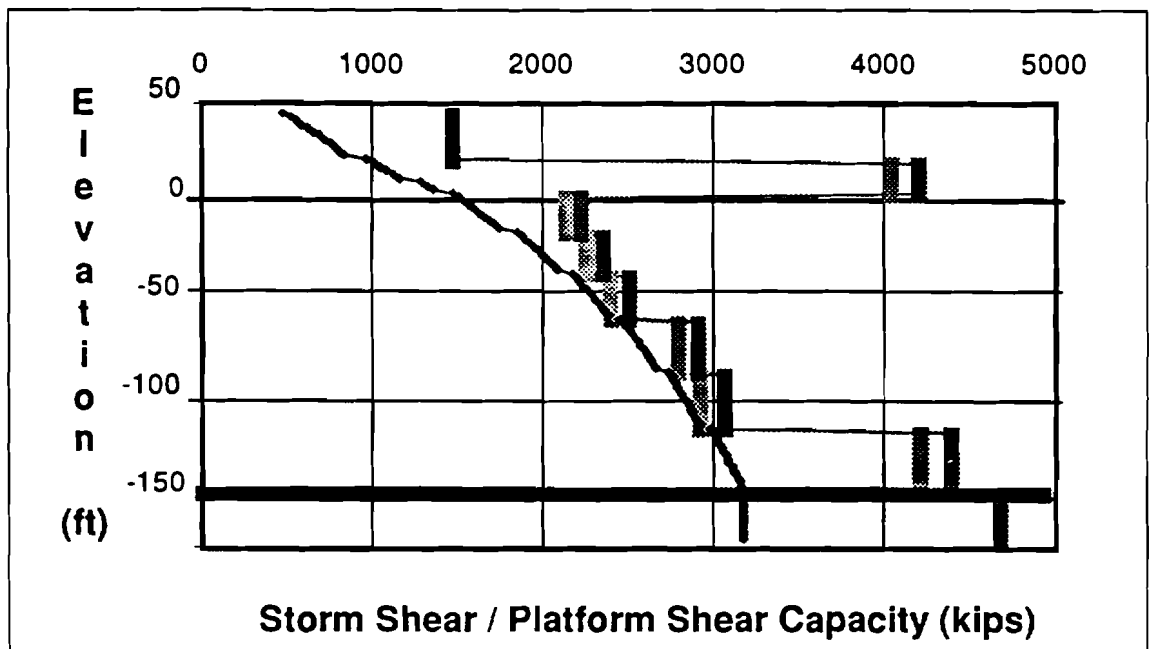
Figure 6.25: Platform C Shear Capacity (ULSLEA)

END-ON LOADING
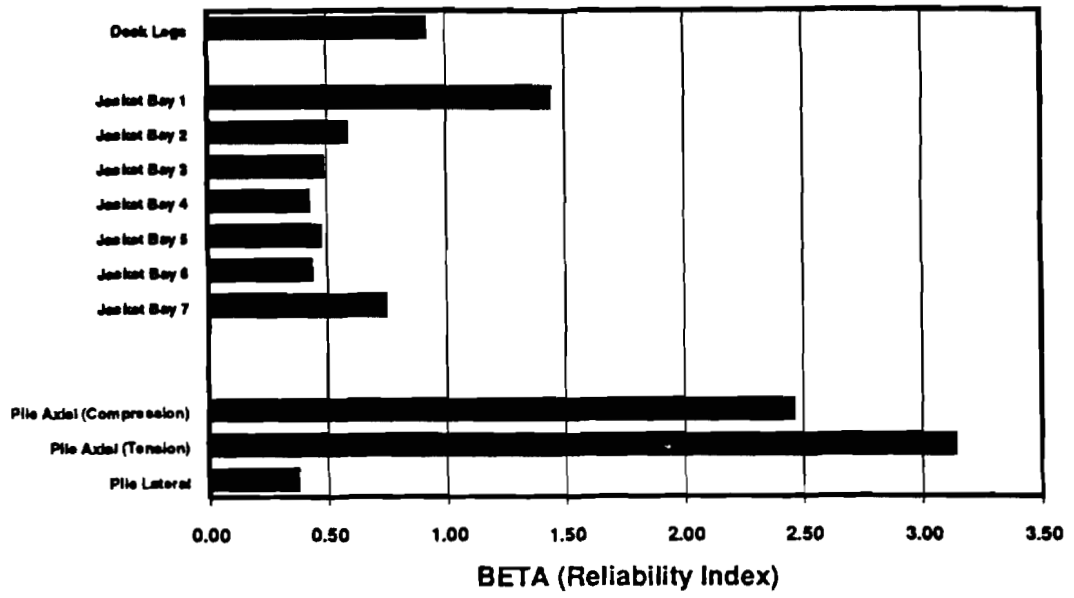
Figure 6.26: Platform C Component Safety Indices ($\beta|_{\text{Wave Height}}$) - End-on Loading

167

6.2.4 Platform D

Platform D is an eight-pile drilling and production platform located in the Gulf of Mexico's South Timbalier region in 137 feet of water (Figure 6.27). This region was subjected to 100 year wave loads during hurricane Andrew (Vannan et al., 1994). The platform was designed and installed in 1964. Cellar and main deck elevations are at + 35 ft and +46 ft respectively. The jacket legs are battered at one to twelve in both broadside framing. The 30 in. piles extend approximately 180 ft below the mudline through firm to very stiff clay. A dense sand layer lies directly beneath the piles ends. The 30 in. deck legs are connected to the tops of the 30 in. piles. The 33 in. diameter legs are ungrouted but have thickened joint sections. The jacket bracing and horizontal framing are made of nominal 36 ksi steel with an average yield strength of 43 ksi.

The broadside wave was set to 56 ft while end-on wave was set at 60 ft. The drag coefficient, C_d, was taken to be 1.2 for both rough and smooth cylinders. The inertia coefficient, C_m, was taken to be 1.2 for rough cylinders and 1.6 for smooth cylinders respectively . A wave kinematics factor equal to 0.88 was used for both the deck and jacket loads. A current blockage factor of 0.80 for broadside loading and 0.70 for end-on loading was also included. All members were given an initial imperfection of 0.003 of their length. Since the legs did have joint cans, the detailed analysis used rigid joints.

The force-displacement plot for end-on loading is shown in Figure 6.28. This curve indicates that the platforms reaches its peak capacity at a total base shear of 2,697 kips.

The force-displacement history indicates that there is some reserve strength in the end-on direction. ULSLEA was able to predict the collapse mechanism and the ultimate lateral loading capacity of 2,700 kips (Figure 6.29). The force-displacement curve for broadside loading is shown in Figure 6.30. This curve indicates that platform fails at a total base shear of 4,475 kips. The maximum strength was controlled by buckling of the end-on braces in the second bay. ULSLEA analysis for this loading direction also indicated a failure mechanism at the second jacket bay at a total base shear of 4,200 kips (Figure 6.31).

The results of the reliability analyses are plotted in Figures 6.32 and 6.33 for end-on and broadside loading directions respectively. According to these results, foundation lateral failure mode is the most likely collapse mechanism for both loading directions. This failure mode was not captured by the deterministic analysis. In case of jacket failure, the simplified reliability analysis results are in agreement with the deterministic analysis results.

Platform D was located close to the path of hurricane Andrew. It collapsed during the storm. Both the ULSLEA and detailed analysis results indicated that the platform should have failed during hurricane Andrew.

120' 40'

EL +34.5' 23.5'

EL +11'

MWL 37

EL -26'

137' 37 148'

EL -63'

EL -100 37

EL -137' 37

90' 65.5'
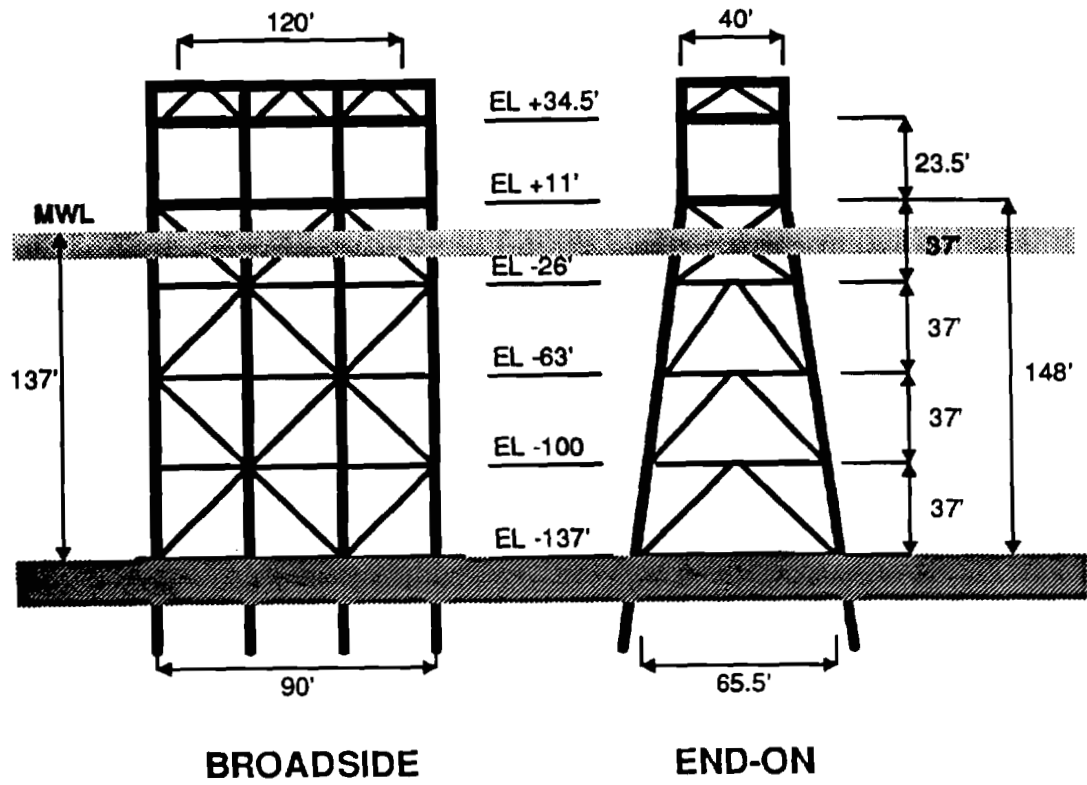
BROADSIDE **END-ON**

Figure 6.27: Platform D Elevations

Figure 6.28: Platform D End-on Loading Force-Displacement History (USFOS)
(Loch, 1995)
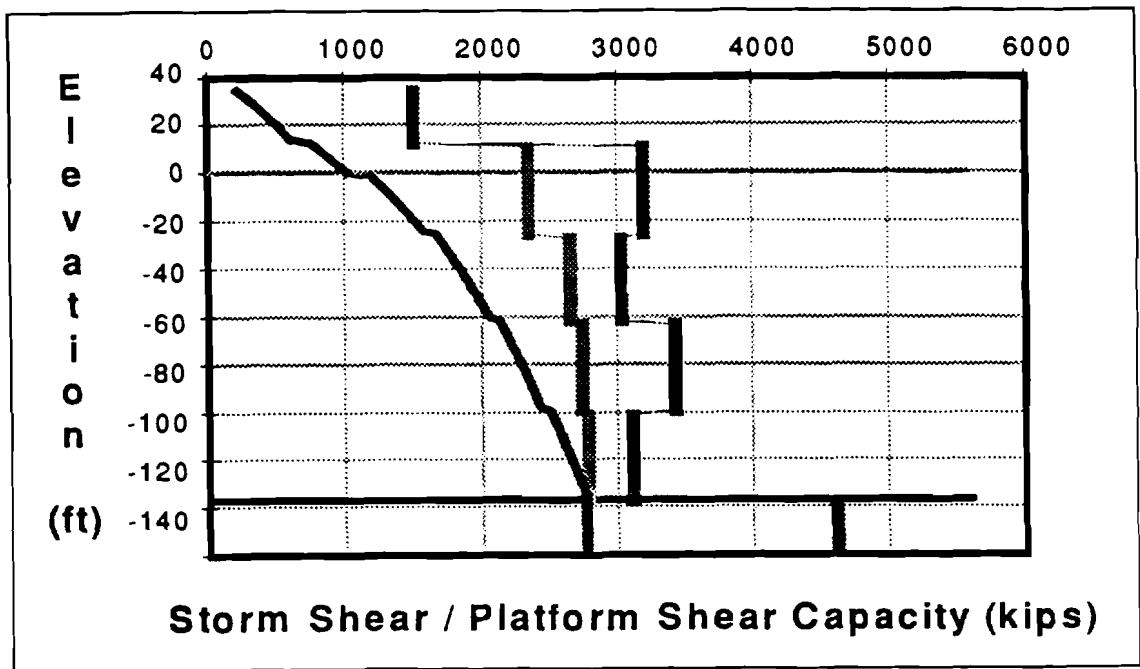
Figure 6.29: Platform D End-on Loading Capacity (ULSLEA)

171
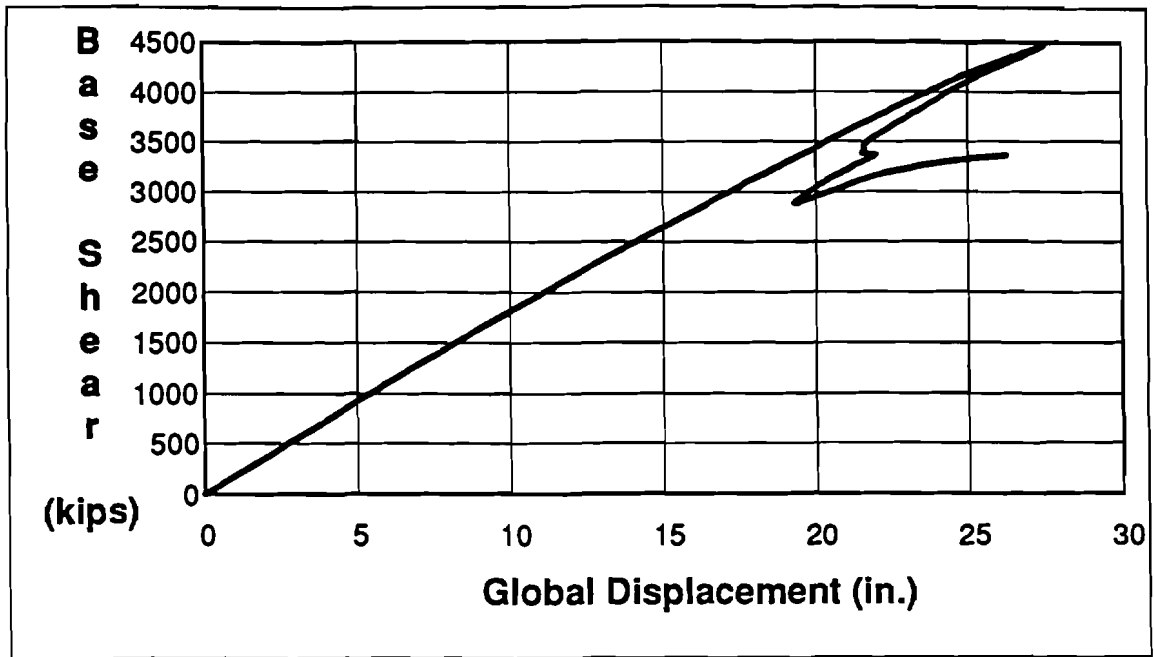
Figure 6.30: Platform D Broadside Loading Force-Displacement History (USFOS) (Loch, 1995)
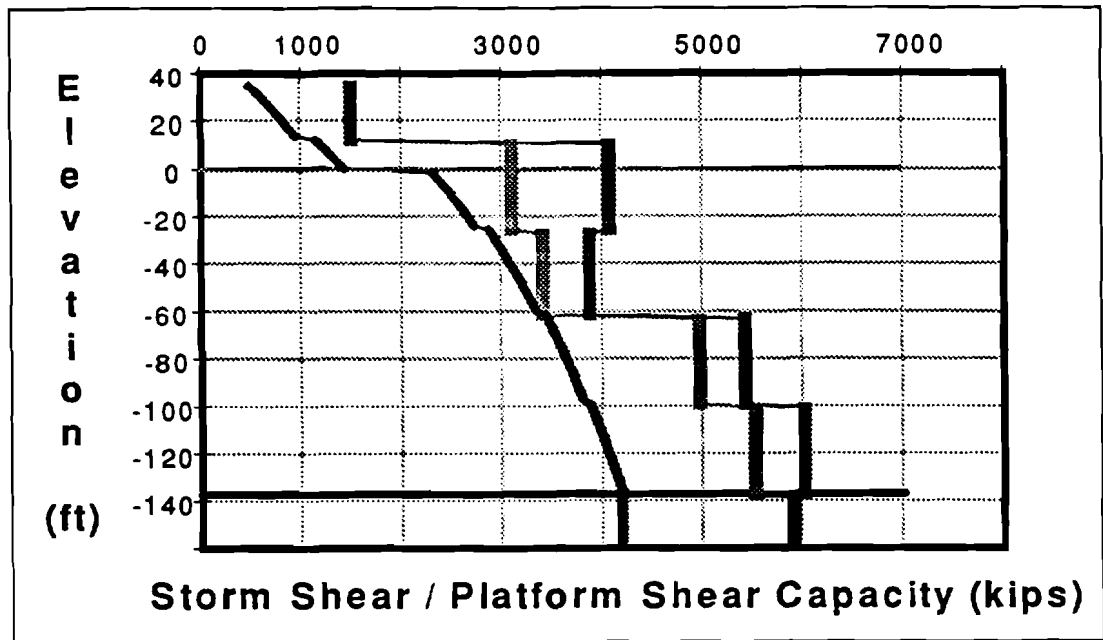
Figure 6.31: Platform D Broadside Loading Capacity (ULSLEA)

END-ON LOADING
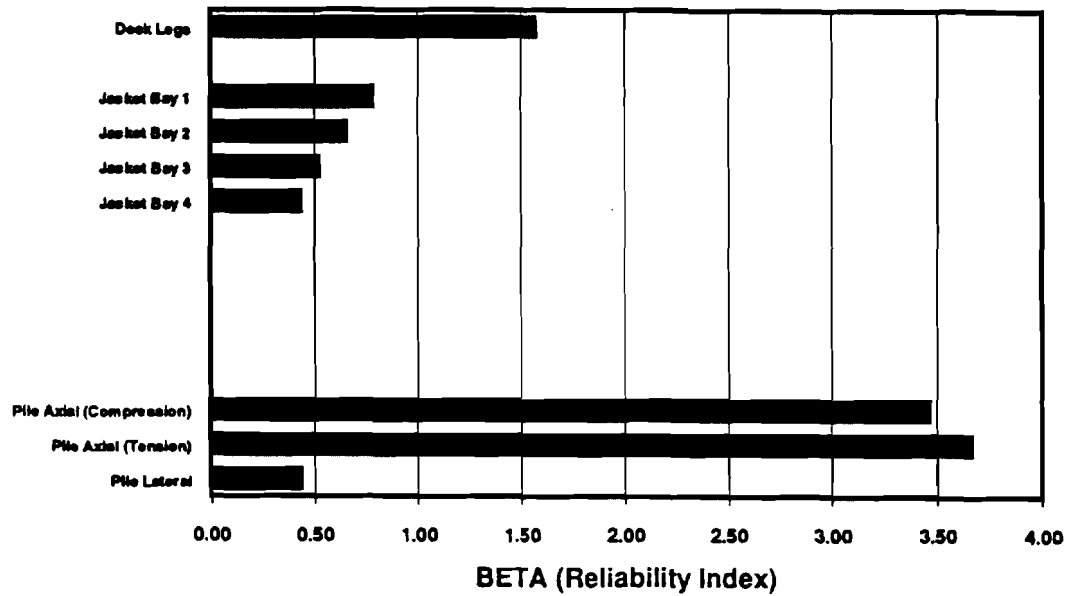
Figure 6.32: Platform D Component Safety Indices ($\beta|_{\text{Wave Height}}$) - End-on Loading
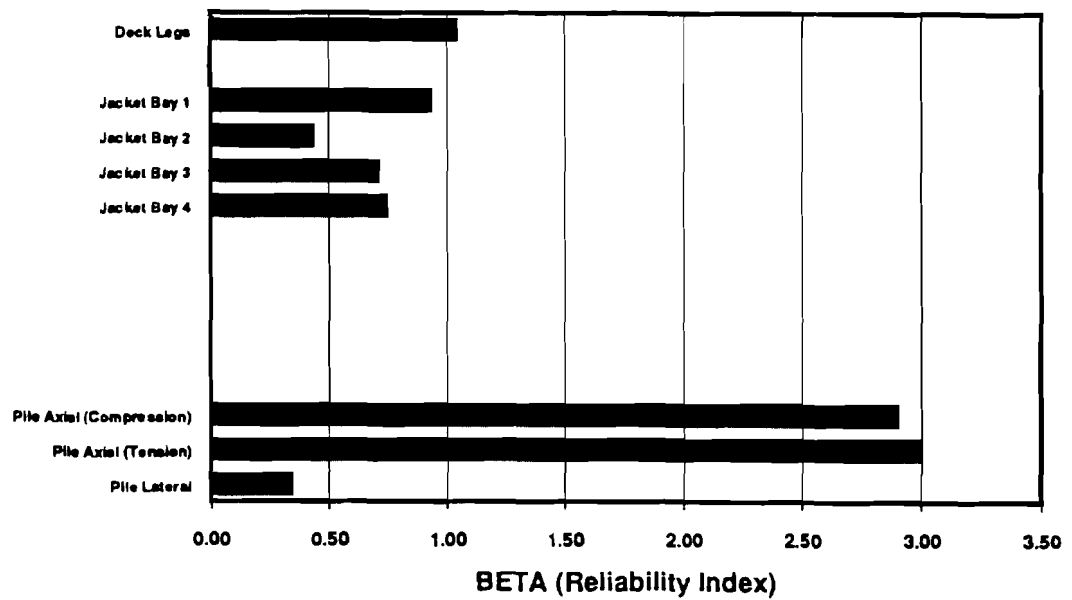
BROADSIDE LOADING

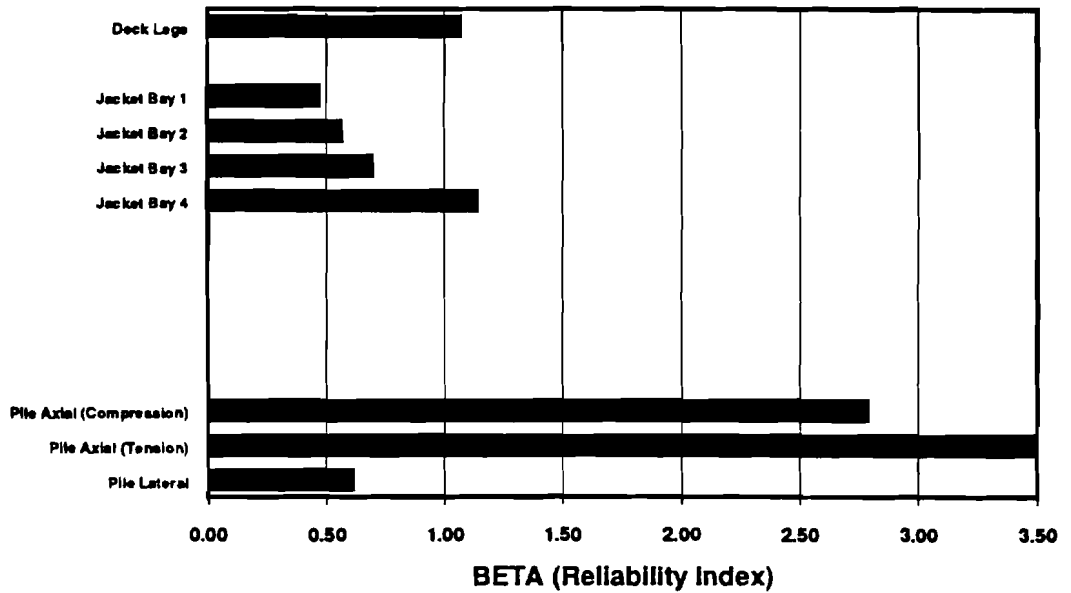**Figure 6.33: Platform D Component Safety Indices ($\beta|_{\text{Wave Height}}$) - Broadside Loading**

173

6.2.5 Platform E

Platform E is also an eight-leg drilling and production platform located in the Gulf of Mexico's South Timbalier region (Figure 6.34). This platform was bridge-connected to Platform D. Both platforms were designed in 1964 and installed in 137 feet of water. Platform E is similar in geometry to platform D except that it is battered at one to ten in both broadside and end-on framing. The same wave and wind conditions and force coefficients were used for both platforms D and E. However, platform E had a much larger base shear for the same storm conditions due to its additional conductors. Similar modeling assumptions were made for both platforms. All members were given an initial imperfection of 0.003 of their length. The analysis used rigid joints for both structures.

The force-displacement plot for broadside loading is shown in Figure 6.35. This curve indicates that platform reaches its maximum capacity at a total base shear of 4,709 kips. As with platform D, the maximum strength was controlled by buckling of the end-on braces in the second bay. This result is in good agreement with results developed using ULSLEA. For this loading direction, the simplified analysis indicated a collapse mechanism in the second jacket bay at a base shear of 4,400 kips (Figure 6.36). The force-displacement curve for end-on loading is shown in Figure 6.37. The detailed analysis indicated that the lowermost broadside braces buckled at a total base shear of 4,577 kips (Figure 6.37). ULSLEA results for this loading direction showed failure due to simultaneous buckling of compression braces at the two lowest jacket bays. The simplified

174

analysis indicated an ultimate lateral loading capacity of 4,450 kips, which is in good agreement with result from the detailed analysis (Figure 6.38).

The conditional component reliability indices are plotted in Figures 6.39 and 6.40. These results are similar to those for verification platform D. The relatively large uncertainties associated with lateral capacity of pile foundation and storm loads are the primary reason for the low reliability indices for the lateral foundation failure mode.

Verification platforms D and E were subjected to significant environmental loading during hurricane Andrew. Hindcast data indicates that the two platforms were loaded close to end-on direction and were exposed to 60 ft waves. One of these apparently identical structures, platform D, collapsed while the other, platform E, survived the storm. According to Vannan et al. (1994), platform D was toppled due to jacket failure in end-on direction. Past work on collapse analysis of these platforms indicated an expected failure of both structures during Andrew (Vannan et al., 1994). For Andrew conditions, ULSLEA was able to predict the collapse and replicate the failure mode of platform D. Based on original hindcast storm wind and wave data, ULSLEA also predicted failure of platform E. However, the simplified analyses indicated a much higher probability of failure for platform D compared to that of platform E (Figures 6.41 and 6.42). Recent updating of hincast data resulted in lower maximum wave heights during Andrew, which could explain the survival of platform E.
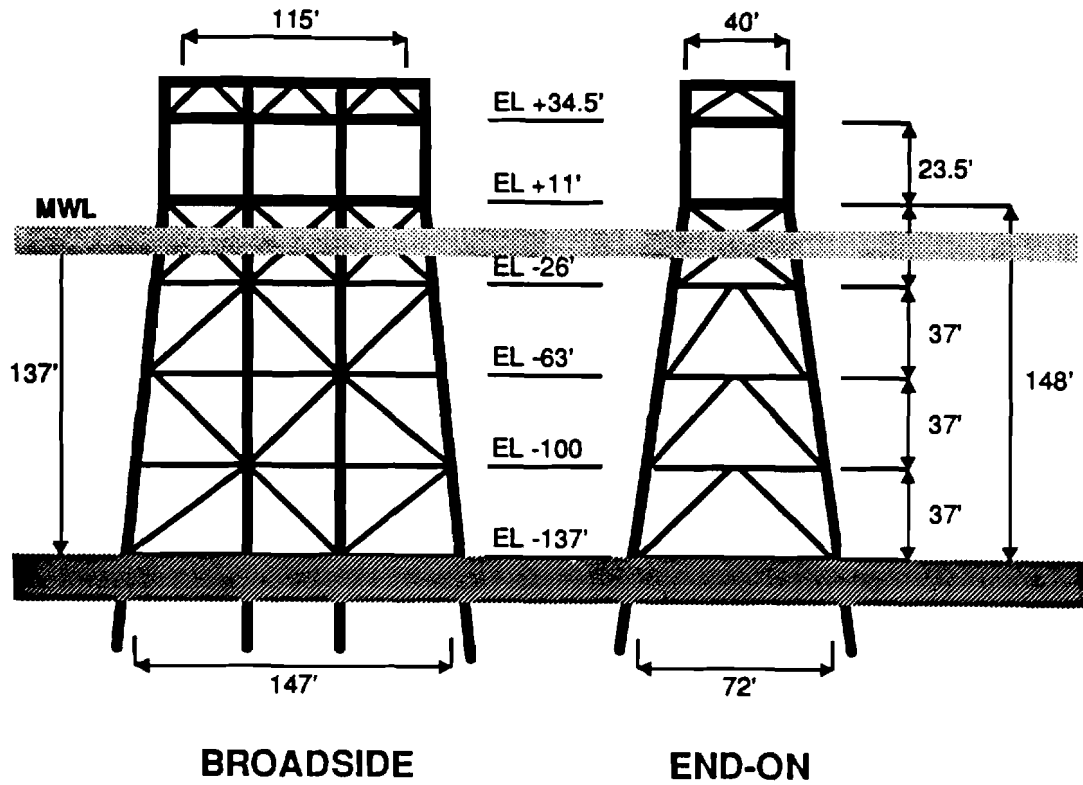
Figure 6.34: Platform E Elevations
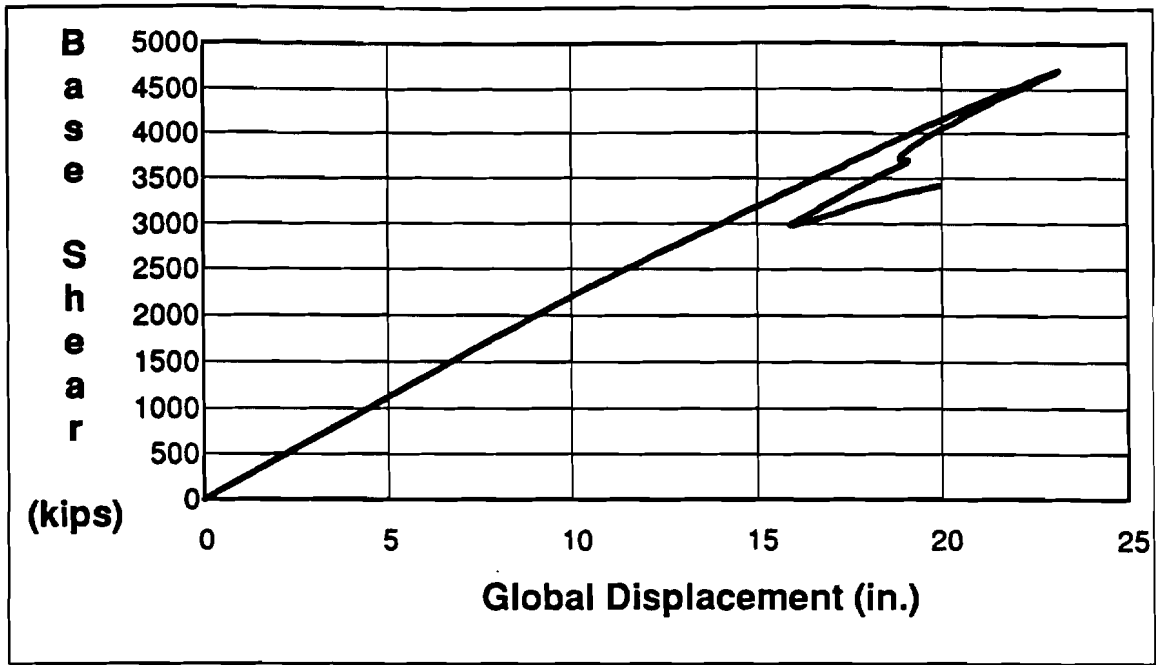
Figure 6.35: Platform E Broadside Loading Force-Displacement History (USFOS)
(Loch, 1995)
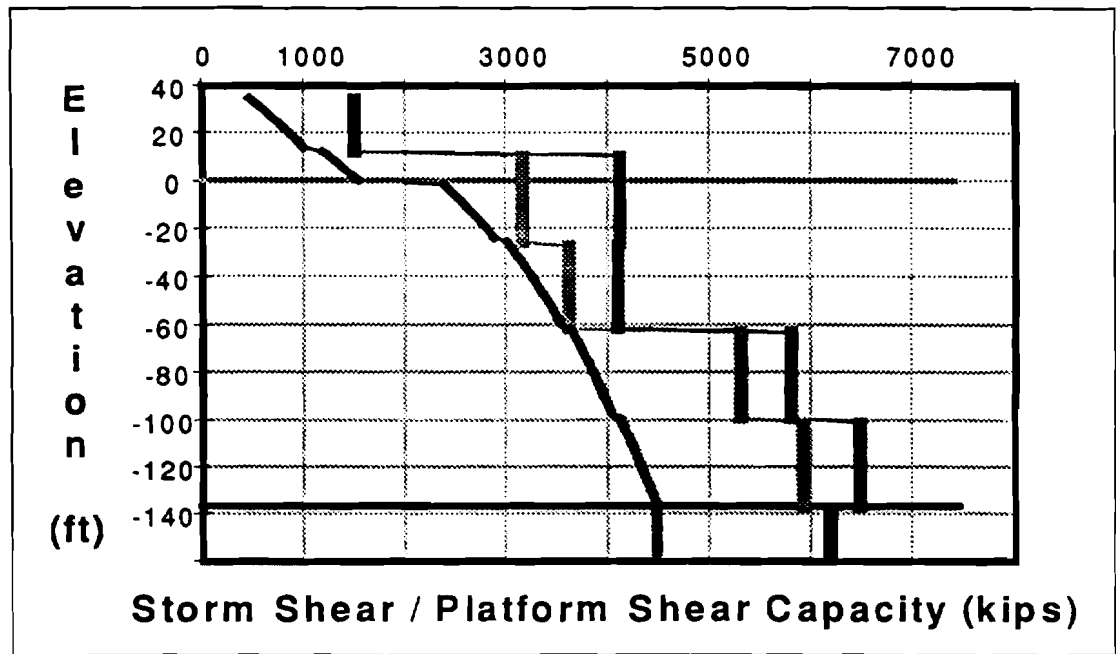
Figure 6.36: Platform E Broadside Loading Capacity (ULSLEA)
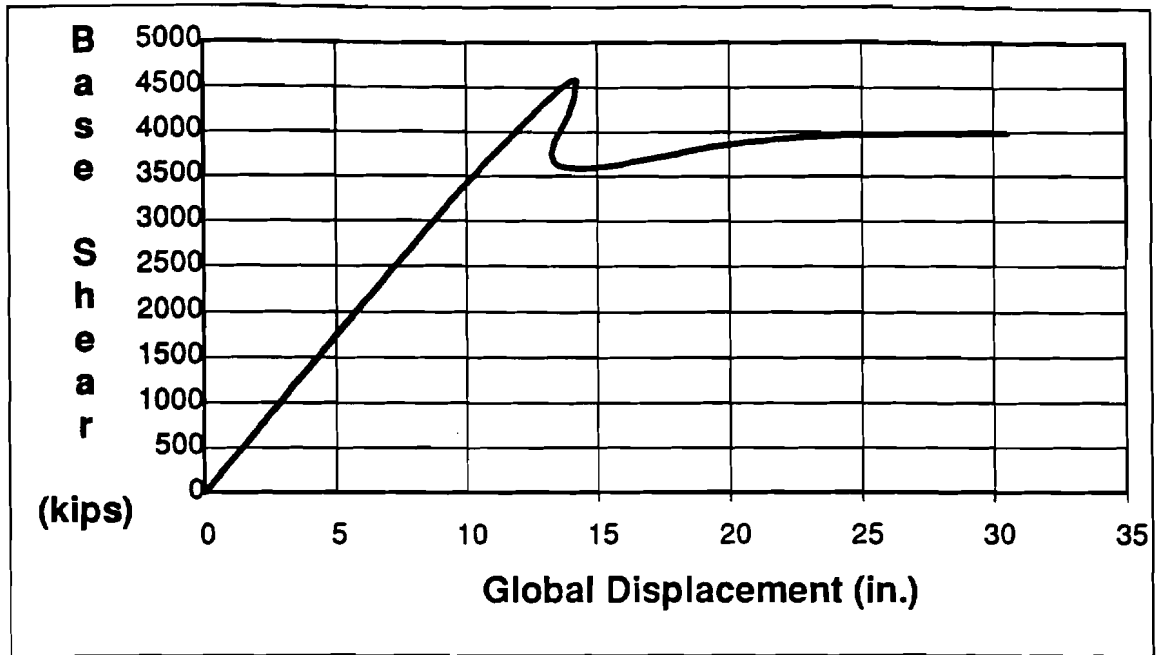
Figure 6.37: Platform E End-on Loading Force-Displacement History (USFOS)
(Loch, 1995)
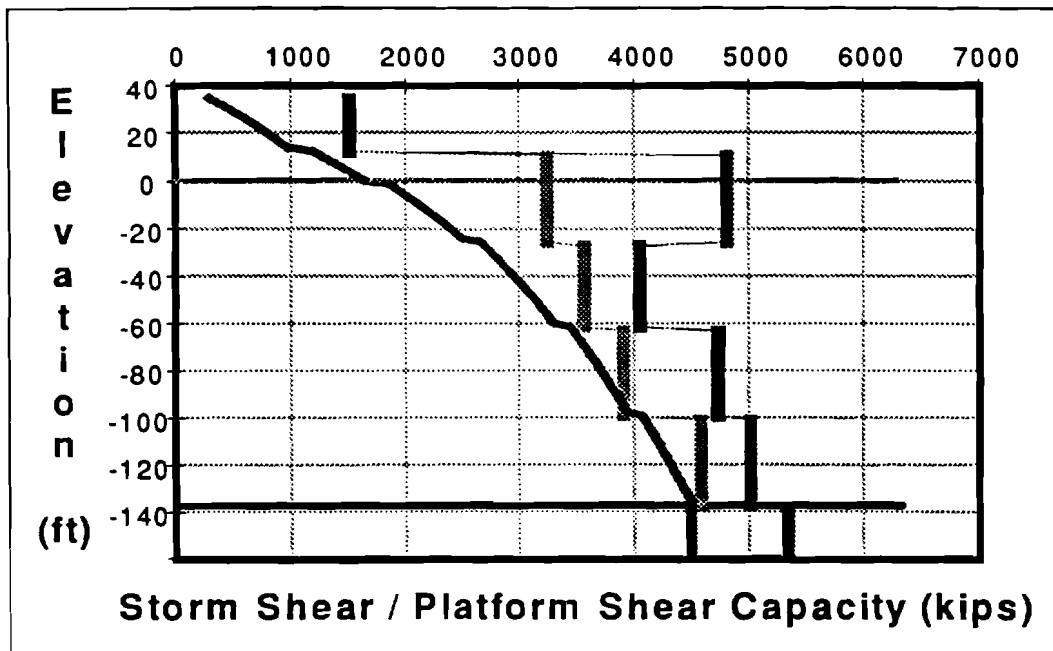
Figure 6.38: Platform E End-on Loading Capacity (ULSLEA)

178
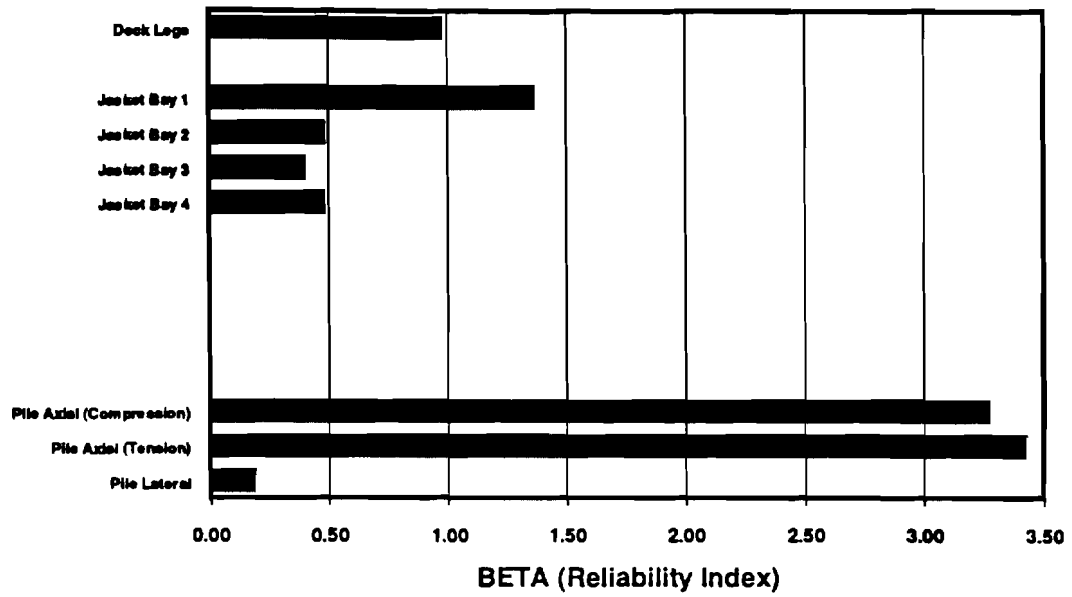
END-ON LOADING

Figure 6.39: Platform E Component Safety Indices ($\beta|_{\text{Wave Height}}$) - End-on Loading
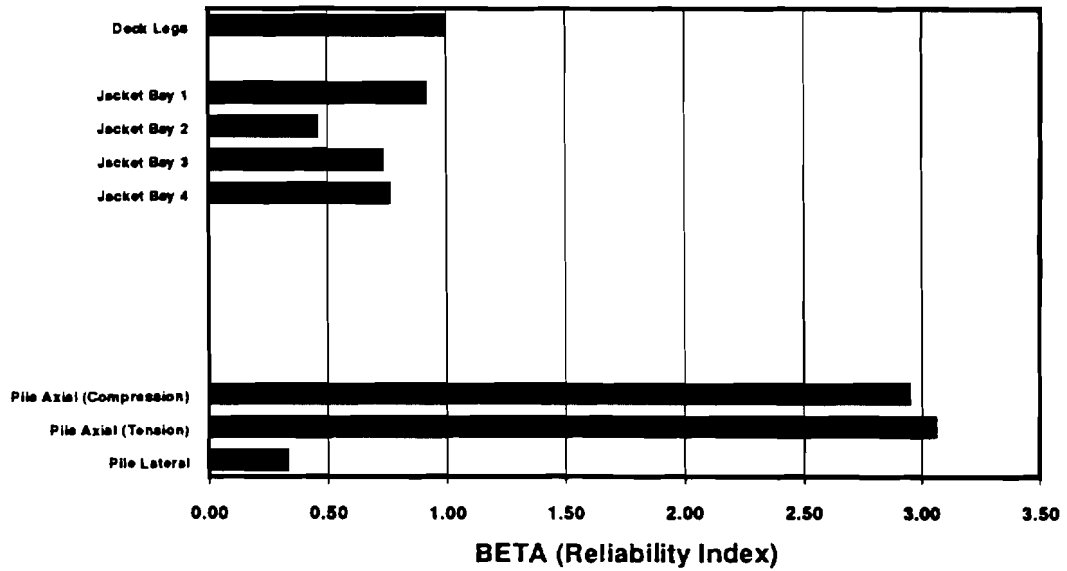
BROADSIDE LOADING

Figure 6.40: Platform E Component Safety Indices ($\beta|_{\text{Wave Height}}$) - Broadside Loading

179

END-ON LOADING

Storm Shear / Platform Shear Capacity (kips)
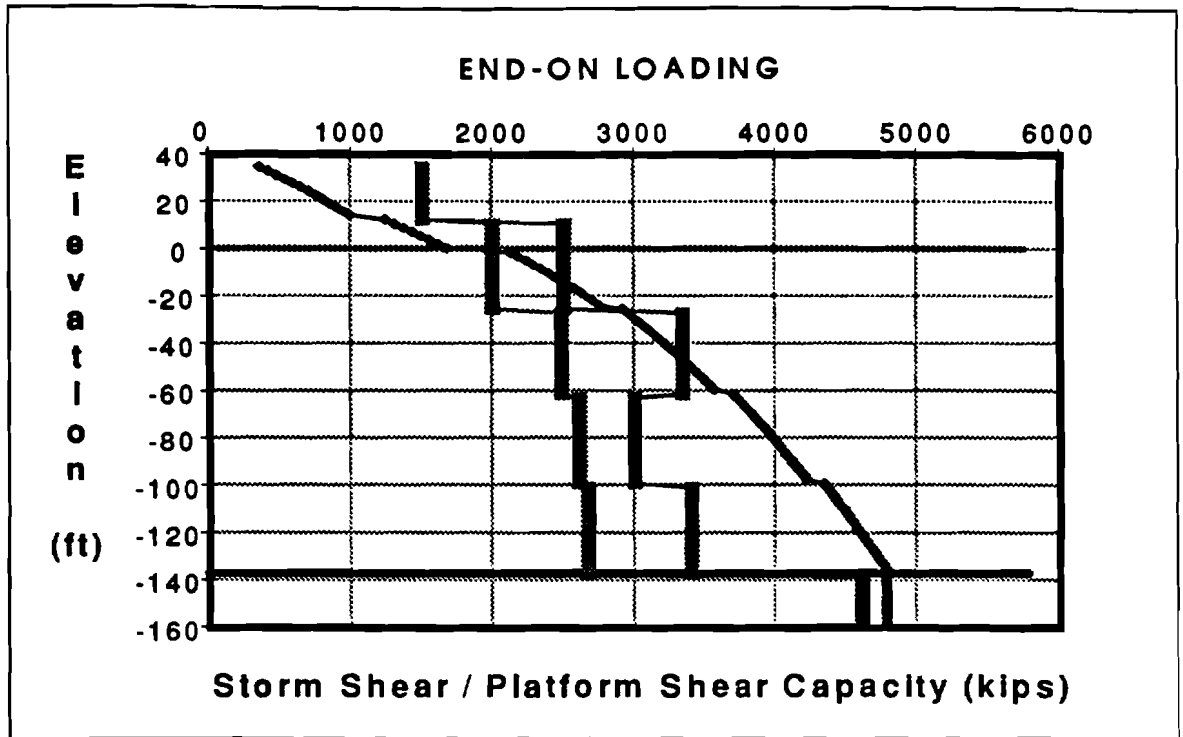
Figure 6.41: Platform D under Hurricane Loading (failed)

END-ON LOADING

Storm Shear / Platform Shear Capacity (kips)
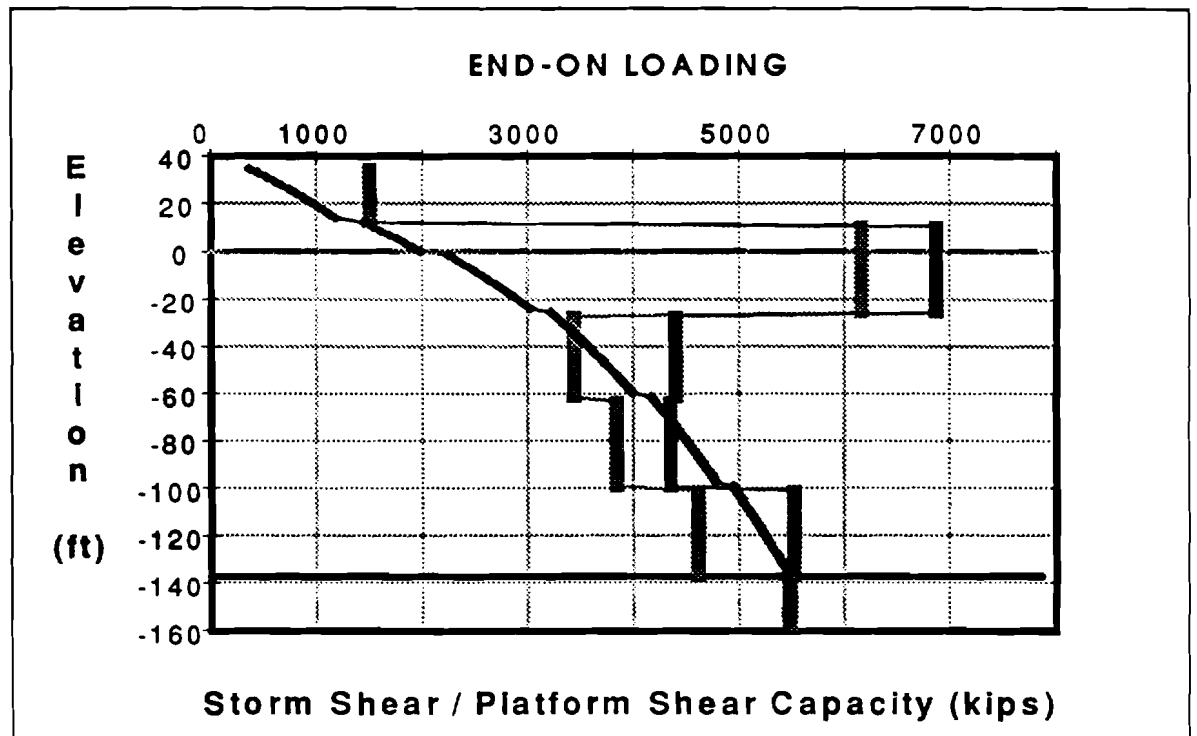
Figure 6.42: Platform E under Hurricane Loading (survived)

180

6.2.6   Platform F

Platform F is an eight-leg self-contained drilling and production platform located in 340 ft of water in the South Pass area of the Gulf of Mexico (Figure 6.43). The bottom of the lower decks has an elevation of 45 ft. The jacket framing consists of main diagonal bracings with diameters ranging from 24 to 30 in. and thicknesses from 0.625 to 1.25 in. This platform supports eighteen 24 in. conductors. The main piles are driven through the jacket legs and shim-connected to the top of the legs. The jacket leg-pile annulus is not grouted. The platform has 8 additional skirt piles which are grouted in skirt pile legs that are within the framing of the bottom jacket bay. All of the piles penetrate to a depth of 180 ft below mudline. The foundation soils consist predominantly of sand.

Plots of deck displacement versus total base shear are shown for end-on and broadside loading cases in Figures 6.44 and 6.46 respectively. ULSLEA was used to perform simplified analyses of this structure. The results are summarized in Figures 6.45 and 6.47. In the case of broadside loading, a wave height of 84 ft, a wave period of 13.5 seconds and a constant current velocity of 3.9 ft/sec were used to develop a loading pattern on the platform. Using a buckling length factor of K=0.65, ULSLEA predicted the buckling capacity of the critical diagonal brace with reasonable accuracy. For this loading direction, ULSLEA predicted a lower-bound capacity of 7,600 kips for the platform. This is an underestimation of approximately 10% comparing to USFOS results (Figure 6.44). The platform failure was initiated by buckling of compression braces at the second jacket bay from the top, which is in agreement with USFOS results.

In the case of end-on loading, a wave height of 80 ft with a period of 13.5 seconds and a constant current velocity of 3.9 ft/sec were used to develop a loading pattern on the platform close to that resulting in actual structure failure. Using a buckling length factor of K=0.65, ULSLEA accurately predicted the buckling capacity of the critical diagonal brace. The failure of the first compression brace occured at a lateral load of 7,000 kips. This is an underestimation of approximately 7% comparing to USFOS results (Figure 6.46). The failure initiating event was the buckling of compression braces at the second jacket bay from the top. In addition, the results indicated that the compression braces in the third and fourth jacket bay were also very likely to fail (Figure 6.45). This failure prediction is also in good agreement with results given by USFOS. A tubular joint failure mode was not considered in any of the loading cases.

Figures 6.48 and 6.49 show the component reliability indices conditional on wave height for end-on and broadside directions respectively. According to these results, an axial pile failure is the most likely collapse mechanism for both loading directions. In addition, the reliability indices associated with lateral foundation failure modes are in the same order as those associated with jacket failures. Non of these potential failure modes were captured by the deterministic analyses. In case of jacket failures, the reliability indices are in agreement with the deterministic analysis results for both loading directions.

Platform F was subjected to extreme wave loads during hurricane Camille in 1969. The maximum wave heights during the storm were estimated to be approximately 75 ft. The platform survived the storm without damage. Both the simplified and detailed analyses were able to predict the observed performance of the platform. The platform should have survived the storm loadings and it did.
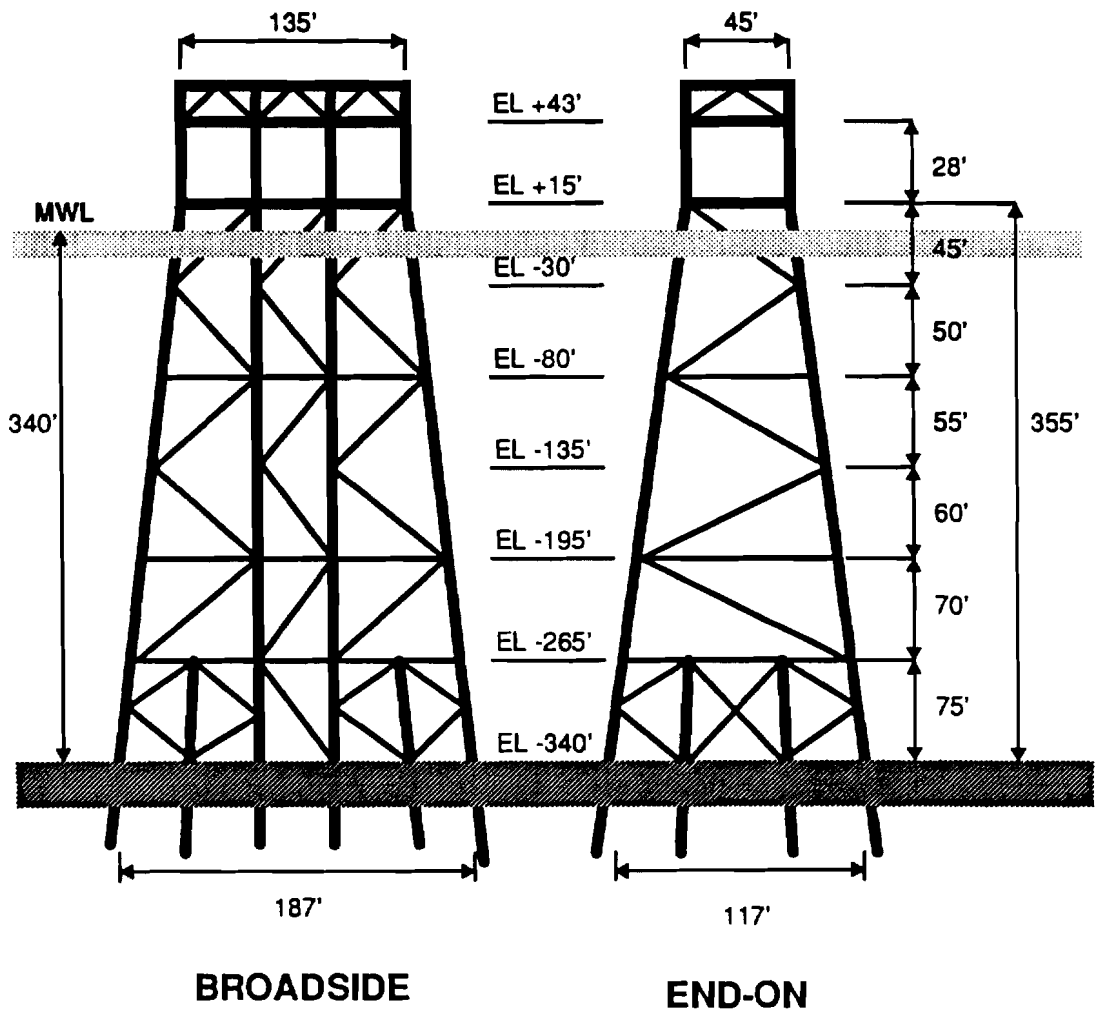
Figure 6.43: Platform F Elevations
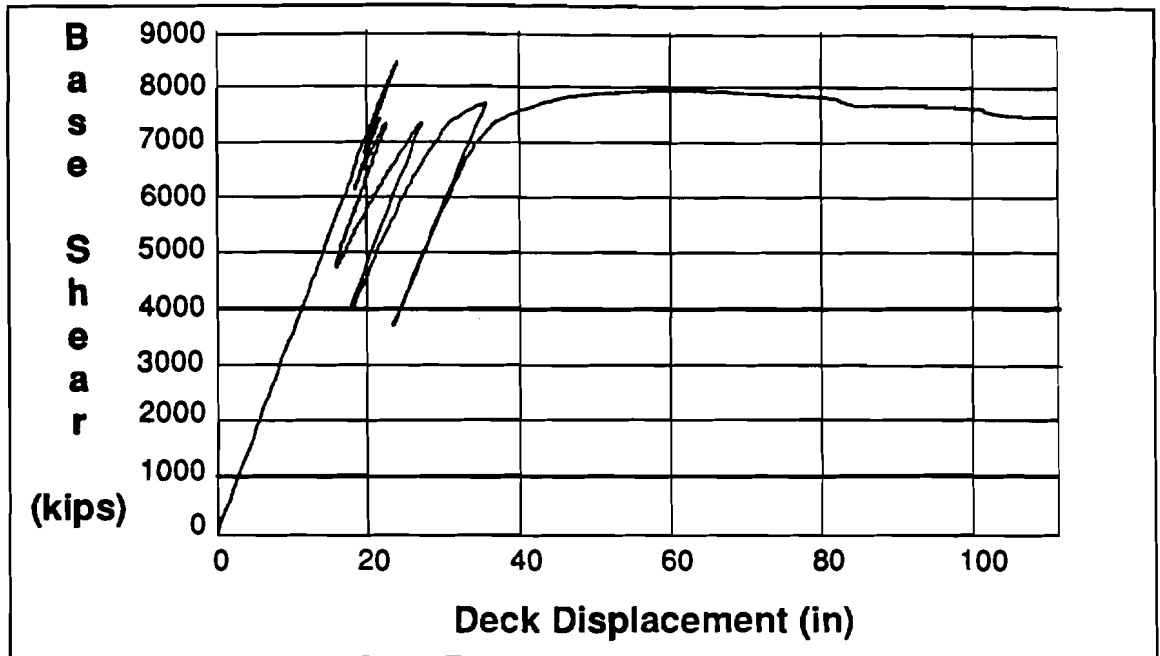
Figure 6.44: Platform F Broadside Loading Force-Displacement History (USFOS)
(Stear, 1995)
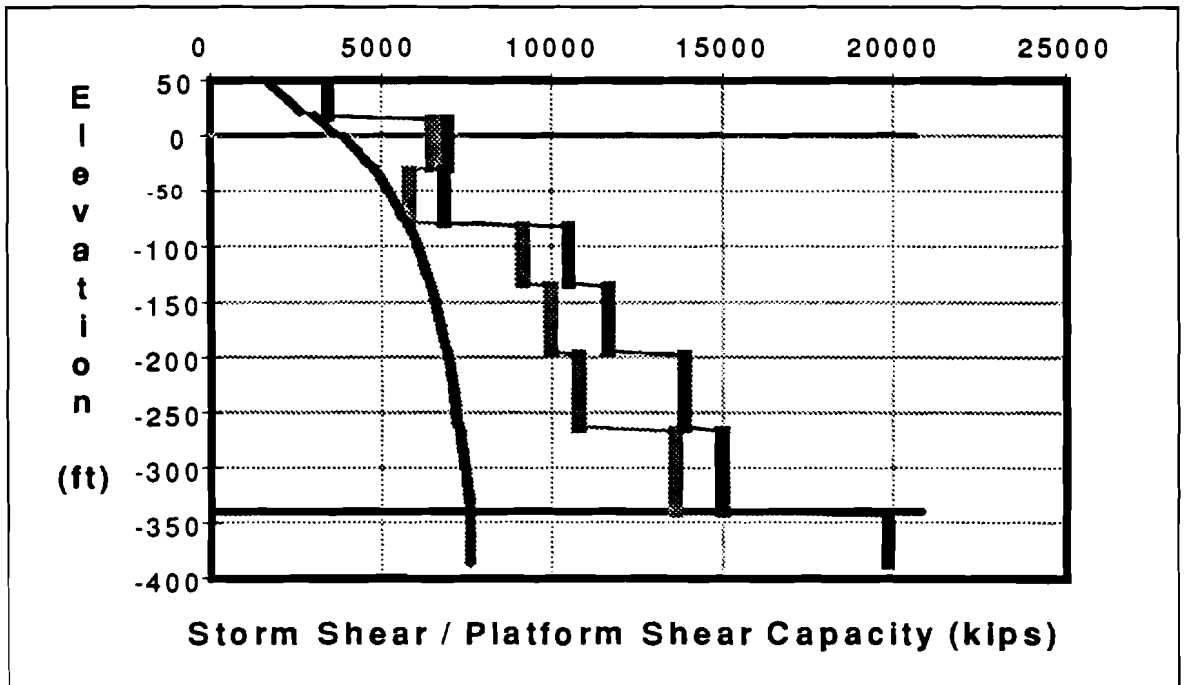
Figure 6.45: Platform F Broadside Loading Capacity (ULSLEA)
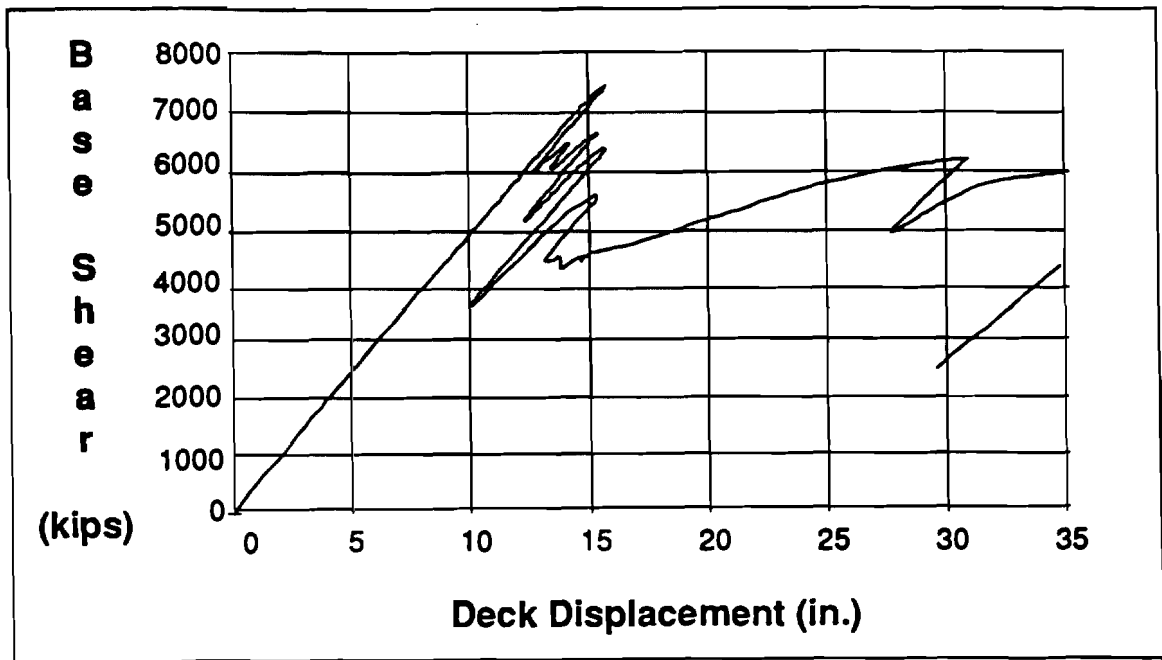
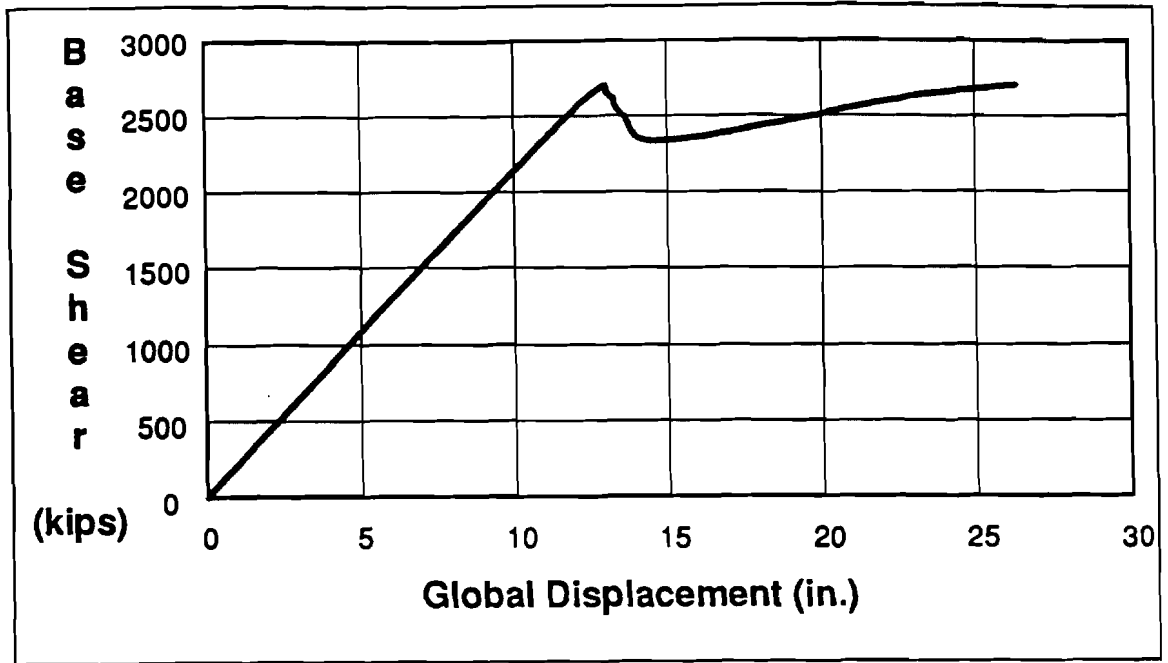**Figure 6.46: Platform F End-on Loading Force-Displacement History (USFOS)**
(Stear, 1995)
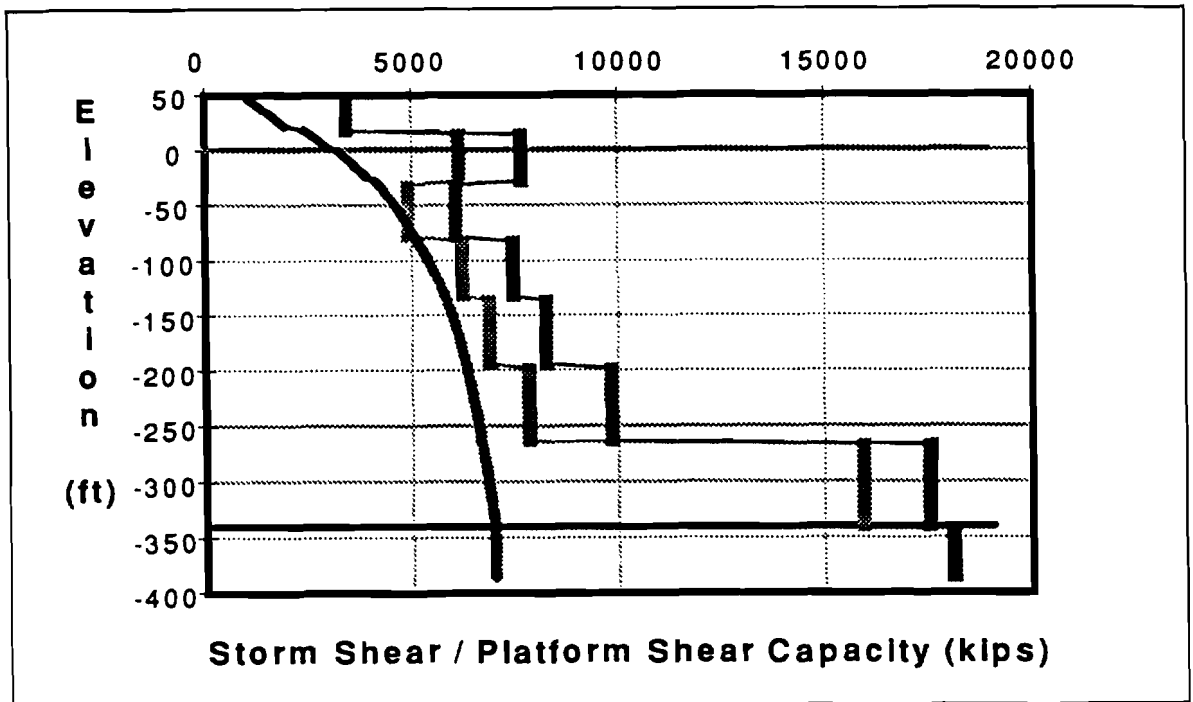
Figure 6.47: Platform F End-on Loading Capacity (ULSLEA)

185
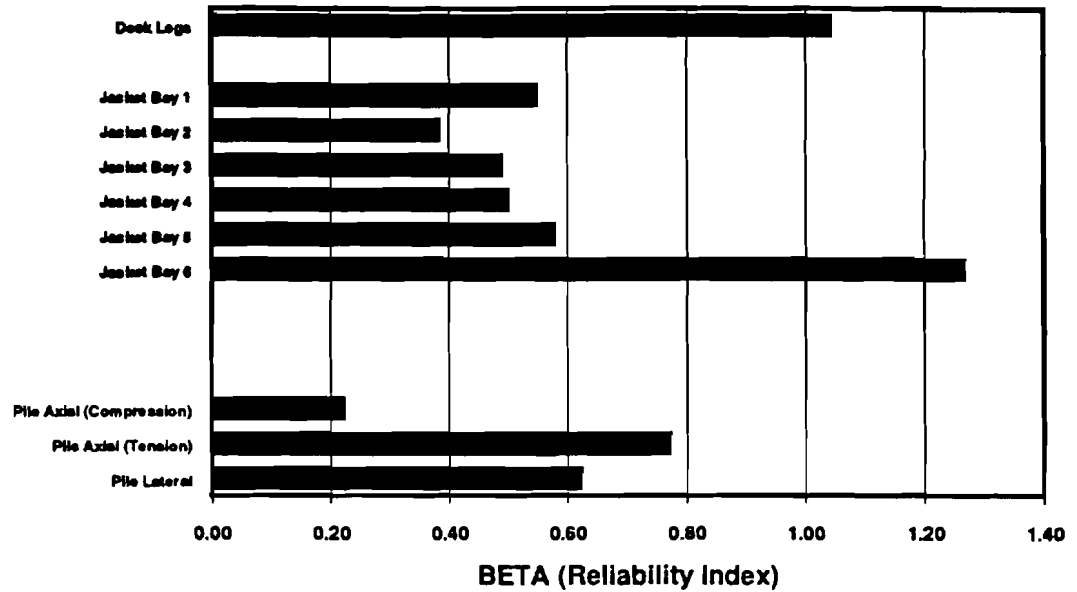
END-ON LOADING

Figure 6.48: Platform F Component Safety Indices ($\beta|_{Wave\ Height}$) -End-on Loading
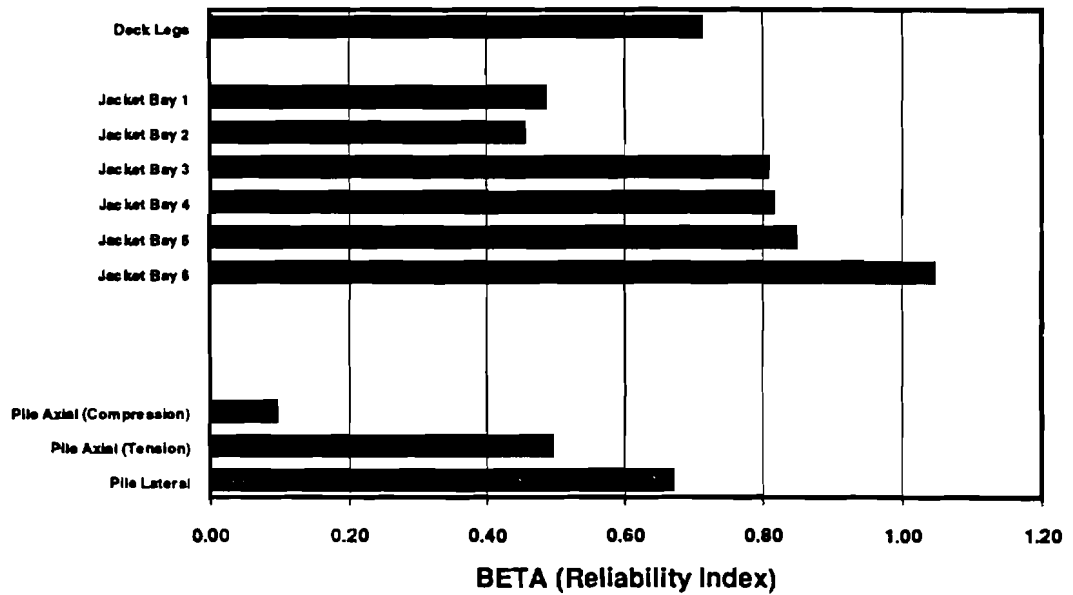
BROADSIDE LOADING

Figure 6.49: Platform F Component Safety Indices ($\beta|_{Wave\ Height}$) - Broadside Loading

186

6.2.7 Summary

The results of the analytical verification case studies are summarized in Tables 6.1 and 6.2. Table 6.1 contains a comparison of total base shears given by the simplified ULSLEA and detailed USFOS analyses and based on the same environmental conditions and force and kinematics coefficients. Defining a bias as the ratio of USFOS over ULSLEA base shears, the mean and the coefficient of variation of the bias are 0.89 and 0.03 respectively. A bias factor less than unity indicates an overprediction of the total base shear by the simplified method. The source of this conservatism is traced to modeling assumptions in the simplified analysis: all of the platform elements are modeled as equivalent vertical cylinders that are concentrated at a single vertical position in the wave crest. It is important to note that for all verification platforms, the wave forces acting on the lower deck areas were calculated according to API RP 2A-Section 17 using the same approach and force coefficients in both types of analysis. Hence, the estimated deck forces were in good agreement and the resulting bias factor reflects the difference in jacket loads only.

Table 6.2 contains a comparison of ultimate lateral loading capacities of the verification platforms given by the two types of analysis. Defining a bias as the ratio of USFOS over ULSLEA ultimate capacities, the mean and the coefficient of variation of the bias are 1.03 and 0.09 respectively. This indicates that compared to detailed nonlinear analyses, the simplified method predicts ultimate capacities which are practically unbiased.

The results of simplified reliability analyses performed on all verification platforms showed that the effects of uncertainties in loads and capacities on the assessment of structural reliability and prediction of potential failure modes can be important. For the platforms studied during this research, the results of the simplified reliability analyses are in good agreement with the results of deterministic nonlinear analyses in terms of potential failure modes, provided that the uncertainties associated with the capacities of pile foundations are neglected. Taking into account the relatively large uncertainties associated with foundation capacities, the reliability analyses results often indicate foundation failures as potential collapse mechanisms, which are not captured by deterministic pushover analyses.

Inclusion of the contribution of well conductors to the lateral foundation capacity and the loading rate effects (Chapter 4) would lead to an increase in the reliability indices associated with foundation failure modes. These effects have not been taken into account in the simplified analyses performed during this research.

Platform	Configuration	Wave Direction	Wave Height ft	Wave Period sec	Current Velocity at SWL	CD*	CB**	DS***	ULSLEA Base Shear (kips)	USFOS Base Shear (kips)	Ratio of USFOS/ULSLEA Base Shears
A	8 leg double battered K-braced	End-on	70	12.8	-	0.7	-	1	2,250	1,900	0.84
		Broadside	70	12.8	-	0.7	-	1	2,500	2,200	0.88
B	8 leg double battered K-braced	End-on	72	14.6	-	1.2	0.7	0.88	3,900	3,500	0.92
		Broadside	64	13.3	2.8	1.2	0.8	0.88	4,400	4,200	0.95
C	4 leg double battered K-braced	End-on	67	14.3	3.1	1.2	0.8	0.88	3,050	2,650	0.87
D	8 leg single battered K-braced	End-on	60	13	3.8	1.2	0.7	0.88	4,900	4,300	0.88
		Broadside	56	13	3.8	1.2	0.8	0.88	5,550	5,050	0.91
E	8 leg double battered K-braced	End-on	60	13	3.8	1.2	0.7	0.88	5,650	5,100	0.90
		Broadside	56	13	3.9	1.2	0.8	0.88	6,450	5,900	0.90
F	8 leg double battered single-braced	End-on	60	13.5	4	1.2	0.8	0.88	8,250	7,100	0.88
		Broadside	84	13.5	4	1.2	0.8	0.88	9,900	8,700	0.88

*) CD=Drag Coefficient
**) CB=Current Blockage Factor
***) DS=Wave Directional Spreading Factor

Table 6.1 : Load Predictions - Comparison of ULSLEA and USFOS Results

Platform	Configuration	Wave Direction	ULSLEA Failure Mode	Base Shear (kips)	USFOS / SEASTAR Failure Mode	Base Shear (kips)	Ratio of USFOS/ULSLEA Base Shears
A	8 leg double battered K-braced	End-on	1st jacket bay	2,900	1st jacket bay	2,600	0.90
		Broadside	2nd jacket bay	3,400	2nd jacket bay	2,900	0.85
B	8 leg double battered K-braced	End-on	1st jacket bay	3,100	1st jacket bay	3,900	1.26
		Broadside	1st jacket bay	3,700	1st jacket bay	3,900	1.05
C	4 leg double battered K-braced	End-on	4th , 5th and 6th jacket bays	3,200	5th and 6th jacket bays	3,400	1.06
		End-on	Foundation	1,900 (1,700)	Foundation	1,700	0.90 (1.00)*
D	8 leg single battered K-braced	End-on	4th jacket bay	2,800	4th jacket bay	2,700	0.96
		Broadside	2nd jacket bay	4,200	2nd jacket bay	4,500	1.07
E	8 leg double battered K-braced	End-on	3rd and 4th jacket bays	4,500	4th jacket bay	4,400	0.98
		Broadside	3rd jacket bay	4,500	3rd jacket bay	4,700	1.04
F	8 leg double battered single-braced	End-on	2nd, 3rd and 4th jacket bays	7,000	2nd, 3rd and 4th jacket bays	7,400	1.06
		BS (+Y)	2nd jacket bay	7,600	2nd jacket bay	8,400	1.11
		BS (-Y)	2nd jacket bay	9,200	2nd jacket bay	9,500	1.03

*) Including the platform selfweight

Table 6.2 : Capacity Predictions - Comparison of ULSLEA and USFOS Results

189

6.3 Frame Tests

6.3.1 Frame Test Program I

Frame test program I was performed in 1986 in behalf of Esso Australia in the process of upgrading some of its older platforms (Grenda et al., 1988). The program was conducted to support the results of nonlinear pushover analyses and the modeling assumptions upon which the analyses were based. Verification of these modeling assumptions were crucial to the validity of the nonlinear analyses results.

The test program included static testing of six two-dimensional single-bay K-braced frames (Figure 6.50). Four of the frames were ungrouted with overlap-joints. In two other cases, the compression diagonals were grout-filled. Two different K-joint can thicknesses were selected. The frames were heavily instrumented and sophisticated data acquisition systems were utilized. The 25 ft x 28 ft frames were loaded laterally using a 250 ton displacement-controlled hydraulic cylinder.

Figure 6.51 shows the load-displacement response of test frames 1-6. The performance of the four ungrouted frames with different joint can thicknesses (tests 1-4) was reported to be similar, each resisting a peak lateral load of approximately 160 kips. In all four cases, the buckling of compression braces was reported to govern the behavior of the frames. The lateral load resisting capacity of the frames began to decrease rapidly after failure of the compression diagonals. This is a typical result for a brittle k-braced frame

configuration. In all four cases, ULSLEA was able to predict the frame failure at the same peak lateral loads (Figure 6.51).

The lateral load capacity of the frames was significantly increased by grouting the diagonal compression braces. Grouting increased the buckling capacity of the diagonal braces in compression so that the diagonal braces in tension were able to fully develop their tensile capacity. This effect resulted in a redundant behavior of the frames. At the time the peak load was reached, both diagonal braces in tension and compression were contributing to the lateral shear resistance with their ultimate strengths. In addition, due to large displacement at collapse, the full portal strength of the frame legs were reported to be developed. However, the observed increase in lateral frame capacity due to frame action should not be overemphasized. In a real multi-bay offshore structure, frame action within one bay is likely to result in failure of diagonals in neighboring bays.

Frame test 6 resulted in an ultimate frame capacity of roughly 300 kips. The result gained using the simplified ULSLEA method indicated an almost simultaneous failure of two diagonal braces at a collapse load of roughly 240 kips (Figure 6.52). This is an underestimation of 20% compared to the test results. A detailed comparison of predicted and actual member forces at collapse indicated that the effect of frame action, observed in the test, was the source of the difference in results. ULSLEA does not take the effect of frame action into account.
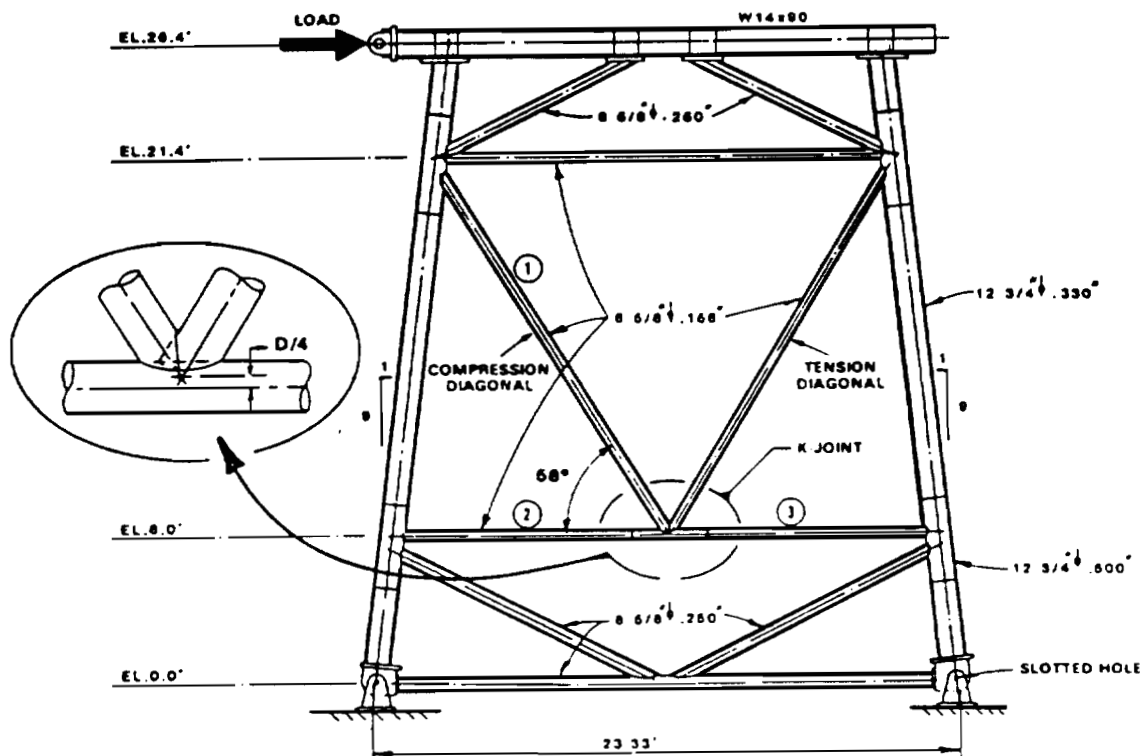
**Figure 6.50: Test Program I - Test Frame Geometry
(Grenda et al.,1988)**

192
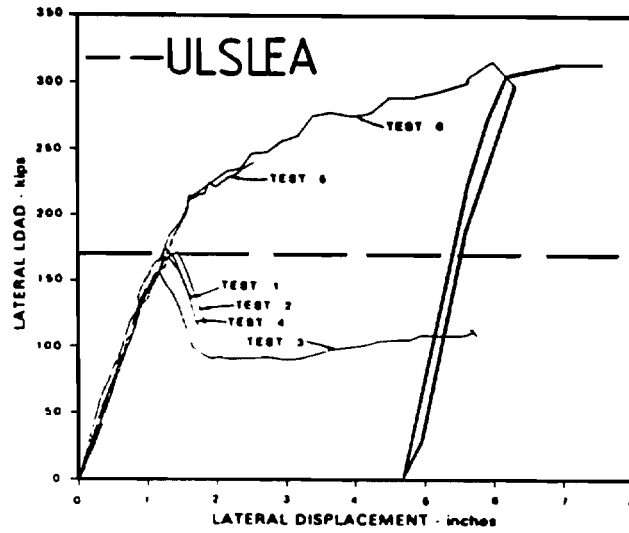
Figure 6.51: Test Program I - Tests 1-4
(Adopted from Grenda et al.,1988)
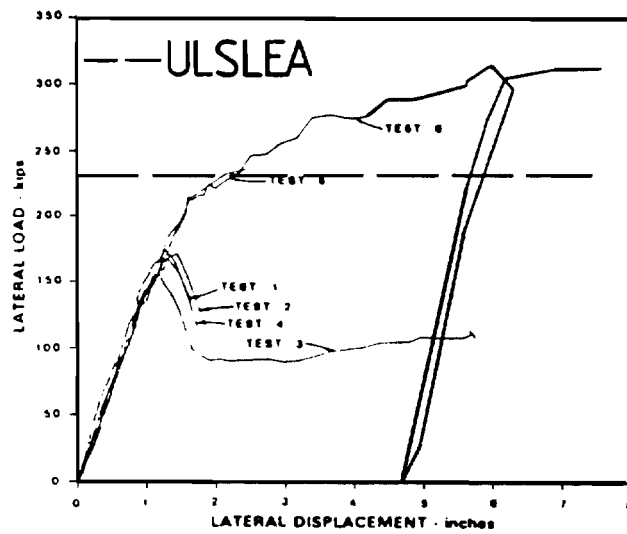
Figure 6.52: Test Program I - Tests 5-6
(Adopted from Grenda et al.,1988)

6.3.2 Frame Test Program II

Frame test program II was initiated in the U.K. in 1987. The program, Frames Project Phase I, was conducted by Billington Osborne-Moss Engineering Limited (BOMEL) as part of a joint industry project with the objectives of providing test data on the collapse behavior of jacket structures and developing a calibrated software for the nonlinear pushover analysis of framed structures (Bolt et al., 1994). Prior to release of the test data, the Health and Safety Executive in the U.K. invited interested companies in the U.K., Norway and U.S. to participate in a benchmarking effort. The results of this benchmarking exercise have been published by Nichols, et al. (1995).

In this phase of the project, four two-bay X-braced frames were pushed to collapse (Figure 6.53). The effects of joint ductility and system redundancy on the ultimate and post-ultimate response of the frames were studied. The frames were heavily instrumented and tested in plane. The hydraulic actuators were located at the top of the frames and were operated in a displacement-controlled manner. The frames were pinned at the bottom. The four frames had virtually the same geometry but differed in the joint can thickness, horizontal bracing, initial imperfections and residual stresses. Frame 2 was similar to frame 1 with the exception of a reduced joint can thickness. Frame 3 was virtually the same as frame 1 with the horizontal brace at the mid height removed. Finally frame 4 had the same configuration as frame 3 with the difference of locked-in prestresses and initial imperfections. Frame test 4 was left out in the verification study.

The test results for frames 1 and 3 are shown in Figure 6.54 in terms of lateral load displacement. In the case of frame 1, the buckling of the compression brace at the top half of the upper bay was reported to govern the ultimate lateral capacity of the frame which was reached at a lateral load of 920 kN. Due to redundancy of the X-bracing configuration and existing horizontal brace at the mid-height, a substantial residual strength in the system could be observed (Figure 6.54, left). Portal action in the legs was also reported to have contributed to this residual capacity. In the case of frame 3, a similar failure mode was observed. However, the peak lateral resistance was reached at a load level of 780 kN. The lower capacity as compared to the frame 1 was reported to be due to differences in the residual stresses and not a result of the missing horizontal brace at the mid-height. The lower residual capacity was, however, attributed to the reduced redundancy and lack of an effective load redistribution after first member failure. This resulted in a premature buckling of the compression brace in the lower bay and a consequent rapid fall of lateral resistance in post-ultimate regime (Figure 6.54, right).

Simplified ULSLEA method was used to predict the ultimate lateral capacity of both frames 1 and 2. ULSLEA predicted almost simultaneous failure of the compression and tension diagonals at the upper bay at a lateral load of roughly 850 kN for both frames. This result is in good agreement with the test results. The minor difference is due to the fact that ULSLEA does not account for residual stresses. The fact that the absence of the horizontal bracing in frame 3 did not change the ultimate capacity of the system, confirms

the assumption made in ULSLEA regarding horizontal framings. In ULSLEA, it is assumed that horizontal bracings exist and are rigid.

The results of the frame test 2 are plotted in Figure 6.55. The X-joint in the upper bay with the reduced wall thickness was the weak link in the frame and started yielding at a lateral load of 689 kN. The flattening of the joint essentially postponed the buckling of the compression diagonal and the tension diagonal developed its full yield strength. After the X-joint was completely compressed, a new load path was created. With further increase in the lateral load, the compression brace in the upper bay buckled and a rapid load shedding followed. The large global deflection at collapse had also resulted in portal action. The peak capacity of 1,080 kN was reached.

ULSLEA underestimated the lateral load at first member failure by 50%. The first member to fail is the X-joint in the upper bay. This underprediction is solely due to the conservatism of the joint capacity equations as given by API RP 2A-LRFD. Using a joint capacity bias factor of 2 would result in a close prediction of the lower-bound capacity. An upper-bound capacity of roughly 1,000 kN was predicted by ULSLEA. This peak lateral load was predicted to be associated with simultaneous failure of the tension and compression diagonals. In this case, the minor difference between ULSLEA and test results was traced back to the additional frame resistance due to portal action in the test.

196
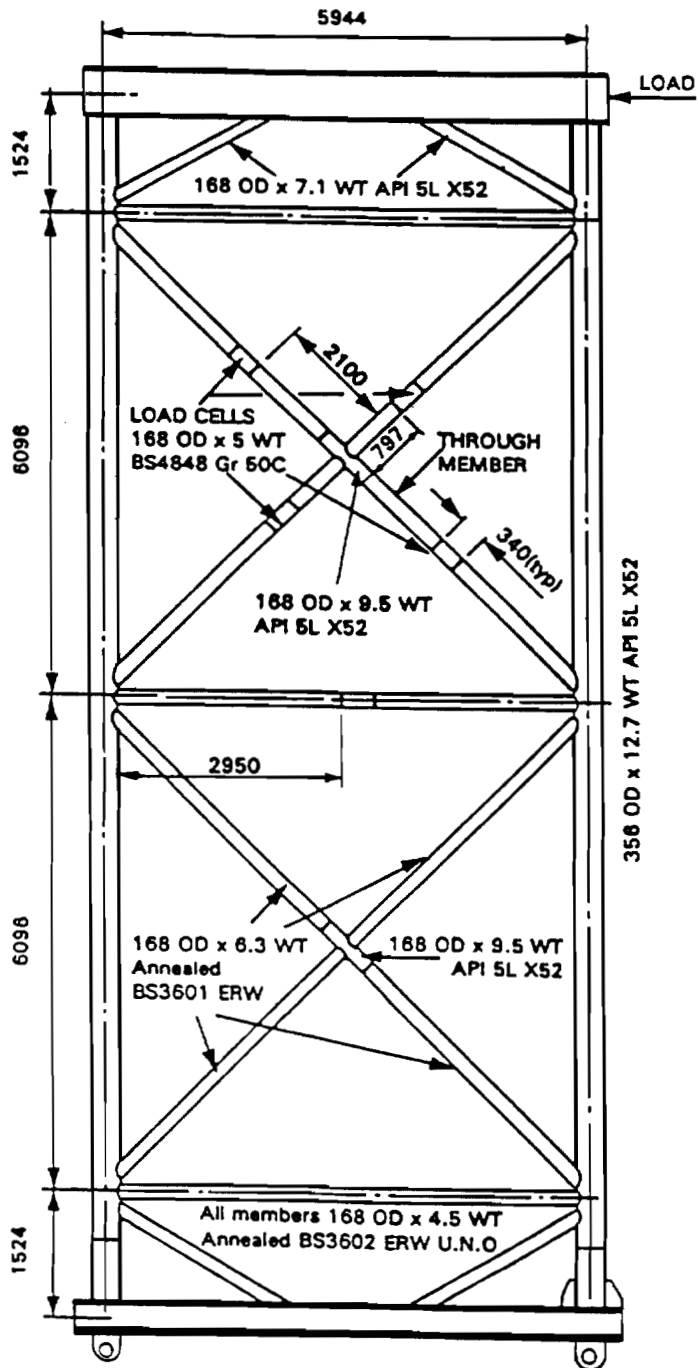
Figure 6.53: Test Program II - Test Frame Geometry (Bolt et al.,1994)
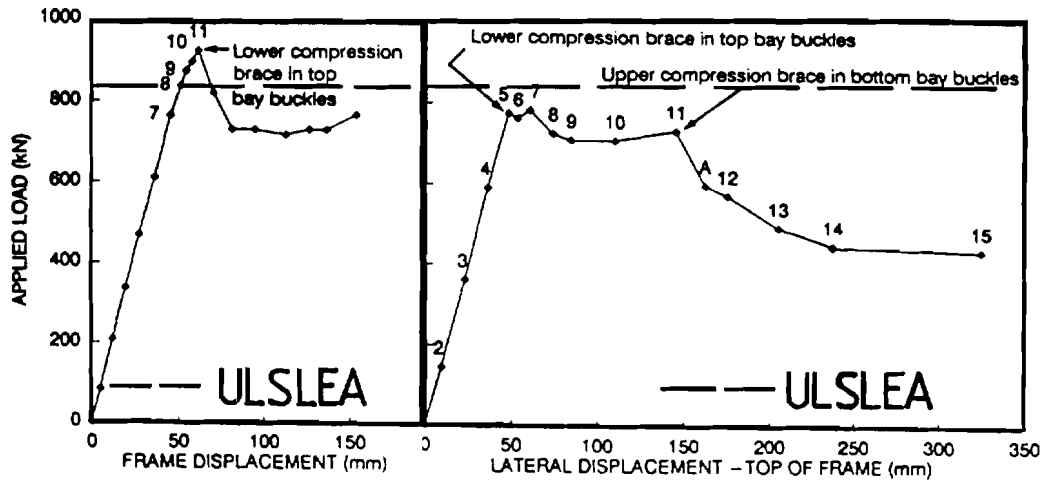
Figure 6.54: Test Program II - Tests 1 and 3
(Adopted from Bolt et al.,1994)
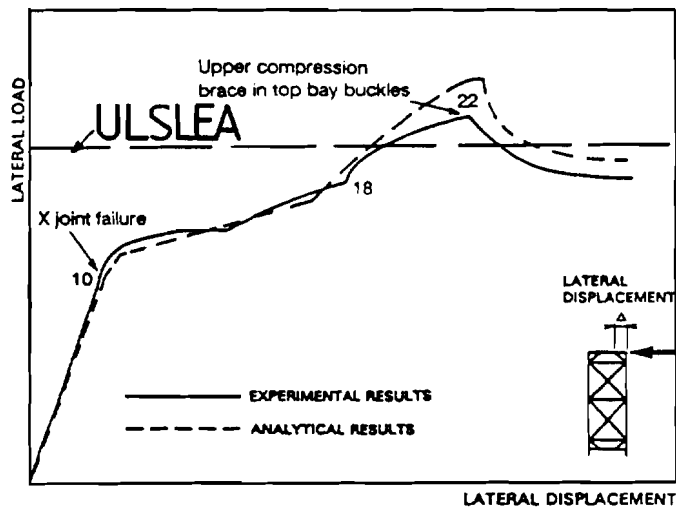
Figure 6.55: Test Program II - Test 2
(Adopted from Bolt et al.,1994)

6.3.3 Frame Test Program III

This frame test program was the second phase of the BOMEL's Frames Project (Bolt, 1995). Two objectives of this phase of the program were to investigate the effect of boundary conditions on joint ultimate capacity performance and to examine the collapse behavior of K-braced frames. In this phase four single bay K-braced frames were laterally pushed to collapse (Figure 6.56). Gap and overlap K-joints were used. The frames were laterally pushed under displacement-control beyond the ultimate load and into post-ultimate regime in order to capture their residual strength.

Figure 6.57 shows the load displacement behavior of one of the frames. The ultimate capacity was governed by the failure of the K-joint. With increasing lateral load, a crack was initiated at the chord side of the tension brace, which rapidly propagated and led to load shedding and a sudden reduction in frame lateral resistance. Compared to test results on isolated joints, it was found that the joint capacity within frames is higher. ULSLEA also predicted K-joint failure, however at a lateral load 50% lower than reported in the test (Figure 6.57). Again, the difference was found to be due to the conservatism in joint capacity formulations in API-RP 2A-LRFD (API, 1993b).
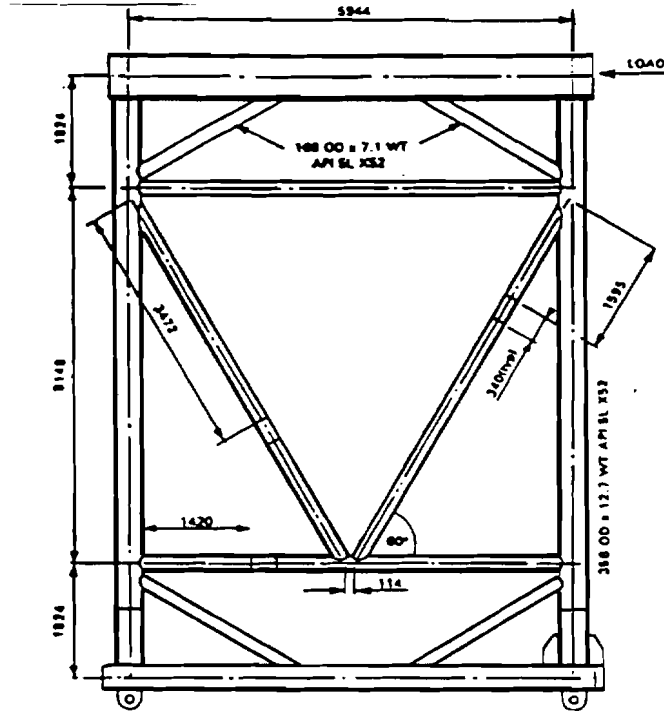
Figure 6.56: Test Program III - Test Frame Geometry (Bolt, 1995)
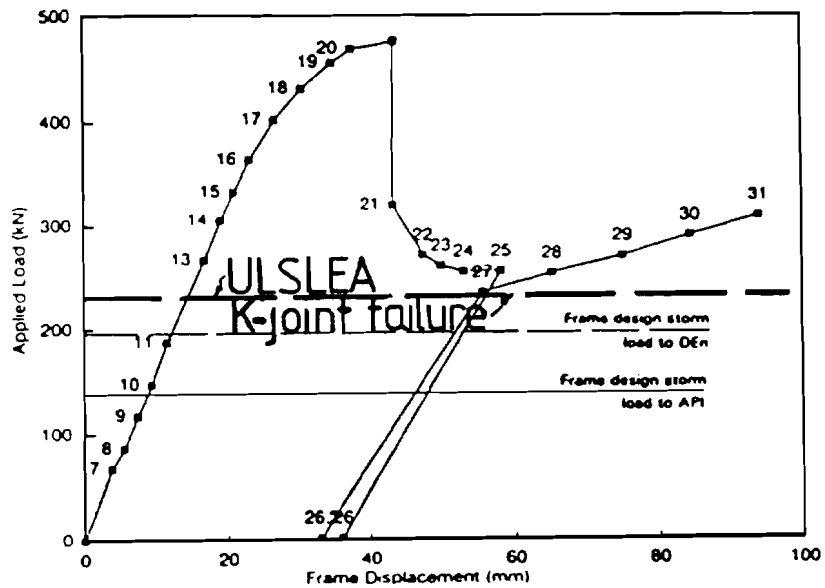
Figure 6.57: Test Program III (Adopted from Bolt, 1995)

200

6.3.4 Summary

Table 6.3 contains a summary of the verification studies based on frame test results. First member failures and ultimate lateral loading capacities of six test frames were predicted using the simplified method. These results were compared with the actual performance of the test frames. Defining a bias as the ratio of test over ULSLEA results, the mean and coefficient of variation of the bias were estimated to be 1.05 and 0.1 respectively for the cases where brace failures governed the capacity. In cases where tubular joint failures governed the frame capacity, the mean and coefficient of variation of the bias were estimated to be 2.03 and 0.01 respectively. The latter set of results can be explained by the conservatism of the API joint capacity equations (API, 1993b), which are adopted by ULSLEA.

Frame Test	Summary Description	Failure Category	Test Result		ULSLEA		Ratio of TEST/ULSLEA Base Shears
			Failure Mode	Base Shear	Failure Mode	Base Shear	
IA	single bay, K-braced, overlap K-joint	1st member failure	comp. brace	160 kips	comp. brace	160 kips	1.00
		ultimate capacity	comp. brace	160 kips	comp. brace	160 kips	1.00
IB	single bay, K-braced, overlap K-joint, grouted compression diagonal	1st member failure	tension brace	240 kN	all braces	240 kN	1.00
		ultimate capacity	all braces	300 kN	all braces	240 kN	1.25
IIA	two bay, X-braced, strong X-joint cans	1st member failure	comp. brace top bay	920 kN	comp. brace top bay	850 kN	1.08
		ultimate capacity	comp. brace top bay	920 kN	comp. brace top bay	850 kN	1.08
IIB	two bay, X-braced, weak X-joints	1st member failure	X-joint top bay	689 kN	X-joint top bay	345 kN	2.00
		ultimate capacity	all braces top bay	1080 kN	all braces top bay	1000 kN	1.08
IIC	two bay, X-braced, strong X-joint cans, no horizontal bracing	1st member failure	comp. brace top bay	780 kN	comp. brace top bay	850 kN	0.92
		ultimate capacity	comp. brace top bay	780 kN	comp. brace top bay	850 kN	0.92
III	single bay, K-braced, gap K-joint	1st member failure	K-joint	470 kN	K-joint	230 kN	2.04
		ultimate capacity	K-joint	470 kN	K-joint	230 kN	2.04

Table 6.3 : Capacity Predictions - Comparison of ULSLEA and Test Results

6.4   Summary

The simplified load and capacity prediction procedures that were developed in the previous chapters have been verified in this chapter. First, both simplified and detailed analyses were performed for six conventional jacket-type Gulf of Mexico platforms. The results of these verification studies are summarized in Tables 6.1 and 6.2. Defining a bias factor as the ratio of static ultimate lateral loading capacity of the platform predicted by USFOS (or SEASTAR) over that predicted by ULSLEA, a mean bias of B=1.03 was achieved. This bias ranged from 0.85 to 1.26 resulting in a coefficient of variation of 0.09 (Table 6.2). These verification case studies further indicated that the simplified loading calculation procedure overestimates the wave on jacket loads by approximately 10% in average (mean bias of 0.89 with a COV of 0.03)(Table 6.1). This difference was found to be due to the simplified platform model used in ULSLEA; all structural and non-structural elements are replaced by equivalent vertical cylinders that are located at the wave crest.

ULSLEA was also able to predict the actual field performance of the verification platforms which were on or very close to path of hurricanes Frederic, Camille, Carmen, and Andrew. Finally, ULSLEA was able to predict the ultimate capacity of the test frames, which have been conducted by offshore industry in the past ten years, reasonably well (Table 6.3). Tubular joint failures can be predicted provided joint capacity bias factors associated with the API joint capacity equations are known.

CHAPTER 7

SUMMARY & CONCLUSIONS

7.1   Summary

Assessment and requalification of offshore platforms is an issue of increasing importance. In recent years, interest in safety assessment of engineering structures against failure has significantly increased due to the awareness of the public of the consequences of their failure. Loss of life, environmental pollution, and loss of resources and property will no longer be easily tolerated. In this study, simplified procedures are developed to assess the structural reliability of steel, template-type, offshore platforms under extreme storm conditions. This research focused on development and verification of simplified procedures to:

a)   determine best estimates of storm loads and load profiles acting on offshore platforms,

b)   determine the ultimate capacity of intact, damaged, and grout repaired structural elements and components of the platforms,

c)   assess the static ultimate lateral loading capacity of the platform systems,

d)   assess the structural reliability of the platforms by taking into account the uncertainties associated with loadings and capacities, and

e)   verify the simplified procedures with results from detailed nonlinear analyses, actual field performance, and large-scale frame tests.

A computer program has been developed and tested to perform the simplified analyses. This program has been identified as ULSLEA (Appendix C). High degrees of user-friendliness have been employed in development of the software to reduce the engineering effort, required expertise, likelihood of errors, costs and time associated with the analyses.

7.2 Conclusions

The results of the verification case studies indicate that the simplified analyses can develop evaluations of both storm loadings on and ultimate lateral capacities of platforms that are good approximations of those derived from complex analyses. Defining a bias factor as the ratio of the results predicted by the detailed analyses (WAJAC and USFOS programs) over that predicted by the simplified analyses (ULSLEA), the mean and coefficient of variation of the loading bias are 0.89 and 0.03 respectively (Table 6.1). A bias factor less than unity indicates an overprediction of the total base shear by the simplified method. The source of this conservatism is traced to modeling assumptions in the simplified analysis. The mean and the coefficient of variation of the capacity bias are 1.03 and 0.09 respectively (Table 6.2). This indicates that compared to detailed nonlinear analyses, the simplified method predicts ultimate capacities which are practically unbiased.

Comparison of the estimated lateral load capacities with the estimated maximum loadings that these platforms have experienced during intense storms and their observed performance characteristics indicates that the analytical evaluations of both storm loadings and platform capacities are also in good agreement with the experience.

Finally, it is shown that the simplified ULSLEA technique is able to predict the ultimate capacity of test frames with reasonable accuracy. ULSLEA is also able to predict tubular joint failures provided joint capacity bias factors are included in the analysis. Defining a bias as the ratio of test over ULSLEA results, the mean and coefficient of variation of the bias is estimated to be 1.05 and 0.1 respectively for the cases where brace failures govern the capacity. In cases where tubular joint failures govern the frame capacity, the mean and coefficient of variation of the bias are estimated to be 2.03 and 0.01 respectively. The latter set of results can be explained by the conservatism of the API joint capacity equations (API, 1993b), which are adopted by ULSLEA.

The results of the simplified reliability analyses performed on all verification platforms show that the effects of uncertainties in loads and capacities on the assessment of structural reliability and prediction of potential failure modes can be important. For the platforms studied during this research, the results of the simplified reliability analyses are in good agreement with the results of deterministic nonlinear analyses in terms of potential failure modes, provided the uncertainties associated with the capacities of pile foundations are neglected. Taking into account the relatively large uncertainties associated with foundation capacities, the reliability analyses results often indicate foundation failures as potential collapse mechanisms, which are not captured by deterministic pushover analyses.

The use of the simplified analytical procedures to estimate reference storm lateral loading and platform capacities, and reserve strength ratios are shown to result in good estimates that can be used in the process of screening platforms that are being evaluated for extended service. In addition, the results from these analyses can be used to help verify results from complex analytical models that are intended to determine the ultimate limit state lateral loading capacities of platforms. In every verification case cited in this report, results from ULSLEA initially helped define major deficiencies and errors in either the complex analysis software or in the input to this software. Lastly, this approach can be applied as a preliminary design tool for design of new platforms.

7.3 Recommended Future Work

Potential research topics for future studies have been identified. These are presented and briefly discussed in this section. Further verification studies need to be performed. The verification studies performed during this research included six platforms located in the Gulf of Mexico. Although the results are extremely encouraging, additional studies on platforms with a variety of bracing patterns, different configurations, and in various water depths would help establish the probabilistic characteristics of the simplified loading and capacity modeling bias and help increase the confidence in simplified analysis techniques.

For the sake of simplicity in estimating the lateral capacity of jacket bays, it is assumed in the present work that the interconnecting horizontal braces are rigid. In reality, however, these horizontal members have diameter and thickness close in size to those of vertical

diagonal braces. The verification studies performed so far indicate that this assumption is reasonable in case of platforms with brittle strength behavior. In other words, the first member failure seems to be independent of the degree of rigidity of the interconnecting horizontals. The next step in verifying the simplified capacity calculation techniques is to investigate how the strength behavior of a redundant structure is affected by nonrigid horizontal framing. Currently, this issue is being investigated at University of California at Berkeley.

The simplified analyses developed and presented in this work include a foundation capacity model that is based on one soil layer. The next step in refining the procedure would be to include additional soil layers in the model. Development and verification of simplified procedures to account for soil sampling, testing, and cyclic-dynamic loading conditions is another potential research topic (Bea, 1987).

One important application of the simplified analysis techniques is preliminary design and optimization of jackets. Research and case studies can be performed to realize and demonstrate the application of the simplified nonlinear analysis method in conceptual plastic design and proportioning of jacket structures considering issues like robustness and damage tolerance.

Based on the simplified loading and capacity prediction procedures developed for extreme storm conditions, similar procedures can be developed to assess seismic loads, seismic

loading effects on and ultimate lateral loading capacity of pile supported offshore platforms or other structurally similar land-based structures such as high-rise buildings. The author is convinced that similar simplified reliability analysis procedures can be developed for screening of large fleets of other types of engineering structures of importance such as bridges and high-rise buildings.

BIBLIOGRAPHY

Aggarwal, R.K., Bea, R.G., Gerwick, B.C., Ibbs, C.W., Reimer, R.B., Lee, G.C., 1990. "Development of a Methodology for Safety Assessment of Existing Steel-Jacket Offshore Platforms." Proceedings, Offshore Technology Conference, OTC No. 6385, Houston, TX.

Aggarwal, R.K., 1991. "Methodology for Assessment by Regulatory Bodies of the Safety of Existing Steel Offshore Platforms." Dissertation, Graduate Division, Univ. of Cal. at Berkeley.

American Petroleum Institute (API), 1993a. "Recommended Practice for Planning, Designing and Constructing Fixed Offshore Platforms - Working Stress Design (RP 2A-WSD)." 20th Edition, July, Washington, D.C.

American Petroleum Institute (API), 1993b. "Recommended Practice for Planning, Designing and Constructing Fixed Offshore Platforms - Load and Resistance Factor Design (RP 2A-LRFD)." First Edition, July, Washington, D.C.

American Petroleum Institute (API), 1994. "API RP 2A-WSD 20th Edition, Draft Section 17.0, Assessment of Existing Platforms." November, Houston, TX.

Bea, R.G., 1973. "Wave Forces, Comparison of Stokes Fifth and Stream Function Theories." Engineering Note No. 40, Environmental Mechanics, April.

Bea, R.G., Lai, N.W., 1978. "Hydrodynamic Loadings on Offshore Structures." Proceedings, Offshore Technology Conference, OTC No. 3064. Houston, TX.

Bea, R.G., Pawsey, S.F., Litton, R.W., 1986. "Measured and Predicted Wave Forces on Offshore Platforms." Proceedings, Offshore Technology Conference, OTC No. 5787. Houston, TX.

Bea, R.G., Smith, C.S., 1987. "AIM (Assessment, Inspection, Maintenance) and Reliability of Offshore Platforms." Marine Structural Reliability Symposium, Virginia. pp57-75.

Bea R.G., 1987. "Dynamic Response of Marine Foundations." Proceedings, Ocean Structural Dynamics Symposium '84, Oregon State University, Corvallis, OR, Sept.

Bea, R.G., Puskar, F.J., Smith, C.S., Spencer, J., 1988. "Development of AIM (Assessment, Inspection, Maintenance) Programs for Fixed and Mobile Platforms." Proceedings, Offshore Technology Conference, OTC No. 5703, Houston, TX.

Bea R.G., 1990, "Reliability Based Design Criteria for Coastal and Ocean Structures." The Institution of Engineers, Australia, 11 National Circuit, Barton, ACT, Australia.

Bea, R.G., 1992. "Requalification of Offshore Platforms." Proceedings, Civil Engineering in the Oceans V, ASCE, College Station, Texas, 1992.

Bea, R.G., DesRoches, R., 1993. "Development and Verification of A Simplified Procedure to Estimate the Capacity of Template-Type Platforms." Proceedings, 5th International Symposium Integrity of Offshore Structures, D. Faulkner et al., Emas Scientific Publications, pp. 129-148.

Bea, R.G., Young, C., 1993. "Loading and Capacity Effects on Platform Performance in Extreme Condition Storm Waves & Earthquakes." Proceedings, Offshore Technology Conference, OTC No. 7140. Houston, TX.

Bea, R.G., Craig, M. J. K., 1993. "Developments in the Assessment and Requalification of Offshore Platforms." Proceedings, Offshore Technology Conference, OTC 7138, Houston TX, May.

Bea, R.G., Mortazavi, M., 1995a. "Simplified Evaluation of the Capacities of Template-Type Offshore Platforms." Proceeding of 5th International Offshore and Polar Engineering Conference, The Hague, The Netherlands, June 11-16.

Bea, R.G., Loch, K., Young, P., 1995b. "Evaluation of Capacities of Template-Type Gulf of Mexico Platforms." Proceedings, 5th International Offshore and Polar Engineering Conference, ISOPE-95, The Hague, The Netherlands, June 11-16.

Bea, R.G., Mortazavi, M., Loch, K., Young, P., 1995c. "Verification of A Simplified Method to Evaluate the Capacities of Template-Type Platforms." Proceedings, Offshore Technology Conference, OTC 7780, Houston TX, May.

Bea, R.G., Mortazavi, M., Loch, K., Young, P., 1995d. "Verification of A Second Generation Simplified Method to Evaluate the Storm Loadings on and Capacities of Steel Template-Type Platforms." Proceedings, Energy and Environmental Expo 95, American Society of Mechanical Engineers, Houston, Texas, Jan.

Bea, R.G., 1995. "Development and Verification of a Simplified Method to Evaluate Storm Loadings on and Capacities of Steel, Template-Type Platforms." Proceedings, Energy and Environmental Expo 95, American Society of Mechanical Engineers, Houston, Texas, Jan.

Billington, C.J., Lloyed, J.R., Digre, K.A., 1993. "Structural Elements, Systems and Analyses." White paper prepared for the International Workshop on Assessment and Requalification of Offshore Production Structures, New Orleans, LA.

Billington, C.J., Bolt, H.M., Ward, J.K. 1993. "Reserve, Residual and Ultimate Strength Analysis of Offshore Structures: State of the Art Review." Proceedings, Third International Offshore and Polar Engineering Conference, Singapore, June, pp. 125-133.

Bolt, H.M., Billington C.J., Ward J.K., 1994. "Results from Large-Scale Ultimate Load Tests on Tubular Jacket Frame Structures." Proceedings, Offshore Technology Conference, OTC 7451, Houston TX, May.

Bolt, H.M., 1995. "Results from Large-Scale Ultimate Strength Tests of K-Braced Jacket Frame Structures." Proceedings, Offshore Technology Conference, OTC 7783, Houston TX, May.

Cox, J.W., 1987. "Tubular Member Strength Equations for LRFD." Final Report API PRAC Project 86-55.

Dean, R.G., 1977. "Hybrid Method of Computing Wave Loading." Proceedings, Offshore Technology Conference, OTC 3029, Houston TX, May.

Der Kiureghian, A., 1994. "Structural Reliability." Lecture Notes, Department of Civil Engineering, University of California, Berkeley.

Det Norske Veritas, 1993. "WAJAC. Wave and Current Loads on Fixed Rigid Frame Structures." DNV SESAM AS. Version 5.4-02.

Digre, K.A., Puskar, F.J., Irick, J.T., Krieger, W., 1995. "Modifications to and Applications of the Guidelines for Assessment of Existing Platforms Contained in Section 17 of API RP 2A." Proceedings, Offshore Technology Conference, OTC 7779, Houston TX, May.

Dunlap, W.A., Ibbs, C.W., 1993. "Assessment and Requalification of Offshore Production Structures." Proceedings of an International Workshop, New Orleans, LA, Dec. 8-10.

Ellinas, C.P., 1984. "Ultimate Strength of Damaged Tubular Bracing Members." Journal of Structural Engineering, Vol. 110, No.2, February 1984.

Fenton, J.D., 1985. "A Fifth Order Stokes Theory for Steady Waves." ASCE Journal of Waterway, Port, Coastal and Ocean Engineering, Vol. 111, No. 2, pp. 216-234.

Focht, J.A., and Kraft, L.M., 1986. "Axial Performance and Capacity of Piles." Planning and Design of Fixed Offshore Platforms, McClelland, B., and Reifel, M.D., pp. 763-801.

Grenda, K.G., Clawson, W.C., Shinners, C.D., 1988. "Large-Scale Ultimate Strength Testing of Tubular K-Braced Frames." Proceedings, Offshore Technology Conference, OTC 5832, Houston TX, May.

Hamilton, J.M., Phillips, R., Dunnavant, T.W., Murff, J.D., 1991. "Centrifuge Study of Laterally Loaded Pile Behavior in Clay." Proceedings, International Conference Centrifuge, ISSMFE.

Haring, R.E., Spencer, L.P., 1979. "The Ocean Test Structure Data Base." Proceedings, Civil Engineering in the Oceans IV, Vol. II, ASCE, New York, September, pp 669-683.

Haver, S., 1995. " Uncertainties in Force and Response Estimates." E&P Forum, The Oil Industry International Exploration & Production Forum, Offshore Structures/Metocean Workshop, E&P Forum Report No. 3.15/229.

Heideman, J.C., Weaver, T.O., 1992. "Static Wave Force Procedure for Platform Design." Proceedings of Civil Engineering in the Oceans V, College Station, Texas, American Society of Civil Engineers, New York.

Hellan, O., Moan, T., Drange, S.O., 1994. "Use of Nonlinear Pushover Analyses in Ultimate Limit State Design and Integrity Assessment of Jacket Structures." Proceedings, 7th International Conference on Behavior of Offshore Structures, Boss '94, Vol. 3, Structures, C. Chryssostomidis (Ed.) Elsevier Science Inc., New York, NY.

Hennegan, N., Abadie, W., Goldberg, L., Winkworth, W., 1993. "Inspections, Surveys and Data Management." White paper prepared for the International Workshop on Assessment and Requalification of Offshore Production Structures, New Orleans, LA.

Imm, G.R., O'Connor, J.M., Light, J.M., Stahl, B., 1994. "South Timbalier 161A: A Successful Application of Platform Requalification Technology." Proceedings, Offshore Technology Conference, OTC 7471, Houston, Texas, May.

Kim W., Ostapenko A., "A Simplified Method to Determine The Ultimate Strength of Damaged Tubular Segment."

Liu, P.L., Lin, H.Z., Der Kiureghian, A., 1989. "CALREL User Manual." Report No.UCB/SEMM-89/18, Dept. of Civil Engineering, University of California at Berkeley.

Loch, K.J., Bea, R.G., 1995. "Determination of the Ultimate Limit States of Fixed Steel-Frame Offshore Platforms Using static Pushover Analyses." Report to U.S. Minerals Management Service and Joint Industry Project Sponsors, Marine Technology Development Group, University of California at Berkeley, May.

Loh, J.T., Kahlich, J.L., Broekers, D.L., 1992. "Dented Tubular Steel Members." Exxon Production Research Company, Offshore Division, Houston, TX, March.

Loh, J.T., 1993. "Ultimate Strength of Dented Tubular Steel Members." Proceedings, 3rd International Offshore and Polar Engineering Conference, Vol. 4, pp. 134-145.

Marshall, P.W., 1986. "Tubular Joint Design." Planning and Design of Fixed Offshore Platforms, McClelland, B., and Reifel, M.D., pp. 624-691.

Marshall, P.W., 1992. "Screening Old Offshore Platforms: Previous Approaches and Further Thoughts." Proceedings, Civil Engineering in the Oceans V, ASCE, Texas 1992.

Matlock, H., 1970. "Correlations for Design of Laterally Loaded Piles in Soft Clay." Proceedings, Offshore Technology Conference, Houston TX, May.

McDonald, D.T., Bando, K., Bea, R.G., Sobey, R.J., 1990. " Near Surface Wave Forces on Horizontal Members and Decks of Offshore Platforms." Final Report, Coastal and Hydraulic Engineering, Dept. of Civil Engineering, University of California at Berkeley, Dec.

Moan, T., 1981. "The Alexander Kielland Accident." Proceedings, The First Robert Bruce Wallace Lecture, Department of Ocean Engineering, Massachusetts Institute of Technology.

Moore, W.H., 1993. "Management of Human and Organizational Error in Operations of marine Systems." Dissertation, Graduate Division, Univ. of Cal. at Berkeley.

Morison, J.R., O'Brien, M.P., Johnson, J.W., Schaff, S.A., 1950. "The Force Exerted by Surface Waves on Piles." Petrol. Trans. AIME, Vol. 189, pp 149-154.

Mortazavi, M., Bea R.G., 1994. "ULSLEA, Simplified Nonlinear Analysis for Offshore Structures." Report to Joint Industry-Government Sponsored Project, Marine Technology and Management Group, Dept. of Civil Engineering, University of California at Berkeley, June.

Mortazavi, M., Bea R.G., 1995. "Screening Methodologies for Use in Platform Assessments and Requalifications." Final Report to Joint Industry-Government Sponsored Project, Marine Technology and Management Group, Dept. of Civil Engineering, University of California at Berkeley, June.

Murff, J.D., Hamilton, J.M., 1993. "P-Ultimate for Undrained Analysis of Laterally Loaded Piles", Journal of Geotechnical Engineering, Vol. 119, No. 1, January.

Nair, V.V.D., Kuhn, J.M., (1993). "Reassessment of Offshore Platforms." Appl. Mech. Rev. vol. 46, no 5, May 1993.

Nichols, N.W., Sharp, J.V., Kam, J.C.P., 1995. "Benchmarking of Collapse Analysis of Large-Scale Ultimate Load Tests on Tubular Jacket Frame Structures."

Nordal, H., 1991. "Application of Ultimate Strength Analysis in Design of Offshore Structural Systems." Integrity of Offshore Structures- 4. ed. Faulkner, D., Glasgow.

Nordal, H., Cornell, C.A., Karamchandani, A., 1988. "A System Reliability Case Study of an Eight-leg Jacket Platform." Report No. RMS-3, Department of Civil Engineering, Stanford University.

Ochi, M.K., Shin, Y.S., 1986. "Wind Turbulent Spectra for Design Consideration of Offshore Structures." Proceedings, Offshore Technology Conference, OTC 5736, Houston, Texas, May.

Ostapenko, A., Wood, B., Chowdhury, A., Hebor, M., 1993. "Residual Strength of Damaged and Deteriorated Tubular Members in Offshore Structures." ATLSS Report No. 93-03, Lehigh University, Betlehem, PA.

Parsanejad S., 1987. "Strength of Grout-Filled Damaged Tubular Members." Journal of Structural Engineering, ASCE, Vol. 113, No. 3, March 1987.

Pate-Cornell, M.E., 1993. "Risk Management for Existing Energy Facilities." Applied Mechanics Review, vol 46, no 5, May 1993, pp 242-245.

Petrauskas, C., Botelho, D.L.R., Krieger, W.F., and Griffin, J.J., 1994. "A Reliability Model for Offshore Platforms and its Application to ST 151 H and K Platforms During Hurricane Andrew (1992)." Proceedings of the Behavior of Offshore Structure Systems, Boss '94, Massachusetts Institute of Technology.

Petrauskas, C., Heideman, J.C., Berek, E.P., 1993. "Extreme Wave-Force Calculation Procedure for the 20th Edition of API RP-2A." Proceedings, Offshore Technology Conference, OTC 7153, Houston, Texas, May.

Petrauskas, C., Heideman, J.C., and Berek, E.P., 1993. "Extreme Wave Force Calculation Procedure for 20th Edition of API RP 2A." Proceedings, Offshore Technology Conference, OTC 7153, Houston, TX.

PMB Engineering Inc., 1994. "Benchmark Analysis, Trial Application of the API-RP 2A-WSD Draft Section 17." Report to Minerals Management Service and Trials JIP Participants, San Francisco, CA., Dec.

PMB Engineering Inc., 1995. "Further Evaluation of Offshore Structures Performance in Hurricane Andrew - Development of Bias Factors for Pile Foundation Capacity." Report to American Petroleum Institute and Minerals Management Service, San Francisco, CA., Dec.

Preston, D.,1994, "An Assessment of the Environmental Loads on the Ocean Motion International Platform." MS Thesis, Department of Naval Architecture and Offshore Engineering, University of California, Berkeley, USA.

Randolph, M.F., Houlsby, G.T., (1984). "The Limiting Pressure on A Circular Pile Loaded Laterally in Cohesive Soil." Geotechnique, London, England, 34(4), pp 613-623.

Reese, L.C., Cox, W.R., Koop, F.D., (1975). "Field Testing and Analysis of Laterally Loaded Piles in Stiff Caly." Proceedings, Offshore Technology Conference, Houston TX, May.

Ricles, J.M., Bruin, W.M., Sooi, T.K., 1992. "Residual Strength and Repair of Dent-Damaged Tubulars and the Implication on Offshore Platform Assessment and Requalification."

Ricles, J.M., Lamport, W.P., Gillum, T.E., 1992. "Residual Strength of Damaged Offshore Tubular Bracing." Proceedings, Offshore Technology Conference, OTC 6938, Houston TX, May.

Ricles, J.M., Gillum, T.E., Lamport, W.P., 1993. "Grout Repair of Dent-Damaged Steel Tubular bracing." Proceedings, Offshore Technology Conference, OTC 7151, Houston TX, May.

Ricles, J.M., Hebor, M.F., 1994. "Residual Strength and Epoxy-based Grout Repair of Corroded Offshore Tubulars." Boss 94.

Sarpkaya, T, Isaacson, M., 1981. "Mechanics of Wave Forces on Offshore Structures" Van Nostrand Reinhold Company.

Shaefer, M.G., 1992. "Selection of Design/Performance Goals for Critical Project Elements." Dam Safety Guidelines, Washington State Department of Ecology.

Sintef, 1994. "USFOS. A Computer Program for Progressive Collapse Analysis of Steel Offshore Structures." Publication N-7034, Trondheim, Norway. Revised Version 6.0.

Skjelbreia, L., and Hendrickson, J., 1961, "Fifth Order Gravity Wave Theory." Proceedings, 7th Conference of Coastal Engineering, pp. 184-196.

Staneff, S.T., Ibbs, C.W., Bea, R.G., 1994, "California Coastal Platform Information Management System - Software Documentation." Report to California State Lands Commission, University of California at Berkeley.

Stear, J.D., Bea, R.G., 1995. "Verification of Screening Methodologies for Use in Gulf of Mexico Platform Requalifications." Progress Report to joint government-industry project sponsors, University of California at Berkeley October.

Tang, W.H. and Gilbert R.B., 1990, "Offshore Lateral Pile Design Reliability." Research Report for Project PRAC 87-29 sponsored by the American Petroleum Institute.

Tang, W.H., 1988, "Offshore Axial Pile Design Reliability", Research Report for Phase 1 of the Project PRAC 86-29B sponsored by the American Petroleum Institute.

Thoft-Christensen, P., Baker, J., 1982. "Structural Reliability Theory and Its Applications." Springer-Verlag.

Titus, P.G., Banon, H., 1988. "Reserve Strength Analyses of Offshore Platforms." Proceedings, 7th Offshore South East Asia, Singapore, 2-5 February.

Vannan, M.T., Thompson, H.M., Griffin, J.J., Gelpi, S.L., 1994. "An Automated Procedure for Platform Strength Assessment." Proceedings, Offshore Technology Conference, OTC 7474, Houston, TX.

Weidler, J.B., 1993. "Platform Removal." Article in Applied Mechanics Review, vol 46, no 5, May 1993, pp176-177.

Wenk, E., Kallman, R.E., Pulsipher, A., 1993. "Considerations and consequences of public policy." White paper prepared for the International Workshop on Assessment and Requalification of Offshore Production Structures, New Orleans, LA.

Yura, J.A., Zettlemoyer, N., Edwards, F.E., 1980. "Ultimate Capacity Equations for Tubular Joints." Proceedings, Offshore Technology Conference, OTC 3690, Houston TX, May.

Zayas, V.A., Popov, E.P., Mahin, S.A., 1980. "Cyclic Inelastic Buckling of Tubular Steel Braces.", University of California, Report No. UCB/EERC-80/16, June.

Zhang, Y., Der Kiureghian, A., 1995. "Finite Element Reliability Analysis of Limit Load." Proceedings, ICASP-7, July, Paris, France.

APPENDIX A

CALREL INPUT & OUTPUT FILES

****

University of California
Department of Civil Engineering

CAL-RELiability program
Developed by
P.L. Liu, H.Z. Lin and A. Der Kiureghian

Last Revision: December 1990
Copyright @ 1989

****

INPUT - LIMIT STATE FUNCTIONS

DECK LEGS

```
    subroutine ugfun(g,x,tp,ig)
    implicit real*8 (a-h,o-z)
    dimension x(1),tp(1)
    go to(10) ig
 10 g = x(1)*cos(tp(1)/x(2))*tp(2)-tp(3)*x(3)*(tp(4)*x(4))**2-tp(5)
    return
    end
```

JACKET END-ON LOADING

```
    subroutine ugfun(g,x,tp,ig)
    implicit real*8 (a-h,o-z)
    dimension x(1),tp(1)
    go to(10) ig
 10 g =tp(1)*x(1)+tp(2)*x(2)+tp(3)*x(3)-tp(4)*x(4)*(tp(5)*x(5))**2
   *+x(6)
    return
    end
```

JACKET BROADSIDE LOADING

```
    subroutine ugfun(g,x,tp,ig)
    implicit real*8 (a-h,o-z)
    dimension x(1),tp(1)
    go to(10) ig
 10 g =x(1)-tp(1)*x(2)*(tp(2)*x(3))**2+tp(3)
    return
    end
```

FOUNDATION

```
    subroutine ugfun(g,x,tp,ig)
    implicit real*8 (a-h,o-z)
    dimension x(1),tp(1)
    go to(10) ig
10  g =tp(1)*x(1)-tp(2)*x(2)*(tp(3)*x(3)**2)
    return
    end
```

DECK LEGS - END-ON LOADING

var	ids	mean	st. dev.	param1	param2	param3	param4	init. pt
x1	2	6.31E+03	6.68E+02	8.74E+00	1.06E-01			6.31E+03
x2	2	6.68E+03	7.82E+02	8.80E+00	1.17E-01			6.68E+03
x3	2	1.00E-01	5.80E-02	-2.45E+00	5.38E-01			1.00E-01
x4	2	3.45E+01	1.16E+01	3.49E+00	3.27E-01			3.45E+01

deterministic parameters in limit-state function:

tp (1) = 1.197E+03
tp (2) = 4.200E-01
tp (3) = 7.000E-01
tp (4) = 1.100E+00
tp (5) = 1.000E+00

>>>> FIRST-ORDER RELIABILITY ANALYSIS <<<<

iteration number ....iter=   7
value of limit-state function..g(x)=-3.016E-05
reliability index ....beta=   4.0956
probability ....Pf1= 2.106E-05

var	design point			sensitivity vectors			
	x*	u*	alpha	gamma	delta	eta	
x1	5.944E+03	-5.067E-01	-.1237	-.1237	.1320	-.0753	
x2	6.623E+03	-1.847E-02	-.0045	-.0045	.0046	-.0006	
x3	3.474E-01	2.582E+00	.6304	.6304	-.0304	-1.1184	
x4	9.133E+01	3.138E+00	.7663	.7663	-.1004	-2.0428	

>>>> SECOND-ORDER RELIABILITY ANALYSIS -- POINT FITTING <<<<

coordinates and ave. main curvatures of fitting points in rotated space

axis	u'i	u'n	G(u)	a'+i	u'i	u'n	G(u)	a'-i
1	3.000	4.096	7.414E-08	-4.689E-06	-3.000	4.096	6.022E-08	-5.780E-06
2	3.000	4.092	1.774E-03	-8.501E-04	-3.000	4.089	4.470E-03	-1.371E-03
3	3.000	4.096	1.215E-11	-7.068E-08	-3.000	4.096	1.156E-11	-7.208E-08

		improved Breitung	Tvedt's EI
generalized reliability index betag =		4.0950	4.0950
probability	Pf2 =	2.111E-05	2.111E-05

218

JACKET BAY 1 - END-ON LOADING

var	ids	mean	st. dev.	param1	param2	param3	param4	init. pt
x1	2	1.15E+03	1.73E+02	7.04E+00	1.49E-01			1.15E+03
x2	2	1.07E+03	1.60E+02	6.96E+00	1.49E-01			1.07E+03
x3	2	1.62E+03	1.30E+02	7.39E+00	8.01E-02			1.62E+03
x4	2	3.56E-01	2.06E-01	-1.18E+00	5.37E-01			3.56E-01
x5	2	3.45E+01	1.16E+01	3.49E+00	3.27E-01			3.45E+01

deterministic parameters in limit-state function:

tp (1) = 1.500E-01
tp (2) = 1.500E-01
tp (3) = 1.000E+00
tp (4) = 7.000E-01
tp (5) = 1.100E+00
tp (6) = 1.000E+00

>>>> FIRST-ORDER RELIABILITY ANALYSIS <<<<

iteration number ....iter=   8
value of limit-state function..g(x)=-9.461E-07
reliability index ....beta=   2.2855
probability ....Pf1= 1.114E-02

var	design point			sensitivity vectors			
	x*	u*	alpha	gamma	delta	eta	
x1	1.134E+03	-3.554E-02		-.0155	-.0155	.0161	-.0028
x2	1.049E+03	-3.288E-02		-.0144	-.0144	.0149	-.0026
x3	1.593E+03	-1.786E-01		-.0781	-.0781	.0799	-.0201
x4	6.701E-01	1.446E+00		.6325	.6325	-.3923	-.4989
x5	5.818E+01	1.761E+00		.7703	.7703	-.4394	-1.0471

>>>> SECOND-ORDER RELIABILITY ANALYSIS -- POINT FITTING <<<<

type of integration scheme used ....itg=   2
 itg=1 ....improved Breitung formula
 itg=2 ....improved Breitung formula
 ....& Tvedt's exact integral
max. number of iterations for each fitting point ..inp=   4

limit-state function   1

---

coordinates and ave. main curvatures of fitting points in rotated space

axis	u'i	u'n	G(u)	a'+i	u'i	u'n	G(u)	a'-i
1	2.279	2.292	-1.459E-06	2.322E-03	-2.281	2.291	-1.961E-06	1.927E-03
2	2.280	2.291	-1.318E-06	2.169E-03	-2.281	2.290	-1.672E-06	1.794E-03
3	2.283	2.288	-4.686E-08	1.024E-03	-2.283	2.288	-1.786E-06	1.110E-03
4	2.286	2.286	-1.372E-12	1.802E-06	-2.286	2.286	-1.212E-12	1.808E-06

	improved Breitung	Tvedt's EI
generalized reliability index betag =	2.2881	2.2881
probability Pf2 =	1.107E-02	1.107E-02

JACKET BAY 2 - END-ON LOADING

var	ids	mean	st. dev.	param1	param2	param3	param4	init. pt
x1	2	1.21E+03	1.81E+02	7.09E+00	1.49E-01			1.21E+03
x2	2	1.25E+03	1.87E+02	7.12E+00	1.49E-01			1.25E+03
x3	2	1.51E+03	1.21E+02	7.32E+00	8.01E-02			1.51E+03
x4	2	4.20E-01	2.40E-01	-1.01E+00	5.32E-01			4.20E-01
x5	2	3.45E+01	1.16E+01	3.49E+00	3.27E-01			3.45E+01
x6	2	1.70E+02	1.70E+02	4.79E+00	8.33E-01			1.70E+02

deterministic parameters in limit-state function:

tp (1) = 1.500E-01
tp (2) = 1.500E-01
tp (3) = 1.000E+00
tp (4) = 7.000E-01
tp (5) = 1.100E+00

>>>> FIRST-ORDER RELIABILITY ANALYSIS <<<<

iteration number ....iter=   7
value of limit-state function..g(x)=-8.777E-06
reliability index ....beta= 2.1190
probability ....Pf1= 1.705E-02

var	design point			sensitivity vectors			
	x*	u*	alpha	gamma	delta	eta	
x1	1.189E+03	-3.397E-02	-.0160	-.0160	.0166	-.0029	
x2	1.228E+03	-3.509E-02	-.0166	-.0166	.0171	-.0030	
x3	1.485E+03	-1.521E-01	-.0718	-.0718	.0732	-.0166	
x4	7.395E-01	1.330E+00	.6277	.6277	-.4253	-.4366	
x5	5.589E+01	1.638E+00	.7729	.7729	-.4711	-.9605	
x6	1.091E+02	-1.162E-01	-.0548	-.0548	.1034	-.0375	

>>>> SECOND-ORDER RELIABILITY ANALYSIS -- POINT FITTING <<<<

type of integration scheme used ....itg=   2
  itg=1 ....improved Breilung formula
  itg=2 ....improved Breilung formula
       ....& Tvedt's exact integral
max. number of iterations for each fitting point ..inp=   4

limit-state function   1
----
coordinates and ave. main curvatures of fitting points in rotated space

axis	u'i	u'n	G(u)	a'+i	u'i	u'n	G(u)	a'-i
1	2.107	2.131	-3.399E-06	5.489E-03	-2.105	2.133	-3.837E-06	6.214E-03
2	2.107	2.131	-3.212E-06	5.323E-03	-2.106	2.132	-3.504E-06	5.872E-03
3	2.079	2.158	-2.352E-05	1.825E-02	-2.039	2.196	-1.152E-05	3.690E-02
4	2.085	2.152	-5.008E-08	1.528E-02	-2.099	2.139	-4.931E-05	9.162E-03
5	2.119	2.119	-2.683E-09	1.593E-04	-2.119	2.119	-4.043E-09	1.500E-04

	improved Breitung	Tvedt's EI
generalized reliability index betag =	2.1439	2.1441
probability Pf2 =	1.602E-02	1.601E-02

JACKET BAY 3 - END-ON LOADING

var	ids	mean	st. dev.	param1	param2	param3	param4	init. pt
x1	2	1.28E+03	1.81E+02	7.14E+00	1.41E-01			1.28E+03
x2	2	1.25E+03	1.87E+02	7.12E+00	1.49E-01			1.25E+03
x3	2	1.66E+03	1.21E+02	7.41E+00	7.30E-02			1.66E+03
x4	2	4.33E-01	2.40E-01	-9.71E-01	5.18E-01			4.33E-01
x5	2	3.45E+01	1.16E+01	3.49E+00	3.27E-01			3.45E+01
x6	2	3.26E+02	3.26E+02	5.44E+00	8.33E-01			3.26E+02

deterministic parameters in limit-state function:

tp (1) = 1.500E-01
tp (2) = 1.500E-01
tp (3) = 1.000E+00
tp (4) = 7.000E-01
tp (5) = 1.100E+00

>>>> FIRST-ORDER RELIABILITY ANALYSIS <<<<

iteration number ....iter= 7
value of limit-state function..g(x)= 8.082E-06
reliability index ....beta= 2.2419
probability ....Pf1= 1.248E-02

var	design point			sensitivity vectors			
	x*	u*	alpha	gamma	delta	eta	
x1	1.258E+03	-3.229E-02	-.0144	-.0144	.0148	-.0025	
x2	1.228E+03	-3.329E-02	-.0148	-.0148	.0153	-.0027	
x3	1.633E+03	-1.446E-01	-.0645	-.0645	.0656	-.0140	
x4	7.744E-01	1.382E+00	.6164	.6164	-.4010	-.4674	
x5	5.794E+01	1.748E+00	.7795	.7795	-.4478	-1.0500	
x6	1.956E+02	-1.974E-01	-.0881	-.0881	.1712	-.0654	

>>>> SECOND-ORDER RELIABILITY ANALYSIS -- POINT FITTING <<<<

type of integration scheme used ....itg= 2
   itg=1 ....improved Breitung formula
   itg=2 ....improved Breitung formula
   ....& Tvedt's exact integral
max. number of iterations for each fitting point ..inp= 4

limit-state function 1

---

coordinates and ave. main curvatures of fitting points in rotated space

221

```
axis u'i  u'n   G(u)      a'+i       u'i  u'n   G(u)      a'-i
  1 2.232 2.252 -3.886E-06 3.927E-03  -2.232 2.252 -3.441E-06 3.879E-03
  2 2.232 2.252 -4.284E-06 4.146E-03  -2.232 2.252 -3.708E-06 4.041E-03
  3 2.193 2.290 -5.534E-05 2.007E-02  -2.157 2.324 -2.416E-05 3.520E-02
  4 2.122 2.356 -1.171E-06 5.069E-02  -2.179 2.303 -5.560E-04 2.572E-02
  5 2.240 2.244 -1.060E-07 7.520E-04  -2.240 2.244 -1.845E-07 6.793E-04
```

		improved Breitung	Tvedt's EI
generalized reliability index betag =		2.2774	2.2778
probability	Pf2 =	1.138E-02	1.137E-02

JACKET BAY 4 - END-ON LOADING

var	ids	mean	st. dev.	param1	param2	param3	param4	init. pt
x1	2	1.21E+03	1.81E+02	7.09E+00	1.49E-01			1.21E+03
x2	2	1.14E+03	1.71E+02	7.03E+00	1.49E-01			1.14E+03
x3	2	1.70E+03	1.36E+02	7.44E+00	7.98E-02			1.70E+03
x4	2	4.35E-01	2.50E-01	-9.75E-01	5.34E-01			4.35E-01
x5	2	3.45E+01	1.16E+01	3.49E+00	3.27E-01			3.45E+01
x6	2	4.84E+02	4.84E+02	5.84E+00	8.33E-01			4.84E+02

deterministic parameters in limit-state function:

```
tp ( 1) = 1.500E-01
tp ( 2) = 1.500E-01
tp ( 3) = 1.000E+00
tp ( 4) = 7.000E-01
tp ( 5) = 1.100E+00
```

>>>> FIRST-ORDER RELIABILITY ANALYSIS <<<<

```
iteration number ..............iter=      9
value of limit-state function..g(x)= 1.083E-06
reliability index ..............beta=  2.2768
probability .....................Pf1= 1.140E-02
```

var	design point			sensitivity vectors			
	x*	u*	alpha	gamma	delta	eta	
x1	1.189E+03	-3.089E-02	-.0136	-.0136	.0140	-.0024	
x2	1.122E+03	-2.919E-02	-.0128	-.0128	.0132	-.0023	
x3	1.676E+03	-1.554E-01	-.0682	-.0682	.0696	-.0160	
x4	8.080E-01	1.426E+00	.6264	.6264	-.3945	-.4861	
x5	5.793E+01	1.747E+00	.7675	.7675	-.4410	-1.0335	
x6	2.744E+02	-2.655E-01	-.1166	-.1166	.2324	-.0924	

>>>> SECOND-ORDER RELIABILITY ANALYSIS -- POINT FITTING <<<<

coordinates and ave. main curvatures of fitting points in rotated space

```
axis u'i  u'n   G(u)      a'+i       u'i  u'n   G(u)      a'-i
  1 2.268 2.286 -4.140E-06 3.442E-03  -2.269 2.285 -3.156E-06 3.165E-03
```

```
2 2.269 2.285 -3.555E-06 3.175E-03  -2.269 2.284 -2.675E-06 2.887E-03
3 2.222 2.331 -8.461E-05 2.185E-02  -2.190 2.360 -3.043E-05 3.477E-02
4 2.103 2.439 -1.129E-04 7.323E-02  -2.182 2.368 -1.486E-03 3.819E-02
5 2.273 2.281 -4.979E-07 1.600E-03  -2.273 2.280 -1.215E-06 1.418E-03
```

		improved Breitung	Tvedt's EI
generalized reliability index betag =		2.3198	2.3203
probability	Pf2 =	1.018E-02	1.016E-02

JACKET BAY 5 - END-ON LOADING

var	ids	mean	st. dev.	param1	param2	param3	param4	init. pt
x1	2	1.19E+03	1.78E+02	7.07E+00	1.49E-01			1.19E+03
x2	2	1.12E+03	1.68E+02	7.01E+00	1.49E-01			1.12E+03
x3	2	1.80E+03	1.44E+02	7.49E+00	7.98E-02			1.80E+03
x4	2	4.37E-01	2.53E-01	-9.72E-01	5.38E-01			4.37E-01
x5	2	3.45E+01	1.16E+01	3.49E+00	3.27E-01			3.45E+01
x6	2	7.44E+02	7.44E+02	6.27E+00	8.33E-01			7.44E+02

deterministic parameters in limit-state function:
```
tp ( 1) = 1.500E-01
tp ( 2) = 1.500E-01
tp ( 3) = 1.000E+00
tp ( 4) = 7.000E-01
tp ( 5) = 1.100E+00
```

>>>> FIRST-ORDER RELIABILITY ANALYSIS <<<<

```
iteration number ..............iter=      9
value of limit-state function..g(x)= 4.783E-06
reliability index ..............beta=   2.3814
probability ....................Pf1= 8.623E-03
```

var	design point			sensitivity vectors			
	x*	u*	alpha	gamma	delta	eta	
x1	1.167E+03	-2.895E-02	-.0122	-.0122	.0125	-.0021	
x2	1.102E+03	-2.733E-02	-.0115	-.0115	.0118	-.0020	
x3	1.774E+03	-1.567E-01	-.0658	-.0658	.0671	-.0155	
x4	8.429E-01	1.491E+00	.6260	.6260	-.3741	-.5181	
x5	5.923E+01	1.815E+00	.7621	.7621	-.4215	-1.0750	
x6	3.900E+02	-3.595E-01	-.1510	-.1510	.3111	-.1298	

>>>> SECOND-ORDER RELIABILITY ANALYSIS -- POINT FITTING <<<<

coordinates and ave. main curvatures of fitting points in rotated space
```
axis u'i  u'n   G(u)      a'+i       u'i    u'n   G(u)       a'-i
  1 2.374 2.389 -5.010E-06 2.805E-03  -2.375 2.388 -3.397E-06 2.446E-03
  2 2.374 2.389 -4.338E-06 2.602E-03  -2.375 2.388 -2.926E-06 2.254E-03
  3 2.326 2.435 -1.387E-04 1.992E-02  -2.304 2.456 -5.407E-05 2.828E-02
```

```
4 2.132 2.607 -1.233E-03 9.919E-02 -2.238 2.517 -3.895E-03 5.410E-02
5 2.372 2.391 -2.431E-06 3.329E-03 -2.373 2.390 -1.016E-05 2.890E-03
```

	improved Breitung	Tvedt's EI
generalized reliability index betag =	2.4312	2.4319
probability Pf2 =	7.524E-03	7.509E-03

FOUNDATION (LATERAL) - END-ON LOADING

var	ids	mean	st. dev.	param1	param2	param3	param4	init. pt
x1	2	7.20E+03	3.82E+03	8.76E+00	4.98E-01			7.20E+03
x2	2	4.37E-01	2.54E-01	-9.73E-01	5.39E-01			4.37E-01
x3	2	3.45E+01	1.16E+01	3.49E+00	3.27E-01			3.45E+01

deterministic parameters in limit-state function:
tp (1) = 8.100E-01
tp (2) = 7.000E-01
tp (3) = 1.100E+00

>>>> FIRST-ORDER RELIABILITY ANALYSIS <<<<

iteration number ....iter=   10
value of limit-state function..g(x)=-1.013E-08
reliability index ....beta= 2.8547
probability ....Pf1= 2.154E-03

var	design point			sensitivity vectors			
	x*	u*	alpha	gamma	delta	eta	
x1	3.101E+03	-1.444E+00	-.5060	-.5060	1.0003	-.8704	
x2	8.795E-01	1.566E+00	.5486	.5486	-.3070	-.4887	
x3	6.090E+01	1.900E+00	.6656	.6656	-.3500	-.9927	

>>>> SECOND-ORDER RELIABILITY ANALYSIS -- POINT FITTING <<<<

coordinates and ave. main curvatures of fitting points in rotated space
axis u'i u'n G(u)   a'+i   u'i u'n G(u)   a'-i
 1 2.855 2.855 2.802E-09 -2.736E-13 -2.855 2.855 1.666E-09 -1.561E-12
 2 2.855 2.855 4.581E-09 -8.648E-13 -2.855 2.855 2.001E-09 -9.700E-13

	improved Breitung	Tvedt's EI
generalized reliability index betag =	2.8547	2.8547
probability Pf2 =	2.154E-03	2.154E-03

FOUNDATION (AXIAL) - END-ON LOADING

var	ids	mean	st. dev.	param1	param2	param3	param4	init. pt
x1	2	4.06E+03	1.26E+03	8.26E+00	3.03E-01			4.06E+03

224

```
x2   2 7.20E-01 4.20E-01 -4.75E-01 5.41E-01         7.20E-01
x3   2 3.45E+01 1.16E+01 3.49E+00 3.27E-01         3.45E+01
```

deterministic parameters in limit-state function:
  tp (1) = 1.500E+00
  tp (2) = 7.000E-01
  tp (3) = 1.100E+00

>>>> FIRST-ORDER RELIABILITY ANALYSIS <<<<

```
------------------------------------------------------------------
iteration number .............iter=       8
value of limit-state function..g(x)= 7.839E-07
reliability index ...........beta=   2.6956
probability ...................Pf1= 3.513E-03
var      design point              sensitivity vectors
         x*        u*       alpha   gamma   delta   eta
x1   2.949E+03  -9.059E-01   -.3360  -.3360   .4643  -.3881
x2   1.493E+00   1.618E+00    .6002   .6002  -.3202  -.5601
x3   6.204E+01   1.957E+00    .7259   .7259  -.3686  -1.1216
------------------------------------------------------------------
```

>>>> SECOND-ORDER RELIABILITY ANALYSIS -- POINT FITTING <<<<

coordinates and ave. main curvatures of fitting points in rotated space
```
axis u'i  u'n  G(u)     a'+i       u'i   u'n  G(u)      a'-i
 1 2.696 2.696 -3.426E-08 1.319E-11 -2.696 2.696 1.178E-07 9.164E-11
 2 2.696 2.696 1.528E-08 4.389E-11 -2.696 2.696 7.024E-08 6.354E-11
```

```
                              improved Breitung    Tvedt's EI
generalized reliability index betag =   2.6956         2.6956
probability                   Pf2 =   3.513E-03      3.513E-03
```


DECK LEGS - BROADSIDE LOADING

```
var  ids  mean    st. dev.  param1   param2   param3   param4  init. pt
x1   2 6.31E+03 6.68E+02 8.74E+00 1.06E-01                  6.31E+03
x2   2 6.68E+03 7.82E+02 8.80E+00 1.17E-01                  6.68E+03
x3   2 1.65E-01 9.60E-02 -1.95E+00 5.40E-01                 1.65E-01
x4   2 3.45E+01 1.16E+01 3.49E+00 3.27E-01                  3.45E+01
```

deterministic parameters in limit-state function:
  tp (1) = 1.197E+03
  tp (2) = 4.200E-01
  tp (3) = 7.000E-01
  tp (4) = 1.100E+00
  tp (5) = 1.000E+00

>>>> FIRST-ORDER RELIABILITY ANALYSIS <<<<

iteration number ....iter=   6

value of limit-state function..g(x)= 1.582E-05
reliability index ....beta= 3.5064
probability ....Pf1= 2.271E-04

var	design point			sensitivity vectors			
	x*	u*	alpha	gamma	delta	eta	
x1	5.990E+03	-4.334E-01	-.1236	-.1236	.1310	-.0662
x2	6.626E+03	-1.579E-02	-.0045	-.0045	.0046	-.0006
x3	4.714E-01	2.214E+00	.6315	.6315	-.1469	-.9171
x4	7.871E+01	2.684E+00	.7655	.7655	-.2112	-1.7108

>>>> SECOND-ORDER RELIABILITY ANALYSIS -- POINT FITTING <<<<

coordinates and ave. main curvatures of fitting points in rotated space

axis	u'i	u'n	G(u)	a'+i	u'i	u'n	G(u)	a'-i
1	3.000	3.506	1.246E-07	-4.645E-06	-3.000	3.506	1.012E-07	-5.722E-06
2	3.000	3.503	3.034E-03	-8.486E-04	-3.000	3.500	7.652E-03	-1.369E-03
3	3.000	3.506	1.954E-11	-6.569E-08	-3.000	3.506	1.886E-11	-6.675E-08

		improved Breitung	Tvedt's EI
generalized reliability index betag =		3.5059	3.5059
probability	Pf2 =	2.276E-04	2.276E-04

JACKET BAY 1 - BROADSIDE LOADING

var	ids	mean	st. dev.	param1	param2	param3	param4	init. pt
x1	2	2.93E+03	2.35E+02	7.98E+00	8.00E-02			2.93E+03
x2	2	4.57E-01	2.60E-01	-9.23E-01	5.30E-01			4.57E-01
x3	2	3.45E+01	1.16E+01	3.49E+00	3.27E-01			3.45E+01

deterministic parameters in limit-state function:
   tp (1) = 7.000E-01
   tp (2) = 1.100E+00
   tp (3) = 0.000E+00

>>>> FIRST-ORDER RELIABILITY ANALYSIS <<<<

iteration number ....iter=   8
value of limit-state function..g(x)=-4.631E-06
reliability index ....beta= 2.4769
probability ....Pf1= 6.627E-03

var	design point			sensitivity vectors			
	x*	u*	alpha	gamma	delta	eta	
x1	2.868E+03	-2.344E-01	-.0946	-.0946	.0971	-.0297
x2	9.030E-01	1.551E+00	.6261	.6261	-.3554	-.5577
x3	6.124E+01	1.917E+00	.7739	.7739	-.4028	-1.1668

>>>> SECOND-ORDER RELIABILITY ANALYSIS -- POINT FITTING <<<<

coordinates and ave. main curvatures of fitting points in rotated space

```
axis u'i  u'n  G(u)    a'+i      u'i  u'n  G(u)    a'-i
 1 2.477 2.477 2.713E-06 -3.212E-10 -2.477 2.477 2.731E-06 -4.792E-10
 2 2.477 2.477 2.776E-06 -3.942E-10 -2.477 2.477 2.776E-06 -4.062E-10
```

<table>
<tr><td></td><td>improved Breitung</td><td>Tvedt's EI</td></tr>
<tr><td>generalized reliability index betag =</td><td>2.4769</td><td>2.4769</td></tr>
<tr><td>probability   Pf2 =</td><td>6.627E-03</td><td>6.627E-03</td></tr>
</table>

JACKET BAY 2 - BROADSIDE LOADING

var	ids	mean	st. dev.	param1	param2	param3	param4	init. pt
x1	2	2.02E+03	1.62E+02	7.61E+00	8.01E-02			2.02E+03
x2	2	5.21E-01	3.00E-01	-7.95E-01	5.35E-01			5.21E-01
x3	2	3.45E+01	1.16E+01	3.49E+00	3.27E-01			3.45E+01
x4	2	6.01E+02	6.01E+02	6.05E+00	8.33E-01			6.01E+02

deterministic parameters in limit-state function:
 tp (1) = 7.000E-01
 tp (2) = 1.100E+00

>>>> FIRST-ORDER RELIABILITY ANALYSIS <<<<

iteration number ....iter=   7
value of limit-state function..g(x)= 1.316E-03
reliability index ....beta=   2.0805
probability ....Pf1= 1.874E-02

var	design point			sensitivity vectors			
	x*	u*	alpha	gamma	delta	eta	
x1	1.987E+03	-1.666E-01	-.0800	-.0800	.0817	-.0197	
x2	9.051E-01	1.300E+00	.6247	.6247	-.4330	-.4153	
x3	5.502E+01	1.590E+00	.7641	.7641	-.4774	-.9148	
x4	3.338E+02	-2.901E-01	-.1398	-.1398	.2811	-.1132	

>>>> SECOND-ORDER RELIABILITY ANALYSIS -- POINT FITTING <<<<

coordinates and ave. main curvatures of fitting points in rotated space
```
axis u'i  u'n  G(u)    a'+i      u'i  u'n  G(u)    a'-i
 1 2.024 2.136 -2.755E-05 2.690E-02 -1.996 2.162 -2.899E-06 4.077E-02
 2 1.921 2.229 -3.830E-04 8.039E-02 -1.984 2.172 -9.648E-04 4.669E-02
 3 2.075 2.086 -1.651E-07 2.575E-03 -2.075 2.085 -1.068E-06 2.306E-03
```

<table>
<tr><td></td><td>improved Breitung</td><td>Tvedt's EI</td></tr>
<tr><td>generalized reliability index betag =</td><td>2.1269</td><td>2.1276</td></tr>
<tr><td>probability   Pf2 =</td><td>1.672E-02</td><td>1.669E-02</td></tr>
</table>

JACKET BAY 3 - BROADSIDE LOADING

var	ids	mean	st. dev.	param1	param2	param3	param4	init. pt
x1	2	2.02E+03	1.62E+02	7.61E+00	8.01E-02			2.02E+03
x2	2	5.21E-01	3.00E-01	-7.95E-01	5.35E-01			5.21E-01
x3	2	3.45E+01	1.16E+01	3.49E+00	3.27E-01			3.45E+01
x4	2	6.01E+02	6.01E+02	6.05E+00	8.33E-01			6.01E+02

deterministic parameters in limit-state function:
tp (1) = 7.000E-01
tp (2) = 1.100E+00

>>>> FIRST-ORDER RELIABILITY ANALYSIS <<<<

iteration number ....iter=   7
value of limit-state function..g(x)= 1.316E-03
reliability index ....beta=   2.0805
probability ....Pf1= 1.874E-02

var	design point			sensitivity vectors			
	x*	u*	alpha	gamma	delta	eta	
x1	1.987E+03	-1.666E-01		-.0800	-.0800	.0817	-.0197
x2	9.051E-01	1.300E+00		.6247	.6247	-.4330	-.4153
x3	5.502E+01	1.590E+00		.7641	.7641	-.4774	-.9148
x4	3.338E+02	-2.901E-01		-.1398	-.1398	.2811	-.1132

>>>> SECOND-ORDER RELIABILITY ANALYSIS -- POINT FITTING <<<<

coordinates and ave. main curvatures of fitting points in rotated space

axis	u'i	u'n	G(u)	a'+i	u'i	u'n	G(u)	a'-i
1	2.024	2.136	-2.755E-05	2.690E-02	-1.996	2.162	-2.899E-06	4.077E-02
2	1.921	2.229	-3.830E-04	8.039E-02	-1.984	2.172	-9.648E-04	4.669E-02
3	2.075	2.086	-1.651E-07	2.575E-03	-2.075	2.085	-1.068E-06	2.306E-03

		improved Breitung	Tvedt's EI
generalized reliability index betag =		2.1269	2.1276
probability	Pf2 =	1.672E-02	1.669E-02

JACKET BAY 4 - BROADSIDE LOADING

var	ids	mean	st. dev.	param1	param2	param3	param4	init. pt
x1	2	2.28E+03	1.82E+02	7.73E+00	7.98E-02			2.28E+03
x2	2	5.36E-01	3.10E-01	-7.68E-01	5.37E-01			5.36E-01
x3	2	3.45E+01	1.16E+01	3.49E+00	3.27E-01			3.45E+01
x4	2	1.85E+03	1.85E+03	7.18E+00	8.33E-01			1.85E+03

deterministic parameters in limit-state function:
tp (1) = 7.000E-01
tp (2) = 1.100E+00

>>>> FIRST-ORDER RELIABILITY ANALYSIS <<<<

iteration number ....iter=   8
value of limit-state function..g(x)= 5.077E-02
reliability index ....beta=   2.4163
probability ....Pf1= 7.840E-03
var   design point   sensitivity vectors
         x*   u*   alpha   gamma   delta   eta
x1   2.239E+03   -1.630E-01   -.0672   -.0672   .0686   -.0163
x2   1.028E+00   1.482E+00   .6129   .6129   -.3690   -.5029
x3   5.904E+01   1.805E+00   .7468   .7468   -.4153 -1.0468
x4   7.974E+02   -5.972E-01   -.2494   -.2494   .5568   -.2572

>>>> SECOND-ORDER RELIABILITY ANALYSIS -- POINT FITTING <<<<

coordinates and ave. main curvatures of fitting points in rotated space
axis u'i u'n G(u)   a'+i   u'i u'n G(u)   a'-i
 1 2.366 2.465 -1.113E-04 1.756E-02 -2.359 2.472 -1.740E-05 1.996E-02
 2 2.105 2.691 -1.294E-02 1.242E-01 -2.179 2.632 -7.859E-03 9.085E-02
 3 2.382 2.450 4.728E-03 1.178E-02 -2.385 2.447 -2.263E-04 1.080E-02

                          improved Breitung   Tvedt's EI
generalized reliability index betag =   2.4773   2.4784
probability   Pf2 =   6.619E-03   6.599E-03

JACKET BAY 5 - BROADSIDE LOADING

var ids mean   st. dev. param1   param2   param3 param4 init. pt
x1   2 2.92E+03 2.34E+02 7.98E+00 7.99E-02   2.92E+03
x2   2 5.38E-01 3.10E-01 -7.63E-01 5.35E-01   5.38E-01
x3   2 3.45E+01 1.16E+01 3.49E+00 3.27E-01   3.45E+01
x4   2 2.78E+03 2.78E+03 7.58E+00 8.33E-01   2.78E+03

deterministic parameters in limit-state function:
 tp (1) = 7.000E-01
 tp (2) = 1.100E+00

>>>> FIRST-ORDER RELIABILITY ANALYSIS <<<<

iteration number ....iter=   9
value of limit-state function..g(x)= 7.134E-02
reliability index ....beta=   2.7467
probability ....Pf1= 3.010E-03
var   design point   sensitivity vectors
         x*   u*   alpha   gamma   delta   eta
x1   2.873E+03   -1.810E-01   -.0662   -.0662   .0676   -.0172
x2   1.143E+00   1.675E+00   .6101   .6101   -.3084   -.6043
x3   6.390E+01   2.047E+00   .7458   .7458   -.3572 -1.2164
x4   1.080E+03   -7.185E-01   -.2592   -.2592   .6013   -.2900

>>>> SECOND-ORDER RELIABILITY ANALYSIS -- POINT FITTING <<<<

coordinates and ave. main curvatures of fitting points in rotated space
axis u'i u'n G(u)   a'+i   u'i u'n G(u)   a'-i
  1 2.687 2.805 -5.700E-04 1.626E-02 -2.675 2.817 -1.215E-04 1.950E-02
  2 2.349 3.094 -1.939E-02 1.259E-01 -2.448 3.016 -2.126E-02 8.986E-02
  3 2.697 2.796 3.531E-02 1.345E-02 -2.704 2.789 -1.222E-03 1.142E-02

                                improved Breitung   Tvedt's EI
generalized reliability index betag =   2.8074   2.8084
probability   ، Pf2 =   2.497E-03   2.490E-03

FOUNDATION (LATERAL) - BROADSIDE LOADING

var ids mean   st. dev. param1   param2   param3   param4 init. pt
x1   2 3.21E+03 2.56E+02 8.07E+00 7.97E-02   3.21E+03
x2   2 5.38E-01 3.10E-01 -7.63E-01 5.35E-01   5.38E-01
x3   2 3.45E+01 1.16E+01 3.49E+00 3.27E-01   3.45E+01
x4   2 2.95E+03 2.95E+03 7.64E+00 8.33E-01   2.95E+03

deterministic parameters in limit-state function:
  tp (1) = 7.000E-01
  tp (2) = 1.100E+00

>>>> FIRST-ORDER RELIABILITY ANALYSIS <<<<

iteration number ....iter=   9
value of limit-state function..g(x)= 9.166E-02
reliability index ....beta=   2.8420
probability ....Pf1= 2.242E-03
var   design point   sensitivity vectors
         x*   u*   alpha   gamma   delta   eta
x1   3.148E+03 -1.890E-01   -.0668 -.0668   .0683 -.0179
x2   1.181E+00   1.736E+00   .6112   .6112 -.2902 -.6378
x3   6.548E+01   2.122E+00   .7471   .7471 -.3401 -1.2714
x4   1.141E+03 -7.256E-01   -.2527 -.2527   .5876 -.2841

>>>> SECOND-ORDER RELIABILITY ANALYSIS -- POINT FITTING <<<<

coordinates and ave. main curvatures of fitting points in rotated space
axis u'i u'n G(u)   a'+i   u'i u'n G(u)   a'-i
  1 2.777 2.906 -9.547E-04 1.655E-02 -2.763 2.919 -2.252E-04 2.026E-02
  2 2.419 3.210 -1.834E-02 1.256E-01 -2.533 3.121 -2.813E-02 8.690E-02
  3 2.791 2.892 9.047E-02 1.276E-02 -2.799 2.884 -1.614E-03 1.069E-02

                                improved Breitung   Tvedt's EI
generalized reliability index betag =   2.9018   2.9027
probability   Pf2 =   1.855E-03   1.850E-03

230

FOUNDATION (AXIAL) - BROADSIDE LOADING

var	ids	mean	st. dev.	param1	param2	param3	param4	init. pt
x1	2	7.70E+03	4.31E+03	8.81E+00	5.22E-01			7.70E+03
x2	2	5.40E-01	3.10E-01	-7.59E-01	5.34E-01			5.40E-01
x3	2	3.45E+01	1.16E+01	3.49E+00	3.27E-01			3.45E+01

deterministic parameters in limit-state function:
tp (1) = 8.100E-01
tp (2) = 7.000E-01
tp (3) = 1.100E+00

>>>> FIRST-ORDER RELIABILITY ANALYSIS <<<<

iteration number ....iter=   9
value of limit-state function..g(x)= 1.137E-05
reliability index ....beta=   2.6657
probability ....Pf1= 3.841E-03

var	design point			sensitivity vectors			
	x*	u*	alpha	gamma	delta	eta	
x1	3.230E+03	-1.402E+00	-.5260	-.5260	1.0600	-.8858	
x2	1.006E+00	1.433E+00	.5375	.5375	-.3367	-.4205	
x3	5.812E+01	1.757E+00	.6592	.6592	-.3767	-.8938	

>>>> SECOND-ORDER RELIABILITY ANALYSIS -- POINT FITTING <<<<

coordinates and ave. main curvatures of fitting points in rotated space
axis u'i u'n G(u)   a'+i   u'i   u'n   G(u)   a'-i
 1 2.666 2.666 7.921E-07 -1.080E-10 -2.666 2.666 1.511E-06 2.475E-09
 2 2.666 2.666 -8.359E-07 6.449E-10 -2.666 2.666 9.216E-07 1.788E-09

		improved Breitung	Tvedt's EI
generalized reliability index betag =		2.6657	2.6657
probability	Pf2 =	3.841E-03	3.841E-03

---

var	ids	mean	st. dev.	param1	param2	param3	param4	init. pt
x1	2	4.06E+03	1.26E+03	8.26E+00	3.03E-01			4.06E+03
x2	2	8.70E-01	5.00E-01	-2.82E-01	5.34E-01			8.70E-01
x3	2	3.45E+01	1.16E+01	3.49E+00	3.27E-01			3.45E+01

deterministic parameters in limit-state function:
tp (1) = 1.500E+00
tp (2) = 7.000E-01
tp (3) = 1.100E+00

>>>> FIRST-ORDER RELIABILITY ANALYSIS <<<<

iteration number ....iter=   8
value of limit-state function..g(x)= 4.626E-09
reliability index ....beta=   2.4931
probability ....Pf1= 6.332E-03

var	design point			sensitivity vectors			
	x*	u*	alpha	gamma	delta	eta	
x1	3.007E+03	-8.417E-01	-.3376	-.3376	.4600	-.3692	
x2	1.667E+00	1.484E+00	.5952	.5952	-.3577	-.4917	
x3	5.929E+01	1.818E+00	.7292	.7292	-.4026	-1.0309	

>>>> SECOND-ORDER RELIABILITY ANALYSIS -- POINT FITTING <<<<

coordinates and ave. main curvatures of fitting points in rotated space

axis	u'i	u'n	G(u)	a'+i	u'i	u'n	G(u)	a'-i
1	2.493	2.493	-2.963E-09	-5.540E-13	-2.493	2.493	1.311E-09	1.256E-12
2	2.493	2.493	1.986E-10	1.348E-12	-2.493	2.493	2.955E-09	-4.818E-13

		improved Breitung	Tvedt's EI
generalized reliability index betag =		**2.4931**	**2.4931**
probability	**Pf2 =**	**6.332E-03**	**6.332E-03**

APPENDIX B

DAMAGED AND REPAIRED MEMBERS

B.1   Loh's Interaction Equations for Dent-Damaged Tubulars (Loh, 1993)

Notations

A_d	effective cross-sectional area of dent section
A_0	cross-sectional area of undamaged member
A_{st}	cross-sectional area of the steel
A_s	cross-sectional area of the soil plug in pile
D	outside diameter of tubular member
dd	dent depth
ΔY	primary out-of-straightness of a dented member
ΔY_0	$=0.001\,L$
E	Young's modulus
f_y	yield stress
I_d	effective moment of inertia of dent cross-section
I_0	moment of inertia of undamaged cross-section
K_0	effective length factor of undamaged member
K	effective buckling length factor
L	unbraced member length
λ	slenderness ratio
λ_d	slenderness parameter of a dented member $= (P_{ud}/P_{Ed})^{0.5}$
M_u	ultimate moment capacity
M_{cr}	critical moment capacity (local buckling)
M_p	plastic moment capacity of undamaged member
M_{ud}	ultimate negative moment capacity of dent section
$M-$	negative moment for dent section
$M+$	positive moment for dent section
M^*	neutral moment for dent section
P_{crd}	critical axial buckling capacity of a dented member ($\Delta/L>0.001$)
P_{crd0}	critical axial buckling capacity of a dented member ($\Delta/L=0.001$)
P_E	Euler load of undamaged member
P_u	axial compression capacity
P_{ud}	axial compression capacity of a short dented member
P_{crl}	axial local buckling capacity
P_{cr}	axial column buckling capacity
P_y	tensile capacity
r	radius of gyration
t	member wall thickness
UC	unity check

233

Undamaged Cross Sectional Capacities

$$P_u = F_y A_u \qquad \text{for} \qquad \frac{D}{t} \leq 60 \qquad \text{(B.1)}$$

$$P_u = F_y A_u \left[1.64 - 0.23 \left(\frac{D}{t} \right)^{0.25} \right] \qquad \text{for} \qquad \frac{D}{t} \geq 60 \qquad \text{(B.2)}$$

$$\frac{M_u}{M_p} = 1.0 \qquad \text{for} \qquad 0 \leq \frac{F_y D}{t} \leq 1500 (ksi) \qquad \text{(B.3)}$$

$$\frac{M_u}{M_p} = 1.13 - 2.58 \frac{F_y D}{E t} \qquad \text{for} \qquad 1500 \leq \frac{F_y D}{t} \leq 3000 \qquad \text{(B.4)}$$

$$\frac{M_u}{M_p} = 0.94 - 0.76 \frac{F_y D}{E t} \qquad \text{for} \qquad 3000 \leq \frac{F_y D}{t} \leq 300 F_y \qquad \text{(B.5)}$$

$$M_p = F_y t (D - t)^2 \qquad \text{(B.6)}$$

Dent-Section Properties

$$\frac{P_{ud}}{P_u} = \frac{A_d}{A_u} = exp \left(-0.08 \frac{dd}{t} \right) \geq 0.45 \qquad \text{(B.7)}$$

$$\frac{M_{ud}}{M_u} = \frac{I_d}{I_u} = exp \left(-0.06 \frac{dd}{t} \right) \geq 0.55 \qquad \text{(B.8)}$$

Strength Check

$$UC = \frac{P}{P_{ud}} + \sqrt{ \left(\frac{M-}{M_{ud}} \right)^2 + \left(\frac{M*}{M_u} \right)^2 } \leq 1.0 \qquad \text{(B.9)}$$

$$UC = \frac{P}{P_{ud}} + \sqrt{ \left(\frac{M+}{M_u} \right)^2 + \left(\frac{M*}{M_u} \right)^2 } \leq 1.0 \qquad \text{(B.10)}$$

Stability Check

$$UC = \frac{P}{P_{crd}} + \sqrt{\left(\frac{M-}{\left(1-\frac{P}{P_{Ed}}\right)M_{bd}}\right)^a + \left(\frac{M*}{\left(1-\frac{P}{P_E}\right)M_b}\right)^2} \leq 1.0 \qquad \text{(B.11)}$$

$$UC = \frac{P}{P_{crd}} + \sqrt{\left(\frac{M+}{\left(1-\frac{P}{P_{Ed}}\right)M_{bd}}\right)^2 + \left(\frac{M*}{\left(1-\frac{P}{P_E}\right)M_b}\right)^2} \leq 1.0 \qquad \text{(B.12)}$$

$$\alpha = 2 - 3 \, dd / D \qquad \text{(B.13)}$$

Critical Buckling Capacities

$$P_{crdo} = P_{ad}\left[1 - 0.25\,\lambda_d^2\right] \qquad\qquad \text{for} \quad \lambda \leq \sqrt{2} \qquad \text{(B.14)}$$

$$P_{crdo} = P_{ad}\frac{1}{\lambda_d^2} = P_{ED} \qquad\qquad \text{for} \quad \lambda \geq \sqrt{2} \qquad \text{(B.15)}$$

$$\frac{P_{crd}}{P_{crdo}} + \frac{P_{crd}\,\Delta Y}{\left(1 - \frac{P_{crd}}{P_{Ed}}\right)M_{bd}} = 1.0 \qquad \text{(B.16)}$$

B.2 Parsanejad's Strength Equation for Grout-Filled Tubulars (Parsanejad, 1987)

<u>**Notations**</u>

A_g	area of grout at the dented section
A_s	area of steel
A_{tr}, A_{tr}^*	transformed areas at the dented and undented cross section
D	mid-thickness diameter
d	depth of denth
E_g	elastic modulus of grout
E_s	elastic modulus of steel
e	external eccentricity of load
e_g	distance between centroid of grout at the dented cross section to the centroid of undented cross section
e_s	distance between centroid of steel at the dented cross section to the centroid of undented cross section
e_t	$= e + \delta + e_{tr}$
e_{tr}	distance between centroid of the dented and undented transformed cross section
I_g	moment of inertia of grout at dented cross section
I_s	moment of inertia of steel at dented cross section
I_{tr}	transformed moment of inertia of dented cross section
k	nondimensionalized parameter $= A_{tr}\, e_t\, / \, Z_{tr}$
l	effective length of member
m	nondimensionalized parameter $= A_{tr} / A_{tr}^*$
n	elastic modular ratio $= E_s \, / \, E_g$
P_u	ultimate axial capacity
P_y	full yield capacity $= A_{tr}^* \, \sigma_y$
r_{tr}	transformed radious of gyration of dented section
t	thickness of tubular member
Z_{tr}	transformed section modulus with respect to the dented side
α	angle shown in fig.
δ	overall bending
λ	reduced slenderness parameter
σ_a	axial stress
σ_b	bending stress
σ_e	Euler buckling stress
σ_u	ultimate axial stress
σ_y	yield stress of steel

$$\left(\frac{\sigma_u}{\sigma_y}\right)^2 - \left(\frac{1+k}{\lambda^2} + m\right)\left(\frac{\sigma_u}{\sigma_y}\right) + \frac{m}{\lambda^2} = 0 \qquad (B.17)$$

$$\lambda = \sqrt{\frac{\sigma_y}{\sigma_e}} = \frac{1}{\pi}\frac{l}{r_{tr}}\sqrt{\frac{\sigma_y}{E_s}} \qquad (B.18)$$

$$k = \frac{A_{tr}\, e_t}{Z_{tr}} \qquad (B.19)$$

$$m = \frac{A_{tr}}{A_{tr}^*} \qquad (B.20)$$

Cross-Sectional Properties

$$A_{tr} = A_s + \frac{A_t}{n} \qquad (B.21)$$

$$A_s = \pi D t \qquad (B.22)$$

$$A_t = \frac{D^2}{4}\left(\pi - \alpha + \frac{1}{2}\sin 2\alpha\right) \qquad (B.23)$$

$$n = \frac{E_s}{E_t} \qquad (B.24)$$

$$\alpha = \cos^{-1}\left(1 - 2\frac{d}{D}\right) \qquad (B.25)$$

$$e_{tr} = \frac{A_s e_s + \frac{A_t}{n} e_t}{A_{tr}} \qquad (B.26)$$

$$e_t = \frac{D}{2\pi}(\sin\alpha - \alpha \cos\alpha) \qquad (B.27)$$

237

$$e_s = \frac{(D \ sin \ \alpha \ )^3}{12 \ A_s} \qquad (B.28)$$

$$Z_{tr} = \frac{I_{tr}}{\frac{D}{2}} cos \ \alpha \ + \ e_{tr} \qquad (B.29)$$

$$r_{tr} = \sqrt{\frac{I_{tr}}{A_{tr}}} \qquad (B.30)$$

$$I_{tr} = I_s + \frac{I_s}{n} + A_s (e_{tr} - e_s)^2 + \frac{A_s}{n} (e_g - e_{tr})^2 \approx I_s + \frac{I_s}{n} \qquad (B.31)$$

$$I_s = \frac{D^2 t}{4} \left[\frac{\pi - \alpha}{2} - \frac{sin \ 2\alpha}{4} + \alpha \ cos^2 \alpha - \frac{(sin \ \alpha - \alpha \ cos \ \alpha)^2}{\pi} \right] \qquad (B.32)$$

$$I_s = \frac{D^4}{64} \left[\pi - \alpha + \frac{sin \ 4\alpha}{4} \right] - \frac{D^4 sin^6 \alpha}{144 \ A_s} \qquad (B.33)$$

$$A_{tr}^{\bullet} = A_s + \frac{\pi \ D^2}{4 \ n} \qquad (B.34)$$

238

APPENDIX C

ULSLEA
Ultimate Limit State Limit Equilibrium Analysis

This software is provided "as is" by the Marine Technology and Management Group (MTMG) at University of California at Berkeley to sponsors of the research project *Screening Methodologies for Use in Platform Assessments and Requalifications*. Any express or implied warranties of merchantability and fitness for a particular purpose are disclaimed. In no event shall the MTMG be liable for any direct, indirect, incidental, special, exemplary, or consequential damages (including, but not limited to, procurement of substitute goods or services; loss of use, data, or profits; or business interruption) however caused on any theory of liability, whether in contract, strict liability, or tort (including negligence or otherwise) arising in any way out of the use of this software, even if advised of possibility of such damage.

C.1   Introduction

ULSLEA is the prototype of a simplified nonlinear structural analysis program developed for level 2 screening of steel, template-type offshore platforms. The program is based on simplified load and capacity calculation procedures developed for the joint industry-government sponsored research project titled "Screening Methodologies for Use in Platform Assessments and Requalifications". This research has been performed at the University of California at Berkeley, Department of Civil Engineering by Research Assistant Mehrdad Mortazavi under supervision of Professor Robert Bea.

The theoretical background of ULSLEA is documented in the previous chapters of this report. This appendix includes information on how to install and use ULSLEA, prepare the input and interpret the output of the program. In the case of an example platform the input parameters and the output are presented.

C.1.1   Application Range of ULSLEA

ULSLEA can be applied to typical, symmetrical, jacket-type platforms with generic geometries; 4-, 6-, 8-, and 12-leg platforms with up to 29 jacket bays. The loading has been calibrated to platforms located in deep and intermediate water depths. ULSLEA is expected to give some what conservative results in case of shallow water platforms. For information on other limitations of the program, refer to the following sections of this appendix.

C.1.2   Program Installation

The program is developed using Microsoft Excel Visual Basic programming language. The following Excel 5.0 files are linked together and comprise the program:

- ULSLEA.XLS
- INP.XLS

240

These files can be found in compressed format on two floppy disks attached to page 261 of this report. To install the program, copy the compressed files into the hard disk of your PC and decompress them. You can start the program by opening the file ULSLEA.XLS in Excel 5.0.

C.2   Input Data

There are principally two ways of defining the input parameters in the program:

<blockquote>

a)   by stepping through the input menu and defining the required parameters or

b)   by opening an input file that has been originally created by stepping through the input menu.

</blockquote>

The data that need to be defined by the user is subdivided into five principal categories:

- Environmental Conditions
- Global Parameters
- Local Parameters
- Material and Soil Properties
- Uncertainties and Biases

Figures C1 and C2 demonstrate the terminology used in defining the platform global and local parameters.

C.2.1   Environmental Conditions

The user is required to define the site specific environmental parameters which are then used to calculate the aero- and hydrodynamic forces acting on the platform. These include water depth, storm surge, wind, wave, and current parameters (Figure C5):

- Water Depth, Storm Surge (ft)
- Wind: velocity @ 30 ft elevation (mph)
- Wave: height (ft) and period (sec)

241

- Current: velocities (fps) @ SWL and mudline current profile: linear/quadratic/constant with depth. If linear or quadratic current velocity profiles are specified, the profile is stretched from still water level up to the wave crest so that the water volume remains unchanged. If a constant current velocity profile is specified, the velocities will be equal to the specified velocity everywhere in the water column.

C.2.2 Global Parameters

These include global data on the platform (Figures C6 - C8):

- Number of supporting legs (4,6,8 or 12)

- Number of jacket bays (=< 29)

- Number of decks (=< 5): for each deck, the top and bottom elevation, end-on and broadside width, hydrodynamic drag coefficient and wind shape factor are required

- Total deck weight (kips)

- Base centerline width (ft): the horizontal distance between the central axis of the two outer jacket legs @ the base of the jacket

- Top centerline width (ft): the horizontal distance between the central axis of the two outer jacket legs @ the top of the jacket

- Middle section width (ft): the horizontal distance between the central axis of the two inner jacket legs

- Bay heights (ft)

- Total number of joints: the sum of the number of joints with different joint parameters in two orthogonal planes (End-on and Broadside) , n= < 99

- Total number of diagonal braces: the sum of the number of vertical diagonal braces in all planes at a given bay and with a given direction (end-on/broadside), n=<12 per jacket bay and direction

C.2.3 Local Parameters

The input data file for local parameters is subdivided into the following sections:

- Decklegs and vertical diagonal braces

- Horizontal braces
- Joints
- Foundation
- Force coefficients
- Boatlanding and appurtenances

C.2.3.1 Decklegs and vertical diagonal braces

Deckleg diameter (in.) and thickness (in.) are to be specified. For each jacket bay, starting from top to the bottom of the jacket, the following data is required (Figures C9 & C10):

- Jacket leg diameter (in.)
- Jacket leg thickness (in.): only for the uppermost jacket bay
- Bracing information: For each vertical diagonal brace in a given bay the diameter, thickness, type of axial loading (tension/compression), position of the brace relative to wave direction (left, center, right) and the brace configuration (S (Single)-braced, K-braced, and X-braced) are to be defined. Wave, current, and wind flow directions are assumed to be from left to the right. In addition, the identification number of the joints at the two ends of each brace element are required. If the program is used to perform a preliminary design, the diameter and thickness properties of diagonal braces do not need to be specified. These properties are selected automatically based on the following ratios:

$$D/t = 40 \qquad \text{for braces at top elevations}$$
$$D/t = 60 \qquad \text{for braces at bottom elevations}$$
$$Kl/r = 70 \qquad \text{for braces at top elevations}$$
$$Kl/r = 80 \qquad \text{for braces at bottom elevations}$$

For damaged or repaired members, the Dent Depth (dd) and Out-of-Straightness (oos) have to be defined. For other types of damage (overall corrosion, fatigue, etc.) capacity bias factors can be defined to reduce the mean element capacity accordingly (see Section C.2.5).
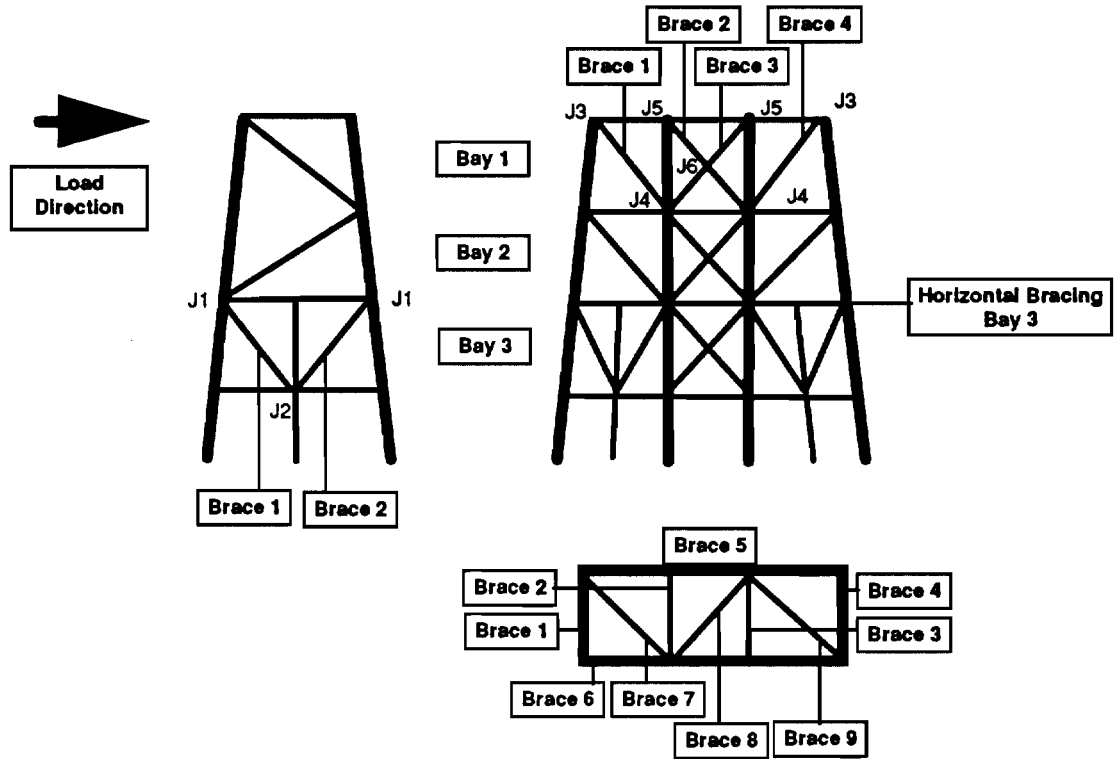
END-ON
(bs loading)

BROADSIDE
(eo loading)
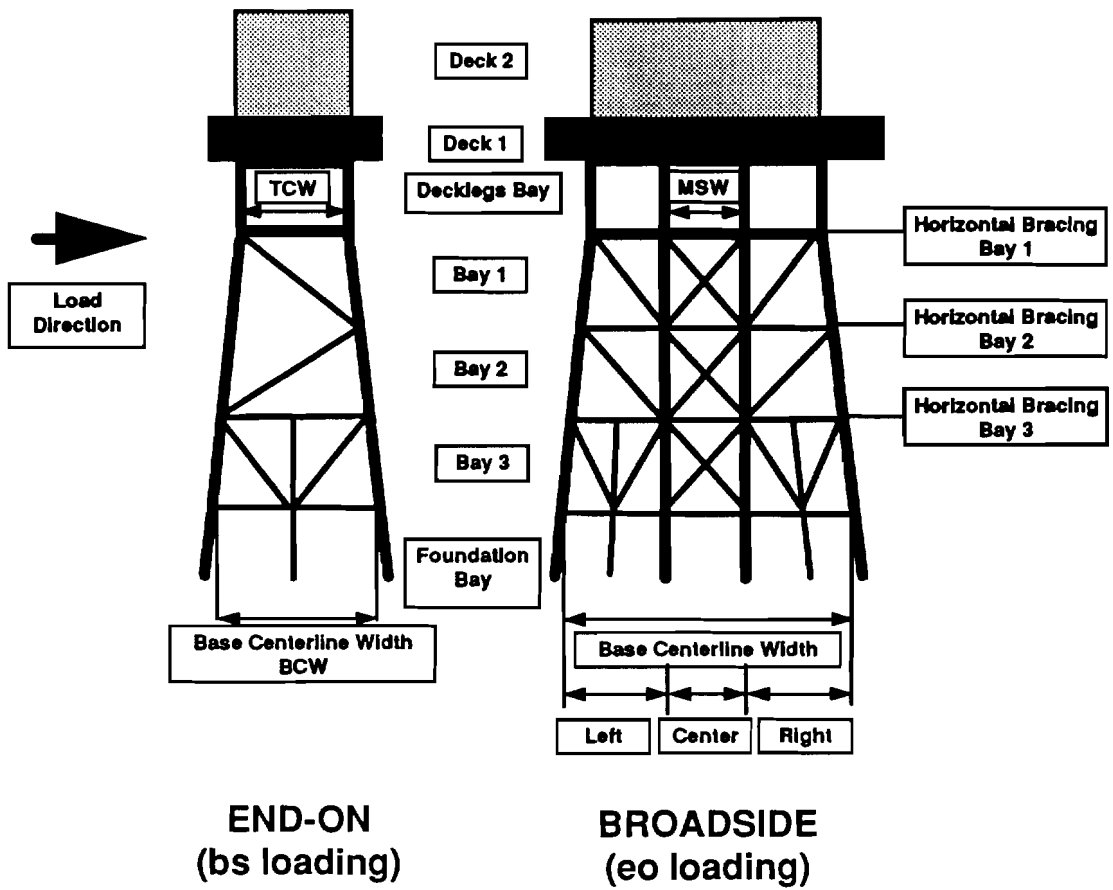
# of Supporting Legs	# of Decks	# of Jacket Bays
8	2	3

# of Diagonal Braces	End-on	Broadside
Bay 1	4	8
Bay 2	4	8
Bay 3	8	12
# of Skirt Piles	2	4

Figure C1: ULSLEA Input Terminology for an Example Platform

**END-ON
(bs loading)**

**BROADSIDE
(eo loading)**

Horizontal Bracing Bay 3 (Plan View)

BS Brace #	Type	Position	Configuration	Joint i	Joint j
1	compression	left	S	3	4
2	compression	center	X	5	6
3	tension	center	X	5	6
4	tension	right	S	3	4

EO Brace #	Type	Position	Configuration	Joint i	Joint j
1	compression	-	K	1	2
2	tension	-	K	1	2

Figure C2: ULSLEA Input Parameters for Diagonal Braces (Example)

245

C.2.3.2 Horizontal braces

For each horizontal framing, the total number of elements, including non-diagonal members, is to be defined (n= <28). For each element the following information is required (Figure C17):

- Diameter (in.)
- Thickness (in.)
- Length (ft)
- Angle (degree): is to be measured from an axis parallel to the end-on face of the platform, $a = < 90°$

C.2.3.3 Joints

For each joint that the user wants to include in the analysis, the following parameters are to be specified (Figure C11):

- Joint type (K, Y, X): see API RP 2A (20th edition) for joint classifications
- Chord diameter (in.)
- Chord thickness (in.)
- Branch diameter (in.)
- Gap in K-joints (in.)
- Chord/branch angle (degree)

C.2.3.4 Foundation

The following data are to be specified for the main and skirt piles (Figure C15):

- Pile length (ft): the embedded pile length
- Pile diameter (in.)
- Pile thickness (in.): no variation over length
- If piles are plugged: yes, if any kind of plug exists inside the piles

C.2.3.5 Force Coefficients

The following coefficients need to be defined (Figure C13):

- Modification factors: current blockage factor, directional spreading factor
- Force coefficients: drag force coefficient for deck areas, wind shape factor for deck areas, drag force coefficient on jacket elements
- Global load factor: defines the magnitude of lateral loading given a fixed loading pattern (Default = 1.0)
- Marine growth (in.): the variation over depth can be specified (Figure C14)

C.2.3.6 Boatlanding and Appurtenances

An equivalent area (ft^2) for boatlanding is to be defined for both end-on and broadside directions. This area is assumed to be at mean water level. An equivalent diameter (ft) for appurtenances (conductors, risers, etc.) is to be defined for deck bay and every jacket bay. In this case, user has to include marine growth thickness in estimating the equivalent diameter for appurtenances (Figure C16).

C.2.4 Member Strength, Material and Soil Properties

The following material and element properties are to be specified (Figure C12):

- Steel yield stress (ksi)
- Steel elastic modulus (ksi)
- Brace buckling length factor
- Brace residual strength factor (default = 1.0 : elastic perfectly plastic behavior)

At present stage only one soil layer can be considered. Soil parameters to be specified are:

- Soil type (clay/sand)
- Linear variation of undrained shear strength (ksf)
- Angle of friction of soil (degree)
- Submerged specific weight of soil (kcf)

- Scour depth (ft)

Bias factors can be specified for axial and lateral pile capacities in sand and clay (see Section C.2.5)

C.2.5 Uncertainties and Biases

ULSLEA includes a simplified first order second moment reliability analysis (FOSM) subroutine. Failure of each component is defined as the "lower-bound" capacity of the component being reached. The resulting reliability indices are conditional on the specified environmental conditions (storm surge, wave, current, and wind). For information on other underlying assumptions, refer to Chapter 5 of this report. Coefficients of variations and biases have to be defined for loadings and capacities:

<u>Loadings:</u>

- Wave deck load

- Wave jacket load: default bias = 0.9. The default bias of 0.9 for the jacket load is a modeling bias, which is based on the verification study results presented in this report. This bias takes into account the conservatism that is introduced by using the simplified load calculation procedure.

<u>Capacities:</u>

- Tubular braces: bias and COV of buckling capacity of tubular braces

- Tubular joints: at this point, the COV associated with joint capacity is not included in the reliability analysis

- Foundation: bias and COV of axial and lateral pile capacities in sand and clay

- Decklegs: default values of B = 1.0 and COV = 0.10 are selected for the moment capacity of the decklegs.

All bias factors are also used in deterministic analysis procedures to predict "best estimate" component capacities and loads acting on these components. The default value for these biases is taken to be B=1.0 (except for jacket loads where B = 0.9).

C.3 Output

The output of ULSLEA is mainly in graphical format. The following charts are produced by the program:

- Kinematics: wave, current, and total velocities vs. platform elevation
- End-on loading: cumulative storm shear force and platform's shear capacity vs. platform elevation
- Broadside loading
- Axial pile performance: RSR = pile axial capacity/pile axial load
- Risk Analysis: conditional component reliability indices for end-on and broadside loading directions

C.3.1 Interpretation of Output Data

The velocity profiles are plotted from mudline to the top of deck legs (bottom of cellar deck). Current velocity profile is based on the input data provided by the user. If linear or quadratic current velocity profiles are specified, the profile is stretched from still water level up to the wave crest so that the water volume remains unchanged. If a constant current velocity profile is specified, the velocities will be set equal to the specified velocity every where in the water column. The water particle velocity due to wave motion is based on Stokes 5th-order theory. The total velocity is the linear summation of velocities due to current and wave (Figure C20).

The cumulative storm shear at a given elevation, is the integrated wind, wave and current forces acting on the portions of platform above that elevation. The ordinate at the top of the plot (top of decklegs) corresponds to total wind, wave and current forces acting on the exposed decks of the platform. These forces are estimated according to API RP2A Chapter 17 (API, 1994). The ordinate at mudline is the total base shear. When the storm shear profile touches the platform shear capacity profile at any elevation, the corresponding total base shear defines the capacity of the platform (Figure C19).

The upper-bound capacity of a given bay is based on failure of all of the load resisting elements. The lower-bound capacity of a given bay is based on first compression member failure and is plotted for jacket bays in addition to the upper-bound capacity. The joint capacity profile is based on first joint failure in each jacket bay. The failure mode for a given bay is independent from other failure modes. As a result, different analyses for a platform with and without a "fixed" base are not required. The load can always be increased to estimate the collapse base shear for any failure mode in deck, jacket or foundation.

The simplified risk analysis subroutine is based on the developments included in Chapter 5 of this report. For each principal orthogonal direction, FOSM reliability indices, b, are plotted for all failure modes. These indices are in general conditional on environmental conditions. (Figure C22).

C.4   Example

C.4.1   Example Platform

The input data and analysis results of a four-leg platform (verification platform C - PMB Benchmark Structure) is included in this appendix. The input file of this 4-leg platform is included in the floppy disk under "EXAMPLE.XLS". The user can run the analysis of this platform by opening the file ULSLEA.XLS, choosing EXAMPLE.XLS as the input file.
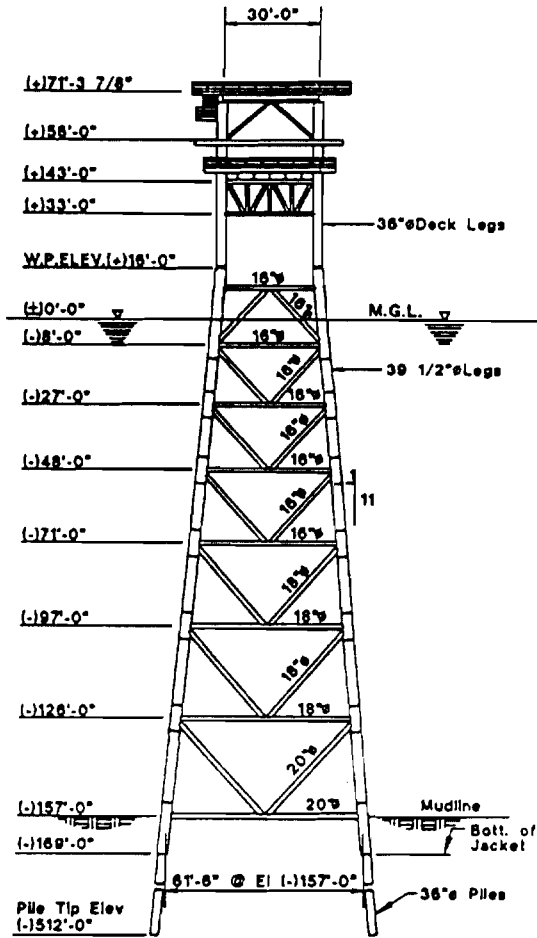
C.4.2 Input Data

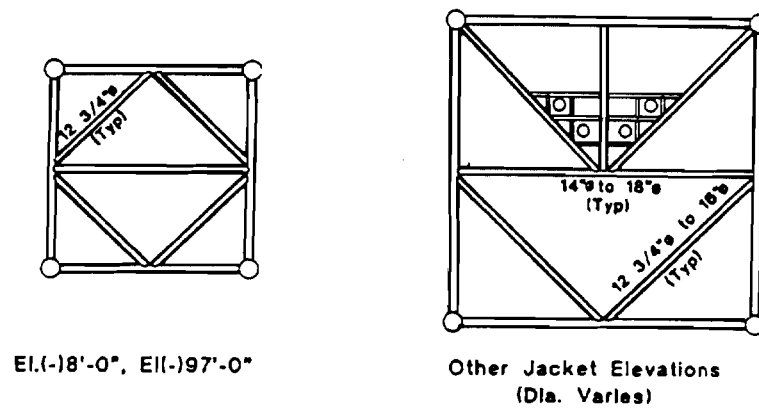**Figure C3: Platform C - Typical Elevation (Digre et. al., 1995)**

El.(-)8'-0", El(-)97'-0"

Other Jacket Elevations
(Dia. Varies)

Figure C4: Platform C - Typical Horizontal Framings (Digre et. al., 1995)

251

Figure C5: Platform C - Environmental Conditions

Figure C6: Platform C - Global Parameters

Figure C9: Platform C - Local Parameters
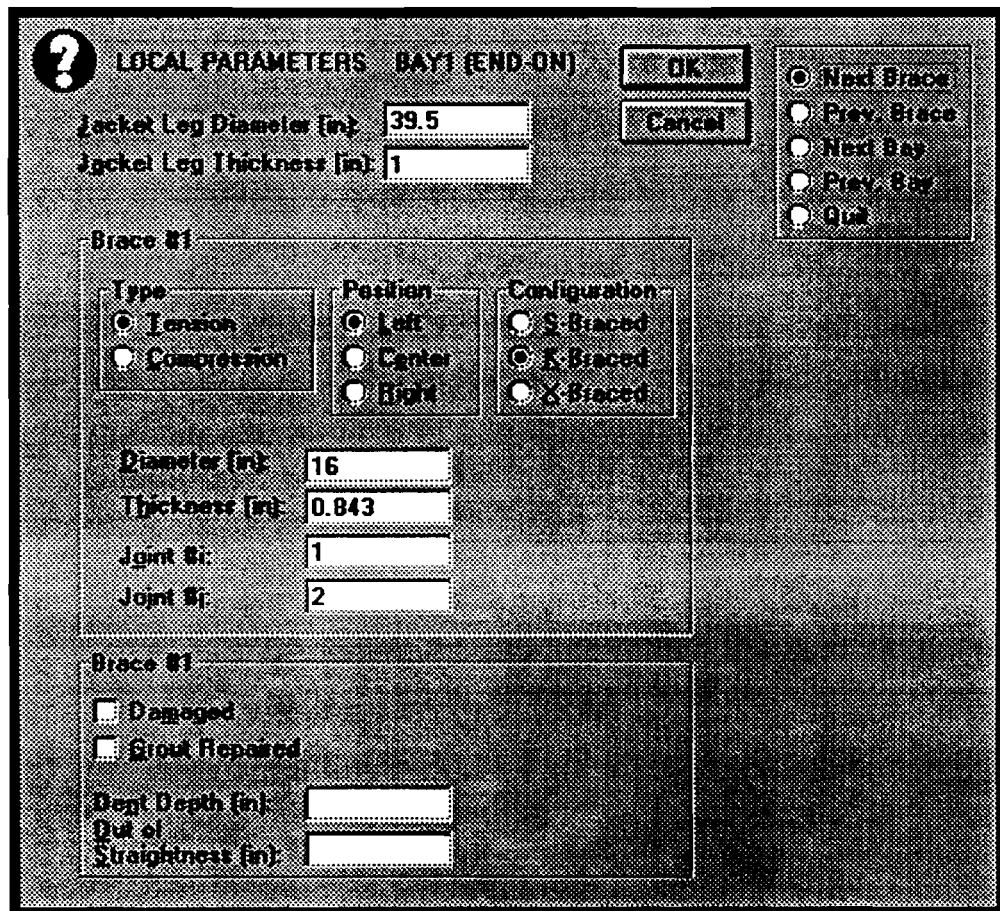
Figure C10: Platform C - Local Parameters (Vertical Diagonal Braces)

Figure C11: Platform C - Local Parameters (Joints)

**Figure C12: Platform C - Local Parameters
(Member Strength, Material and Soil Properties)**

255

Figure C13: Platform C - Local Parameters (Force Coefficients)

Figure C14: Platform C - Local Parameters (Marine Growth)

Figure C15: Platform C - Local Parameters (Foundation)

Figure C16: Platform C - Local Parameters (Boatlanding and Appurtenances)

Figure C17: Platform C - Local Parameters (Horizontal Bracing - Bay1)

Figure C18: Platform C - Uncertainties and Biases

258

C.4.3 Output
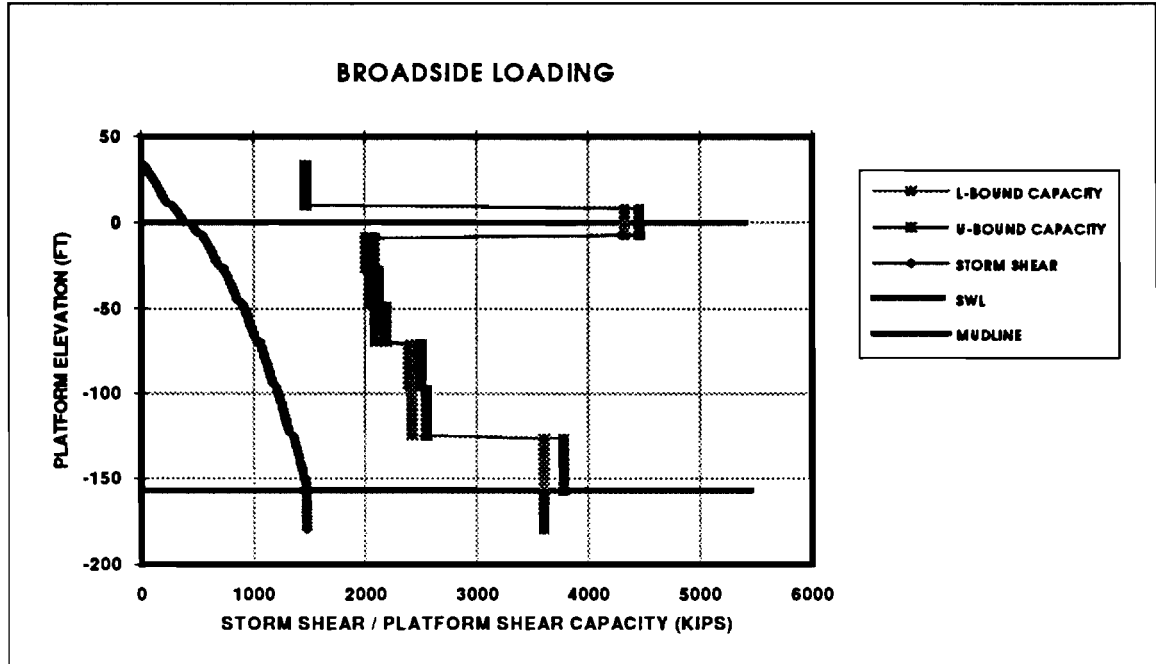
Figure C19: Platform C - Storm Shear vs Shear Capacity
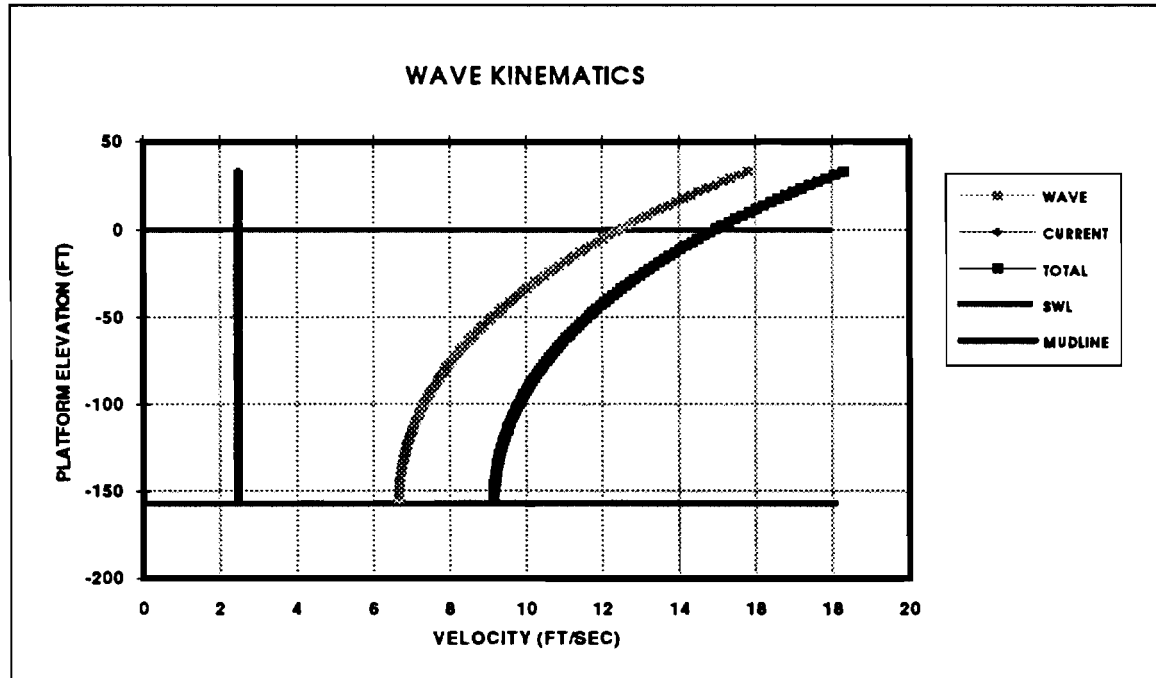
Figure C20: Platform C - Kinematics

259
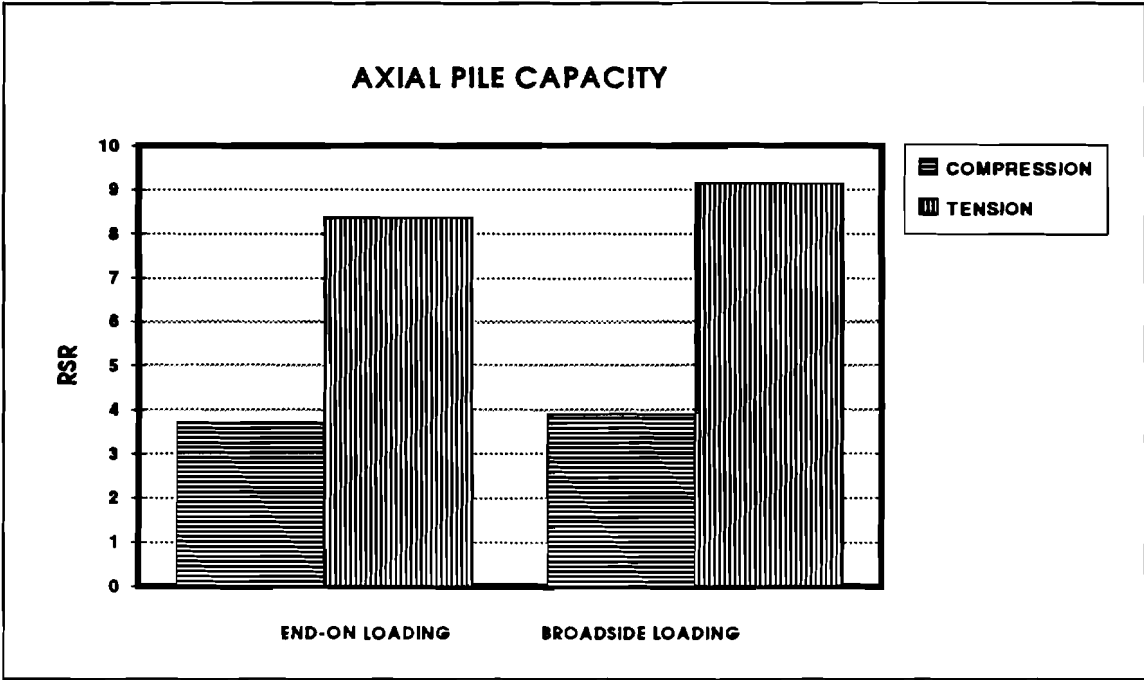
Figure C21: Platform C - Axial Pile Performance
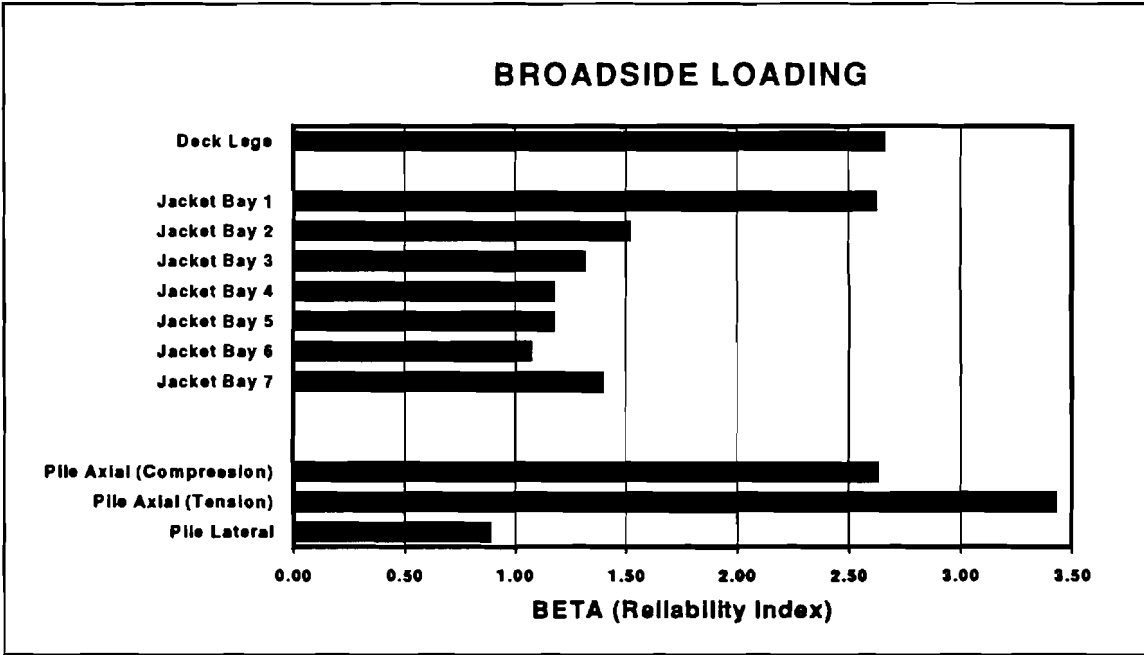
Figure C22: Platform C - Risk Analysis (Broadside Loading)

ULSLEA
Ultimate Limit State Limit Equilibrium Analysis
Simplified Reliability Analysis Program for Offshore Platforms

by

Mehrdad Mortazavi
and
Robert G. Bea

Marine Technology and Management Group
Department of Civil Engineering
University of California at Berkeley

' VARIABLE DECLARATION
'

Public wdep, sdep, vrh, wavh, wavp, cswl, cmdl, cprof, nleg, nbay, qdeck, pltype
Public ecdw(2), ecdh(2), edw(2), edh(2), bcw(2), tcw(2), msw
Public ndeck, deckw(2, 6), ok(6), uk(6), vcrest, cdd(6), wsc(6), decka(2, 6)
Public fhydro(2, 6), fhydroh(6), faero(2, 6), faeroh(6), deckh(6), faerobar(2), fhydrobar(2)
Public njoint, ndb(2, 30), bayh(30)
Public dld, dlt, jld(2, 30), jlt(2), dbtype(2, 30, 30), dbpos(2, 30, 30), theta(2, 30, 30), thetax(2, 30, 30)
Public dbconf(2, 30, 30), dbd(2, 30, 30), dbt(2, 30, 30), dbcond(2, 30, 30), dbjointi(2, 30, 30)
Public dbjointj(2, 30, 30), dbdam(2, 30, 30), dbrep(2, 30, 30), ddep(2, 30, 30), oos(2, 30, 30)
Public jtype(100), jgrout(100), jchd(100), jcht(100), jbrd(100), jbrt(100), jgap(100), jang(100), jpu(2, 30, 30), jput(100), jpuc(100), jpuh(2, 30, 30), jcap(2, 30), jcapbar(2, 100)
Public fy, e, kbuck, bres, stype, su1, su2, sphi, gammas, scour, cdj, cb, ds, lf
Public marineg, mg(30), pilet, piled, pilel, pgrout, plug, skirt, boatl(2), dequapp(30), dequ(2, 30)
Public spilet, spiled, spilel, splug, nskirt(2), nsk
Public nhb(30), hbd(30, 28), hbt(30, 28), hbl(30, 28), hbang(30, 28), hbequa(2, 30)
Public wdbias, wdcov, wjbias, wjcov, btbias, btcov, bcbias, bccov, jtbias, jtcov, jcbias, jccov
Public cabias, cacov, clbias, clcov, sabias, sacov, slbias, slcov
Public lh(2, 30), lht(2, 30), alpha(2), htotal
Public dbl(2, 30, 30), dblx(2, 30, 30), dbalpha(2, 30, 30)
Public phi(5), eta(5), wvel(100), cvel(100), vel(100), wvcrest, elev(100), velocity(30)
Public elevation(31), interval, f(2, 100), cumf(2, 100)
Public jbeta(100), jgamma(100), jqg(100), jdummy(100), jqbeta(100)
Public h(100, 30), m(2, 100, 30), mbar(2, 30), legf(2, 30), legfh(2, 30)
Public dla, dli, ibay1(2), dlzp, dlr, dlmp, dlmcr, dlm, dlcs(2), dlcm(2), dldelta(2), dlcap(2)
Public shear(2), dlmbar(2, 2)
Public dba(2, 30, 30), dbzp(2, 30, 30), dblam(2, 30, 30), dbdeque(2, 30, 30), dbdequb(2, 30, 30), dbdequebar(2, 30), dbdequbbar(2, 30), dbpe(2, 30, 30)
Public dbpy(2, 30, 30), dbpcr(2, 30, 30), dbmp(2, 30, 30), dbmcr(2, 30, 30), dbpcrl(2, 30, 30), dbr(2, 30, 30)
Public dbi(2, 30, 30)
Public dummye(2, 30), dummyb(2, 30)
Public dbw(30, 30), dbeps0(2, 30, 30), dbdelta(2, 30, 30), dbki(2, 30, 30)
Public dbpu(2, 30, 30), dbpuh(2, 30, 30), dbpuhu(2, 30, 30), epsilon, Formula, Formula1

```
Public dbalhpa(2, 30, 30), dbes(2, 30, 30), dbag(2, 30, 30), dbeg(2, 30, 30), dbatr(2, 30, 30), dbesdbeg(2,
30, 30), dbetr(2, 30, 30), dbis(2, 30, 30)
Public dbig(2, 30, 30), dbitr(2, 30, 30), dbrtr(2, 30, 30), dbztr(2, 30, 30), dbastr(2, 30, 30)
Public dblamp(2, 30, 30), dbm(2, 30, 30), dbk(2, 30, 30), dbkis(2)
Public dbpcrld(2, 30, 30), dbmcrd(2, 30, 30), dblamd(2, 30, 30), dbpcrd0(2, 30, 30), dbpcrd(2, 30, 30)
Public pilea, pilepy, pilezp, piler, pilemp, pilemcr, pilem, n(2)
Public spilea, spilepy, spilezp, spiler, spilemp, spilemcr, spilem
Public ff, wp, dummy, qcc, qtc, bca, a, b, seta, psi, pucbar, puc(2), bcl, nq, qmax, ffmax, fas, qcs, qts, bsa,
bsl
Public kp, pusbar, pus(2)
Public swp, sqcc, sqtcs, spuc(2), sqcs, sqts, spus(2)
Public cap(2, 30), capu(2, 30), rsrcc(2), rsrtc(2), rsrcs(2), rsrts(2), rsrc(2), rsrt(2)
Public lbcap(2, 31), lbcapbar(2, 100), ubcap(2, 31), ubcapbar(2, 100), fcap(2)
Public meanload(2, 30), meanmarg(2, 30), covload(2, 30), covcap(2, 30), covlfcap(2), covafcap(2)
Public sigmacap(2, 30), sigmaalpha(2, 30), sigmamarg(2, 30), sigmapu(2, 30), sumksq(2, 30)
Public meanmargacf(2), meanmargatf(2), sigmamargaf(2), betaacf(2), betaatf(2), beta(2, 30)
Public prelim, steelg, steelw, steelv, decklegsw, jacketw, pilew
'
'        ASSIGN VALUE TO VARIABLES
'        ENVIRONMENTAL CONDITIONS
'
Sub Macro1()
'
Windows("INP.XLS").Activate
prelim = ActiveSheet.Cells(873, 8)
wdep = ActiveSheet.Cells(5, 8)
sdep = ActiveSheet.Cells(7, 8)
vrh = ActiveSheet.Cells(10, 8)
wavh = ActiveSheet.Cells(13, 8)
wavp = ActiveSheet.Cells(15, 8)
cswl = ActiveSheet.Cells(22, 8)
cmdl = ActiveSheet.Cells(24, 8)
cprof = ActiveSheet.Cells(18, 8)
'
'        GLOBAL PARAMETERS
'
pltype = ActiveSheet.Cells(52, 8)
If pltype = 1 Then
    nleg = 4
Elself pltype = 2 Then
    nleg = 6
Elself pltype = 3 Then
    nleg = 8
Else
    nleg = 12
End If
nbay = ActiveSheet.Cells(72, 8)
qdeck = ActiveSheet.Cells(76, 8)
bcw(1) = ActiveSheet.Cells(59, 8)
tcw(1) = ActiveSheet.Cells(61, 8)
bcw(2) = ActiveSheet.Cells(64, 8)
tcw(2) = ActiveSheet.Cells(66, 8)
msw = ActiveSheet.Cells(68, 8)
ndeck = ActiveSheet.Cells(73, 8)
```

```
'
'           Deck Areas
'
For i = 1 To ndeck
    uk(i) = ActiveSheet.Cells(815 + 7 * i, 8)
    ok(i) = ActiveSheet.Cells(816 + 7 * i, 8)
    deckw(2, i) = ActiveSheet.Cells(817 + 7 * i, 8)
    deckw(1, i) = ActiveSheet.Cells(818 + 7 * i, 8)
    cdd(i) = ActiveSheet.Cells(819 + 7 * i, 8)
    wsc(i) = ActiveSheet.Cells(820 + 7 * i, 8)
Next i
'
'           #of Joints, # of Diagonal Braces, Bay Heights
'
njoint = ActiveSheet.Cells(666, 8)
For i = 1 To 2
    For j = 1 To 10
        ndb(i, j) = ActiveSheet.Cells(668 + 2 * (i - 1) + 4 * (j - 1), 8)
        If nbay > 10 Then ndb(i, j + 10) = ActiveSheet.Cells(715 + 2 * (i - 1) + 4 * (j - 1), 8)
        If nbay > 20 Then ndb(i, j + 20) = ActiveSheet.Cells(762 + 2 * (i - 1) + 4 * (j - 1), 8)
    Next j
Next i
For i = 0 To nbay
    bayh(i) = ActiveSheet.Cells(477 + 2 * i, 8)
Next i
If nbay > 14 Then
    For i = 0 To 15
        bayh(i + 15) = ActiveSheet.Cells(513 + 2 * i, 8)
    Next i
Else
End If
'
'           LOCAL PARAMETERS
'           Deck legs and Vertical Diagonal Braces
'
dld = ActiveSheet.Cells(343, 8)
dlt = ActiveSheet.Cells(345, 8)
For i = 1 To 2
jlt(i) = ActiveSheet.Cells(6 + 1399 * (i - 1), 16)
    For j = 1 To nbay
    jld(i, j) = ActiveSheet.Cells(8 + 1399 * (i - 1), 16 + 8 * (j - 1))
        For k = 1 To ndb(i, j)
        dbd(i, j, k) = ActiveSheet.Cells(14 + 1399 * (i - 1) + 46 * (k - 1), 16 + 8 * (j - 1))
        dbt(i, j, k) = ActiveSheet.Cells(16 + 1399 * (i - 1) + 46 * (k - 1), 16 + 8 * (j - 1))
        dbpos(i, j, k) = ActiveSheet.Cells(18 + 1399 * (i - 1) + 46 * (k - 1), 16 + 8 * (j - 1))
        dbtype(i, j, k) = ActiveSheet.Cells(23 + 1399 * (i - 1) + 46 * (k - 1), 16 + 8 * (j - 1))
        dbconf(i, j, k) = ActiveSheet.Cells(36 + 1399 * (i - 1) + 46 * (k - 1), 16 + 8 * (j - 1))
        dbjointi(i, j, k) = ActiveSheet.Cells(27 + 1399 * (i - 1) + 46 * (k - 1), 16 + 8 * (j - 1))
        dbjointj(i, j, k) = ActiveSheet.Cells(29 + 1399 * (i - 1) + 46 * (k - 1), 16 + 8 * (j - 1))
        dbcond(i, j, k) = ActiveSheet.Cells(48 + 1399 * (i - 1) + 46 * (k - 1), 16 + 8 * (j - 1))
        ddep(i, j, k) = ActiveSheet.Cells(32 + 1399 * (i - 1) + 46 * (k - 1), 16 + 8 * (j - 1))
        oos(i, j, k) = ActiveSheet.Cells(34 + 1399 * (i - 1) + 46 * (k - 1), 16 + 8 * (j - 1))
        Next k
    Next j
```

```
Next i
'
'          Horizontal Bracings
'
For i = 1 To nbay
    nhb(i) = ActiveSheet.Cells(2846, 16 + 8 * (i - 1))
    For j = 1 To 7
        hbd(i, j) = ActiveSheet.Cells(2806 + 5 * (j - 1), 16 + 8 * (i - 1))
        hbt(i, j) = ActiveSheet.Cells(2807 + 5 * (j - 1), 16 + 8 * (i - 1))
        hbl(i, j) = ActiveSheet.Cells(2808 + 5 * (j - 1), 16 + 8 * (i - 1))
        hbang(i, j) = ActiveSheet.Cells(2809 + 5 * (j - 1), 16 + 8 * (i - 1))
        hbd(i, j + 7) = ActiveSheet.Cells(2857 + 5 * (j - 1), 16 + 8 * (i - 1))
        hbt(i, j + 7) = ActiveSheet.Cells(2858 + 5 * (j - 1), 16 + 8 * (i - 1))
        hbl(i, j + 7) = ActiveSheet.Cells(2859 + 5 * (j - 1), 16 + 8 * (i - 1))
        hbang(i, j + 7) = ActiveSheet.Cells(2860 + 5 * (j - 1), 16 + 8 * (i - 1))
        hbd(i, j + 14) = ActiveSheet.Cells(2906 + 5 * (j - 1), 16 + 8 * (i - 1))
        hbt(i, j + 14) = ActiveSheet.Cells(2907 + 5 * (j - 1), 16 + 8 * (i - 1))
        hbl(i, j + 14) = ActiveSheet.Cells(2908 + 5 * (j - 1), 16 + 8 * (i - 1))
        hbang(i, j + 14) = ActiveSheet.Cells(2909 + 5 * (j - 1), 16 + 8 * (i - 1))
        hbd(i, j + 21) = ActiveSheet.Cells(2955 + 5 * (j - 1), 16 + 8 * (i - 1))
        hbt(i, j + 21) = ActiveSheet.Cells(2956 + 5 * (j - 1), 16 + 8 * (i - 1))
        hbl(i, j + 21) = ActiveSheet.Cells(2957 + 5 * (j - 1), 16 + 8 * (i - 1))
        hbang(i, j + 21) = ActiveSheet.Cells(2958 + 5 * (j - 1), 16 + 8 * (i - 1))
    Next j
Next i
'
'          Tubular Joints
'
For i = 1 To njoint
    jtype(i) = ActiveSheet.Cells(3015, 8 + 8 * i)
    jgrout(i) = ActiveSheet.Cells(3027, 8 + 8 * i)
    jchd(i) = ActiveSheet.Cells(3005, 8 + 8 * i)
    jcht(i) = ActiveSheet.Cells(3007, 8 + 8 * i)
    jbrd(i) = ActiveSheet.Cells(3009, 8 + 8 * i)
    jgap(i) = ActiveSheet.Cells(3011, 8 + 8 * i)
    jang(i) = ActiveSheet.Cells(3013, 8 + 8 * i)
    If njoint > 30 Then
        jtype(i + 30) = ActiveSheet.Cells(3046, 8 + 8 * i)
        jgrout(i + 30) = ActiveSheet.Cells(3058, 8 + 8 * i)
        jchd(i + 30) = ActiveSheet.Cells(3036, 8 + 8 * i)
        jcht(i + 30) = ActiveSheet.Cells(3038, 8 + 8 * i)
        jbrd(i + 30) = ActiveSheet.Cells(3040, 8 + 8 * i)
        jgap(i + 30) = ActiveSheet.Cells(3042, 8 + 8 * i)
        jang(i + 30) = ActiveSheet.Cells(3044, 8 + 8 * i)
    ElseIf njoint > 60 Then
        jtype(i + 60) = ActiveSheet.Cells(3077, 8 + 8 * i)
        jgrout(i + 60) = ActiveSheet.Cells(3089, 8 + 8 * i)
        jchd(i + 60) = ActiveSheet.Cells(3077, 8 + 8 * i)
        jcht(i + 60) = ActiveSheet.Cells(3079, 8 + 8 * i)
        jbrd(i + 60) = ActiveSheet.Cells(3071, 8 + 8 * i)
        jgap(i + 60) = ActiveSheet.Cells(3073, 8 + 8 * i)
        jang(i + 60) = ActiveSheet.Cells(3075, 8 + 8 * i)
    Else
End If
```

```
Next i
'
'          Foundation: Main and Skirt Piles
'
pilel = ActiveSheet.Cells(209, 8)
piled = ActiveSheet.Cells(211, 8)
pilet = ActiveSheet.Cells(213, 8)
plug = ActiveSheet.Cells(214, 8)
skirt = ActiveSheet.Cells(215, 8)
spilet = ActiveSheet.Cells(226, 8)
spiled = ActiveSheet.Cells(224, 8)
spilel = ActiveSheet.Cells(228, 8)
splug = ActiveSheet.Cells(233, 8)
nskirt(2) = ActiveSheet.Cells(221, 8)
nskirt(1) = ActiveSheet.Cells(222, 8)
'
'          Force Coeficients
'
cdj = ActiveSheet.Cells(171, 8)
cb = ActiveSheet.Cells(173, 8)
ds = ActiveSheet.Cells(175, 8)
lf = ActiveSheet.Cells(177, 8)
marineg = ActiveSheet.Cells(178, 8)
For i = 0 To 30
    mg(i) = ActiveSheet.Cells(571 + 2 * i, 8)
Next i
'
'          Boatlanding and Appurtenances
'
boatl(1) = ActiveSheet.Cells(374, 8)
boatl(2) = ActiveSheet.Cells(376, 8)
For i = 0 To 10
    dequapp(i) = ActiveSheet.Cells(378 + 2 * i, 8)
    If nbay > 10 Then dequapp(i + 10) = ActiveSheet.Cells(403 + 2 * i, 8)
    If nbay > 20 Then dequapp(i + 20) = ActiveSheet.Cells(430 + 2 * i, 8)
Next i
'
'          MEMBER STRENGTH, MATERIAL AND SOIL PROPERTIES
'
fy = ActiveSheet.Cells(129, 8)
e = ActiveSheet.Cells(131, 8)
kbuck = ActiveSheet.Cells(133, 8)
bres = ActiveSheet.Cells(135, 8)
stype = ActiveSheet.Cells(137, 8)
su1 = ActiveSheet.Cells(121, 8)
su2 = ActiveSheet.Cells(143, 8)
sphi = ActiveSheet.Cells(123, 8)
gammas = ActiveSheet.Cells(125, 8)
scour = ActiveSheet.Cells(127, 8)
If bres = 0 Then bres = 1
'
'          UNCERTAINTIES AND BIASES
'
wdbias = ActiveSheet.Cells(292, 8)
```

```
If wdbias = 0 Then wdbias = 1
wdcov = ActiveSheet.Cells(293, 8)
wjbias = ActiveSheet.Cells(295, 8)
If wjbias = 0 Then wjbias = 0.9
wjcov = ActiveSheet.Cells(296, 8)
btbias = ActiveSheet.Cells(298, 8)
If btbias = 0 Then btbias = 1
btcov = ActiveSheet.Cells(299, 8)
bcbias = ActiveSheet.Cells(298, 8)
If bcbias = 0 Then bcbias = 1
bccov = ActiveSheet.Cells(299, 8)
jtbias = ActiveSheet.Cells(314, 8)
If jtbias = 0 Then jtbias = 1
jtcov = ActiveSheet.Cells(315, 8)
jcbias = ActiveSheet.Cells(314, 8)
If jcbias = 0 Then jcbias = 1
jccov = ActiveSheet.Cells(315, 8)
cabias = ActiveSheet.Cells(302, 8)
If cabias = 0 Then cabias = 1
cacov = ActiveSheet.Cells(303, 8)
clbias = ActiveSheet.Cells(305, 8)
If clbias = 0 Then clbias = 1
clcov = ActiveSheet.Cells(306, 8)
sabias = ActiveSheet.Cells(308, 8)
If sabias = 0 Then sabias = 1
sacov = ActiveSheet.Cells(309, 8)
slbias = ActiveSheet.Cells(311, 8)
If slbias = 0 Then slbias = 1
slcov = ActiveSheet.Cells(312, 8)
Windows("U.XLS").Activate
'
End Sub
'
'          ULSLEA
'
Sub Macro2()
'
steelg = 0.42 'kcf
decklegsw = 0
jacketw = 0
pilew = 0
'
'          Stoke's V Kinematics
'
'          Storm Shear Profile
'
htotal = 0
For i = 1 To nbay
    htotal = bayh(i) + htotal
Next i
elevation(0) = htotal + bayh(0)
elevbar = elevation(0)
interval = elevation(0) / 100
For j = 1 To 100
```

266

```
        elev(j) = elevbar
        elevbar = elevbar - interval
Next j
g = 32.174
Pi = 3.14159
stk = 0
stlambda=0
If wdep = 0 Then wdep = 1
If wavp = 0 Then wavp = 1
If wavh = 0 Then wavh = 1
Do
        stkd = stk * (wdep + sdep)
        sts = (Application.Cosh(2 * stkd)) ^ (-1)
        stc0 = (Application.Tanh(stkd)) ^ 0.5
        stc2 = (stc0 * (2 + 7 * sts ^ 2)) / (4 * (1 - sts) ^ 2)
        stc4 = (stc0 * (4 + 32 * sts - 116 * sts ^ 2 - 400 * sts ^ 3 - 71 * sts ^ 4 + 146 * sts ^ 5)) / (32 * (1
        - sts) ^ 5)
        Formula = 100000 * ((((stk / g) ^ 0.5) * 0) - (2 * Pi / (wavp * ((g * stk) ^ 0.5))) + (stc0) + ((wavh
        * stk / 2) ^ 2 * stc2) + (((stk * wavh / 2) ^ 4) * stc4))
        stk = stk + 0.0001
Loop While Formula > 0.0001
Do
        stcosh = Application.Cosh(stkd)
        stsinh = Application.Sinh(stkd)
        c1 = (8 * stcosh ^ 4 - 8 * stcosh ^ 2 + 9) / (8 * stsinh ^ 4)
        c2 = (3840 * stcosh ^ 12 - 4096 * stcosh ^ 10 - 2592 * stcosh ^ 8 - 1008 * stcosh ^ 6 + 5944 *
        stcosh ^ 4 - 1830 * stcosh ^ 2 + 147) / (512 * stsinh ^ 10 * (6 * stcosh ^ 2 - 1))
        Formula = 100000 * (1 + c1 * stlambda ^ 2 + c2 * stlambda ^ 4 - 4 * Pi ^ 2 / (g * wavp ^ 2 * stk
        * Application.Tanh(stk * wdep)))
        stlambda = stlambda + 0.0001
Loop While Formula > 0.0001
a11 = 1 / stsinh
a13 = -(stcosh ^ 2 * (5 * stcosh ^ 2 + 1)) / (8 * stsinh ^ 5)
a15 = -(1184 * stcosh ^ 10 - 1440 * stcosh ^ 8 - 1992 * stcosh ^ 6 + 2641 * stcosh ^ 4 - 249 * stcosh ^ 2 +
18) / (1536 * stsinh ^ 11)
a22 = 3 / (8 * stsinh ^ 4)
a24 = (192 * stcosh ^ 8 - 424 * stcosh ^ 6 - 312 * stcosh ^ 4 + 480 * stcosh ^ 2 - 17) / (768 * stsinh ^ 10)
a33 = (13 - 4 * stcosh ^ 2) / (64 * stsinh ^ 7)
a35 = (512 * stcosh ^ 12 + 4224 * stcosh ^ 10 - 6800 * stcosh ^ 8 - 12808 * stcosh ^ 6 + 16704 * stcosh ^
4 - 3154 * stcosh ^ 2 + 107) / (4096 * stsinh ^ 13 * (6 * stcosh ^ 2 - 1))
a44 = (80 * stcosh ^ 6 - 816 * stcosh ^ 4 + 1338 * stcosh ^ 2 - 197) / (1536 * stsinh ^ 10 * (6 * stcosh ^ 2
- 1))
a55 = -(2880 * stcosh ^ 10 - 72480 * stcosh ^ 8 + 324000 * stcosh ^ 6 - 432000 * stcosh ^ 4 + 163470 *
stcosh ^ 2 - 16245) / (61440 * stsinh ^ 11 * (6 * stcosh ^ 2 - 1) * (8 * stcosh ^ 4 - 11 * stcosh ^ 2 + 3))
b22 = (2 * stcosh ^ 2 + 1) * stcosh / (4 * stsinh ^ 3)
b24 = stcosh * (272 * stcosh ^ 8 - 504 * stcosh ^ 6 - 192 * stcosh ^ 4 + 322 * stcosh ^ 2 + 21) / (384 *
stsinh ^ 9)
b33 = 3 * (8 * stcosh ^ 6 + 1) / (64 * stsinh ^ 6)
b35 = (88128 * stcosh ^ 14 - 208224 * stcosh ^ 12 + 70848 * stcosh ^ 10 + 54000 * stcosh ^ 8 - 21816 *
stcosh ^ 6 + 6264 * stcosh ^ 4 - 54 * stcosh ^ 2 - 81) / (12288 * stsinh ^ 12 * (6 * stcosh ^ 2 - 1))
b44 = stcosh * (768 * stcosh ^ 10 - 448 * stcosh ^ 8 - 48 * stcosh ^ 6 + 48 * stcosh ^ 4 + 106 * stcosh ^ 2
- 21) / (384 * stsinh ^ 9 * (6 * stcosh ^ 2 - 1))
```

```
b55 = (192000 * stcosh ^ 16 - 262720 * stcosh ^ 14 + 83680 * stcosh ^ 12 + 20160 * stcosh ^ 10 - 7280 *
stcosh ^ 8 + 7160 * stcosh ^ 6 - 1800 * stcosh ^ 4 - 1050 * stcosh ^ 2 + 225) / (12288 * stsinh ^ 10 * (6 *
stcosh ^ 2 - 1) * (8 * stcosh ^ 4 - 11 * stcosh ^ 2 + 3))
phi(1) = stlambda * a11 + stlambda ^ 3 * a13 + stlambda ^ 5 * a15
phi(2) = stlambda ^ 2 * a22 + stlambda ^ 4 * a24
phi(3) = stlambda ^ 3 * a33 + stlambda ^ 5 * a35
phi(4) = stlambda ^ 4 * a44
phi(5) = stlambda ^ 5 * a55
eta(1) = stlambda
eta(2) = stlambda ^ 2 * b22 + stlambda ^ 4 * b24
eta(3) = stlambda ^ 3 * b33 + stlambda ^ 5 * b35
eta(4) = stlambda ^ 4 * b44
eta(5) = stlambda ^ 5 * b55
celerity = (g * (wdep + sdep) * Application.Tanh(stkd) / stkd * (1 + stlambda ^ 2 * c1 + stlambda ^ 4 *
c2)) ^ 0.5
dummy = 0
For i = 1 To 5
    dummy = dummy + eta(i)
Next i
crest = dummy / stk + wdep + sdep
For i = 1 To 100
    wvel(i) = 0 'initialize
Next i
wvcrest = 0
For i = 1 To 5
    wvcrest = wvcrest + i * Application.Cosh(i * crest * stk) * phi(i)
    For j = 1 To 100
        If elev(j) > crest Then
            wvel(j) = 0
        Else
            wvel(j) = wvel(j) + i * Application.Cosh(i * elev(j) * stk) * phi(i)
        End If
    Next j
Next i
wvcrest = celerity * wvcrest * ds
For j = 1 To 100
    wvel(j) = celerity * wvel(j) * ds
Next j
'
'        Current Velocity
'
For i = 1 To 100
    If elev(i) > crest Then
        cvel(i) = 0
    ElseIf cprof = 3 Then
        cvel(i) = cswl
    ElseIf cprof = 1 Then
        cvel(i) = cswl - (cswl - cmdl) / crest * Application.Min(0, crest - elev(i))
    Else
        cvel(i) = cswl - (cswl - cmdl) / crest ^ 2 * (Application.Min(0, crest - elev(i))) ^ 2
    End If
    cvel(i) = Application.Max(0, cvel(i)) * cb
    cvcrest = cswl * cb
Next i
```

```
'
'           Total Velocities
'
vcrest = wvcrest + cvcrest
For i = 1 To 100
    vel(i) = wvel(i) + cvel(i)
Next i
'
'velocity(j)@ each bay
'
i = 0
elevation(0) = htotal + bayh(0)
Do
    elevation(i + 1) = elevation(i) - bayh(i)
    i = i + 1
Loop While i <= nbay
elevbar = elevation(0)
interval = elevation(0) / 100
k = 1
For j = 1 To 100
    velocity(k) = vel(j)
    If elevbar < elevation(k) Then k = k + 1
    elevbar = elevbar - interval
Next j
'
'           Bay Horizontal dimensions
'
For i = 1 To 2
    alpha(i) = Atn((bcw(i) - tcw(i)) / 2 / htotal)
Next i
i = 1 'eo (bs-load)
For j = 1 To nbay
    If nleg < 12 Then
        lh(i, 1) = tcw(i)
        lh(i, j + 1) = lh(i, j) + 2 * (bayh(j) * Tan(alpha(i)))
        lht(i, j) = lh(i, j)
    Else
        lh(i, 1) = tcw(i) / 2
        lh(i, j + 1) = lh(i, j) + (bayh(j) * Tan(alpha(i)))
        lht(i, j) = 2 * lh(i, j)
    End If
Next j
i = 2 'bs (eo-load)
For j = 1 To nbay
    If nleg = 4 Then
        lh(i, 1) = tcw(i)
        lh(i, j + 1) = lh(i, j) + 2 * (bayh(j) * Tan(alpha(i)))
        lht(i, j) = lh(i, j)
    ElseIf nleg = 6 Then
        lh(i, 1) = tcw(i) / 2
        lh(i, j + 1) = lh(i, j) + (bayh(j) * Tan(alpha(i)))
        lht(i, j) = 2 * lh(i, j)
    Else
        lh(i, 1) = (tcw(i) - msw) / 2
```

```
         lh(i, j + 1) = lh(i, j) + (bayh(j) * Tan(alpha(i)))
         lht(i, j) = 2 * lh(i, j) + msw
    End If
Next j
'
'         Diagonal Brace Properties
'         End-on (bs-load)
'
i = 1
If nleg < 12 Then
   For j = 1 To nbay
      For k = 1 To ndb(i, j)
         If dbconf(i, j, k) = 1 Then
            dbl(i, j, k) = Sqr(((lh(i, j + 1) + lh(i, j)) / 2) ^ 2 + bayh(j) ^ 2)
         ElseIf dbconf(i, j, k) = 2 Then
            If dbtype(i, j, k) = 1 Then
               If dbpos(i, j, k) = 1 Then
                  dbl(i, j, k) = Sqr((((lh(i, j + 1)) / 2) ^ 2 + bayh(j) ^ 2)
               Else
                  dbl(i, j, k) = Sqr((((lh(i, j)) / 2) ^ 2 + bayh(j) ^ 2)
               End If
            Else
               If dbpos(i, j, k) = 1 Then
                  dbl(i, j, k) = Sqr((((lh(i, j)) / 2) ^ 2 + bayh(j) ^ 2)
               Else
                  dbl(i, j, k) = Sqr((((lh(i, j + 1)) / 2) ^ 2 + bayh(j) ^ 2)
               End If
            End If
         Else
            dbl(i, j, k) = Sqr(((lh(i, j + 1) + lh(i, j)) / 2) ^ 2 + bayh(j) ^ 2)
         End If
      Next k
   Next j
Else
   For j = 1 To nbay
      For k = 1 To ndb(i, j)
         If dbconf(i, j, k) = 1 Then
            If dbtype(i, j, k) = 1 Then
               If dbpos(i, j, k) = 1 Then
                  dbl(i, j, k) = Sqr(lh(i, j + 1) ^ 2 + bayh(j) ^ 2)
               Else
                  dbl(i, j, k) = Sqr(lh(i, j) ^ 2 + bayh(j) ^ 2)
               End If
            Else
               If dbpos(i, j, k) = 1 Then
                  dbl(i, j, k) = Sqr(lh(i, j) ^ 2 + bayh(j) ^ 2)
               Else
                  dbl(i, j, k) = Sqr(lh(i, j + 1) ^ 2 + bayh(j) ^ 2)
               End If
            End If
         ElseIf dbconf(i, j, k) = 2 Then
            If dbtype(i, j, k) = 1 Then
               If dbpos(i, j, k) = 1 Then
                  dbl(i, j, k) = Sqr((lh(i, j + 1) - lh(i, j) / 2) ^ 2 + bayh(j) ^ 2)
```

```
                Else
                    dbl(i, j, k) = Sqr(((lh(i, j)) / 2) ^ 2 + bayh(j) ^ 2)
                End If
            Else
                If dbpos(i, j, k) = 1 Then
                    dbl(i, j, k) = Sqr(((lh(i, j)) / 2) ^ 2 + bayh(j) ^ 2)
                Else
                    dbl(i, j, k) = Sqr((lh(i, j + 1) - lh(i, j) / 2) ^ 2 + bayh(j) ^ 2)
                End If
            End If
        Else
            If dbtype(i, j, k) = 1 Then
                If dbpos(i, j, k) = 1 Then
                    dbl(i, j, k) = Sqr(lh(i, j + 1) ^ 2 + bayh(j) ^ 2)
                Else
                    dbl(i, j, k) = Sqr(lh(i, j) ^ 2 + bayh(j) ^ 2)
                End If
            Else
                If dbpos(i, j, k) = 1 Then
                    dbl(i, j, k) = Sqr(lh(i, j) ^ 2 + bayh(j) ^ 2)
                Else
                    dbl(i, j, k) = Sqr(lh(i, j + 1) ^ 2 + bayh(j) ^ 2)
                End If
            End If
        End If
    Next k
  Next j
End If
'
'         Broadside (eo-load)
'
i = 2
If nleg = 4 Then
  For j = 1 To nbay
    For k = 1 To ndb(i, j)
        If dbconf(i, j, k) = 1 Then
            dbl(i, j, k) = Sqr(((lh(i, j + 1) + lh(i, j)) / 2) ^ 2 + bayh(j) ^ 2)
        ElseIf dbconf(i, j, k) = 2 Then
            If dbtype(i, j, k) = 1 Then
                If dbpos(i, j, k) = 1 Then
                    dbl(i, j, k) = Sqr(((lh(i, j + 1)) / 2) ^ 2 + bayh(j) ^ 2)
                Else
                    dbl(i, j, k) = Sqr(((lh(i, j)) / 2) ^ 2 + bayh(j) ^ 2)
                End If
            Else
                If dbpos(i, j, k) = 1 Then
                    dbl(i, j, k) = Sqr(((lh(i, j)) / 2) ^ 2 + bayh(j) ^ 2)
                Else
                    dbl(i, j, k) = Sqr(((lh(i, j + 1)) / 2) ^ 2 + bayh(j) ^ 2)
                End If
            End If
        Else
            dbl(i, j, k) = Sqr(((lh(i, j + 1) + lh(i, j)) / 2) ^ 2 + bayh(j) ^ 2)
        End If
```

271

```
            Next k
        Next j
    ElseIf nleg = 6 Then
      For j = 1 To nbay
        For k = 1 To ndb(i, j)
          If dbconf(i, j, k) = 1 Then
            If dbtype(i, j, k) = 1 Then
              If dbpos(i, j, k) = 1 Then
                dbl(i, j, k) = Sqr(lh(i, j + 1) ^ 2 + bayh(j) ^ 2)
              Else
                dbl(i, j, k) = Sqr(lh(i, j) ^ 2 + bayh(j) ^ 2)
              End If
            Else
              If dbpos(i, j, k) = 1 Then
                dbl(i, j, k) = Sqr(lh(i, j) ^ 2 + bayh(j) ^ 2)
              Else
                dbl(i, j, k) = Sqr(lh(i, j + 1) ^ 2 + bayh(j) ^ 2)
              End If
            End If
          ElseIf dbconf(i, j, k) = 2 Then
            If dbtype(i, j, k) = 1 Then
              If dbpos(i, j, k) = 1 Then
                dbl(i, j, k) = Sqr((lh(i, j + 1) - lh(i, j) / 2) ^ 2 + bayh(j) ^ 2)
              Else
                dbl(i, j, k) = Sqr(((lh(i, j)) / 2) ^ 2 + bayh(j) ^ 2)
              End If
            Else
              If dbpos(i, j, k) = 1 Then
                dbl(i, j, k) = Sqr(((lh(i, j)) / 2) ^ 2 + bayh(j) ^ 2)
              Else
                dbl(i, j, k) = Sqr((lh(i, j + 1) - lh(i, j) / 2) ^ 2 + bayh(j) ^ 2)
              End If
            End If
          Else
            If dbtype(i, j, k) = 1 Then
              If dbpos(i, j, k) = 1 Then
                dbl(i, j, k) = Sqr(lh(i, j + 1) ^ 2 + bayh(j) ^ 2)
              Else
                dbl(i, j, k) = Sqr(lh(i, j) ^ 2 + bayh(j) ^ 2)
              End If
            Else
              If dbpos(i, j, k) = 1 Then
                dbl(i, j, k) = Sqr(lh(i, j) ^ 2 + bayh(j) ^ 2)
              Else
                dbl(i, j, k) = Sqr(lh(i, j + 1) ^ 2 + bayh(j) ^ 2)
              End If
            End If
          End If
        Next k
      Next j
    Else
      For j = 1 To nbay
        For k = 1 To ndb(i, j)
          If dbconf(i, j, k) = 1 Then
```

```
If dbtype(i, j, k) = 1 Then
    If dbpos(i, j, k) = 1 Then
        dbl(i, j, k) = Sqr(lh(i, j + 1) ^ 2 + bayh(j) ^ 2)
    ElseIf dbpos(i, j, k) = 2 Then
        dbl(i, j, k) = Sqr(msw ^ 2 + bayh(j) ^ 2)
    Else
        dbl(i, j, k) = Sqr(lh(i, j) ^ 2 + bayh(j) ^ 2)
    End If
Else
    If dbpos(i, j, k) = 1 Then
        dbl(i, j, k) = Sqr(lh(i, j) ^ 2 + bayh(j) ^ 2)
    ElseIf dbpos(i, j, k) = 2 Then
        dbl(i, j, k) = Sqr(msw ^ 2 + bayh(j) ^ 2)
    Else
        dbl(i, j, k) = Sqr(lh(i, j + 1) ^ 2 + bayh(j) ^ 2)
    End If
End If
ElseIf dbconf(i, j, k) = 2 Then
    If dbtype(i, j, k) = 1 Then
        If dbpos(i, j, k) = 1 Then
            dbl(i, j, k) = Sqr((lh(i, j + 1) - lh(i, j) / 2) ^ 2 + bayh(j) ^ 2)
        ElseIf dbpos(i, j, k) = 2 Then
            dbl(i, j, k) = Sqr((msw / 2) ^ 2 + bayh(j) ^ 2)
        Else
            dbl(i, j, k) = Sqr(((lh(i, j)) / 2) ^ 2 + bayh(j) ^ 2)
        End If
    Else
        If dbpos(i, j, k) = 1 Then
            dbl(i, j, k) = Sqr(((lh(i, j)) / 2) ^ 2 + bayh(j) ^ 2)
        ElseIf dbpos(i, j, k) = 2 Then
            dbl(i, j, k) = Sqr((msw / 2) ^ 2 + bayh(j) ^ 2)
        Else
            dbl(i, j, k) = Sqr((lh(i, j + 1) - lh(i, j) / 2) ^ 2 + bayh(j) ^ 2)
        End If
    End If
Else
    If dbtype(i, j, k) = 1 Then
        If dbpos(i, j, k) = 1 Then
            dbl(i, j, k) = Sqr(lh(i, j + 1) ^ 2 + bayh(j) ^ 2)
        ElseIf dbpos(i, j, k) = 2 Then
            dbl(i, j, k) = Sqr(msw ^ 2 + bayh(j) ^ 2)
        Else
            dbl(i, j, k) = Sqr(lh(i, j) ^ 2 + bayh(j) ^ 2)
        End If
    Else
        If dbpos(i, j, k) = 1 Then
            dbl(i, j, k) = Sqr(lh(i, j) ^ 2 + bayh(j) ^ 2)
        ElseIf dbpos(i, j, k) = 2 Then
            dbl(i, j, k) = Sqr(msw ^ 2 + bayh(j) ^ 2)
        Else
            dbl(i, j, k) = Sqr(lh(i, j + 1) ^ 2 + bayh(j) ^ 2)
        End If
    End If
End If
```

273

```
      Next k
   Next j
End If
'
'         Angles theta
'
For i = 1 To 2
   For j = 1 To nbay
      For k = 1 To ndb(i, j)
         theta(i, j, k) = Application.Asin(bayh(j) / dbl(i, j, k))
         If dbconf(i, j, k) = 1 Or dbconf(i, j, k) = 2 Then
            dblx(i, j, k) = dbl(i, j, k)
         ElseIf i = 1 And nleg < 12 Then                    '...X-Braced Elements...
            dblx(i, j, k) = lh(i, j + 1) / 2 / Sin(theta(i, j, k))
         ElseIf i = 1 And nleg = 12 Then
            If dbpos(i, j, k) = 1 Then
               thetax(i, j, k) = Atn((bayh(j) / lh(i, j + 1)))
               dblx(i, j, k) = Sin(thetax(i, j, k)) * lh(i, j + 1) / Sin(3.14 - theta(i, j, k) - thetax(i, j, k))
            Else
               thetax(i, j, k) = Atn((bayh(j) / lh(i, j)))
               dblx(i, j, k) = Sin(thetax(i, j, k)) * lh(i, j + 1) / Sin(3.14 - theta(i, j, k) - thetax(i, j, k))
            End If
         ElseIf i = 2 And nleg = 4 Then
            dblx(i, j, k) = lh(i, j + 1) / 2 / Sin(theta(i, j, k))
         ElseIf i = 2 And nleg = 6 Then
            If dbpos(i, j, k) = 1 Then
               thetax(i, j, k) = Atn((bayh(j) / lh(i, j + 1)))
               dblx(i, j, k) = Sin(thetax(i, j, k)) * lh(i, j + 1) / Sin(3.14 - theta(i, j, k) - thetax(i, j, k))
            Else
               thetax(i, j, k) = Atn((bayh(j) / lh(i, j)))
               dblx(i, j, k) = Sin(thetax(i, j, k)) * lh(i, j + 1) / Sin(3.14 - theta(i, j, k) - thetax(i, j, k))
            End If
         Else                              '...i=2 and nleg >=8...
            If dbpos(i, j, k) = 1 Then
               thetax(i, j, k) = Atn((bayh(j) / lh(i, j + 1)))
               dblx(i, j, k) = Sin(thetax(i, j, k)) * lh(i, j + 1) / Sin(3.14 - theta(i, j, k) - thetax(i, j, k))
            ElseIf dbpos(i, j, k) = 2 Then
               dblx(i, j, k) = dbl(i, j, k) / 2
            Else
               thetax(i, j, k) = Atn((bayh(j) / lh(i, j)))
               dblx(i, j, k) = Sin(thetax(i, j, k)) * lh(i, j + 1) / Sin(3.14 - theta(i, j, k) - thetax(i, j, k))
            End If
         End If
      Next k
   Next j
Next i
'For i = 1 To 2
'For j = 1 To nbay
'For k = 1 To ndb(i, j)
'Worksheets(15).Cells(k, j + nbay * (i - 1)) = theta(i, j, k)
'Next k
'Next j
'Next i
'
```

274

```
'       PRELIMINARY DESIGN
'
If prelim = True Then
   For i = 1 To 2
      For j = 1 To nbay
         If j <= nbay / 2 Then
            For k = 1 To ndb(i, j)
               dummy = kbuck * dblx(i, j, k) * 12 / 70 / 0.35
               dbd(i, j, k) = Application.Round(dummy, 0)
               dummy = dbd(i, j, k) / 40
               dbt(i, j, k) = Application.Round(dummy, 1)
            Next k
         Else
            For k = 1 To ndb(i, j)
               dummy = kbuck * dblx(i, j, k) * 12 / 80 / 0.35
               dbd(i, j, k) = Application.Round(dummy, 0)
               dummy = dbd(i, j, k) / 60
               dbt(i, j, k) = Application.Round(dummy, 1)
            Next k
         End If
      Next j
   Next i
Else
End If
'
'       Horizontal Bracings
'
For i = 1 To 2
   For j = 1 To nbay
      dummy = 0
      For k = 1 To nhb(j)
      If i = 2 Then
         dummy = dummy + (hbd(j, k) + 2 * mg(j)) / 12 * hbl(j, k) * (Cos(hbang(j, k) * 3.14 / 180)) ^ 3
      Else
         dummy = dummy + (hbd(j, k) + 2 * mg(j)) / 12 * hbl(j, k) * (Sin(hbang(j, k) * 3.14 / 180)) ^ 3
      End If
      Next k
      hbequa(i, j) = dummy
   Next j
Next i
For j = 1 To nbay
      For k = 1 To nhb(j)
         jacketw = jacketw + steelg * (3.14 * hbd(j, k) + hbt(j, k) * hbl(j, k))
      Next k
Next j
'
'       Deck Forces (According to API RP2A Ch.17)
'
For i = 1 To 2
   faerobar(i) = 0
   fhydrobar(i) = 0
   For j = 1 To ndeck
      deckh(j) = ok(j) - uk(j)
      decka(i, j) = deckh(j) * deckw(i, j)
```

```
        If crest > ok(j) Then
           fhydro(i, j) = (vcrest ^ 2 * cdd(j) * decka(i, j)) / 1000
           fhydroh(j) = uk(j) + deckh(j) / 2
           faero(i, j) = 0
           faeroh(j) = 0
        ElseIf crest < uk(j) Then
           fhydro(i, j) = 0
           fhydroh(j) = 0
           faero(i, j) = (0.00256 * vrh ^ 2 * wsc(j) * decka(i, j)) / 1000 'check units
           faeroh(j) = uk(j) + deckh(j) / 2
        Else
           fhydro(i, j) = (vcrest ^ 2 * cdd(j) * (crest - uk(j)) * deckw(i, j)) / 1000
           fhydroh(j) = (uk(j) + crest - wdep) / 2
           faero(i, j) = (0.00256 * vrh ^ 2 * wsc(i) * (decka(i, j) - (crest - uk(j)) * deckw(i, j))) / 1000
           faeroh(j) = (ok(j) + crest - wdep) / 2
        End If
        faerobar(i) = faerobar(i) + faero(i, j)
        fhydrobar(i) = fhydrobar(i) + wdbias * fhydro(i, j)
     Next j
Next i
'
'         Joint Capacities
'
For i = 1 To njoint
   jbeta(i) = jgap(i) / jchd(i)
   jgamma(i) = jbrd(i) / (2 * jcht(i))
   If jbeta(i) < 0.6 Then
      jqbeta(i) = 1
   Else
      jqbeta(i) = 0.3 / (jbeta(i) * (1 - 0.8333 * jbeta(i)))
   End If
   If jgamma(i) <= 20 Then
      jqg(i) = 1.8 - 0.1 * (jgap(i) / jcht(i))
   Else
      jqg(i) = 1.8 - 4 * (jgap(i) / jchd(i))
   End If
   If jqg(i) < 1 Then jqg(i) = 1
   jdummy(i) = fy * jcht(i) ^ 2 / Sin(jang(i) * 2 * 3.14 / 360)
   If jtype(i) = 1 Then
      jput(i) = jcbias * jdummy(i) * (3.4 + 19 * jbeta(i)) * jqg(i)
      jpuc(i) = jcbias * jdummy(i) * (3.4 + 19 * jbeta(i)) * jqg(i)
   Else
      jput(i) = jcbias * jdummy(i) * (3.4 + 19 * jbeta(i))
      If jtype(i) = 3 Then
         jpuc(i) = jcbias * jdummy(i) * (3.4 + 13 * jbeta(i)) * jqbeta(i)
      Else
         jpuc(i) = jcbias * jdummy(i) * (3.4 + 19 * jbeta(i)) * jqg(i)
      End If
   End If
Next i
'
'         Diagonal Brace Cross-sectional Properties and Capacities
'
For i = 1 To 2
```

```
    For j = 1 To nbay
       dummye(i, j) = 0
       dummyb(i, j) = 0
    Next j
 Next i
 For i = 1 To 2
    For j = 1 To nbay
       l = 1
       ll = 1
       cap(i, j) = 0
       capu(i, j) = 0
       jcap(i, j) = 0
       sumksq(i, j) = 0
          For k = 1 To ndb(i, j)
          dba(i, j, k) = (dbd(i, j, k) - dbt(i, j, k)) * dbt(i, j, k) * 3.14
          dbr(i, j, k) = 1 / 4 * (dbd(i, j, k) ^ 2 + (dbd(i, j, k) - 2 * dbt(i, j, k)) ^ 2) ^ 0.5
          dbi(i, j, k) = dbr(i, j, k) ^ 2 * dba(i, j, k)
          dbzp(i, j, k) = 1.3 * 3.14 / 32 * (dbd(i, j, k) ^ 4 - (dbd(i, j, k) - 2 * dbt(i, j, k)) ^ 4) / dbd(i, j, k)
          dblam(i, j, k) = (1 / 3.14) * (fy / e) ^ 0.5 * kbuck * (dblx(i, j, k) * 12) / dbr(i, j, k)
          If i = 1 Then
             dbdeque(2, j, k) = ((dbd(1, j, k) + 2 * mg(j)) / Sin(theta(1, j, k))) / 12
             dbdeque(1, j, k) = ((dbd(1, j, k) + 2 * mg(j)) * Sin(theta(1, j, k)) ^ 2) / 12
             dbdequb(1, j, k) = 0
             dbdequb(2, j, k) = 0
          Else
             dbdequb(1, j, k) = ((dbd(2, j, k) + 2 * mg(j)) / Sin(theta(2, j, k))) / 12
             dbdequb(2, j, k) = ((dbd(2, j, k) + 2 * mg(j)) * Sin(theta(2, j, k)) ^ 2) / 12
             dbdeque(2, j, k) = 0
             dbdeque(1, j, k) = 0
          End If
          dummye(1, j) = dummye(1, j) + dbdeque(1, j, k)
          dummye(2, j) = dummye(2, j) + dbdeque(2, j, k)
          dummyb(1, j) = dummyb(1, j) + dbdequb(1, j, k)
          dummyb(2, j) = dummyb(2, j) + dbdequb(2, j, k)
          dbpe(i, j, k) = 3.14 ^ 2 * e * dba(i, j, k) / (kbuck * dblx(i, j, k) * 12 / dbr(i, j, k)) ^ 2
          dbpy(i, j, k) = fy * dba(i, j, k)
          If dblam(i, j, k) < 2 ^ 0.5 Then
             dbpcr(i, j, k) = (1 - 0.25 * dblam(i, j, k) ^ 2)
          Else
             dbpcr(i, j, k) = 1 / (dblam(i, j, k) ^ 2)
          End If
          dbpcr(i, j, k) = dbpcr(i, j, k) * fy * dba(i, j, k)
          If dbd(i, j, k) / dbt(i, j, k) <= 60 Then
             dbpcrl(i, j, k) = dbpy(i, j, k)
          Else
             dbpcrl(i, j, k) = dbpy(i, j, k) * (1.64 - 0.23 * (dbd(i, j, k) / dbt(i, j, k)) ^ 0.25)
          End If
          dbmp(i, j, k) = dbzp(i, j, k) * fy / 12
          If fy * dbd(i, j, k) / dbt(i, j, k) < 1500 Then
             dbmcr(i, j, k) = 1
          ElseIf fy * dbd(i, j, k) / dbt(i, j, k) < 3000 Then
             dbmcr(i, j, k) = (1.13 - 2.58 * fy * dbd(i, j, k) / dbt(i, j, k) / e)
          Else
             dbmcr(i, j, k) = (0.94 - 0.76 * fy * dbd(i, j, k) / dbt(i, j, k) / e)
```

277

```
End If
dbmcr(i, j, k) = dbmcr(i, j, k) * dbmp(i, j, k)
'
'           Brace Buckling Formulation
'
dbw(j, k) = wjbias * ((velocity(j) * Sin(theta(i, j, k))) ^ 2 * cdj * (dbd(i, j, k) + 2 * mg(j)) / 12 /
1000) * If
dbeps0(i, j, k) = dblx(i, j, k) * 12 * (dbpcr(i, j, k) / e / dbi(i, j, k)) ^ 0.5
dbdelta(i, j, k) = Abs(Cos(3.1416 / 2 * dbpcr(i, j, k) / dbpy(i, j, k)) * dbmcr(i, j, k) / ((1 / (1 + 2 *
Sin(0.5 * dbeps0(i, j, k)) / Sin(dbeps0(i, j, k)))) * 1 / (dbeps0(i, j, k) ^ 2) * (1 / Cos(dbeps0(i, j, k) / 2) - 1)
* 8 * dbpcr(i, j, k)))
dbki(i, j, k) = e * dba(i, j, k) * Cos(theta(i, j, k)) ^ 2 / dbl(i, j, k)
If dbtype(i, j, k) = 1 Then
  jpu(i, j, k) = Application.Min(jput(dbjointi(i, j, k)), jput(dbjointj(i, j, k)))
  dbpu(i, j, k) = dbpy(i, j, k)
  dbpuhu(i, j, k) = dbpy(i, j, k) * Cos(theta(i, j, k))
ElseIf dbcond(i, j, k) = 1 Then
  dbpu(i, j, k) = dbpcr(i, j, k)
  Do
          Formula = ((1 / (1 + 2 * Sin(0.5 * dbeps0(i, j, k)) / Sin(dbeps0(i, j, k))) * 1 / dbeps0(i, j,
          k) ^ 2 * (1 / Cos((dbeps0(i, j, k)) / 2) - 1) * (dbw(j, k) * dblx(i, j, k) ^ 2 + 8 * dbpu(i, j,
          k) * dbdelta(i, j, k))) / dbmcr(i, j, k)) - Cos(3.1416 / 2 * dbpu(i, j, k) / dbpy(i, j, k))
          Formula1 = ((1 / (1 + 2 * Sin(0.5 * dbeps0(i, j, k)) / Sin(dbeps0(i, j, k))) * 1 / dbeps0(i,
          j, k) ^ 2 * (1 / Cos((dbeps0(i, j, k)) / 2) - 1) * (8 * dbdelta(i, j, k))) / dbmcr(i, j, k)) +
          3.1416 / 2 / dbpy(i, j, k) * Sin(3.1416 / 2 * dbpu(i, j, k) / dbpy(i, j, k))
          dbpu(i, j, k) = dbpu(i, j, k) - Formula / Formula1
  Loop While Abs(Formula) > 1
  dbpu(i, j, k) = bcbias * dbpu(i, j, k)
ElseIf dbcond(i, j, k) = 2 Then
'
'           Damaged Members (Loh's Equations)
'
  dbpcrld(i, j, k) = dbpcrl(i, j, k) * Application.Max(0.45, Exp(-0.08 * ddep(i, j, k) / dbt(i, j, k)))
  dbmcrd(i, j, k) = dbmcr(i, j, k) * Application.Max(0.55, Exp(-0.06 * ddep(i, j, k) / dbt(i, j, k)))
  dblamd(i, j, k) = (dbpcrld(i, j, k) / dbpe(i, j, k)) ^ 0.5
  If dblamd(i, j, k) < 2 ^ 0.5 Then
    dbpcrd0(i, j, k) = (1 - 0.25 * dblamd(i, j, k) ^ 2) * dbpcrld(i, j, k)
  Else
    dbpcrd0(i, j, k) = (1 / dblamd(i, j, k) ^ 2) * dbpcrld(i, j, k)
  End If
  dbpcrd(i, j, k) = dbpcrd0(i, j, k)
  Do
    dbpcrd(i, j, k) = dbpcrd(i, j, k) - 0.1
    Formula = Abs(1 - dbpcrd(i, j, k) / dbpcrd0(i, j, k) - dbpcrd(i, j, k) * oos(i, j, k) / 12 / (1 -
    dbpcrd(i, j, k) / dbpe(i, j, k)) / dbmcrd(i, j, k))
  Loop While Formula > 0.01
  dbpu(i, j, k) = dbpcrd(i, j, k)
  Do
    dbpu(i, j, k) = dbpu(i, j, k) - 0.1
    Formula = 1 - dbpu(i, j, k) / dbpcrd(i, j, k) - ((dbw(j, k) * dblx(i, j, k) ^ 2 / 24 / (1 - dbpu(i, j,
    k) / dbpe(i, j, k)) / dbmcrd(i, j, k)) ^ (2 - 3 * ddep(i, j, k) / dbd(i, j, k))) ^ 0.5
  Loop While Formula > 0.01
  dbpu(i, j, k) = bcbias * dbpu(i, j, k)
Else
```

```vb
' 
'       Grout Repaired Members (Parsanejad's Equations)
' 

    dbalhpa(i, j, k) = Application.Acos(1 - 2 * ddep(i, j, k) / dbd(i, j, k))
    dbag(i, j, k) = dbd(i, j, k) ^ 2 / 4 * (3.14 - dbalpha(i, j, k) + 0.5 * Sin(2 * dbalpha(i, j, k)))
    dbatr(i, j, k) = dba(i, j, k) + dbag(i, j, k) / 7
    dbes(i, j, k) = dbd(i, j, k) / (2 * 3.14) * (Sin(dbalpha(i, j, k)) - dbalpha(i, j, k) * Cos(dbalpha(i, j,
        k)))
    dbeg(i, j, k) = (dbd(i, j, k) * Sin(dbalpha(i, j, k))) ^ 3 / 12 / dbag(i, j, k)
    dbetr(i, j, k) = (dba(i, j, k) * dbes(i, j, k) + dbag(i, j, k) / 7 * dbeg(i, j, k)) / dbatr(i, j, k)
    dbis(i, j, k) = dbd(i, j, k) ^ 3 * dbt(i, j, k) / 4 * ((3.14 - dbalpha(i, j, k)) / 2 - Sin(2 * dbalpha(i, j,
        k)) / 4 + dbalpha(i, j, k) * (Cos(dbalpha(i, j, k))) ^ 2 - (Sin(dbalpha(i, j, k)) - dbalpha(i, j, k) *
        Cos(dbalpha(i, j, k))) ^ 2 / 3.14)
    dbig(i, j, k) = dbd(i, j, k) ^ 4 / 64 * (3.14 - dbalpha(i, j, k) + Sin(4 * dbalpha(i, j, k)) / 4) - dbd(i,
        j, k) ^ 4 * (Sin(dbalpha(i, j, k))) ^ 6 / 144 / dbag(i, j, k)
    dbitr(i, j, k) = dbis(i, j, k) + dbig(i, j, k) / 7 + dba(i, j, k) * (dbetr(i, j, k) - dbes(i, j, k)) ^ 2 +
        dbag(i, j, k) / 7 * (dbeg(i, j, k) - dbetr(i, j, k)) ^ 2
    dbrtr(i, j, k) = (dbitr(i, j, k) / dbatr(i, j, k)) ^ 0.5
    dbztr(i, j, k) = dbitr(i, j, k) / (dbd(i, j, k) / 2 * Cos(dbalpha(i, j, k)) + dbes(i, j, k))
    dbastr(i, j, k) = dba(i, j, k) + 3.14 * dbd(i, j, k) ^ 2 / 4 / 7
    dblamp(i, j, k) = 1 / 3.14 * kbuck * dblx(i, j, k) * 12 / dbrtr(i, j, k) * (fy / e) ^ 0.5
    dbm(i, j, k) = dbatr(i, j, k) / dbastr(i, j, k)
    dbpu(i, j, k) = 0
    Do
        dbpu(i, j, k) = dbpu(i, j, k) + 0.1
        dbk(i, j, k) = dbatr(i, j, k) * (dbetr(i, j, k) + oos(i, j, k) + dbw(j, k) * 12 * dblx(i, j, k) ^ 2 / 24
            / dbpu(i, j, k)) / dbztr(i, j, k)
        Formula = Abs((dbpu(i, j, k) / dbastr(i, j, k) / fy) ^ 2 - ((1 + dbk(i, j, k)) / (dblamp(i, j, k) ^ 2)
            + dbm(i, j, k)) * (dbpu(i, j, k) / dbastr(i, j, k) / fy) + dbm(i, j, k) / (dblamp(i, j, k) ^ 2))
    Loop While Formula > 0.01
    dbpu(i, j, k) = bcbias * dbpu(i, j, k)
End If
If dbtype(i, j, k) = 2 Then jpu(i, j, k) = Application.Min(jpuc(dbjointi(i, j, k)), jpuc(dbjointj(i, j,
    k)))
dbpu(i, j, 0) = 10 ^ 10
jpu(i, j, 0) = 10 ^ 10
dbki(i, j, 0) = 1
If jpu(i, j, k) / dbki(i, j, k) < jpu(i, j, k - 1) / dbki(i, j, k - 1) Then 11 = k
If dbpu(i, j, k) / dbki(i, j, k) < dbpu(i, j, k - 1) / dbki(i, j, k - 1) Then l = k
dbkis(i) = dbkis(i) + dbki(i, 1, k)
jpuh(i, j, k) = jpu(i, j, 11) / dbki(i, j, 11) * dbki(i, j, k) * Cos(theta(i, j, k))
dbpuh(i, j, k) = dbpu(i, j, l) / dbki(i, j, l) * dbki(i, j, k) * Cos(theta(i, j, k))
jcap(i, j) = jcap(i, j) + jpuh(i, j, k) 'Joint Capacity
cap(i, j) = cap(i, j) + dbpuh(i, j, k) 'L-Bound Capacity
If dbtype(i, j, k) = 2 Then dbpuhu(i, j, k) = bres * dbpu(i, j, k) * Cos(theta(i, j, k))
capu(i, j) = capu(i, j) + dbpuhu(i, j, k) 'U-Bound Capacity
sumksq(i, j) = sumksq(i, j) + dbki(i, j, k) ^ 2
sigmapu(i, j) = ((bccov * dbpu(i, j, l)) ^ 2 + (dbl(i, j, l) ^ 2 / 8 / dbdelta(i, j, l)) ^ 2 * (wjcov *
    dbw(j, l)) ^ 2) ^ 0.5
sigmaalpha(i, j) = sigmapu(i, j) / dbki(i, j, l)
jacketw = jacketw + steelg * (3.14 * dbd(i, j, k) / 12 * dbt(i, j, k) / 12 * dbl(i, j, k))
Next k
dbdequebar(1, j) = dummye(1, j)
dbdequebar(2, j) = dummye(2, j)
```

```
      dbdequbbar(1, j) = dummyb(1, j)
      dbdequbbar(2, j) = dummyb(2, j)
   Next j
Next i
htotal*cos(application.atn((tan(alpha(1))^2+(tan(alpha(2))^2)^0.5)
jacketw = jacketw + steelg * nleg * 3.14 * jld(1, 1) / 12 * jlt(1) / 12 * htotal
'
'        Deck Legs
'
For i = 1 To 2
   dla = (dld - dlt) * dlt * 3.14
   dli = 3.14 / 64 * (dld ^ 4 - (dld - 2 * dlt) ^ 4)
   If pgrout = True Then
      ibay1(i) = 3.14 / 64 * (jld(i, 1) ^ 4 - (piled - 2 * pilet) ^ 4)
   Else
      ibay1(i) = 3.14 / 64 * (jld(i, 1) ^ 4 - (jld(i, 1) - 2 * jlt(i)) ^ 4)
   End If
   dlzp = 1.3 * 3.14 / 32 * (dld ^ 4 - (dld - 2 * dlt) ^ 4) / dld
   dlr = 1 / 4 * (dld ^ 2 + (dld - 2 * dlt) ^ 2) ^ 0.5
   dlmp = dlzp * fy / 12
   If fy * dld / dlt < 1500 Then
      dlmcr = 1
   ElseIf fy * dld / dlt < 3000 Then
      dlmcr = (1.13 - 2.58 * fy * dld / dlt / e)
   Else
      dlmcr = (0.94 - 0.76 * fy * dld / dlt / e)
   End If
   dlmcr = dlmcr * dlmp
   dlm = dlmcr * Cos(3.14 / 2 * qdeck / nleg / fy / dla)
   dlcs(i) = dbkis(i) / nleg
   dlcm(i) = (bayh(1) / (e * ibay1(i) / 144) - 3 * dlcs(i) * bayh(1) ^ 4 / (4 * dlcs(i) * bayh(1) ^ 3 * e *
         ibay1(i) / 144 + 12 * (e * ibay1(i) / 144) ^ 2)) ^ -1
   dldelta(i) = dlm * bayh(0) * (bayh(0) / (6 * e * dli / 144) + 1 / dlcm(i))
   dlcap(i) = (2 * nleg * dlm - qdeck * dldelta(i)) / bayh(0)
   dlmbar(i, 0) = Abs(Application.Min((faerobar(i) + fhydrobar(i)) / nleg * bayh(0) * ((bayh(0) / (2 * e *
         dli / 144) + 1 / dlcm(i)) / (bayh(0) / (e * dli / 144) + 1 / dlcm(i))), dlm))
   dlmbar(i, 1) = Abs(Application.Min(dlmbar(i, 0) - (faerobar(i) + fhydrobar(i)) / nleg * bayh(0), dlm))
   shear(i) = dlmbar(i, 1) / bayh(1) * nleg
   dbdequebar(i, 0) = 0
   dbdequbbar(i, 0) = 0
   jld(i, 0) = dld
Next i
decklegsw = steelg * dla / 144 * bayh(0) * nleg
'
'        FOUNDATION CAPACITY
'        Cross-sectional Properties (Main Piles)
'
pilea = (piled - pilet) * pilet * 3.14
pilepy = pilea * fy
pilezp = 1.3 * 3.14 / 32 * (piled ^ 4 - (piled - 2 * pilet) ^ 4) / piled
piler = 1 / 4 * (piled ^ 2 + (piled - 2 * pilet) ^ 2) ^ 0.5
pilemp = pilezp * fy / 12
If fy * piled / pilet < 1500 Then
   pilemcr = 1
```

```
ElseIf fy * piled / pilet < 3000 Then
    pilemcr = (1.13 - 2.58 * fy * piled / pilet / e)
Else
    pilemcr = (0.94 - 0.76 * fy * piled / pilet / e)
End If
pilemcr = pilemcr * pilemp
pilem = pilemcr * Cos(3.14 / 2 * qdeck / nleg / fy / pilea)
pilew = steelg * nleg * pilea / 144 * (pilel + htotal)
'
'           Cross-sectional Properties (Skirt Piles)
'
If skirt = True Then
    spilea = (spiled - spilet) * spilet * 3.14
    spilepy = spilea * fy
    spilezp = 1.3 * 3.14 / 32 * (spiled ^ 4 - (spiled - 2 * spilet) ^ 4) / spiled
    spiler = 1 / 4 * (spiled ^ 2 + (spiled - 2 * spilet) ^ 2) ^ 0.5
    spilemp = spilezp * fy / 12
    If fy * spiled / spilet < 1500 Then
        spilemcr = 1
    ElseIf fy * spiled / spilet < 3000 Then
        spilemcr = (1.13 - 2.58 * fy * spiled / spilet / e)
    Else
        spilemcr = (0.94 - 0.76 * fy * spiled / spilet / e)
    End If
    spilemcr = spilemcr * spilemp
    spilem = spilemcr
Else
End If
pilew = pilew + steelg * nsk * spilea / 144 * spilel
steelw = decklegsw + jacketw + pilew
'
'           Pile Capacity
'
If nleg = 4 Then
        n(1) = 2
        n(2) = 2
    ElseIf nleg = 6 Then
        n(1) = 3
        n(2) = 2
    ElseIf nleg = 8 Then
        n(1) = 4
        n(2) = 2
    Else
        n(1) = 4
        n(2) = 3
End If
nsk = nskirt(1) + nskirt(2)
If stype = 2 Then
'
'           Axial Pile Capacity in Clay
'           Main Piles
'
    su = (su1 + su2) / 2
    If su < 0.5 Then
```

```
        ff = su
ElseIf su > 1.5 Then
        ff = 0.5 * su
Else
        ff = (1 - (su - 0.5) / 2) * su
End If
wp = 0
If plug = True Then wp = gammas * 3.14 * ((piled - 2 * pilet) / 12) ^ 2 / 4
wp = wp + 0.42 * 3.14 * ((piled / 12) ^ 2 - ((piled - 2 * pilet) / 12) ^ 2) / 4
If plug = True Then
        dummy = Application.Min(9 * su2 * 3.14 * (piled / 12) ^ 2 / 4, ff * 3.14 * (piled - 2 * pilet) / 12 *
            pilel)
Else
        dummy = 9 * su2 * 3.14 * (piled / 12) * pilet
End If
qcc = cabias * (Application.Min(pilepy, dummy + (ff * 3.14 * piled / 12 - wp) * pilel))
qtc = cabias * (Application.Min(pilepy, (ff * 3.14 * piled / 12 + wp) * pilel))
'
'       Axial Pile Capacity in Clay
'       Skirt Piles
'
If skirt = True Then
    swp = 0
    If splug = True Then swp = gammas * 3.14 * ((spiled - 2 * spilet) / 12) ^ 2 / 4
    swp = swp + 0.42 * 3.14 * ((spiled / 12) ^ 2 - ((spiled - 2 * spilet) / 12) ^ 2) / 4
    If splug = True Then
        dummy = Application.Min(9 * su2 * 3.14 * (spiled / 12) ^ 2 / 4, ff * 3.14 * (spiled - 2 * spilet) /
            12 * spilel)
    Else
        dummy = 9 * su2 * 3.14 * (spiled / 12) * spilet
    End If
    sqcc = cabias * (Application.Min(spilepy, dummy + (ff * 3.14 * spiled / 12 - swp) * spilel))
    sqtc = cabias * (Application.Min(spilepy, (ff * 3.14 * spiled / 12 + swp) * spilel))
Else
    sqcc = 0
    sqtc = 0
End If

'       Lateral Pile Capacity in Clay
'       Main Piles
'
a = 9 * su1 * piled / 12
b = 9 * su2 * piled / 12
seta = (b - a) / pilel
psi = 1.5 * piled + scour
pucbar = 0
Do
    pucbar = pucbar + 1
    If su1 = su2 Then
        c = pucbar / a
    Else
        c = 1 / seta * (-(a + seta * psi) + ((a + seta * psi) ^ 2 + 2 * seta * pucbar) ^ 0.5)
    End If
    dummy = pucbar * (c + psi) - 2 * pilem - (a + seta * psi) * c ^ 2 / 2 - seta / 2 * c ^ 3 / 3
```

282

```
Loop While dummy > 1
For i = 1 To 2
    puc(i) = clbias * pucbar * nleg
Next i
'
'       Lateral Pile Capacity in Clay
'           Skirt Piles
'
If skirt = True Then
    a = 9 * su1 * spiled / 12
    b = 9 * su2 * spiled / 12
    seta = (b - a) / spilel
    psi = 1.5 * spiled + scour
    pucbar = 0
    Do
        pucbar = pucbar + 1
        If su1 = su2 Then
            c = pucbar / a
        Else
            c = 1 / seta * (-(a + seta * psi) + ((a + seta * psi) ^ 2 + 2 * seta * pucbar) ^ 0.5)
        End If
        dummy = pucbar * (c + psi) - 2 * spilem - (a + seta * psi) * c ^ 2 / 2 - seta / 2 * c ^ 3 / 3
    Loop While dummy > 1
    For i = 1 To 2
        spuc(i) = clbias * pucbar * nsk
    Next i
Else
    For i = 1 To 2
        spuc(i) = 0
    Next i
End If
Else
'
'       Axial Pile Capacity in Sand
'           Main Piles
'
If sphi < 20 Then
    nq = 8
ElseIf sphi > 35 Then
    nq = 40
ElseIf sphi > 30 Then
    nq = 40 - (35 - sphi) * 4
ElseIf sphi > 25 Then
    nq = 20 - (30 - sphi) * 1.6
Else
    nq = 12 - (25 - sphi) * 0.8
End If
qmax = 5 * nq
If sphi < 20 Then
    ffmax = 1
ElseIf sphi > 35 Then
    ffmax = 2
ElseIf sphi > 25 Then
    ffmax = 2 - (35 - sphi) * 0.06
```

```
Else
    ffmax = 1.4 - (25 - sphi) * 0.08
End If
plc = ffmax / (gammas * (Tan((sphi - 5) * 3.14 / 180)))
plt = ffmax / (0.7 * gammas * Tan((sphi - 5) * 3.14 / 180)) ' 0.7 ??
If pilel < plc Then
    fas = 0.5 * pilel ^ 2 * gammas * Tan((sphi - 5) * 3.14 / 180)
Else
    fas = ffmax * (pilel - 0.5 * plc) * piled / 12 * 3.14
End If
dummy = 0
If plug = True Then dummy = Application.Min(qmax, nq * pilel * gammas) * 3.14 * (piled / 12) ^ 2 /
        4
qcs = sabias * (Application.Min(pilepy, fas + dummy) - wp * pilel)
If pilel < plt Then
    dummy = 0.7 * 0.5 * pilel ^ 2 * gammas * Tan((sphi - 5) * 3.14 / 180) ' 0.7 ??
Else
    dummy = ffmax * (pilel - 0.5 * plt)
End If
qts = sabias * (Application.Min(pilepy, dummy * 3.14 * piled / 12 + wp * pilel))
'
'       Axial Pile Capacity in Sand
'       Skirt Piles
'
If skirt = True Then
    If spilel < plc Then
        fas = 0.5 * spilel ^ 2 * gammas * Tan((sphi - 5) * 3.14 / 180)
    Else
        fas = ffmax * (spilel - 0.5 * plc) * spiled / 12 * 3.14
    End If
    dummy = 0
    If splug = True Then dummy = Application.Min(qmax, nq * spilel * gammas) * 3.14 * (spiled / 12)
        ^ 2 / 4
    sqcs = sabias * (Application.Min(spilepy, fas + dummy) - swp * spilel)
    If spilel < plt Then
        dummy = 0.7 * 0.5 * spilel ^ 2 * gammas * Tan((sphi - 5) * 3.14 / 180) ' 0.7 ??
    Else
        dummy = ffmax * (spilel - 0.5 * plt)
    End If
    sqts = sabias * (Application.Min(spilepy, dummy * 3.14 * spiled / 12 + swp * spilel))
Else
    sqcs = 0
    sqts = 0
End If
'
'       Lateral Pile Capacity in Sand
'       Main Piles
'
kp = (Tan((45 + sphi / 2) * 3.14 / 180)) ^ 2
If scour = 0 Then
    pusbar = (2.382 * pilem ^ (2 / 3) * (gammas * piled * kp) ^ (1 / 3))
Else
    pusbar = (2.382 * pilem ^ (2 / 3) * (gammas * piled * kp) ^ (1 / 3))
    Do
```

```
            pusbar = pusbar - 1
            dummy = pusbar - (2 * pilem / (scour + 0.544 * (pusbar / gammas / piled / kp)) ^ 0.5)
        Loop While dummy > 1
    End If
    For i = 1 To 2
        pus(i) = slbias * pusbar * nleg
    Next i
'
'       Lateral Pile Capacity in Sand
'       Skirt Piles
'
    If skirt = True Then
        If scour = 0 Then
            pusbar = (2.382 * spilem ^ (2 / 3) * (gammas * spiled * kp) ^ (i / 3))
        Else
            pusbar = (2.382 * spilem ^ (2 / 3) * (gammas * spiled * kp) ^ (1 / 3))
            Do
                pusbar = pusbar - 1
                dummy = pusbar - (2 * spilem / (scour + 0.544 * (pusbar / gammas / spiled / kp)) ^ 0.5)
            Loop While dummy > 1
        End If
        For i = 1 To 2
            spus(i) = slbias * pusbar * nsk
        Next i
    Else
        For i = 1 To 2
            spus(i) = 0
        Next i
    End If
End If
'
'       Storm Shear Profile
'
i = 0
elevation(0) = htotal + bayh(0)
Do
    elevation(i + 1) = elevation(i) - bayh(i)
    i = i + 1
Loop While i <= nbay
For i = 1 To 2
elevbar = elevation(0)
interval = elevation(0) / 100
    dummy = 0
    For j = 1 To ndeck
        dummy = dummy + fhydro(i, j) + faero(i, j)
    Next j
    cumf(i, 0) = dummy
    For l = 0 To nbay
        dequ(i, l) = dbdequebar(i, l) + dbdequbbar(i, l) + dequapp(l) + nleg * (jld(i, l) + 2 * mg(l)) / 12
    Next l
    k = 0
    For j = 1 To 100
        If elevbar > elevation(k + 1) Then
            f(i, j) = wjbias * cdj * dequ(i, k) * interval * vel(j) ^ 2 / 1000 * If
```

285

```
      Else
        If k = 0 Then
           f(i, j) = wjbias * cdj * (dequ(i, k + 1) * interval + hbequa(i, k + 1) + boatl(i)) * vel(j) ^ 2 / 1000
           * lf
        Else
           f(i, j) = wjbias * cdj * (dequ(i, k + 1) * interval + hbequa(i, k + 1)) * vel(j) ^ 2 / 1000 * lf
        End If
        k = k + 1
      End If
      elev(j) = elevbar
      elevbar = elevbar - interval
      If elevbar < 0 Then Exit For
      cumf(i, j) = cumf(i, j - 1) + f(i, j)
   Next j
Next i
'
'        Jacket Leg Forces
'
For i = 1 To 2
   For j = 1 To nbay + 1
      dummy = 0
      For k = 1 To ndeck
         dummy = dummy + fhydro(i, k) * (fhydroh(k) + wdep - elevation(j)) + faero(i, k) * (faeroh(k) +
wdep - elevation(j))
      Next k
      mbar(i, j) = dummy
   Next j
   For j = 1 To 100
      For k = 1 To nbay + 1
         h(j, k) = elev(j) - elevation(k)
         If h(j, k) > 0 Then
            m(i, j, k) = f(i, j) * h(j, k)
         Else
            m(i, j, k) = 0
         End If
         mbar(i, k) = mbar(i, k) + m(i, j, k)
         If k > nbay Then lht(i, k) = bcw(i)
         legf(i, k) = mbar(i, k) / lht(i, k)
         legfh(i, k) = legf(i, k) * Sin(alpha(i))
      Next k
   Next j
Next i
'
'        Platform Lateral Loading Capacity
'
For i = 1 To 2
   lbcap(i, 0) = dlcap(i)
   ubcap(i, 0) = dlcap(i)
   For j = 1 To nbay
      jcap(i, j) = jcap(i, j) + 2 * legfh(i, j)
      lbcap(i, j) = cap(i, j) + 2 * legfh(i, j)
      ubcap(i, j) = capu(i, j) + 2 * legfh(i, j)
      If j = 1 Then jcap(i, j) = jcap(i, j) - shear(i)
      If j = 1 Then lbcap(i, j) = lbcap(i, j) - shear(i)
```

```
        If j = 1 Then ubcap(i, j) = ubcap(i, j) - shear(i)
     Next j
     If stype = 1 Then
        fcap(i) = pus(i) + spus(i) + 2 * legfh(i, nbay + 1)
        rsrcs(i) = (qcs * n(i) + sqcs * nskirt(i) / 2) / (n(i) + nskirt(i) / 2) / (qdeck / (nleg + nskirt(1) +
           nskirt(2)) + legf(i, nbay + 1) / (nskirt(i) / 2 + n(i)))
        rsrts(i) = Application.Max(0, (qts * n(i) + sqts * nskirt(i) / 2) / (n(i) + nskirt(i) / 2) / (-qdeck / (nleg
           + nskirt(i) / 2) + legf(i, nbay + 1) / (nskirt(i) / 2 + n(i))))
        rsrc(i) = rsrcs(i)
        rsrt(i) = rsrts(i)
Else
        fcap(i) = puc(i) + spuc(i) + 2 * legfh(i, nbay + 1)
        rsrcs(i) = (qcc * n(i) + sqcc * nskirt(i) / 2) / (n(i) + nskirt(i) / 2) / (qdeck / (nleg + nskirt(1) +
           nskirt(2)) + legf(i, nbay + 1) / (nskirt(i) / 2 + n(i)))
        rsrts(i) = Application.Max(0, (qtc * n(i) + sqtc * nskirt(i) / 2) / (n(i) + nskirt(i) / 2) / (-qdeck / (nleg
           + nskirt(i) / 2) + legf(i, nbay + 1) / (nskirt(i) / 2 + n(i))))
        rsrc(i) = rsrcc(i)
        rsrt(i) = rsrtc(i)
     End If
Next i
'
'          Capacity Profile
'
For i = 1 To 2
elevbar = elevation(0)
interval = elevation(0) / 100
k = 0
   For j = 1 To 100
     If elevbar > elevation(k + 1) Then
        jcapbar(i, j) = jcap(i, k)
        lbcapbar(i, j) = lbcap(i, k)
        ubcapbar(i, j) = ubcap(i, k)
     Else
        jcapbar(i, j) = jcap(i, k)
        lbcapbar(i, j) = lbcap(i, k + 1)
        ubcapbar(i, j) = ubcap(i, k + 1)
        k = k + 1
     End If
     meanload(i, k) = cumf(i, j)
     elevbar = elevbar - interval
     If elevbar < 0 Then Exit For
   Next j
   meanload(i, nbay + 1) = cumf(i, j)
Next i
'
'          RELIABILTY ANALYSIS
'
For i = 1 To 2
   dummy = 0
   For j = 1 To ndeck
     dummy = dummy + fhydro(i, j)
   Next j
   For j = 0 To nbay
     If dummy = 0 Then
```

```
        covload(i, j) = wjcov
    Else
        covload(i, j) = (wdcov ^ 2 + wjcov ^ 2) ^ 0.5
    End If
    If j = 0 Then
        '....cov of Mcr = 0.1 , cov of Pcrl = 0 assumed!
        sigmacap(i, j) = (0.1 * dlmcr) * 2 * nleg / bayh(0) * Cos(3.14 / 2 * qdeck / nleg / fy / dla)
    Else
        sigmacap(i, j) = (sigmaalpha(i, j) ^ 2 * sumksq(i, j) + (covload(i, j) * meanload(i, j)) ^ 2) ^ 0.5
    End If
    covcap(i, j) = sigmacap(i, j) / lbcap(i, j)
    If meanload(i, j) = o Then meanload(i, j) = 0.01
    meanmarg(i, j) = Application.Ln(lbcap(i, j) / meanload(i, j) * ((1 + covload(i, j) ^ 2) / (1 + covcap(i,
        j) ^ 2)) ^ 0.5)
    sigmamarg(i, j) = (Application.Ln(1 + covcap(i, j) ^ 2) + Application.Ln(1 + covload(i, j) ^ 2)) ^ 0.5
    If sigmamarg(i, j) = 0 Then
        beta(i, j) = 0
    Else
        beta(i, j) = meanmarg(i, j) / sigmamarg(i, j)
    End If
Next j
If stype = 1 Then
    covlfcap(i) = (slcov ^ 2 + covload(i, nbay) ^ 2) ^ 0.5
    covafcap(i) = sacov
Else
    covlfcap(i) = (clcov ^ 2 + covload(i, nbay) ^ 2) ^ 0.5
    covafcap(i) = cacov
End If
If meanload(i, nbay + 1) = o Then meanload(i, nbay + 1) = 0.01
meanmarg(i, nbay + 1) = Application.Ln(fcap(i) / meanload(i, nbay + 1) * ((1 + covload(i, nbay) ^ 2) /
    (1 + covlfcap(i) ^ 2)) ^ 0.5)
sigmamarg(i, nbay + 1) = (Application.Ln(1 + covlfcap(i) ^ 2) + Application.Ln(1 + covload(i, nbay) ^
    2)) ^ 0.5
If sigmamarg(i, nbay + 1) = 0 Then
    beta(i, nbay + 1) = 0
Else
    beta(i, nbay + 1) = meanmarg(i, nbay + 1) / sigmamarg(i, nbay + 1)
End If
If stype = 1 Then
    meanmargacf(i) = Application.Ln(qcs / (qdeck / nleg + legf(i, nbay + 1) / n(i)) * ((1 + covload(i,
        nbay) ^ 2) / (1 + sacov ^ 2)) ^ 0.5)
    meanmargatf(i) = Application.Ln(qts / (-qdeck / nleg + legf(i, nbay + 1) / n(i)) * ((1 + covload(i,
        nbay) ^ 2) / (1 + sacov ^ 2)) ^ 0.5)
    sigmamargaf(i) = (Application.Ln(1 + sacov ^ 2) + Application.Ln(1 + covload(i, nbay) ^ 2)) ^ 0.5
    If sigmamargaf(i) = 0 Then
        betaacf(i) = 0
        betaatf(i) = 0
    Else
        betaacf(i) = meanmargacf(i) / sigmamargaf(i)
        betaatf(i) = meanmargatf(i) / sigmamargaf(i)
    End If
Else
    meanmargacf(i) = Application.Ln(qcc / (qdeck / nleg + legf(i, nbay + 1) / n(i)) * ((1 + covload(i,
        nbay) ^ 2) / (1 + sacov ^ 2)) ^ 0.5)
```

288

```vba
        meanmargatf(i) = Application.Ln(qtc / (-qdeck / nleg + legf(i, nbay + 1) / n(i)) * ((1 + covload(i,
            nbay) ^ 2) / (1 + sacov ^ 2)) ^ 0.5)
        sigmamargaf(i) = (Application.Ln(1 + sacov ^ 2) + Application.Ln(1 + covload(i, nbay) ^ 2)) ^ 0.5
        If sigmamargaf(i) = 0 Then
            betaacf(i) = 0
            betaatf(i) = 0
        Else
            betaacf(i) = meanmargacf(i) / sigmamargaf(i)
            betaatf(i) = meanmargatf(i) / sigmamargaf(i)
        End If
    End If
Next i
End Sub
Sub Macro3()
'
'       Output
'
For i = 1 To 100
    Worksheets(2).Cells(8 + i, 2) = elev(i) - wdep
    Worksheets(2).Cells(8 + i, 3) = wvel(i)
    Worksheets(2).Cells(8 + i, 4) = cvel(i)
    Worksheets(2).Cells(8 + i, 5) = vel(i)
    Worksheets(2).Cells(8 + i, 6) = f(2, i)
    Worksheets(2).Cells(8 + i, 7) = cumf(2, i)
    Worksheets(2).Cells(8 + i, 8) = jcapbar(2, i)
    Worksheets(2).Cells(8 + i, 9) = lbcapbar(2, i)
    Worksheets(2).Cells(8 + i, 10) = ubcapbar(2, i)
    Worksheets(2).Cells(8 + i, 11) = f(1, i)
    Worksheets(2).Cells(8 + i, 12) = cumf(1, i)
    Worksheets(2).Cells(8 + i, 13) = jcapbar(1, i)
    Worksheets(2).Cells(8 + i, 14) = lbcapbar(1, i)
    Worksheets(2).Cells(8 + i, 15) = ubcapbar(1, i)
Next i
For i = 1 To 10
    Worksheets(2).Cells(108 + i, 2) = -wdep - i
    Worksheets(2).Cells(108 + i, 9) = fcap(2)
    Worksheets(2).Cells(108 + i, 10) = fcap(2)
    Worksheets(2).Cells(108 + i, 14) = fcap(1)
    Worksheets(2).Cells(108 + i, 15) = fcap(1)
Next i
For i = 1 To 2
    Worksheets(2).Cells(3, 17 + i) = rsrc(i)
    Worksheets(2).Cells(4, 17 + i) = rsrt(i)
Next i
For i = 1 To 2
    Worksheets(2).Cells(8, 25 + i) = beta(i, 0)
    For j = 1 To nbay + 1
        Worksheets(2).Cells(9 + j, 25 + i) = beta(i, j)
        Worksheets(2).Cells(9 + j, 25) = j
    Next j
    Worksheets(2).Cells(9 + nbay + 2, 25 + i) = betaacf(i)
    Worksheets(2).Cells(9 + nbay + 3, 25 + i) = betaatf(i)
Next i
Worksheets(2).Cells(9 + nbay + 1, 25) = "Foundation Lateral"
```

289

```
Worksheets(2).Cells(9 + nbay + 2, 25) = "Foundation Axial(Compression)"
Worksheets(2).Cells(9 + nbay + 3, 25) = "Foundation Axial (Tension)"
'
'           INPUT ECHO
'
Worksheets(3).Cells(10, 5) = "ULSLEA"
Worksheets(3).Cells(11, 5) = "Ultimate Limit State Limit Equilibrium Analysis"
Worksheets(3).Cells(15, 5) = "Input Parameters"
'
'           ENVIRONMENTAL CONDITIONS
'
Worksheets(3).Cells(59, 2) = "ENVIRONMENTAL CONDITIONS"
Worksheets(3).Cells(60, 1) = "water depth"
Worksheets(3).Cells(60, 2) = "surge"
Worksheets(3).Cells(60, 3) = "wind vel."
Worksheets(3).Cells(60, 4) = "wave H"
Worksheets(3).Cells(60, 5) = "wave T"
Worksheets(3).Cells(60, 6) = "current vel."
Worksheets(3).Cells(60, 7) = "current vel."
Worksheets(3).Cells(61, 1) = "(ft)"
Worksheets(3).Cells(61, 2) = "(ft)"
Worksheets(3).Cells(61, 3) = "(mph)"
Worksheets(3).Cells(61, 4) = "(ft)"
Worksheets(3).Cells(61, 5) = "(sec)"
Worksheets(3).Cells(61, 6) = "swl (fps)"
Worksheets(3).Cells(61, 7) = "mdl (fps)"

Worksheets(3).Cells(62, 1) = wdep
Worksheets(3).Cells(62, 2) = sdep
Worksheets(3).Cells(62, 3) = vrh
Worksheets(3).Cells(62, 4) = wavh
Worksheets(3).Cells(62, 5) = wavp
Worksheets(3).Cells(62, 6) = cswl
Worksheets(3).Cells(62, 7) = cmdl
'
'           GLOBAL PARAMETERS
'
Worksheets(3).Cells(64, 2) = "GLOBAL PARAMETERS"
Worksheets(3).Cells(65, 1) = "# legs"
Worksheets(3).Cells(65, 2) = "# bays"
Worksheets(3).Cells(65, 3) = "# decks"
Worksheets(3).Cells(65, 4) = "deck weight"
Worksheets(3).Cells(65, 5) = "eo base"
Worksheets(3).Cells(65, 6) = "eo top"
Worksheets(3).Cells(65, 7) = "bs base"
Worksheets(3).Cells(65, 8) = "bs top"
Worksheets(3).Cells(65, 9) = "bs middle"
Worksheets(3).Cells(66, 4) = "(kips)"
Worksheets(3).Cells(66, 5) = "width (ft)"
Worksheets(3).Cells(66, 6) = "width (ft)"
Worksheets(3).Cells(66, 7) = "width (ft)"
Worksheets(3).Cells(66, 8) = "width (ft)"
Worksheets(3).Cells(66, 9) = "width (ft)"
```

290

```
Worksheets(3).Cells(67, 1) = nleg
Worksheets(3).Cells(67, 2) = nbay
Worksheets(3).Cells(67, 3) = ndeck
Worksheets(3).Cells(67, 4) = qdeck
Worksheets(3).Cells(67, 5) = bcw(1)
Worksheets(3).Cells(67, 6) = tcw(1)
Worksheets(3).Cells(67, 7) = bcw(2)
Worksheets(3).Cells(67, 8) = tcw(2)
Worksheets(3).Cells(67, 9) = msw
'
'          Deck Areas
'
Worksheets(3).Cells(69, 2) = "Platform Deck Areas"
Worksheets(3).Cells(70, 1) = "deck #"
Worksheets(3).Cells(70, 2) = "bottom elev."
Worksheets(3).Cells(70, 3) = "top elev."
Worksheets(3).Cells(70, 4) = "eo width"
Worksheets(3).Cells(70, 5) = "bs width"
Worksheets(3).Cells(70, 6) = "drag coef."
Worksheets(3).Cells(70, 7) = "shape coef."
Worksheets(3).Cells(71, 2) = "(ft)"
Worksheets(3).Cells(71, 3) = "(ft)"
Worksheets(3).Cells(71, 4) = "(ft)"
Worksheets(3).Cells(71, 5) = "(ft)"

For i = 1 To ndeck
    Worksheets(3).Cells(71 + i, 1) = i
    Worksheets(3).Cells(71 + i, 2) = uk(i)
    Worksheets(3).Cells(71 + i, 3) = ok(i)
    Worksheets(3).Cells(71 + i, 4) = deckw(2, i)
    Worksheets(3).Cells(71 + i, 5) = deckw(1, i)
    Worksheets(3).Cells(71 + i, 6) = cdd(i)
    Worksheets(3).Cells(71 + i, 7) = wsc(i)
Next i
'
'          Bay Heights
'
Worksheets(3).Cells(77, 2) = "Jacket Bays"
Worksheets(3).Cells(78, 1) = "bay #"
Worksheets(3).Cells(78, 2) = "bay height"
Worksheets(3).Cells(78, 3) = "eo # of diag."
Worksheets(3).Cells(78, 4) = "bs # of diag."
Worksheets(3).Cells(79, 2) = "(ft)"
Worksheets(3).Cells(79, 3) = "braces"
Worksheets(3).Cells(79, 4) = "braces"
For i = 1 To 2
    For j = 1 To nbay
        Worksheets(3).Cells(79 + j, 1) = j
        Worksheets(3).Cells(79 + j, 2) = bayh(j)
        Worksheets(3).Cells(79 + j, 2 + i) = ndb(i, j)
    Next j
Next i
'
'          LOCAL PARAMETERS
```

```
        Worksheets(3).Cells(6 + i, 48) = "Y"
    Else
        Worksheets(3).Cells(6 + i, 48) = "X"
    End If
    Worksheets(3).Cells(6 + i, 49) = jgrout(i)
    Worksheets(3).Cells(6 + i, 50) = jchd(i)
    Worksheets(3).Cells(6 + i, 51) = jcht(i)
    Worksheets(3).Cells(6 + i, 52) = jbrd(i)
    Worksheets(3).Cells(6 + i, 53) = jgap(i)
    Worksheets(3).Cells(6 + i, 54) = jang(i)
    Worksheets(3).Cells(6 + i, 55) = Application.Round(jput(i), 0)
    Worksheets(3).Cells(6 + i, 56) = Application.Round(jpuc(i), 0)
Next i
'
'       Foundation
'
Worksheets(3).Cells(118, 2) = "Foundation"
Worksheets(3).Cells(119, 1) = "main piles"
Worksheets(3).Cells(119, 2) = "d (in)"
Worksheets(3).Cells(119, 3) = "t (in)"
Worksheets(3).Cells(119, 4) = "l (ft)"
Worksheets(3).Cells(119, 5) = "plug"
Worksheets(3).Cells(121, 1) = "skirt piles"
Worksheets(3).Cells(121, 2) = "d (in)"
Worksheets(3).Cells(121, 3) = "t (in)"
Worksheets(3).Cells(121, 4) = "l (ft)"
Worksheets(3).Cells(121, 5) = "plug"

Worksheets(3).Cells(120, 2) = piled
Worksheets(3).Cells(120, 3) = pilet
Worksheets(3).Cells(120, 4) = pilel
Worksheets(3).Cells(122, 5) = plug
Worksheets(3).Cells(122, 2) = spiled
Worksheets(3).Cells(122, 3) = spilet
Worksheets(3).Cells(122, 4) = spilel
Worksheets(3).Cells(122, 5) = splug
'
'       Force Coeficients
'
Worksheets(3).Cells(124, 2) = "Force Coefficients"
Worksheets(3).Cells(125, 1) = "cd"
Worksheets(3).Cells(125, 2) = "cb"
Worksheets(3).Cells(125, 3) = "ds"
Worksheets(3).Cells(125, 4) = "lf"

Worksheets(3).Cells(126, 1) = cdj
Worksheets(3).Cells(126, 2) = cb
Worksheets(3).Cells(126, 3) = ds
Worksheets(3).Cells(126, 4) = lf
'
'       Boatlandings
'
Worksheets(3).Cells(128, 2) = "Boatlandings"
Worksheets(3).Cells(129, 1) = "eo boatl."
```

```
Worksheets(3).Cells(129, 2) = "bs boatl."
Worksheets(3).Cells(130, 1) = "(sqf)"
Worksheets(3).Cells(130, 2) = "(sqf)"
Worksheets(3).Cells(131, 1) = boatl(2)
Worksheets(3).Cells(131, 2) = boatl(1)
'
'       MEMBER STRENGTH, MATERIAL AND SOIL PROPERTIES
'
Worksheets(3).Cells(133, 3) = "Member Strength, Material and Soil Properties"
Worksheets(3).Cells(134, 1) = "fy"
Worksheets(3).Cells(134, 2) = "e"
Worksheets(3).Cells(134, 3) = "k"
Worksheets(3).Cells(134, 4) = "alpha"
Worksheets(3).Cells(134, 5) = "su1"
Worksheets(3).Cells(134, 6) = "su2"
Worksheets(3).Cells(134, 7) = "phi"
Worksheets(3).Cells(134, 8) = "gamma"
Worksheets(3).Cells(134, 9) = "scour"

Worksheets(3).Cells(135, 1) = "(ksi)"
Worksheets(3).Cells(135, 2) = "(ksi)"
Worksheets(3).Cells(135, 5) = "(ksf)"
Worksheets(3).Cells(135, 6) = "(ksf)"
Worksheets(3).Cells(135, 8) = "(kcf)"
Worksheets(3).Cells(135, 9) = "(ft)"

Worksheets(3).Cells(136, 1) = fy
Worksheets(3).Cells(136, 2) = e
Worksheets(3).Cells(136, 3) = kbuck
Worksheets(3).Cells(136, 4) = bres
Worksheets(3).Cells(136, 5) = su1
Worksheets(3).Cells(136, 6) = su2
Worksheets(3).Cells(136, 7) = sphi
Worksheets(3).Cells(136, 8) = gammas
Worksheets(3).Cells(136, 9) = scour
'
'       UNCERTAINTIES AND BIASES
'
Worksheets(3).Cells(138, 2) = "Uncertainties and Biases"
Worksheets(3).Cells(141, 1) = "cov"
Worksheets(3).Cells(142, 1) = "bias"

Worksheets(3).Cells(139, 2) = "wave in"
Worksheets(3).Cells(139, 3) = "jacket"
Worksheets(3).Cells(139, 4) = "brace"
Worksheets(3).Cells(139, 5) = "joint"
Worksheets(3).Cells(139, 6) = "axial pile"
Worksheets(3).Cells(139, 7) = "lateral pile"
Worksheets(3).Cells(139, 8) = "axial pile"
Worksheets(3).Cells(139, 9) = "lateral pile"
Worksheets(3).Cells(140, 2) = "deck ldg."
Worksheets(3).Cells(140, 3) = "ldg."
Worksheets(3).Cells(140, 4) = "capacity"
Worksheets(3).Cells(140, 5) = "capacity"
```

```
Worksheets(3).Cells(140, 6) = "cap.(sand)"
Worksheets(3).Cells(140, 7) = "cap.(sand)"
Worksheets(3).Cells(140, 8) = "cap.(clay)"
Worksheets(3).Cells(140, 9) = "cap.(clay)"

Worksheets(3).Cells(142, 2) = wdbias
Worksheets(3).Cells(141, 2) = wdcov
Worksheets(3).Cells(142, 3) = wjbias
Worksheets(3).Cells(141, 3) = wjcov
Worksheets(3).Cells(142, 4) = bcbias
Worksheets(3).Cells(141, 4) = bccov
Worksheets(3).Cells(142, 5) = jcbias
Worksheets(3).Cells(141, 5) = jccov
Worksheets(3).Cells(142, 6) = sabias
Worksheets(3).Cells(141, 6) = sacov
Worksheets(3).Cells(142, 7) = slbias
Worksheets(3).Cells(141, 7) = slcov
Worksheets(3).Cells(142, 8) = cabias
Worksheets(3).Cells(141, 8) = cacov
Worksheets(3).Cells(142, 9) = clbias
Worksheets(3).Cells(141, 9) = clcov
'
'        Steel Tonnage
'
Worksheets(3).Cells(144, 2) = "Steel Tonnage"
Worksheets(3).Cells(145, 1) = "deck"
Worksheets(3).Cells(145, 2) = "jacket"
Worksheets(3).Cells(145, 3) = "piles"
Worksheets(3).Cells(145, 4) = "total"
Worksheets(3).Cells(146, 1) = "(kip)"
Worksheets(3).Cells(146, 2) = "(kip)"
Worksheets(3).Cells(146, 3) = "(kip)"
Worksheets(3).Cells(146, 4) = "(kip)"

Worksheets(3).Cells(147, 1) = Application.Round(decklegsw, 0)
Worksheets(3).Cells(147, 2) = Application.Round(jacketw, 0)
Worksheets(3).Cells(147, 3) = Application.Round(pilew, 0)
Worksheets(3).Cells(147, 4) = Application.Round(steelw, 0)

End Sub
```